Sede Amministrativa: Università degli Studi di Padova

Dipartimento di Principi ed Impianti di Ingegneria Chimica (DIPIC) “I. Sorgato”

SCUOLA DI DOTTORATO DI RICERCA IN INGEGNERIA INDUSTRIALE

INDIRIZZO INGEGNERIA CHIMICA

XXII CICLO

# BIOETHANOL: A CONTRIBUTION TO BRIDGE THE GAP BETWEEN FIRST AND SECOND GENERATION PROCESSES

**Direttore della Scuola:** Prof. Paolo F. Bariani

**Coordinatore d’indirizzo:** Prof. Alberto Bertucco

**Supervisore:** Prof. Alberto Bertucco

**Dottoranda**: Giada Franceschin

# Contents

**CHAPTER 5**

**Second generation ethanol: a technical and energetic assessment of an industrial process**



**CHAPTER 6**

**Conversion of rye straw into fuel and xylitol: a technical and economical assessment based on experimental data**



**CHAPTER 7**

**LHW pretreatment of wheat bran**

# Riassunto

A causa del prezzo altalenante del petrolio, del consistente impatto ambientale provocato dal massiccio utilizzo di combustibili fossili e della sempre più concreta possibilità che queste fonti di energia stiano per esaurirsi, negli ultimi anni si è rinnovato l'interesse per la questione dell'approvvigionamento energetico.
Le previsioni riguardo all'anno in cui si presenterà il picco di Hubbert (il punto di produzione massima, oltre il quale la produzione del petrolio può soltanto diminuire) sono soggette a incertezze derivanti dalle diverse assunzioni sull'aumento della popolazione mondiale, il consumo pro capite e le politiche energetiche adottate dai diversi Paesi, ma la necessità di cercare al più presto un'alternativa ai combustibili fossili è un dato di fatto.
Cercare di sostituire, almeno in parte, i prodotti di origine fossile con altri basati su risorse di tipo rinnovabile può essere la soluzione a breve e medio periodo per ridurre la dipendenza dal petrolio ed evitare una crisi economica dalle conseguenze imprevedibili.
Il problema energetico riguarda in particolare la crescita repentina della richiesta di prodotti petroliferi, per il settore dei trasporti, che si è ulteriormente aggravata con l'ingresso massiccio di Paesi emergenti, come Cina e India, nel mercato internazionale del greggio. Infatti, mentre per sopperire al fabbisogno di elettricità e calore esistono già alternative tecnologiche (come l'energia eolica, solare, geotermica e le biomasse), per il problema dei carburanti per autotrasporto la scelta si fa più ristretta a causa della necessità di disporre di un combustibile fluido che abbia un'alta densità energetica. Se poi si cerca un'alternativa a breve termine che permetta di mantenere l'attuale struttura logistica così come di utilizzare la tecnologia esistente, le possibilità si restringono ulteriormente.
Bioetanolo e biodiesel sono i candidati più probabili a sostituire benzina e gasolio essenzialmente perché possono essere utilizzati nei motori attualmente disponibili e perché i processi di produzione sono già ben conosciuti.

**Tabella 1** *Costo di produzione del biodiesel da fonti rinnovabili (Demirbas, 2009).*

| Materia prima | Costo [$/gallone] |
|---|---|
| Grassi animali | 1.35 |
| Olio di colza | 1.46 |
| Olio di girasole | 2.35 |
| Olio di soia | 1.26 |

Il costo del biodiesel rappresenta il maggior ostacolo alla sua commercializzazione ed è principalmente dovuto al fatto che gli oli vegetali, utilizzati come materie prime, sono molto costosi.
L'impiego di oli di scarto come materia prima, la possibilità di ottenere processi di trans esterificazione continui e il recupero di glicerolo con un elevato grado di purezza sono i primi passi da considerare per superare il problema. In Tabella 1 è sottolineato come il costo del diesel ottenuto da fonti rinnovabili sia di molto maggiore a quello del gasolio ottenuto da fonti fossili.
Ma un altro ostacolo ben più grave alla larga diffusione del biodiesel è la bassa produttività di oli vegetali per ettaro. In Tabella 2 sono riportate le rese ottenibili da diverse coltivazioni.

**Tabella 2** *Resa in olio di diverse materie prime (Chisti, 2007).*

| Materia prima | Resa in olio [L/ha] |
|---|---|
| Mais | 172 |
| Soia | 446 |
| Noce di cocco | 2,689 |
| Olio di palma | 5,950 |
| Microalghe [a] | 136,900 |
| Microalghe [b] | 58,700 |

a 70% olio (w/w)
b 30% olio (w/w)

Se si volesse sostituire anche solo il 5.75% dei 49.1 milioni di tonnellate equivalenti di petrolio che sono annualmente consumate in Italia come combustibile bisognerebbe convertire a coltivazioni energetiche almeno 3.2 milioni di ettari di terreno coltivato (Russi, 2008). Un altro problema da risolvere sarebbe lo smaltimento dei 0.4 milioni di tonnellate di glicerina prodotte. Dalla Tabella 2 le microalghe appaiono essere le sole specie vegetali potenzialmente in grado di sostituire una fetta importante del combustibile fossile, ma la loro produzione su larga scala non è ancora stata ottenuta con rese soddisfacenti.

Il bioetanolo è l'altro principale candidato per la sostituzione della benzina. Al giorno d'oggi il bioetanolo di prima generazione (ottenuto da mais e canna da zucchero) è caratterizzato da un mercato maturo e tecnologie conosciute, ed è infatti il biocarburante maggiormente prodotto su scala mondiale (Figura 1). In particolare, l'etanolo ottenuto a partire da canna da zucchero, è economicamente vantaggioso (il costo di produzione si aggira sui 0.22 $/L) ed ha rese elevate. La canna da zucchero, però, cresce solamente in climi tropicali o sub tropicali e necessita di almeno 600 mm di precipitazioni annue. Di conseguenza in paesi come gli Stati Uniti e l'Europa tale materia prima non può essere presa in considerazione (The Economist, 2007). In questi casi il bioetanolo è ottenuto a partire dal mais ma, a causa del più complesso processo produttivo e del maggior costo della materia prima, il costo di produzione è maggiore del 30%.

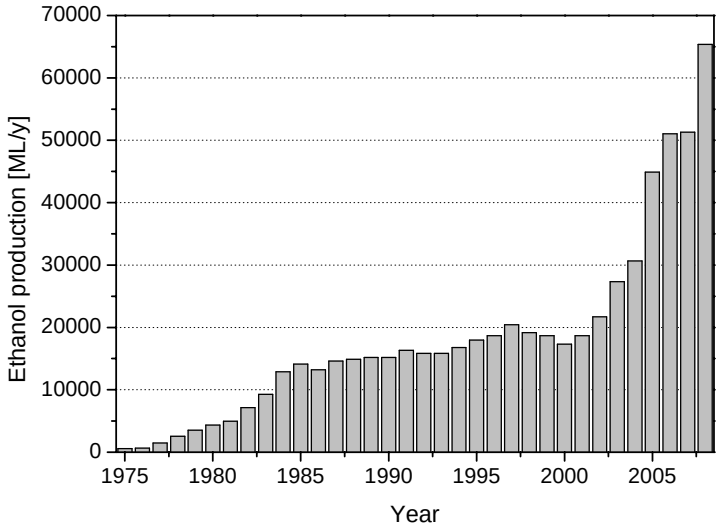


**Figura 1** *Produzione mondiale di bioetanolo dal 1975 al 2007 (Licht, 2006 , Renewable Fuels Association, 2009).*

Il bioetanolo prodotto da mais ha svolto e sta svolgendo un ruolo sicuramente molto importante nell'aprire la strada verso i biocombustibili, ma non può essere considerato la soluzione né a lungo né a medio termine per le ragioni già citate, e soprattutto per questioni di natura etica derivanti dal fatto di utilizzare una risorsa alimentare per fini energetici.

Il bioetanolo di seconda generazione sembrerebbe l'unica soluzione in grado di superare il problema. In questo caso le materie prime utilizzate possono essere, infatti, scarti dell'industria agro forestale, del legno e della carta, oppure possono essere ottenute tramite culture marginali in grado di crescere in terreni non adatti alle altre culture e con una quantità di acqua ridotta (Detchon *et al.*, 2005). Le materie primi non sono in competizione con l'industria alimentare; e il processo di produzione, nel complesso, produce meno anidride carbonica dei processi di prima generazione (Deurwaarder, 2005).

Sfortunatamente, sebbene il bioetanolo da materiali lignocellulosici stia catalizzando l'attenzione sia della ricerca sia delle politiche di molti paesi, il suo sviluppo su scala industriale non è ancora avvenuto. Al momento il problema principale è l'alto costo di produzione causato principalmente dall'elevato costo degli enzimi utilizzati nel processo (Balat and Balat, 2009).

Il grande interesse da parte della comunità scientifica internazionale per la questione energetica e la conclusione che il bioetanolo nel breve periodo è uno dei candidati più probabili per la parziale sostituzione dei combustibili fossili sono state le ragioni che hanno portato allo sviluppo di questa tesi.

Considerando che il bioetanolo da canna da zucchero è già economico ed il processo già ampiamente ottimizzato, l'attenzione è stata rivolta alla produzione di etanolo da mais e da materiali lignocellulosici. Lo scopo è stato quello di studiare i processi produttivi,

focalizzando l'attenzione sugli aspetti che limitano una produzione economica nel primo caso e la diffusione su scala industriale nel secondo.

Nel *Capitolo 1* i due processi produttivi sono presentati assieme alle innovazioni apportate negli ultimi anni e lo stato dell'arte.

Nel *Capitolo 2* un tipico impianto di prima generazione è presentato in dettaglio, grazie ai risultati ottenuti dalla simulazione di processo con il software Aspen Plus$^{TM}$. Una volta sviluppato il modello, l'impianto è stato ottimizzato a livello energetico e si sono eseguite alcune analisi di sensitività. In particolare si è esaminata la possibile influenza delle future innovazioni (mais con un contenuto più elevato in amido e lieviti maggiormente resistenti ad alte concentrazioni di etanolo) sulle prestazioni del processo.

Considerazioni di tipo economico, ottenute grazie ai risultati delle simulazioni, hanno permesso di individuare il costo del mais come maggiore contributo al costo di produzione finale (68.8%), seguito dalle richieste energetiche del processo (16.2%). Considerata l'impossibilità di agire sul costo del mais che segue regole di mercato, si è focalizzata l'attenzione sulla possibilità di ridurre le richieste energetiche del processo, in particolare quelle della distillazione.

L'analisi bibliografica presentata nel *Capitolo 3* ha permesso di individuare nell'estrazione dell'etanolo mediante $CO_2$ supercritica una possibile alternativa alla distillazione tradizionale. L'azeotropo acqua-etanolo può, infatti, essere eliminato in presenza di $CO_2$ supercritica, e di conseguenza il bioetanolo anidro potrebbe essere ottenuto mediante un solo passaggio. A seguito dell'implementazione dell'equilibrio ternario nel software Aspen Plus$^{TM}$ l'estrazione supercritica è stata integrata nel processo di prima generazione.

I risultati delle simulazioni e l'analisi economica presentati nel *Capitolo 4* hanno portato alla conclusione che tale soluzione, sebbene presentata in letteratura come valida alternativa alla distillazione, sia svantaggiosa a causa dell'alto investimento di capitale richiesto e dei costi operativi elevati.

Nei capitoli successivi sono stati esaminati i processi di seconda generazione. Tra tutti i tipi di pretrattamento quello con acqua calda sotto pressione è stato individuato come uno dei più promettenti, ed è stato quindi stato scelto come base per il presente lavoro di ricerca.

Nei processi di seconda generazione la materia prima incide in maniera assai inferiore sul costo di produzione finale, in quanto possono essere utilizzati anche materiali di scarto, per cui gli aspetti energetici assumono un'importanza maggiore. In particolare il pretrattamento con acqua calda ha il vantaggio di non utilizzare altre sostanze chimiche, ma l'acqua deve essere portata ad alta temperatura e pressione, con conseguente aumento della richiesta energetica. Nel *Capitolo 5* il processo di produzione di bioetanolo da paglia è stato simulato in dettaglio giungendo a dimostrare che i residui solidi del processo sono in grado di sostenere le richieste energetiche dello stesso anche con il pretrattamento ad acqua calda.

Un altro grande problema del bioetanolo di seconda generazione è la non competitività economica. Nel *Capitolo 6* si è scelto di verificare l'impatto di un secondo prodotto ad alto valore sulla profittabilità dell'intero processo. I risultati dell'analisi tecnoeconomica sulla contemporanea produzione di bioetanolo (dagli zuccheri a sei atomi di carbonio) e xilitolo (dallo xilosio) hanno dimostrato che anche impianti di media taglia possono diventare competitivi se viene considerata questa opzione.

Nei *Capitoli 7* e *8* sono presentati i risultati sperimentali ottenuti dal pretrattamento della crusca e della carta con acqua calda. In entrambi i casi è stato dimostrato che mediante pretrattamento seguito da idrolisi enzimatica è possibile ottenere zuccheri monomerici, i quali possono essere poi fermentati a etanolo.

Infine nel *Capitolo 9* sono proposti due semplici modelli in grado di rappresentare il pretrattamento con acqua calda in un reattore semi continuo. Tali modelli sono in grado di riprodurre quantitativamente l'andamento della solubilizzazione della biomassa alle diverse temperature, prevedere le concentrazioni di zuccheri monometrici e dei prodotti di degradazione.

## Riferimenti Bibliografici

Balat, M. and H. Balat (2009). Recent Trends in Global Production and Utilization of Bio-ethanol Fuel. *Appl. Energy*, **86**, 2273-2282.

Chisti, Y. (2007). Biodiesel from Microalgae. *Biotechnol. Adv.*, **25**, 294–306.

Demirbas, A. (2009). Progress and Recent Trends in Biodiesel Fuels. *Energy Convers. Manage.*, **50**, 14–34.

Detchon, R, (2005). *Biofuels for Our Future: A Primer*. UN Foundation. Available at: http://www.globalproblems-globalsolutions-files.org/unf_website/PDF/biofuels_faq.pdf [Accessed 29 December 2009].

Deurwaarder, E.P. (2005). *Overview and Analysis of National Reports of the EU Biofuel Directive: Prospects and Barriers for 2005*. Available at: http://www.ecn.nl/docs/library/report/2005/c05042.pdf [Accessed 17 November 2009].

Licht, F.O. (2006). *World Ethanol and Biofuels Report*, vol. 4, no. 17.

Renewable fuel association (2008). *Statistics*. Available at: http://www.ethanolrfa.org/industry/statistics/ [Accessed 17 November 2009].

Russi, D. (2008). An Integrated Assessment of a Large-scale Biodiesel Production in Italy: Killing Several Birds With One Stone? *Energy Policy*, **36,** 1169-1180.

The Economist (2007). *Fuel for Friendship,* p. 44 ,March 3-9th.

# Abstract

In this PhD thesis the development of a number of alternative solutions to overcome some of the main obstacles to the widespread diffusion of bioethanol production plants was addressed. The work was performed through both modelling, process simulation and optimization, and an experimental part concerning the pretreatment of lignocellulosic materials.

A first generation ethanol production process was simulated and optimized. Some key sensitivities about the more likely improvements expected for the years to come, and the possibility to use supercritical $CO_2$ extraction (SFE) instead of distillation were addressed. It was demonstrated that SFE is not economical because of high capital investment and high operation costs.

About second generation bioethanol processes the simulation and energy optimization allowed identifying the best distillation configuration and demonstrating that the process is energetically selfsufficient even though an energy intensive pretreatment like the liquid hot water (LHW) one is chosen. The simulation tool was once more utilized to investigate the economical consequence of the additional xylose production to the traditional second generation process bioethanol. It was found that this high value product could make competitive even a medium size plant.

The experimental work was focused on the pretreatment of both wheat bran and office paper with the liquid hot water technique. The tests on wheat bran were carried out in Germany at the TUHH University (Hamburg) while a lab scale reactor has been built to study the pretreatment of paper at DIPIC Università di Padova. In both cases it was demonstrated that with LHW pretreatment followed by enzymatic treatment it is possible to obtain monomeric sugars from the biomass. A model of the semibatch reactor was also developed to reproduce the experimental data about biomass solubilization.

# Foreword

Most of the research activities that lead to the achievements outlined in this thesis have been developed at the Department of Chemical Engineering Principles and Practice of the University of Padua (DIPIC) under the supervision of Prof. Alberto Bertucco. Part of the work has been carried out at the Institut für Thermische Verfahrenstechnik of the Hamburg University of Technology (TUHH) with the advice of Prof. Irina Smirnova and Prof. Gerd Brunner. As a tangible result of the work completed during the three years of my "Dottorato di Ricerca", a number of publications and presentations to conferences have been produced, as listed below. In addition, three research activities as "Tesi di Laurea" were co-tutored:

1. "Processo di produzione di bioetanolo con $CO_2$ supercritica: simulazione ed ottimizzazione energetica" A.A. 2007/2008. Laureanda: Chiara Vianello, Ingegneria chimica.
2. "Pretrattamento della carta con tecnica dell'acqua liquida calda" scheduled for A.A. 2009-2010. Laureanda: Chiara Favaron, Ingegneria chimica.
3. "Reattore semibatch per il pretrattamento della biomassa: modello di reattore semibatch" scheduled for A.A. 2009-2010. Laureanda: Sarah Lupu, Ingegneria chimica.

## Paper in referred journals

1. Franceschin, G., A. Zamboni, F. Bezzo, and A. Bertucco (2007). Ethanol from Corn: a Technical and Economical Assessment Based on Different Scenarios. *Chemical Engineering Research and Design*, **86**, 488-498.
2. Franceschin G., M. Sudiro, T. Ingram, I. Smirnova, G. Brunner, and A. Bertucco (2009). Conversion of Rye Straw into Fuel and Xylitol: a Technical and Economical Assessment based on Experimental Data Xylitol production. Submitted to: *Chemical Engineering Research and Design*.
3. Franceschin G., T. Ingram, A. Bertucco, G. Brunner, and I. Smirnova (2009). Batch and Semi-Continuous Liquid Hot Water Pretreatment of Wheat Bran. Submitted to: *Biomass and Bioenergy*.
4. Franceschin G., M. Sudiro, and A. Bertucco (2009). Ethanol from Rye Straw: Technical and Energetic Assessment of an Industrial Process. Submitted to: *Renewable Energy*.

## Section in volumes

1. Franceschin, G., M. Sudiro, A. Zamboni, F. Bezzo and A. Bertucco (2007). Energy and economic assessment of bioethanol production by a dry milling process, *AIDIC Conference Series*, Vol. 8, 141-150.

2. Bertucco, A, G. Franceschin (2008). Supercritical Fluid Extraction of Medicinal and Aromatic Plants: Fundamentals and Application. (In S.S. Handa, S.P.S. Khanuja, G. Longo, D.D. Rakesh Eds.) *Extraction Technologies for Medicinal and Aromatic Plants*. UNIDO, Trieste.

## Paper in referred conference proceedings

1. Bertucco, A. and G. Franceschin (2006). Supercritical Fluid Extraction of Medicinal and Aromatic Plants: Fundamentals and Applications. In Proceedings of: *South East Asian (SEA) Regional workshop on Extraction technology for medicinal and aromatics plants.* Lucknow (India), November 29-1.
2. Sudiro, M., G. Franceschin, A. Bertucco (2007). Minimization of Energy Duties and Water Consumption in the Production of Bioethanol by a Dry Milling Process. In Proceedings of: *15st European Biomass Conference & Exhibition*, Berlin (Germany), May 7 - 11. Ref. No. V2.8.II.10.
3. Franceschin, G., M. Sudiro, A. Zamboni, F. Bezzo, A. Bertucco (2007). Energy and Economic Assessment of Bioethanol Production by a Dry Milling Process. In Proceedings of: *ICheaP-8 the eight International Conference on Chemical & Process Engineering*, Ischia (Italy), June 24 - 27.
4. Franceschin, G., A. Bertucco (2008). Integration of Supercritical $CO_2$ Extraction into Existing Bioethanol Production Plant: a Technical and Economical Assessment. In Proceedings of: *11th European Meeting on Supercritical Fluids*. May , 4-7 Barcelona (Spain).
5. Franceschin, G., A. Bertucco, T. Ingram, G. Brunner, and I. Smirnova (2009). Semi Continuous Liquid Hot Water Pretreatment of Wheat Bran. In Proceedings of: *17th European Biomass Conference & Exhibition From Research to Industry and Markets*, 29 June - 3 July, Hamburg (Germany).
6. Franceschin, G., T. Ingram, I. Smirnova, G. Brunner, and A. Bertucco (2009). Conversion of Rye Straw into Fuel, Valuable Product and Energy. In Proceedings of: *17th European Biomass Conference & Exhibition From Research to Industry and Markets*, 29 June - 3 July, Hamburg (Germany).

## Participation to scientific conference

1. Franceschin, G., M. Sudiro, C. Piccolo, A. Zamboni, F. Bezzo, A. Bertucco (2008). Sviluppo di Carburanti Alternativi: dalla Definizione del Processo all'Ottimizzazione della Filiera Produttiva. *Convegno GR.I.C.U.*, 14-17 Sept. La Castella (KR).

Padova
27-01-2010

# Introduction

In the last years the energy supply problem has gained increased interest in the community worldwide. In fact, even thought future projections are quite different, it is a matter fact that the fossil fuels reserves are dwindling and sooner or later we can expect a peak in the oil production. The peak oil will occur when the maximum rate of global petroleum extraction will be reached, after which it will enter its terminal decline. The concept is based on the observed production rates of individual oil wells, and the combined production rate of a field of related oil wells. A first study of this type, based on a scientific analysis of the problem was developed and introduced in Hubbert (1949). Although, when first presented, this theory engendered different reactions, the general idea of a future peak of oil production is now well accepted from the scientific community. The forecasts of the exact time frame of the peak oil are really different and even more difficult is to forecast the oil depletion. This because the projections involve different scenarios and ensue from several hypotheses on the world population growth, the pro capita energy demand, and the energy policy of the years to come.

The Cambridge Energy Research Associates (CERA: Jackson, 2006) as mainstream media (New York Times: Mouawad, 2007), dedicated information organizations (IEA, 2006; EIA, 2006), and even oil extraction companies (Exxon: Tillerson, 2007) still assert that the peak oil problem is not very important. In 2006 CERA declared that the remaining global oil resource bases were suppose to be 3.74 trillion barrels, three times as large as the 1.2 trillion barrels estimated by the other theory. It was claimed that the peak oil argument is based on faulty analysis which could, if accepted, distort critical policy and investment decisions and cloud the debate over the energy future. CERA asserted the peak oil will occur after 2035 (Jackson, 2006).

An important question is: is it really less alarming think about the reach of the peak oil in 25 or even 30 years?

Statistical data from IEA (2007) confirm that the world economy is strictly bound to fossil fuels. The fossil energy is about 81% of the total commercial energy consumed in the world and about 98% of the energy used in the transport sector. These data show that, at present, the combined alternatives to fossil energy represent a relatively small portion of the total energy produced. Nuclear energy accounts for 6.3%, hydro for 2.2%, geothermal and solar 0.5% and finally combustible renewable and waste 10.0%. So, the shift from an economy completely based on fossil fuels to one based on “alternative energies” is not a matter of few years, but being optimistic it will involve decades.

Regardless of the specific time of peak oil production, it is clear that the energy issue should be one of the most important of the period to come. In fact on the one hand the oil barrel price is uncertain and, on the other hand, private investments are not encouraged as long as renewable energies are not competitive with fossil fuels. To the oil supply issue the recent concerns about environment must be added. Burning fossil fuels is responsible for environmental degradation that deserves high attention in the political agenda of these days. Examples are greenhouse gas accumulation, acidification, air pollution, water pollution, damage to land surface, and ground-level ozone. At a conclusion, the research in this field is really crucial.
From the regulatory standpoint the European Commission approved several directives that involve alternative energies and consequently biofuels:

- 2001: "Communication on alternative fuels for road transport" (biofuels are identified as potential future transport fuels);
- 2003: Biofuels Directive was adopted (2003/30 EC) It was fixed the replacement of 2% in 2005 and 5.75% in 2010 of all gasoline and diesel for transport purposes with renewable fuels;
- 2003: Energy taxation Directive (2003/96 EC) which allowed de-taxation of biofuels;
- 2005: "Biomass Action Plan" was presented;
- 2006: "An EU strategy for biofuels" presented in view of the revision of the 2003/30 EC Directive;
- 2007: "Road Map for Renewable Energy in Europe" presented.

On 5 June 2009 Directive 2009/28/EC has been published in the Official Journal of the European Community. This new legislative act related to the use of energy from renewable sources forms part of a series of measures being implemented to position the EU at the forefront of world energy policy and to reduce greenhouse gas emissions by 20% by 2020. The aim of this Directive is to achieve by 2020 a 20% share of energy from renewable sources in the EU's final consumption of energy and a 10% share of energy from renewable sources in each Member state's transport energy consumption. Member States have time until 5 December 2009 to transpose the Directive.

Although there are several alternatives in order to supply electricity or heat, among which sun, wind, hydro, and geothermal energy as well as biomass combustion, there is not the "perfect" renewable energy so that the choice will be necessary tied to political decisions. However, within the energy problem, the one of fuels for transportation is an even more complex issue, this because it involves the problem to have a fuel with a high energy

density. If we are looking for a short term alternative in this field in order to maintain the present logistics and fuel distribution network and the current engine technology, the alternatives are really few.

They are basically: Biodiesel, bioethanol, Fisher Tropsch -diesel, methanol, dimethyl ether, and biomethane. Figure 1 shows the routes to these biofuels starting from possible raw materials.

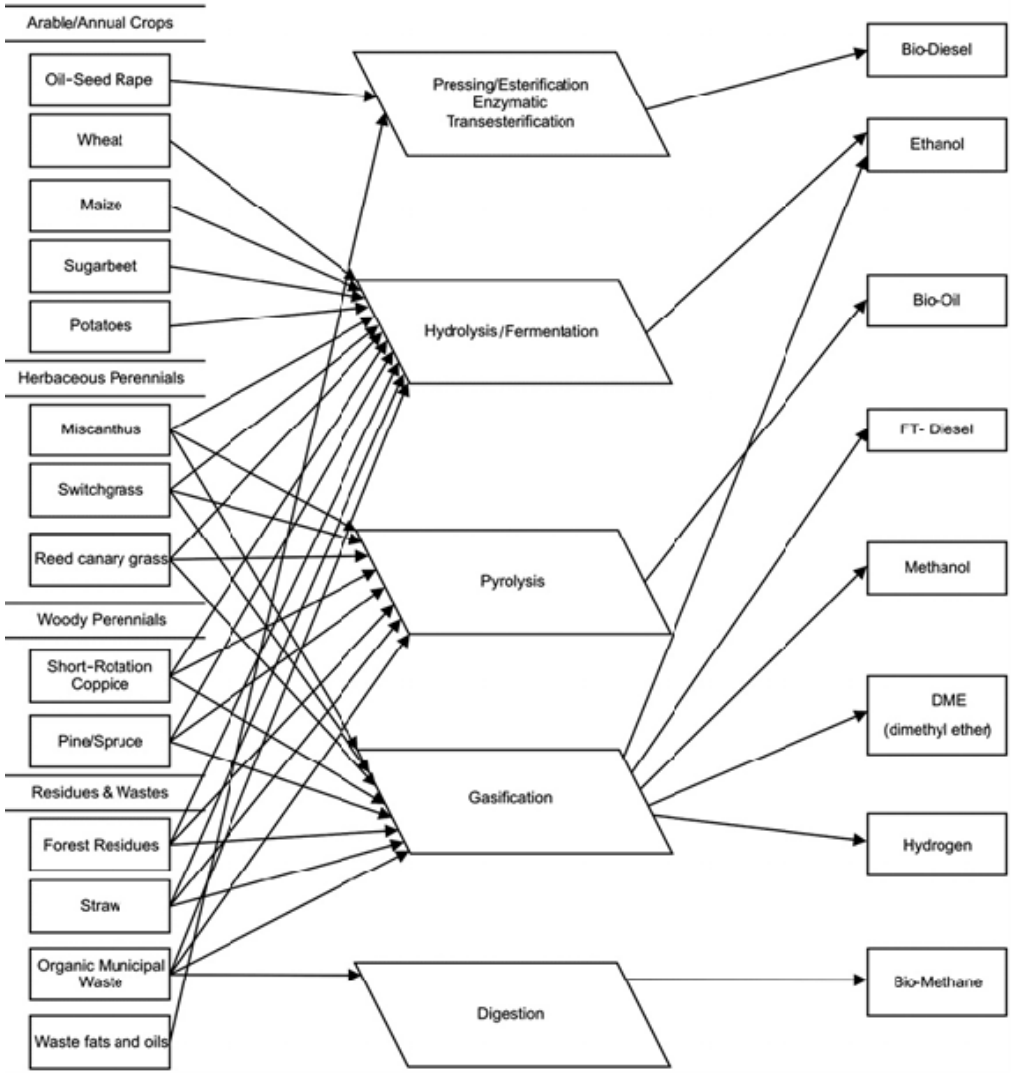


**Figure 1** *Schematic representation of biofuel pathways (Hammond et al., 2008).*

Each one of these biofuels has advantages and disadvantages and different are the reasons because none of these, but first generation ethanol and biodiesel, are nowadays industrial scale processes.

Indeed bioethanol and biodiesel are the current chief candidates as a petroleum replacement for internal combustion engines, primarily because they can be used in present engines and infrastructure, and second because the production technology are completely known and technologically ready.

Biodiesel is mostly produced in Europe; Figure 2 presents details and a comparison between U.S.A. and Europe. Despite a decreasing growth with respect to the previous years, the European Union remains the major producer in the world: 8,733 ML, approximately 60-65% of the total, in 2008; with 2,649 ML, according to the US National Biodiesel Board (2009), the U.S.A. come second, ahead of Brazil (approx. 1,000 ML).

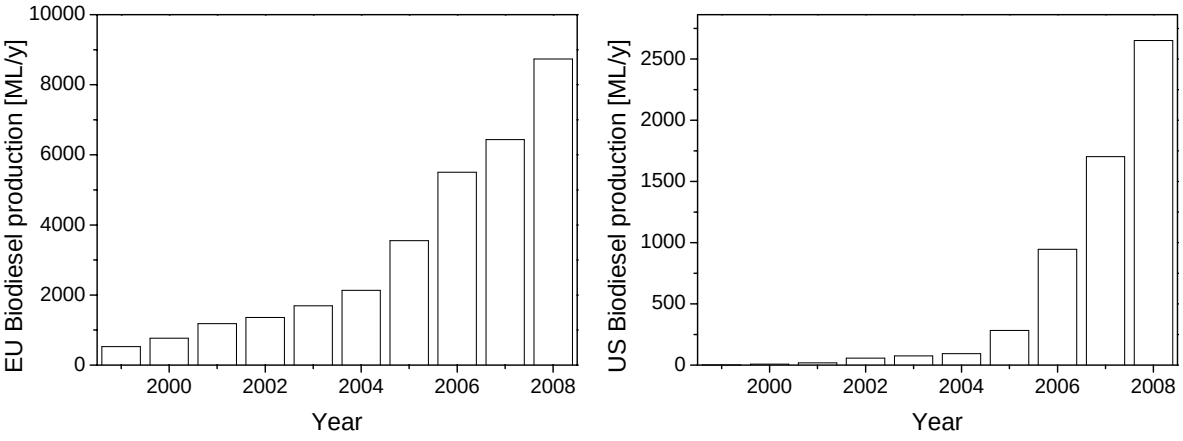


*(a)* *(b)*

**Figure 2** *Evolution of biodiesel production in the EU-27 (Biofuel Platform, 2009) and in the U.S.A. (US National Biodiesel Board, 2009).*

The cost of biodiesel, however, is the main obstacle to commercialization of the product, as vegetal oils are more and more expensive. Use of cooking oil as raw material, the viability of a continuous transesterification process and the recovery of high-quality glycerol as byproduct are primary options to be considered to overcome the problem. Table 1 underlines that biodiesel production costs from different feedstocks are at least 1.5-3 times the cost of fossil fuel diesel.

**Table 1** *Costs per gallons for biodiesel from different feedstocks (Demirbas, 2009).*

| Feedstock | Cost [$/gallon] |
|---|---|
| Animal fats | 1.35 |
| Rapeseed oil | 1.46 |
| Sunflower oil | 2.35 |
| Soybean oil | 1.26 |

Another obstacle to the large diffusion of this fuel is the low productivity for hectare. Table 2 shows the oil yield of different raw materials from which vegetal oils are obtained.
Some fast calculations show how it would be impossible to produce in Italy an amount of biodiesel able to replace even the 5.75% of the fuel presently consumed.

**Table 2** *Oil yield of different sources of biodiesel (Chisti, 2007).*

| Crop | Oil yield [L/ha] |
|---|---|
| Corn | 172 |
| Soybean | 446 |
| Coconut | 2,689 |
| Oil palm | 5,950 |
| Microalgae [a] | 136,900 |
| Microalgae [b] | 58,700 |

a 70% oil (w/w) biomass
b 30% oil (w/w) biomass

The problem of internal production of biodiesel in Italy was addressed by Russi (2008). Try to replace the 5.75% of the 49.1 million t of oil equivalent (toe) estimated as total energy consumption for transport in Italy in 2010 would mean that 2.8 million toe should be obtained annually from biofuels, i.e. 3.2 million tonnes of biodiesel. When considering the actual proportion of feedstock used (20% sunflower and 80% rapeseed, Comitato Termotecnico Italiano, 2000) 3.4 million of hectares should be cultivated with rapeseed and 0.7 with sunflower. But out of the 30.1 million hectares of the Italian territory, 27.9 are already occupied by mountains, forests, pastures, and agricultural land. The remaining 2.2 million hectares include cities and roads, and also not tillable land. Assuming that 0.5 million hectares of marginal, abandoned and set-aside land that can be dedicated to energy farming, 3.2 million hectares more of existing crops would have to be replaced.

Another problem to solve, in case the biodiesel needed to meet the 5.75% target were produced in Italy, is the destiny of the 0.4 million tonnes glycerine and 4 million tonnes cake meal that would be produced. A market outlet for such large amounts is really difficult to find.

In view of Table 2, microalgae appear to be the only source of biodiesel that has the potential to completely displace fossil diesel. Unlike other oil crops, microalgae grow extremely rapidly and many are exceedingly rich in oil. Plenty of papers claim microalgae as the optimal biomass to produce biodiesel, because microalgae commonly double their biomass within 24 h, the doubling times during exponential growth are commonly as short as 3.5 h, and the oil content can be up to 80% by weight of dry biomass (Chisti, 2007).

In spite of the great potential of this biomass only lab scale data are available while outdoor cultivations present several problems which decrease enormously the productivity. Among other we cite: the need to select and grow highly productive lipid-rich algal strains; the difficulty of maintaining selected species in outdoor culture; the very limited availability of data on large-scale microalgae cultures; the high energy inputs required for water pumping, $CO_2$ transfer, mixing of the culture suspension and harvesting/dewatering the algal biomass, potentially resulting in a negative NER (net energy ratio) for the process. By now only open ponds are run at the industrial scale. The main problems in open systems are the

contamination of the culture by other algal species and the efficient utilization of the solar energy.
The development of photobioreactors (close reactors) able to maximize the efficiency of conversion of solar energy is one of the hot research topics, but industrial plants are still not documented. An average value of overall areal productivity 36.3 g/($m^2$ day) and efficiency of conversion of visible solar radiation of 9.4% were obtained with outdoor full-scale columns (Chini Zittelli, 2006) while the maximum theoretical efficiency of conversion is equal to 12%.

As already mentioned, the other chief candidate as a biofuel is bioethanol, whose world production is greater than biodiesel. Nowadays the 1$^{st}$ generation bioethanol (from sugar cane and starchy materials) is characterized by mature commercial markets and well understood technologies. In 2007 the bioethanol worldwide production was 49,595 millions litres that increased up to 65,362 in 2008 (Renewable fuel association, 2009). Main producers are U.S.A. and Brazil that together cover almost 90% of the total production (Figure 3).

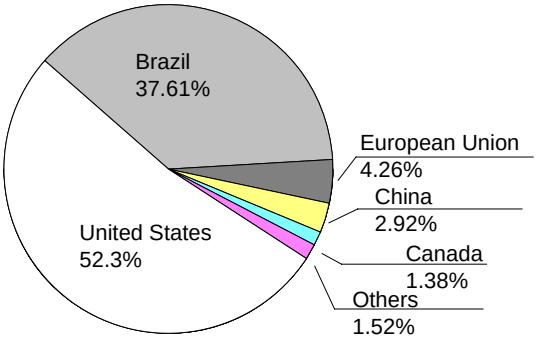


**Figure 3** *Bioethanol producers in 2008.*

Brazil's sugar cane-based industry is far more efficient than the U.S. corn-based one. Brazilian distillers are able to produce ethanol for 22 cents per litre, compared with the 30 cents per litre for corn-based ethanol. In fact sugarcane is one of the most efficient photosynthesizers in the plant kingdom, able to convert up to 2% of incident solar energy into biomass. But sugarcane cultivation requires a tropical or subtropical climate, with a minimum of 600 mm of annual rainfall and obviously it cannot be cultivated efficiently in U.S.A. and Europe (The Economist, 2007).
U.S. corn-derived ethanol costs 30% more for a simple reason: corn starch must first be converted to sugar before being fermented into alcohol. Despite this production cost difference, in contrast to Japan and Sweden, the U.S. does not import much of Brazilian ethanol because of U.S. trade barriers corresponding to a tariff of 54-cent per gallon – a levy

designed to offset the 51-cent per gallon blender's federal tax credit that is applied to ethanol no matter its Country of origin (Cseke *et al.,* 2009).
So, it is clear as the vast majority of first-generation biofuel feedstocks, especially in the case of the European Union and U.S.A., constitute comestible materials, which has led to concerns about biomass previously destined for human consumption being diverted to fuel production.

If the United States, along with Canada and the EU, were to replace only 10 per cent of their current transport fuels with biofuels, it would require an investment of between 30–70 per cent of their national crop areas, at least with current production and crop-yield levels (OECD 2006).
Furthermore, in order to substitute just under 6 per cent of petrol and diesel, the EU would have to convert 19 per cent of its arable land from food crops to fuel crops (OECD 2006). Even the EU's modest target of 20 per cent reliance on alternative fuels (including biofuels) by 2020 would consume the majority of its cropland, although Bulgaria and Romania's recent accession to the EU will doubtless improve the availability of agricultural lands (EU, 2005).
For these reasons and in order to be able to substitute an important part of the fossil fuels, second generation bioethanol, should be considered as the only solution. In fact it is derived from feedstocks not traditionally used for human consumption. As a result, there is much less concern about the use of these fuels leading to famine in developing Countries, or adversely affecting consumer prices in developed nations.
The benefits of using second-generation biofuels are many. Aside from reducing the threat of food supplies being diverted to fuel production, they are more environmentally friendly and produce less greenhouse gases (GHGs) than first-generation ones (Deurwaarder, 2005). In addition they are also expected to be produced at a more competitive price due to the possibility to use waste materials as feedstock. Indeed, the choice of starting material is wide, including various types of hardy grasses (e.g., switchgrass, Detchon *et al.*, 2005) that can grow with a low consumption of water and fertilizer so that marginal area, usually not suitable for crops grow, can be used for their production.
Unfortunately although "Second Generation bioethanol" is nowadays receiving much attention by politicians, especially in the EU, as a more $CO_2$ friendly alternative to fossil transport fuels than corn, wheat or sugar beet bioethanol, its exploitation at a large industrial scale is not developed yet.
At the moment the main issue with bioethanol from lignocellulosic biomass is that it is by far more expensive than the one obtained by traditional feedstock based processes, due to the additional treatment required and to costly enzymes involved in the process (Balat and Balat, 2009).

In Table 3 cost of ethanol production from corn and cellulosic feedstocks are compared (Collins, 2007).

**Table 3** *Comparison between first generation and second generation ethanol production cost (Collins, 2007).*

| | Corn ethanol cost [$/gallon] | Cellulosic ethanol cost currently [$/gallon] | Cellulosic ethanol cost 2010-12 [$/gallon] |
|---|---|---|---|
| Feed stock | 1.17 (3.22$/bushel) | 1.00 (60$/ton) | 0.33 (30$/ton) |
| Enzymes | 0.04 | 0.40 | 0.10 |
| Other costs(1) | 0.62 | 0.80 | 0.22 |
| Capital costs | 0.20 | 0.55 | 0.54 |
| **Total costs** | **2.03** | **2.75** | **1.19** |
| By product | -0.38 | -0.10 | -0.09 |
| **Net costs** | **1.65** | **2.65** | **1.10** |

(1) Includes pre-processing, fermentation, labour costs.

Another problem when processing these raw materials comes from the difficult of fermentation of the hemicellulose fraction. In fact, while hexoses can be easily converted to glucose by *Saccharomyces cerevisiae* with well-known technology, pentoses, i.e. the main constituents of hemicellulose, are more cumbersome to ferment. Yeasts and bacteria able to ferment simultaneously hexoses and pentoses are currently under development (Hägerdal *et al.*, 2007), as conventional organisms are not suitable to this scope.
These considerations highlight how first generation bioethanol has been certainly an important step that contributed to smooth the way to the lignocellulosic bioethanol, but only biodiesel from microalgae and second generation bioethanol can be considered as realistic solution in order to reduce the dependence on fossil fuels and have environmental beneficial effects.
However at present breakthroughs have to be done in the research field before the industrial commercialization of these techniques.

Great scientific community interest on the energetic issue and the conclusion that in the short period bioethanol is one of the more likely candidates were the reasons that lead to develop this thesis project.

The aim is to investigate the bioethanol production process from both starchy material and lignocellulosic feedstocks. Focusing on the actual issues that limit an economical production in the first case and the industrial scale diffusion in the second one, a number of process schemes and commercial alternatives were proposed and investigated.

Regarding first generation ethanol and considering that industrial plants (also from starch feedstocks) are already in operation and the main technical problems are already solved, the attention was focused on the analysis of the process itself especially from the energetic point of view and on alternatives to decrease the final production cost. As already argued, the second generation ethanol is not already developed at the industrial scale and the reasons in this case are both technical and economical so that, at the simulation tasks, were joined also experimental investigations.
As for the first generation ethanol the plant was studied by means of process simulations and alternatives were screened and studied deeply. In particular the experimental part was aimed to study the pretreatment step, which is nowadays one of the steps that are still not optimized.

Getting down into details about the content of each Chapter:
The *first Chapter* introduces the first and second generation bioethanol processes, giving a look to the innovations and advances obtained in the last years.
In the *second Chapter* a typical first generation plant is illustrated in detail by presenting simulation results (obtained with Aspen Plus$^{TM}$). A model to simulate the process was developed, the process was energetically optimized, and some sensitivities on process variables done. In this way it was possible to determine how these variables influence the production cost and how future biotechnological advances (yeast ethanol tolerance and corn starch content) can change it. The calculations with a process simulation software permitted to consider the entire plant and valuate overall energy and mass balances. The energy optimization allowed determining the more energetically expensive operation and screening possible technical modifications.
In *Chapter 3* and *Chapter 4* the supercritical $CO_2$ extraction as a process alternative to the simple distillation of ethanol is investigated, by simulating the extraction process and performing an economical and financial analysis. In fact the ethanol, obtained from the fermentation, is in mixture with water at low concentration. The common recovery with distillation is a high energy demanding operation and is limited by the azeotrope. The supercritical extraction alternative was investigated, as a consequence to literature experimental investigations that showed the possibility to break the azeotrope and reduce to a single step the achievement of absolute ethanol.
*Chapter 5* marks the switch from first generation ethanol to second generation one. In this case it is possible to use waste products as raw material. For this reason and due to the lower concentration of ethanol after the fermentation, the portion of total ethanol production cost related to energy utilities is higher in respect to the first generation plant. The energy optimization of a second generation plant was addressed focusing on the possibility to

obtain the whole amount of energy needed directly from the lignin rich solid residue of the plant.

On the biorefinery point of view, an opportunity to make second generation ethanol economically competitive could be the contemporaneous production of a second high value product. In *Chapter 6* the results of a techno economical analysis on the production of ethanol and xylitol are presented.

In *Chapter 7* and *8* the lignocellulosic biomass pretreatment, identified as one of the main issues in obtaining cellulosic ethanol is dealt with. Experimental results on the liquid hot water pretreatment of wheat bran and white office paper are presented.

Finally *Chapter 9* suggest possible mathematical models that could be implemented in order to represent a semi continuous reactor for the LHW pretreatment.

## References

Balat, M. and H. Balat (2009). Recent Trends in Global Production and Utilization of Bio-ethanol Fuel. *Appl. Energy*, **86**, 2273-2282.

Biofuels Platform (2009). *Production of biodiesel in the EU*. Available at: http://www.biofuels-platform.ch/en/infos/eu-biodiesel.php [Accessed 29 December 2009].

Chini, Zittelli, G., L. Rodolfi, N. Biondi, and M.R. Tredici (2006). Productivity and Photosynthetic Efficiency of Outdoor Cultures of *Tetraselmis suecica* in Annular columns. *Aquaculture*, **261,** 932–943.

Chisti, Y. (2007). Biodiesel from Microalgae. *Biotechnol. Adv.*, **25**, 294–306.

Cseke, L.J., G.K. Podila, A. Kirakosyan, and P.B. Kaufman (2009). Plants as Sources of Energy. In: *Recent Advances in Plant Biotechnology* (P.B. Kaufman, A. Kirakosyan, Eds.) Springer Publishing Co. Inc., New York (U.S.A.).

Collins, K. (2007). The New World of Biofuels: Implications for Agriculture and Energy. In proceedings of: *EIA Energy Outlook, Modeling, and Data Conference*, Washington, (U.S.A.), March 28.

Comitato Termotecnico Italiano (2000): http://cti2000.it/virt/cti2000/Headbio.htmS .

Demirbas, A. (2009). Progress and Recent Trends in Biodiesel Fuels. *Energy Convers. Manage.*, **50**, 14–34.

Detchon, R, (2005). *Biofuels for Our Future: A Primer*. UN Foundation. Available at: http://www.globalproblems-globalsolutions-files.org/unf_website/PDF/biofuels_faq.pdf [Accessed 29 December 2009].

Deurwaarder, E.P. (2005). *Overview and Analysis of National Reports of the EU Biofuel Directive: Prospects and Barriers for 2005*. Available at: http://www.ecn.nl/docs/library/report/2005/c05042.pdf [Accessed 17 November 2009].

EIA, Energy Information Administration (2006). *International Energy Outlook 2006*. Available at: http://www.fypower.org/pdf/EIA_IntlEnergyOutlook(2006).pdf [Accessed 15 September 2009]

European Union (Energy Research Centre of the Netherlands) (2005). *Biomass Action Plan*. Available at: http://ec.europa.eu/ [Accessed 17 November 2009].

Ghisolfi, G. (2009). Biocarburanti. Vale la Pena? Presented at: *2°Bio-ethanol Conference*, *Etanolo di seconda generazione: una realtà possibile*, Milano (Italy), March 4.

Hägerdal, B.H., K. Karhumaa, C. Fonseca, I. Spencer-Martins, and M.F. Gorwa-Grauslund (2007). Towards Industrial Pentose-fermenting Yeast Strains. *Appl. Microbiol. Biotechnol.*, **74**, 937-953.

Hammond, G.P. (2008). Development of Biofuels for the UK Automotive Market. *Appl. Energy*, **85**, 506-515.

Hubbert, M.K. (1949). Energy from Fossil Fuels. *Science,* **109**, 103-109.

IEA, International Energy Agency, Paris (2006). *World energy outlook 2006*. Available at: http://www.iea.org/textbase/nppdf/free/2006/weo2006.pdf [Accessed 29 December 2009].

IEA, International Energy Agency, Paris (2007). *Key World Energy Statistics*. Available at: http://www.iea.org/textbase/nppdf/free/2007/Key_Stats_2007.pdf [Accessed 29 December 2009].

Jackson, P., Client Services Cambridge, MA, USA (2006). *Why the Peak Oil Theory Falls Down - Myths, Legends, and the Future of Oil*. CERA, Available at: http://www.cera.com/aspx/cda/client/report/reportpreview.aspx?CID=8437&KID= [Accessed 29 December 2009].

Mouawad, J. (2007). Oil Innovations Pump New Life into Old Wells. *New York Times*, March 5.

OECD (2006). *Agricultural Market Impacts of the Future Growth in the Production of Biofuels*. Available at: www.oecd.org/dataoecd/58/62/36074135.pdf [Accessed: December 2009]

Renewable fuel association (2008). *Statistics*. Available at: http://www.ethanolrfa.org/industry/statistics/ [Accessed 17 November 2009].

Russi, D. (2008). An Integrated Assessment of a Large-scale Biodiesel Production in Italy: Killing Several Birds With One Stone? *Energy Policy*, **36,** 1169-1180.

The Economist (2007). *Fuel for Friendship,* p. 44 ,March 3-9th.

Tillerson, R. (2007). The State of the Energy Industry: Strengths, Realities and Solutions. Presented at: *CERA Week 2007 Conference*, Houston Texas (U.S.A.), February 12- 16.

U.S. National biodiesel board (2009). Available at: http://www.biodiesel.org [Accessed 17 November 2009].

# Chapter 1

# Bioethanol: state of the art

Processes that convert biomass into ethanol can be divided into two classes: 1st generation processes that use basically starch or fermentable sugars as feed material, and 2nd generation ones that start from the whole plant and try to convert sugar polymers like cellulose and hemicellulose. This Chapter introduces the production processes actually used, reports the advances achieved in the last years and the future trends.

## 1.1 First generation bioethanol

The alcohol industry is quite old and for this reason processes to produce bioethanol from starch and sugar cane are well known and nearly optimized. In 2008 the world bioethanol production was 65,362 millions of litres (Biofuels Platform, 2009) and almost the total amount was produced from sugar cane (Brazil) or starchy materials (other Countries). Both the processes are well known and are described in the following. Figure 1.1 reports the global ethanol production from 1975 to 2008. It is interesting to see how the production was stable from 1984 until 2001/2002, then a rapid increase follows. This was mainly due to the increase of U.S. production.

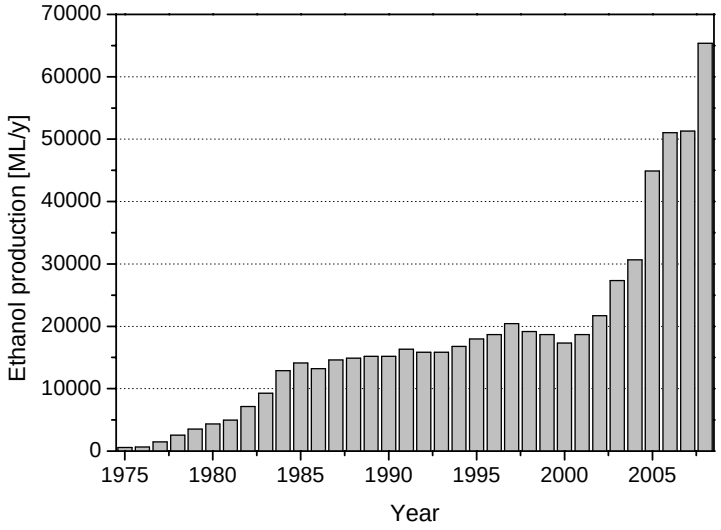


**Figure 1.1** *Global ethanol production from 1975 to 2007 (Data between 1975 and 2005 were obtained from Licht, 2006 while more recent data from the Renewable Fuels Association, 2009).*

### 1.1.1 Bioethanol from crops

Starch is a high yield feedstock for ethanol production, but its hydrolysis is required to obtain ethanol by fermentation. Starch was traditionally hydrolyzed by acids, but the specificity of the enzymes, their mild reaction conditions and the absence of secondary reactions have made the amylases to be the catalysts generally used for this process.
α-amylase can be obtained from thermoresistant bacteria like *Bacillus licheniformis* or from engineered strains of *Escherichia coli* or *Bacillus subtilis* (Sanches and Cardona, 2008).
Corn is the most used fuel crop, especially in the U.S.A.. Two are the main existing processes: the wet mill process and the dry grind one. In Europe (2007 data) ethanol is produced from different feedstocks. The 39% of it is obtained from wheat, the 24% from beet juice and only 13% from corn. This happened especially after the shift to beet juice of lots of Germany plants due to the corn price rise. Other feedstocks are barley (12% of the ethanol), raw alcohol (8%), rye (3%), and pulp (1%) (European biofuel association, 2008). Cassava represents an important alternative source of starch not only for ethanol production, but also for glucose syrups. In fact, cassava is the tuber that has gained most interest due to its availability in tropical Countries being one of the top ten more important tropical crops. Besides, ethanol can be produced also from triticale (Wang *et al.*, 1997), and sorghum (Zhan *et al.*, 2003).

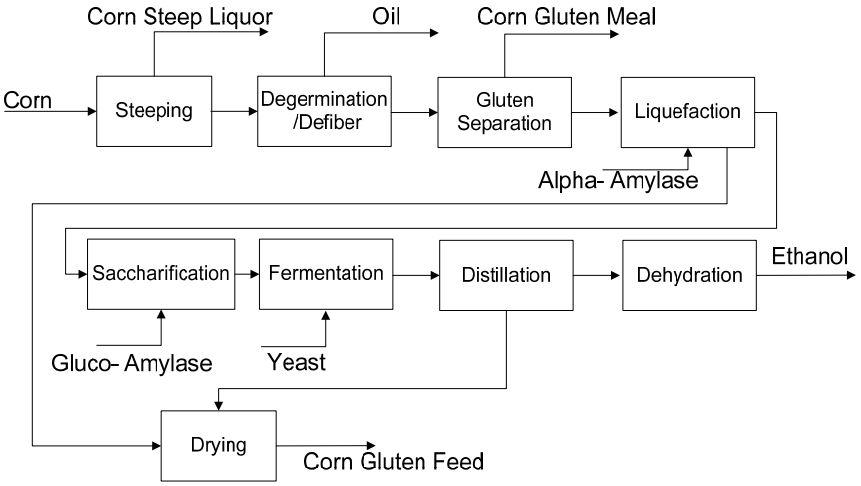


**Figure 1.2** *Block flow diagram of the wet mill process that produce ethanol from corn (Adapted from Wyman, 1996).*

The wet milling process was originally devised for the starch industry and adapted for fuel-ethanol production. Accordingly, the corn (or wheat) kernel is steeped in warm water; this helps to break down the proteins, releases the starch present in the corn, and helps to soften the kernel for the milling process. The corn is then milled to obtain germ, fibre and starch products. The germ is extracted to produce corn oil and the starch fraction undergoes centrifugation and saccharification to produce gluten wet cake. After fermentation the

ethanol is extracted by distillation. The block flow diagram of the process is represented in Figure 1.2 (adapted from Wyman, 1996).

The first large-scale dry-mill ethanol plant was built by New Energy Corporation in South Bend, Indiana in 1985. It was innovative in respect to the wet mill technology due to both its size and technology. Dry-grind ethanol plants (DGP) require lower capital and production investments than wet-mills. The economies of scale are also lower. Therefore, average production capacity for a dry-mill plant is about 30 million of gallons per year vs. 100 and greater for wet mills (BBI International, 2009).

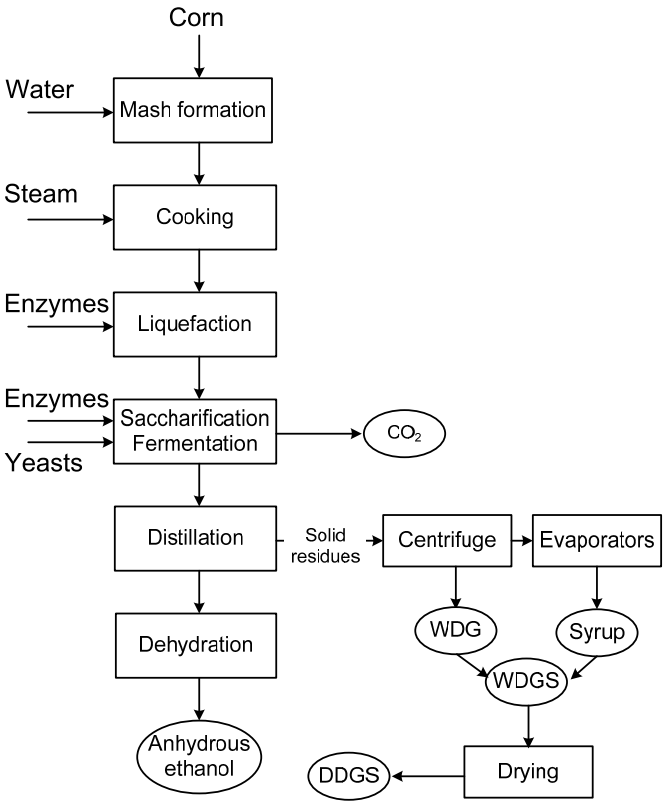


**Figure 1.3** *Block Flow Diagram of the Dry Grind process.*

The DGP is nowadays the preferred choice in to produce bioethanol from crops and also in this thesis it was adopted as a reference and investigated deeper by process simulation (§ Chapter 2). The process Block Flow Diagram of Figure 1.3 show as the raw material is turned into the two products: ethanol and DDGS (Distiller's Dried Grains with Solubles).

### *1.1.2 Sugar cane bioethanol*

Sugar cane (*Saccharum officinarum*) is a drought-tolerant, tropical and subtropical crop that contains 12-17% total sugars on a wet-weight basis with 68-72% moisture (90% sucrose and 10% glucose or fructose). The average extraction efficiency to produce cane juice by crushing is approximately 95% and the remaining solid residue is cane fibre (bagasse).

Sugar cane bioethanol process is very similar to the DGP, with the difference that no enzymes are needed because from sugar cane fermentable sugars are directly obtained. In factories that only produce ethanol, the cane juice is heated up to 110 °C to reduce microbial contamination, decanted, sometimes concentrated by evaporation and then fermented. In combined sugar ethanol plants (annexed distilleries) sucrose crystals that are formed after cane-juice concentration are removed by centrifugation, leaving syrup (molasses) that contains up to 65% w/w sugars. Both sugar-cane juice and molasses (after adjusting the sugar concentration) normally contain sufficient minerals and organic nutrients to be immediately suitable for ethanol production by fermentation with *Saccharomyces cerevisiae* (Wheals *et al.*, 1999). About 79% of ethanol in Brazil is produced from fresh sugar cane juice and the remaining percentage from cane molasses (Wilkie *et al.,* 2000).

The *Melle-Boinot* process is typical for fuel ethanol production by batch fermentation. This process comprises the weight and sterilization of feedstock, followed by the adjustment of pH with $H_2SO_4$ and of the Brix degrees to values of 14-22. After fermentation the produced wine is decanted, centrifuged and sent to the ethanol separation stage, whereas the yeasts are recycled to the fermentation in order to reach high cell concentration during cultivation (Kosaric and Velikonja, 1995).

Fed batch reactor is the most employed technology in Brazil for bioethanol production due to the possibility of achieving higher volumetric productivities. For fed-batch cultures, Alfenore *et al.,* (2004) showed that higher ethanol concentrations (147 g/L) can be obtained in cultures.

Continuous processes have several advantages compared to conventional batch processes mainly due to the reduced construction costs of the bioreactors, lower maintenance and operation requirements, better process control, and higher productivities. For those reasons 30% of ethanol production facilities in Brazil comes from continuous fermentation processes (Monte Alegre *et al.,* 2003).

### *1.1.3 Innovation/advances*

Since the early 80s, plant construction costs have dropped from an average of 2.25 $ per gallon to around $1.00 per gallon. Most of this cost reduction has been the result of the small incremental improvements in the design for each new plant, the tweaking of the process, and the ability to negotiate for lower costs with suppliers because of the increasing volume.

During the 1990s the price of ethanol was fairly stable with the exception of 1995 when corn prices skyrocketed to over $5.00 per bushel (1 bushel = 25.4 kg). For a brief time, this increased feedstock cost forced ethanol plants to do everything possible to reduce other operating costs.

By the late 90s, plant capacities moved into the 20 to 30 million-gallon range, taking further advantage of economies of scale. As corn-to-ethanol conversions improved, plant sizes increased, reducing operating costs and improving the overall bottom line profits even further. Technological advancements implemented throughout the operation reduced equipment requirements, enabling plants to become more streamlined. This drove additional savings to the bottom line.

During the late 1990s and into the current decade, average capacities of new dry mills reached 40 million gallons of ethanol per year while today new plants production is 45-100 (Novozymes & BBI International, 2005).

The most important innovations used in modern ethanol plants are (National Biobased Products and Bioenergy Coordination Office, 2009):

*Molecular sieves.* If there is one predominant advancement in the ethanol industry, it is the introduction of the molecular sieve to dehydrate ethanol near absolute levels. Molecular sieve dehydration technology utilizes microporous particles such as alumino-silicates, possessing a very precise pore size. The pores make possible to separate small molecules from large ones through selective adsorption. For example, ethanol dehydration is accomplished with molecular sieves having a pore diameter of 3Å, which traps water molecules which have a diameter of 2.5Å. Ethanol molecules, which have a diameter of 4Å, cannot enter, and therefore flow around the material. Molecular sieves first entered the ethanol industry in the 1970s. The first designs utilized liquid phase separation. The advantages were the elimination of hazardous solvents and reduced distillation complexity. However, process equipment size restrictions kept liquid phase molecular sieves from making significant inroads into the ethanol industry.

Then, in the late 1980s, vapour phase molecular sieves were introduced, eliminating the capacity restraints that held back liquid phase systems. Vapour phase molecular sieve technology quickly became the system of choice for dehydration, for several reasons:

1. Elimination of cyclohexane or benzene (both carcinogenic) from the distillation process. These materials are also classified as “Hazardous Air Pollutants” so potential new regulatory requirements were avoided.
2. The elimination of one distillation column, saving as much as $250,000 per installation.
3. A reduction in the energy consumed by distillation of up to 20%.

*Thermal integration*. Engineering companies are providing turnkey services enabling a more streamlined production process and integrated energy saving technologies.

*Enzymes.* Improvements in enzyme technology and reductions in the cost of producing enzymes have lowered the price of ethanol by more than 6 cents per gallon. Enzyme manufacturers have increased enzyme production yield 5-fold in the last 15 years. Furthermore, the new enzymes are effective in hydrolyzing starches to fermentable sugars

and they no longer require the addition of lime for pH balance. Ammonia is now used, providing nutrients (nitrogen) to the yeast, and making it more effective during fermentation.

*Yeasts.* Most ethanol plants today propagate their own yeast. The practice of "pitching", which was the discarding of spent yeast and replacing it with a batch of new yeast, is no longer used. Ethanol plants that previously purchased truckloads of yeast per month now need to purchase only kilograms, primarily for propagation purposes. This has reduced the cost of yeast for ethanol production from about 1.5 cents per gallon to less than 0.5 cents per gallon.

*Automation.* Automation of the production process has been streamlined by using distributed control systems and monitoring variables in the production process to better allocate raw materials and increase overall plant efficiencies. This has resulted in reduced manpower needs.

### *1.1.4 Future of the dry grind corn ethanol industry*

BBI expects very few new ethanol plants to be built once the ones under construction are completed, due to the amount of ethanol produced and the amount of corn used. Instead, the opinion is that the future of the ethanol dry grind industry will be driven by modifications to existing plants.

The most important trend that will continue in the future is the increased use of fractionation technology in dry grind facilities. Traditionally, the starch is used to produce ethanol, and the remainder of the corn kernel ends up in the DDGS. If fractionation is carried out the corn fiber (bran) and germ (protein and oil) would be separated from the starch. Fractionation technology will reduce the amount of starch that is fermented by 3-5% due to separation losses. This operation can be done before fermentation, which increases the throughput of the fermenters, as a purer starch stream will be processed compared to a typical dry grind without fractionation. In addition, this front-end fractionation could easily yield higher value, food-grade products. The alternative is back-end fractionation, where the DDGS is further processed to remove components such as the oil that may have higher value applications than DDGS' typical use as animal feed, such as the production of biodiesel.

The separation of the fibre offers also the opportunity to produce a limited amount of cellulosic ethanol from the corn fiber. Actual production will depend on the cost of and incentives for cellulosic ethanol, and the availability of alternative markets for the fiber such as dietary fiber. If cellulosic ethanol is produced, the yield per corn mass unit could increase by up to 10%.

In parallel advances, the development of corn strains with higher starch contents are expected. Currently, corn contains about 68% starch, and it could reach 74% over the next 10 to 20 years. As a result, ethanol yields may reach over 3 gallons per bushel at 74% starch content (90% of theoretical limit) without the use of fractionation.
Technologies that reduce natural gas consumption are closer to commercialization and will continue to receive attention from the existing ethanol plants. For example, the cold cook process (raw starch hydrolysis) could reduce natural gas use by as much as 10-15%. This possibility has been demonstrated in several full-scale production plants. It combines new and novel processes and enzymes to achieve the production of ethanol without the need to gelatinize and cook the starch. Advantages include: reduced energy for cooking and subsequent cooling, better retention of yeast nutrients, and reduced dryer emissions.
Yeast strains that are able to withstand higher solids concentrations are required for “high gravity fermentation”, which can increase the concentration of ethanol to up to 25%, thus reducing energy use in the distillation process. (BBI, 2007)

## 1.2 Second generation bioethanol

The first process developed in order to obtain ethanol from wood was proposed in Germany in 1898. It used dilute acid to hydrolyze the cellulose to glucose, and was able to produce 7.6 litres of ethanol per 100 kg of wood waste (18 gal per ton). After this attempt Germans developed an industrial process optimized for yields of around 50 gallons per ton of biomass. This process, during World War I, arrived also in the United States where two commercial plants were built. These plants used a one-stage dilute sulphuric acid hydrolysis that was called "the American Process". Though the yields were half that of the original German process (25 gallons of ethanol per ton versus 50), the throughput of the American process was much higher. After the end of World War I the plants were closed but the USDA's Forest Products Laboratory (Saeman, 1945, Harris *et al.*, 1945, Conner and Lorenz, 1986) continued the research on the topic. During World War II, the US turned again to cellulosic ethanol, this time for conversion to butanediol for the production of synthetic rubber. This plant achieved an ethanol yield of 50 gal/dry ton but was still not profitable and was closed after the war (Katzen and Shell, 2006).
In the late 1970s, a renewed interest in this technology took hold in the United States because of the petroleum shortages experienced in that decade.
In the last years, the interest on cellulosic bioethanol from researchers and companies has increased due to the fluctuations of the oil price and due to environmental issues.
Volkmann (2009) identified a total of 61 active companies and entities, 3 of them went out of business, in the area of cellulosic ethanol technology and production, of which more than

75% are based in the United States of America. This might be driven by the fact that the US government has the biggest pockets for supporting R&D efforts for this technology.
Due to the fact that most of the technologies are still in the R&D phase companies just are not able to give the numbers, or these are just confidential. For this reason it is not easy to understand exactly the state of the art of the industrial processes and the preferred technological choices.
Three technologies that are presently considered:

- Acid hydrolysis
- Enzymatic process
- Biogas synthetic gas process

In Figure 1.4 the production processes are shown:

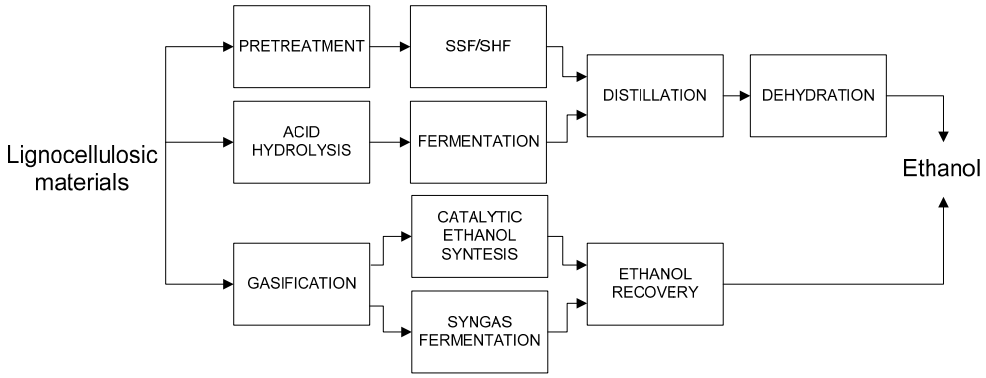


**Figure1.4** *Lignocellulosic materials to ethanol processes.*

## *1.2.1 Biochemical route*

Lignocellulosic biomass can be converted to bioethanol by hydrolysis of the polymeric sugars and subsequent fermentation. Acid hydrolysis and enzymatic hydrolysis differ in the way to hydrolyse polysaccharides to monomeric sugars, downstream the processes are similar.

### 1.2.1.1 Acid hydrolysis

Biomass can be hydrolyzed using different acids to produce xylose, arabinose, glucose, and acetic acid by cleavage of the β-1,4 linkage of glucose or xylose monomers, acetyl groups, and other products in cellulose and hemicellulose components of biomass. The overall fermentable sugar available by acid hydrolysis may be up to 90% of the theoretical value of the sugar present in cellulosic biomass (Lavarack *et al.,* 2002).
Dilute acid processes are carried out under high temperatures (120 to 200 °C) and high pressures (15 psi to 75 psi), and have reaction times in the range of 30 min to 2 h by

continuous processes (Kim *et al.,* 2002). The concentrated acid processes have been somewhat more successful, producing higher sugar yields. These processes typically involve the use of 60 to 90% sulphuric acid, mild temperatures, and moderate pressures. The primary advantage of the concentrated acid process is the high sugar recovery efficiency, which can be larger than 90% for both xylose and glucose sugars (Badger, 2002). The concentrated acid disrupts the hydrogen bond between cellulose chains, converting it to a completely amorphous state. Once cellulose has been decrystallized, it forms a homogeneous gel with the acid (Faraone and Cuzens, 1996). Some researchers used nitric acid and phosphoric acid at varying concentrations, reaction time, and temperature to hydrolyze the sugar cane bagasse (Rodríguez-Chong *et al.,* 2004). Hydrochloric acid was found to be less effective for degradation of xylose than sulphuric acid (Lavarack *et al.,* 2002).

Acid hydrolysis processes have a main disadvantage due to the formation of toxic compounds, such as furfural, hydroxylmethylfurfural (HMF), acetic acid, formic acid, levulinic acid etc., which inhibit the fermentation. Removal of these compounds increases the additional costs. The use of lime to neutralize acid has the disadvantage of significant loss of sugar in gypsum. These disadvantages have lead to an increased interest in using enzymes.

#### 1.2.1.2 Enzymatic hydrolysis

Hydrolysis of cellulose to glucose in aqueous media catalyzed by the cellulase enzyme suffers from slow reaction rates due to the highly crystalline structure of cellulose which makes the penetration of enzymes to the active sites very difficult (Dadi *et al.,* 2006). Therefore, a pretreatment step (Figure 1.4) is necessary for obtaining the maximum yield of sugars by enzymatic hydrolysis (Mosier *et al.,* 2005). Typically, enzymatic hydrolysis sugar yields are less than 20% of theoretical quantity without pretreatment, whereas more than 90% of theoretical quantity is obtained with pretreatment (Ghosh and Ghose, 2003).

Both bacteria and fungi can produce cellulases for the hydrolysis of lignocellulosic materials. These microorganisms can be aerobic or anaerobic, mesophilic or thermophilic. Bacteria belonging to *Clostridium, Cellulomonas, Bacillus, Thermomonospora, Ruminococcus, Bacteriodes, Erwinia, Acetovibrio, Microbispora, and Streptomyces* can produce cellulases (Sun, 2002). Enzymatic hydrolysis is a promising alternative that generally provides hydrolysates with a lower inhibitory impact on the fermentation step, but it is more expensive than chemical hydrolysis (Pongsawatmanit *et al.*, 2007) due to the high cost of enzymes. On the other hand the use of enzymes holds several advantages, such as the quite high efficiency, low by-product formation, less expensive materials for construction due to mild process conditions, and low process energy requirement (Yu *et al.,* 2003).

If the enzymatic hydrolysis is performed simultaneously with the fermentation the process is called Simultaneous Saccharification and Fermentation (SSF); otherwise, if two different reactors are used it is named Separate Hydrolysis and Fermentation (SHF).
The enzymes cellulases (endoglucanase, exoglucanase, and β-glucosidase) responsible for enzymatic hydrolysis of pretreated cellulosic biomass are strongly inhibited by the hydrolysis products (glucose, xylose, cellobiose, and other oligosaccharide). Simultaneous saccharification and fermentation (SSF) plays an effective role to overcome enzyme inhibition. SSF combines enzymatic hydrolysis with ethanol fermentation to keep low the concentration of glucose. The accumulation of ethanol in the fermenter does not inhibit cellulases as much as high concentrations of glucose, so SSF is a good strategy for increasing the overall rate of cellulose to ethanol conversion.
A drawback of SSF is that the optimum conditions for the cellulases and micro-organisms differ to some extent. The difference in optimal pH is small, but the temperature optimum differs more. A micro-organism such as *Saccharomyces cerevisiae* limits the reaction temperature to below 40 °C, which is lower than the temperature of highest cellulases activity.
Most scientific papers about experimental investigation on lignocellulosic bioethanol are concentrated on the pretreatment. This is so because the first process step has large influence on the following ones and every raw materials show different behaviour and optimal condition. The aim of a pre-treatment is the decrease of cellulose crystallinity by removal of hemicelluloses and lignin as well as the increase of cellulose porosity. But it is important to remember that the real goal is not the complete solubilization of the biomass rather it is obtain the best hydrolysable suspension and best fermentable mixture: therefore reactions of mono-sugars to degradation products have to be avoided.

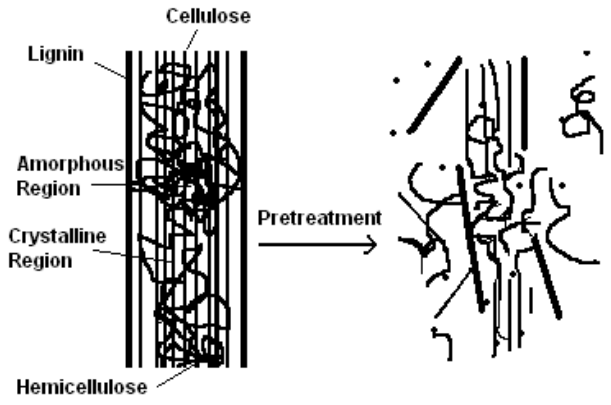


**Figure 1.5** *Effect of the pretreatment (Mosier et al., 2005).*

In Figure 1.5 the effect of the pretreatment on the biomass is shown while in Figure 1.6 the chemical routes to the degradation products are clarified.

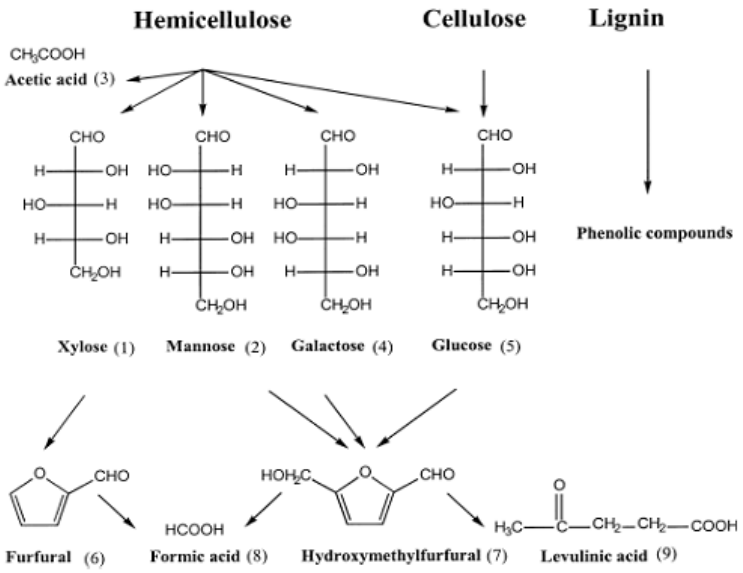


**Figure 1.6** *Compounds obtainable from the pretreatment and following transformation into degradation products (Palmqvist and Häagerdal, 2000).*

Pretreatments may be either of physical or chemical type. Physical pretreatment methods include comminution, steam explosion, and hydrothermolisys, while chemical ones refer to the use of chemical agents (steam and water are excluded). The most commonly acid and base used to promote hydrolysis are $H_2SO_4$ and NaOH respectively; they improve the yield of glucose recovery from cellulose by removing hemicellulose or lignin. Alkaline $H_2O_2$ (Saha and Cotta, 2006), ozone, organosolv (Berlin *et al.*, 2006, Ewanick *et al.*, 2007), glycerol (Sun and Chen, 2008) dioxane, phenol or ethylene glycol are cellulose solvers. However only some pretreatments are cost effective, among them those using: steam explosion, liquid hot water (Lynd, 1996), diluited acid (Ewanick *et al.,* 2007), Balat et *al.*, 2008), lime and ammonia (Balat *et al.*, 2008).

Steam explosion: is the most commonly used method (McMillan, 1994). The chipped biomass is treated with high-pressure saturated steam and then the pressure is swiftly reduced, thus making the materials undergo an explosive decompression. Steam explosion is typically initiated at a temperature of 160–260 °C (corresponding pressure 0.69–4.83 MPa) for several seconds to a few minutes before the material is exposed to atmospheric pressure. The process causes hemicellulose degradation and lignin transformation due to high temperature. Ninety percent efficiency of enzymatic hydrolysis has been achieved in 24 h for poplar chips pretreated by steam explosion, compared to only 15% hydrolysis of untreated hips (Grous *et al.*, 1986). Addition of $H_2SO_4$ (or $SO_2$) or $CO_2$ in steam explosion can effectively improve enzymatic hydrolysis, decrease the production of inhibitory compounds, and lead to more complete removal of hemicellulose (Morjanoff and Gray,

1987). Steam explosion is recognized as one of the most cost effective pretreatment processes for hardwoods and agricultural residues, but it is less effective for softwoods (Clark and Mackie, 1987). It increases the surface area and the removes hemicellulose while only a minor effect is exerted to the lignin structure. An advantage of this pretreatment is the relatively low dilution of the sugars.
Limitations of steam explosion include destruction of a portion of the xylan fraction, incomplete disruption of the lignin–carbohydrate matrix, and generation of compounds that may be inhibitory to microorganisms used in downstream processes (Mackie *et al.*, 1985). Because of this fact, pretreated biomass needs to be washed by water to remove the inhibitory materials along with water-soluble hemicellulose (McMillan, 1994). Typically, 20–25% of the initial dry matter is removed by water wash with a decrease in the overall saccharification yields (Mes-Hartree *et al.*, 1988).

Ammonia fiber explosion (AFEX): is another type of physico-chemical pretreatment. Lignocellulosic materials are exposed to liquid ammonia at high temperature and pressure for a period of time, and then the pressure is swiftly reduced. The concept of AFEX is similar to steam explosion. In a typical AFEX process, the dosage of liquid ammonia is 1–2 kg ammonia/kg dry biomass, temperature is 90 °C, and residence time 30 min.
The AFEX pretreatment does not significantly solubilise hemicellulose compared to acid pretreatment and acid-catalyzed steam explosion (Mes-Hartree *et al.*, 1988; Vlasenko *et al.*, 1997). It turned out not to be very effective for the biomass with high lignin content such as newspaper (18–30% lignin) and aspen chips (25% lignin). Hydrolysis yield of AFEX-pretreated newspaper and aspen chips was reported as only 40% and below 50%, respectively (McMillan, 1994). The ammonia pretreatment does not produce inhibitors for the downstream biological processes, so a water wash step is not necessary (Dale *et al.*, 1984; Mes-Hartree *et al.*, 1988).

Dilute acid hydrolysis: has been successfully developed for pretreatment of lignocellulosic materials. The dilute sulphuric acid pretreatment can achieve high reaction rates and significantly improve cellulose hydrolysis (Esteghlalian *et al.*, 1997). At moderate temperature, direct saccharification suffered from low yields because of sugar decomposition. There are primarily two types of dilute acid pretreatment processes: high temperature (T > 160 °C), a continuous-flow process for low solids loading (5– 10% weight of substrate/weight of reaction mixture) (Brennan *et al.*, 1986; Converse *et al.*, 1989), and low temperature (T < 160 °C), a batch process for high solids loading (10–40%) (Cahela *et al.*, 1983; Esteghlalian *et al.*, 1997). Although dilute acid pretreatment can significantly improve the cellulose hydrolysis, its cost is usually higher than some physico-chemical

pretreatment processes such as steam explosion or AFEX. A neutralization of pH is necessary for the downstream enzymatic hydrolysis or fermentation processes.
Alkaline pretreatments: can also be used for conditioning of lignocellulosic materials; their effect depends on the lignin content of the materials (Fan *et al.*, 1987; McMillan, 1994). The mechanism of alkaline hydrolysis is believed to be saponification of intermolecular ester bonds crosslinking xylan hemicelluloses and other components (for example lignin and other hemicellulose). The porosity of the lignocellulosic materials increases with the removal of the cross links (Tarkow and Feist, 1969). Dilute NaOH treatment of lignocellulosic materials caused swelling, leading to an increase in internal surface area, a decrease in the degree of polymerization, and in crystallinity, the separation of structural linkages between lignin and carbohydrates, and disruption of the lignin structure (Fan *et al.,* 1987). The digestibility of NaOH-treated hardwood increased from 14% to 55%, with the decrease of lignin content from 24–55% to 20%. However, no effect of dilute NaOH pretreatment was observed for softwoods with lignin content greater than 26% (Millet *et al*., 1976).

Organosolv process: uses, an organic or aqueous organic solvent mixture with inorganic acid catalysts (HCl or $H_2SO_4$) to break the internal lignin and hemicellulose bonds (Berlin *et al.*, 2006, Ewanick *et al.,* 2007). The organic solvents that can be utilized in the process include methanol, ethanol, acetone, ethylene glycol, triethylene glycol and tetrahydrofurfuryl alcohol (Chum *et al.*, 1988; Thring *et al.*, 1990). Organic acids such as oxalic, acetylsalicylic and salicylic acid can also be used as catalysts (Sarkanen, 1980). At high temperatures (above 185 °C), the addition of catalyst was unnecessary for satisfactory delignification (Sarkanen, 1980; Aziz and Sarkanen, 1989). Usually, a high yield of xylose can be obtained by adding acids. Solvents used in the process need to be drained from the reactor, evaporated, condensed and recycled to reduce the cost. Removal of solvents from the system is necessary because the solvents may be inhibitory to the growth of organisms, enzymatic hydrolysis, and fermentation.

Liquid hot water (LHW): involves the use of water at high temperature and pressure without any addition of chemicals. LHW has been reported to have the potential to enhance cellulose digestibility, sugar extraction, and pentose recovery, with the advantage of producing prehydrolysates containing little or no inhibitor of sugar fermentation. (Zheng *et al.,* 2009). Nevertheless, solid load is much less than for steam explosion, which is usually greater than 50%. Negro *et al.,* (2003) compared steam explosion and LHW pretreatments for poplar biomass and showed best results for the latter at 210 C during 4 min (Sanchez and Cardona, 2008). A detailed description of the effect of this pretreatment is reported in Chapter 7.

#### 1.2.1.3 Fermentation

Biomass fibre contains two principal sugars sources: cellulose and hemicellulose. The hemicellulose layer in plant fibres is a complex structure of both 5-carbon and 6-carbon sugars. The problem for utilizing the pentose potential is that the commonly used yeast strains, *S. cerevisiae*, are unable to convert C5 sugars. In order to obtain a commercially acceptable conversion of plant fibre into ethanol, the sugar potential in the hemicellulose fraction must be exploited. A limited number of bacteria, yeasts, and fungi can convert hemicellulose or its monomers (xylose, arabinose, mannose, and galactose) into ethanol with a satisfactory yield and productivity. The ethanol yield ranges from 20 to 51% of the substrate weight (Murphy and McCarthy, 2005). Consequently, most research efforts have been devoted to the development of efficient microorganisms that are capable to ferment glucose and xylose separately or simultaneously. In recent years, metabolic engineering concepts have been used for the production of fuel ethanol. Ethanologenic recombinant bacteria such as *Escherichia coli*, *Klebsiella oxytoca*, and *Zymomonas mobilis* and the yeast *Saccharomyces cerevisiae* were successfully used in fermentation of mixed sugars obtained from biomass containing glucose, xylose, arabinose, and galactose to produce ethanol (Bothast *et al.*, 1999). An alternative option fraction could be transform the hemicellulose into other products such as furfural, xylitol or other chemicals.

### *1.2.2 Thermochemical route*

The gasification process does not rely on chemical decomposition of the cellulose chain (cellulolysis). Instead of breaking the cellulose into sugar molecules, the carbon in the raw material is converted into synthesis gas.
Biomass gasification reaction is:

$$C + H_2O \rightarrow CO + H_2 \qquad (1.1)$$

This method is particularly important because up to one third of cellulosic biomass (the lignin-rich parts) cannot be easily converted biochemically. The carbon monoxide, carbon dioxide and hydrogen can then be fed into a special kind of fermenter using a microorganism named *Clostridium ljungdahlii* (Rajagopalan *et al.*, 2002) (Coskata Technology) or converted by a catalytic process. Numerous efforts have been made since then to develop commercially viable thermochemical-to-ethanol processes. Ethanol yields up to 50% have been obtained. Some processes that first produce methanol and then use catalytic shifts to ethanol have gained ethanol yields in the range of 80%. Unfortunately, like for other processes, a cost effective thermochemical route is difficult to find (Balat and Balat, 2009).

### 1.2.3 Existing second generation ethanol plant

The work of Volkmann (2009) was based on literature information or web ones but the analysis showed that about 47 plants are planned or under construction and 20 are already operating (Table 1.1). Very recently, an Italian company (Mossi & Ghisolfi) announced that a 200,000 t/y bioethanol plant is going to be started in 2010 (Ghisolfi, 2009).

**Table 1.1** *Second generation ethanol operating plants (Volkmann, 2009).*

| Company | Country | Plant location | Capacity [$m^3$/y] | Process type | Feedstock |
|---|---|---|---|---|---|
| AE Biofuels | USA | Montana | 567 | Enzymatic hydr. | Corn/corn stover |
| Blue Fire Ethanol | USA | Izumi, JP | - | Enzymatic hydr. | Wood waste |
| Chempolis Oy | FIN | Oulu, Finland | - | Acidic acid hydr. | Straw, reeds, corn stem and bagasse |
| Enerkem | CAN | Quebec | 4,921 | Syngas to ethanol | Treated wood |
| Gulf Coast energy | USA | Florida | 94,635 | Gasification | Woody biomass |
| IOGEN | CAN | Ontario | 2,000 | Enzymatic hydr. | Wheat, oat and barely straw |
| KL Energy | USA | Wyoming | 5,678 | Not acid pretr. | Wood |
| Lignol Energy | CAN | Vancouver | - | Enzymatic hydr. | Wood |
| Mascoma | USA | New York | 1,892 | Enzymatic hydr. | Wood chip, corn stover, bagasse |
| POET | USA | S. Dakota | 75 | | Corn cobs |
| Range Fuels | USA | Colorado | pilot | Gasification | 30 non food feedstocks |
| Sekab | SWE | Sweden | - | | Wood chips |
| ST1 | FIN | Lappeenranta | 1,000 | Fermentation | Food dough |
| ST1 | FIN | Hamina | 1,000 | Fermentation | Bakery waste |
| ST1 | FIN | Närpiö | 1,000 | Fermentation | Potato flake |
| St. Petersburg State Forest Technical Academ. | RUS | 13 plants in Russia | - | - | wood |
| SunOpta | Can | China | - | Enzymatic hydr. | Corn Stover |
| Univ. Of Florida | - | - | - | Waste material | - |
| Verenium | USA | Louisiana | 5,300 | - | Bagasse, energy cane |
| Verenium | USA | Japan | 4,920 | - | Wood constr. waste |

Acronyms:
DDGS: Distiller's Dried Grains with Solubles
DGP: Dry grind process
HMF: hydroxylmethylfurfural
LHW: Liquid hot water

## 1.3 References

Akiya, N. and P.E. Savage (2002). Roles of Water for Chemical Reactions in High-Temperature Water. *Chem. Rev*., **102,** 2725-2750.

Alfenore, S., X. Cameleyre, L. Benbadis, C. Bideaux, J.L. Uribelarrea, G. Goma, C. Molina-Jouve, and S.E. Guillouet (2004). Aeration Strategy: a Need for Very High Ethanol Performance in Saccharomyces cerevisiae Fed-batch Process. *Appl. Microbiol. Biotechnol.,* **63**, 537-542.

Aziz, S. and K. Sarkanen (1989). Organosolv Pulping – a Review. *Tappi. J.,* **72**, 169–175.

Badger, P.C. (2002). *Trends in New Crops and New Uses* (J. Janick, A. Whipkey Eds.), ASHS Press, Alexandria, VA (U.S.A.).

Balat, M. and H. Balat (2009). Recent Trends in Global Production and Utilization of Bio-ethanol Fuel. *Appl. Energy,* **86**, 2273-2282.

Balat, M., H. Balat, and C. Öz (2008). Progress in Bioethanol Processing. *Prog. Energy Combust. Sci.*, **34**, 551-573.

BBI International (2009). *The U.S. Dry Mill Ethanol Industry*. Available at: http://www.brdisolutions.com/ [Accessed June 2009].

Berlin, A., V. Maximenko, R. Bura, K.Y. Kang, N. Gilkes, and J. Saddler (2006). A Rapid Microassay to Evaluate Enzymatic Hydrolysis of Lignocellulosic Substrates. *Biotechnol. Bioeng.*, **93,** 880-886.

Biofuels Platform (2009). *Production of Biofuels in the World in 2008*. Available at: http://www.biofuels-platform.ch/en/infos/production.php?id=bioethanol [Accessed June 2009].

Bothast, R.J., N.N. Nichols, and B.S. Dien (1999). Fermentations With New Recombinant Organisms. *Biotechnol. Prog.*, **15**, 867-875.

Brennan, A.H., W. Hoagland, and D.J. Schell (1986). High Temperature Acid Hydrolysis of Biomass Using an Engineering-scale Plug Flow Reactor: Result of Low Solids Testing. *Biotechnol. Bioeng. Symp.*, **17**, 53-70.

Buhler, W., E. Dinjus, H.J. Ederer, A. Kruse, and C. Mas (2002). Ionic Reactions and Pyrolysis of Glycerol as Competing Reaction Pathways in Near- and Supercritical Water. *J. Supercrit. Fluids,* **22**, 37-53.

Cahela, D.R., Y.Y. Lee, and R.P. Chambers (1983). Modeling of Percolation Process in Hemicellulose Hydrolysis. *Biotechnol. Bioeng.,* **25**, 3-17.

Chum, H.L., D.K. Johnsoon, and S. Black (1988). Organosolv Pretreatment for Enzymatic Hydrolysis of Poplars: 1. Enzyme Hydrolysis of Cellulosic Residues. *Biotechnol. Bioeng.,* **31**, 643-649.

Clark, T.A. and K.L. Mackie (1987). Steam Explosion of the Soft-wood Pinus radiata with Sulphur Dioxide Addition. I. Process optimization. *J. Wood Chem. Technol.,* **7,** 373-403.

Conner, A.H. and L.F. Lorenz (1986). Kinetic Modeling of Hardwood Prehydrolysis. Part III. Water and Dilute Acetic Acid Prehydrolysis of Southern Red Oak. *Wood Fiber Sci.*, **18**, 248–263.

Converse, A.O., I.K. Kwarteng, H.E. Grethlein, and H. Ooshima (1989). Kinetics of thermochemical pretreatment of lignocellulosic materials. *Appl. Biochem. Biotechnol*., **20/21**, 63–78.

Dadi, A.P., S. Varanasi, and C.A. Schall (2006). Enhancement of Cellulose Saccharification Kinetics Using an Ionic Liquid Pretreatment Step. *Biotechnol. Bioeng.,* **95,** 904-910.

Dale, B.E., L.L. Henk, and M. Shiang (1984). Fermentation of Lignocellulosic Materials Treated by Ammonia Freeze-explosion. *Dev. Ind. Microbiol*., **26**, 223-233.

Esteghlalian, A., A.G. Hashimoto, J.J. Fenske, and M.H. Penner (1997). Modeling and Optimization of the Dilute-sulfuric-acid Pretreatment of Corn Stover, Poplar and Switchhgrass. *Bioresour. Technol*., **59**, 129-136.

European biofuel association (2009). *The EU market Production and Consumption*. Available at: http://www.ebio.org/EUmarket.php [Accessed September 2009].

Ewanick, S.M., R. Bura, and J.N. Saddler (2007). Acid-catalyzed Steam Pretreatment of Lodgepole Pine and Subsequent Enzymatic Hydrolysis and Fermentation to Ethanol. *Biotechnol. Bioeng.*, **98**, 737-746.

Fan, L.T., M.M. Gharpuray, and Y.H. Lee (1987). *Cellulose Hydrolysis (biotechnology monographs, Vol. 3)*, Springer, Berlin (Germany).

Farone, W.A. and J.E. Cuzens (1996). *Method of Producing Sugars Using Strong Acid Hydrolysis of Cellulosic and Hemicellulosic materials*. US Patent 5 562 777.

Ghisolfi, G. (2009). Biocarburanti. Vale la Pena? Presented at: *2°Bio-ethanol Conference*, *Etanolo di seconda generazione: una realtà possibile*, Milano (Italy), March 4.

Ghosh, P. and K.T. Ghose (2003). Bioethanol in India: Recent Past and Emerging Future, *Adv. Biochem. Eng./Biotechnol.*, **85**, 1-27.

Grous, W.R., A.O. Converse, and H.E. Grethlein (1986). Effect of Steam Explosion Pretreatment on Pore Size and Enzymatic Hydrolysis of Poplar. *Enzyme Microb. Technol.* **8**, 274-280.

Harris, E.E., E. Beglinger, G.J. Hajny, and E.C. Sherrard (1945). Hydrolysis of Wood: Treatment with Sulfuric Acid in a stationary digester. *Ind. Eng. Chem*., **37**, 12–23.

Katzen, R. and J. Schell (2006). Lignocellulosic feedstock Biorefinery: History and Plant Development for Biomass Hydrolysis. In: *Biorefineries - Industrial Processes and Products*, (B. Kamm, P.R. Gruber, and M. Kamm, Eds.) Wiley-VCH, Weinheim (Germany).

Kim, K. H., M.P. Tucker and Q.A. Nguyen (2002). Effects of Pressing Lignocellulosic Biomass on Sugar Yield in Two-stage Dilute-acid Hydrolysis Process. *Biotechnol. Prog.*, **18**, 489-494.

Kosaric, N. and J. Velikonja (1995). Liquid and Gaseous Fuels from Biotechnology: Challenge and Opportunities. *FEMS Microbiol. Rev.*, **16**, 111-142.

Kruse, A. and E. Dinjus (2007). Hot Compressed Water as Reaction Medium and Reactant: Properties and Synthesis Reactions. *J. Supercrit. Fluids*, **39,** 362-380.

Lavarack, B.P., G.J. Griffin, and D. Rodman (2002). The Acid Hydrolysis of Sugarcane Bagasse Hemicellulose to Produce Xylose, Arabinose, Glucose and Other Products. *Biomass Bioenergy,* **23,** 367-380.

Licht, F.O. (2006). *World Ethanol and Biofuels Report*, vol. 4, no. 17.

Lynd, R.L. (1996). Overview and Evaluation of Fuel Ethanol from Cellulosic Biomass: Technology, Economics, the Environment, and Policy, *Annu. Rev. Energy Environ.*, **21**, 403-465.

Mackie, K.L., H.H. Brownell, K.L. West, and J.N. Saddler (1985). Effect of Sulphur Dioxide and Sulphuric Acid on Steam Explosion of Aspenwood. *J. Wood Chem. Technol.,* **5**, 405-425.

McMillan, J.D. (1994). Pretreatment of Lignocellulosic Biomass. In: *Enzymatic Conversion of Biomass for Fuels Production*, (M.E. Himmel, J.O. Baker and R.P. Overend, Eds.), American Chemical Society Washington, DC.

Mes-Hartree, M., B.E. Dale, and W.K. Craig (1988). Comparison of Steam and Ammonia Pretreatment for Enzymatic Hydrolysis of Cellulose. *Appl. Microbiol. Biotechnol.,* **29**, 462–468.

Millet, M.A., A.J. Baker, and L.D. Scatter (1976). Physical and Chemical Pretreatment for Enhancing Cellulose Saccharification. *Biotech. Bioeng. Symp.,* **6**, 125–153.

Monte Alegre, R., M. Rigo, and I. Joekes (2003). Ethanol Fermentation of a Diluted Molasses Medium by Saccharomyces Cerevisiae Immobilized on Chrysotile. *Braz. Arch. Biol. Technol.*, **46**, 751–757.

Morjanoff, P.J. and P.P. Gray (1987). Optimization of Steam Explosion as Method for Increasing Susceptibility of Sugarcane Bagasse to Enzymatic Saccharification. *Biotechnol. Bioeng.* **29**, 733–741.

Mosier, N., C. Wyman, B. Dale R. Elander, Y.Y. Lee, M. Holtzapple, and M. Ladisch (2005). Features of Promising Technologies for Pretreatment of Lignocellulosic Biomass. *Bioresour. Technol.,* **96,** 673–686.

Murphy, J. D. and K. McCarthy (2005). Ethanol Production from Energy Crops and Wastes for Use as a Transport Fuel in Ireland. *Appl. Energy*, **82**, 148-166.

National Biobased Products and Bioenergy Coordination Office (2009). *The U.S. Dry Mill Ethanol Industry*. Available at: http://www.brdisolutions.com/pdfs/drymill_ethanol_industry.pdf [Accessed 29 December 2009].

Negro, M.J., P. Manzanares, I. Ballesteros, J.M. Oliva, A. Cabanas, and M. Ballesteros (2003). Hydrothermal Pretreatment Conditions to Enhance Ethanol Production from Poplas Biomass. *Appl. Biochem. Biotechnol.* **105–108**, 87–100.

Novozymes & BBI International (2005). *Fuel Ethanol, a Technological Evolution*. Available at: http://www.ethanolrfa.org/objects/documents/76/fuelethanol-lr-05.pdf [Accessed 29 December 2009].

Palmqvist, E. and B.H. Hägerdal (2000). Fermentation of Lignocellulosic Hydrolysates. II: Inhibitors and Mechanisms of Inhibition. *Bioresour. Technol.,* **74**, 25-33.

Pongsawatmanit, R., T. Temsiripong, and T. Suwonsichon (2007). Thermal and Rheological Properties of Tapioca Starch and Xyloglucan Mixtures in the Presence of Sucrose. *Food Res. Int.,* **40**, 239-248.

Rajagopalan, S., R.P. Datar, and R.S. Lewis (2002). Formation of Ethanol from Carbon Monoxide Via a New Microbial Catalyst. *Biomass Bioenergy*, **23**, 487–493.

Renewable fuel association (2008). *Statistics*. Available at: http://www.ethanolrfa.org/industry/statistics/ [Accessed 17 November 2009].

Rodríguez-Chong, A., J.A. Ramírez, G. Garrote, and M. Vázquez (2004). Hydrolysis of Sugar Cane Bagasse Using Nitric Acid: a Kinetic Assessment. *J. Food Eng.,* **61,** 143-152.

Saeman, J.F. (1945). Kinetics of Wood Saccharification: Hydrolysis of Cellulose and Decomposition of Sugars in Dilute Acid at High Temperature. *Ind. Eng. Chem.*, **37**, 43–52.

Saha, B. C. and M. A. Cotta (2006). Ethanol Production from Alkaline Peroxide Pretreated Enzymatically Saccharified Wheat Straw. *Biotechnol. Prog.,* **22**, 449-453.

Sánchez, Ó.J. and C.A. Cardona (2008). Trends in Biotechnological Production of Fuel Ethanol from Different Feedstocks. *Bioresour. Technol*, **99,** 5270–5295.

Sarkanen, K.V., (1980). Acid-catalyzed Delignification of Lignocellulosics in Organic Solvents. *Prog. Biomass Convers.,* **2**, 127–144.

Sun, F. and H. Chen (2008). Comparison of Atmospheric Aqueous Glycerol and Steam Explosion Pretreatments of Wheat Straw for Enhanced Enzymatic Hydrolysis. *J. Chem. Technol. Biotechnol.,* **83,** 707-714.

Sun, Y., (2002). Enzymatic Hydrolysis of Rye Straw and Bermuda Grass for Ethanol Production. *PhD thesis*, Biological and Agricultural Engineering, North Carolina State University.

Tarkow, H. and W.C. Feist (1969). A Mechanism for Improving the Digestibility of Lignocellulosic Materials with Dilute Alkali and Liquid $NH_3$, In: *Advance Chemistry Series 95*, American Chemical Society, Washington, DC.

Vlasenko, E.Y., H. Ding, J.M. Labavitch, and S.P. Shoemaker (1997). Enzymatic Hydrolysis of Pretreated Rice Straw. *Bioresour. Technol*., **59**, 109–119.

Volkmann, D. (2009). Lignocellulosic Ethanol: Competitors in the Market and Technologies to Convert Biomass to Sugar, Presented at: *17th European Biomass Conference & Exhibition,* Hamburg (Germany), July 29 – August 3.

Wang, S., K. Sosulski, F. Sosulski, and M. Ingledew (1997). Effect of Sequential Abrasion on Starch Composition of Five Cereals for Ethanol Fermentation. *Food Res. Int.,* **30**, 603–609.

Wheals, A.E., L.C. Basso, D. M.G. Alves, and H.V. Amorim (1999). Fuel Ethanol After 25 Years. *Trends in Biotechnology*, **17**, 482-487.

Wilkie, A.C., K.J. Riedesel, and J.M. Owens (2000). Stillage Characterization and Anaerobic Treatment of Ethanol Stillage from Conventional and Cellulosic Feedstocks. *Biomass Bioenergy*, **19**, 63–102.

Wyman, C. E. (1996) *Handbook On Bioethanol: Production And Utilization: Production & Utilization.* Taylor & Francis, Washington, DC (U.S.A.).

Yu, J., A.B. Corripio, O.P. Harrison, and R.J. Copeland (2003). Analysis of the Sorbent Energy Transfer System (SETS) for Power Generation and $CO_2$ Capture. *Adv. Environ.,* **7**, 335–345.

Zhan, X., D. Wang, M.R. Tuinstra, S. Bean, P.A. Seib, and X.S. Sun (2003). Ethanol and Lactic Acid Production as Affected by Sorghum Genotype and Location. *Ind. Crops Prod.*, **18**, 245–255.

Zheng, Y., Z. Pan, and R. Zhang (2009). Overview of Biomass Pretreatment for Cellulosic Ethanol Production. *Int. J. Agric. & Biol. Eng.*, **2**, 51-68.

# Chapter 2

# First generation ethanol: a technical and economical assessment based on different scenarios[1]

In the first part of this Chapter process simulation is used to represent a "standard" dry grind production process which is presented in details together with the Aspen Plus™ model. The second part deals with the energy optimization of the dry grind process and the results of some key sensitivities on main process variables. This simulation work permitted to obtain the base input information for the economical and financial analysis carried out by another PhD student. The aim of the whole work was to provide a snapshot on the present business situation and to evaluate a number of potential short-term scenarios.

## 2.1 Introduction

In Italy, although ethanol has a long tradition in the beverage industry (i.e. wine and spirits), it is not clear when the production of ethanol as biofuel will start. Corn will be the obvious choice as a raw material, considering the very high yield which can be obtained in Northern Italy (10-14 t/ha). The ethanol production from corn is definitely a mature process, but its optimisation potential and economics have become a real issue only very recently, i.e. as soon as the production scale has dramatically increased and has determined great price variability. Since the bioethanol production energy costs are second only to the raw material costs, the industry has continued to improve its energy efficiency profile (e.g., U.S. E.P.A, 2006) and to assess new technological solutions for heat and power generation (Morey *et al.*, 2006). The use of process simulators (e.g., Kwiatkowski *et al.,* 2006) and optimisation techniques (Peschel *et al.,* 2006) has recently been applied to assess new processing alternatives and products from starch-based commodities.

## 2.2 The Dry Grind Process (DGP)

The DGP roughly comprises five main sections:

[1] Part of this Chapter has been published in: *Chem. Eng. Res. Des.,* (see Page XV).

1. Grinding, Cooking and Liquefaction
2. Saccharification and Fermentation
3. Distillation and Dehydration
4. Water evaporation and recycling
5. Drying of the non-fermentable fraction

The base case nominal feed capacity of the plant is assumed to be approximately 41,900 kg/h of corn. Table 2.1 shows the simplified composition of corn used in the simulation model; note that proteins and lipids are not accounted for, although essential components of the DDGS, because they are not relevant to the present study.

**Table 2.1** *Corn composition used in simulation.*

| Component | Mass fraction |
|---|---|
| Water | 0.150 |
| Xylose | 0.062 |
| Starch | 0.595 |
| Hemicellulose | 0.131 |
| Cellulose | 0.057 |
| Lignin | 0.005 |

In section 1, the corn is milled down to the proper particle size (< 2 mm) in order to facilitate the subsequent penetration of water, and is sent to a slurry tank together with approximately 77,000 kg/h of process water. The slurry is "cooked" by using steam at 4 bar: the process temperature (110 °C) allows sterilisation of the slurry and breaks the starch hydrogen bonds so that water can be absorbed (the starch granules swell and increase the surface area). This step is termed gelatinisation because the resulting mixture has a highly viscous, gelatinous consistency.

The liquefaction step (85 °C) is accomplished by the action of α−amylase enzyme on the exposed starch molecules. Alpha-amylase is added at 0.082% (dry basis with respect to corn): the effect is a random breakage of the α−1,4 glucosidic amylose and amylopectin linkages, thus decreasing the viscosity. The mash from the liquefaction vessel is added to a backset stream (described in the following) and cooled down to 35 °C, ready for the fermentation step.

In section 2, a simultaneous saccharification and fermentation occurs (SSF): starch oligosaccharides are almost completely hydrolysed (99%) into glucose molecules by glucoamylase enzyme (added at 0.11% db) and *Saccharomices cerevisiae* yeasts catalyse the reaction:

$$C_6H_{12}O_6 \rightarrow 2\ C_2H_5OH + 2\ CO_2 \quad (2.1)$$

with a glucose conversion of about 97%.

The outlet stream from the fermenter (beer) contains also small quantities of several secondary products such as acetaldehyde, methanol, butanol, acetic acid, and glycerol. Our simulation model considers only the last two species, obtained through the reaction:

$$2\ C_6H_{12}O_6 + H_2O \rightarrow C_2H_4O_2 + 2\ C_3H_8O_3 + CH_3CH_2OH + 2\ CO_2 \quad (2.2)$$

Note that a large amount of carbon dioxide is also produced (about 13,100 kg/h): most part of which is immediately purged; the rest is supposed to be removed in a degasser drum after heating the beer prior to the distillation section (discussed in the following). Since the gas purge stream is not free of ethanol, an absorption column is used to recover it and clean the gas before venting. The scrubbing water is recycled upstream to the slurry tank.
It is assumed that the distillation (section 3) involves three columns: the fermentation broth is split into two streams fed to two stripping columns at different pressure conditions (1.7 and 0.5 bar). The distillate products (with an ethanol content of about 50% by weight) are sent to the final rectifying column (working at 5 bar). This last unit is designed to obtain a 92% w/w ethanol purity in the distillate, so that a molecular sieve section downstream can dehydrate ethanol up to required fuel grade (99.8%).
The condensing heat of the rectifier column supplies the energy demand of the 1.7 bar stripping column reboiler; in cascade, the heat of condensation of the distillate in this latter column is exploited to boil up the bottoms of the vacuum stripping column.
In section 4 the non fermentable products of the feedstock (known as whole stillage), consisting of suspended grain solids, dissolved materials (both solids and liquids) and water, are sent to a centrifuge where a wet cake (35% of solids by weight) and a thin stillage (8% of solids by weight) are obtained. Part of this last stream (19,450 kg/h) is recycled as backset, while the rest is sent to a multiple-effect evaporator. Here it is concentrated up to a final solid content of 35% by weight (syrup). The syrup and the wet cake are mixed together and dried up to produce the DDGS, with a moisture content of about 10%, suitable for animal feeding. The natural gas consumption for the DDGS drying is calculated as 1,125 kg/h. In Figure 2.1 and 2.2 the Aspen Plus$^{TM}$ flow sheet of the plant simulated is shown, while Table 2.2 and 2.3 summarise all the input and output streams of the process.

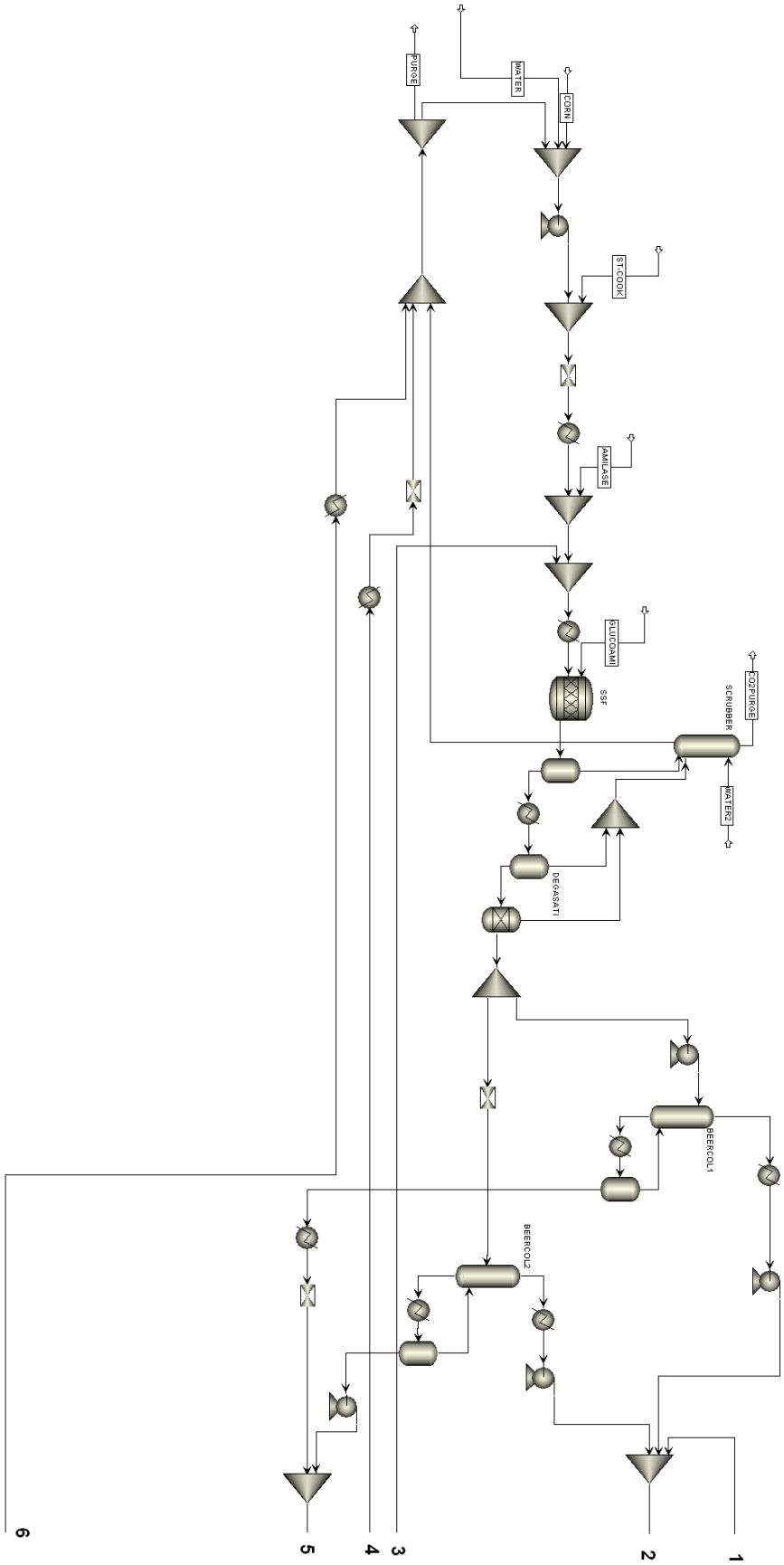


**Figure 2.1** *Aspen Plus™ Flow sheet of the first generation bioethanol plant simulated in this Chapter.*

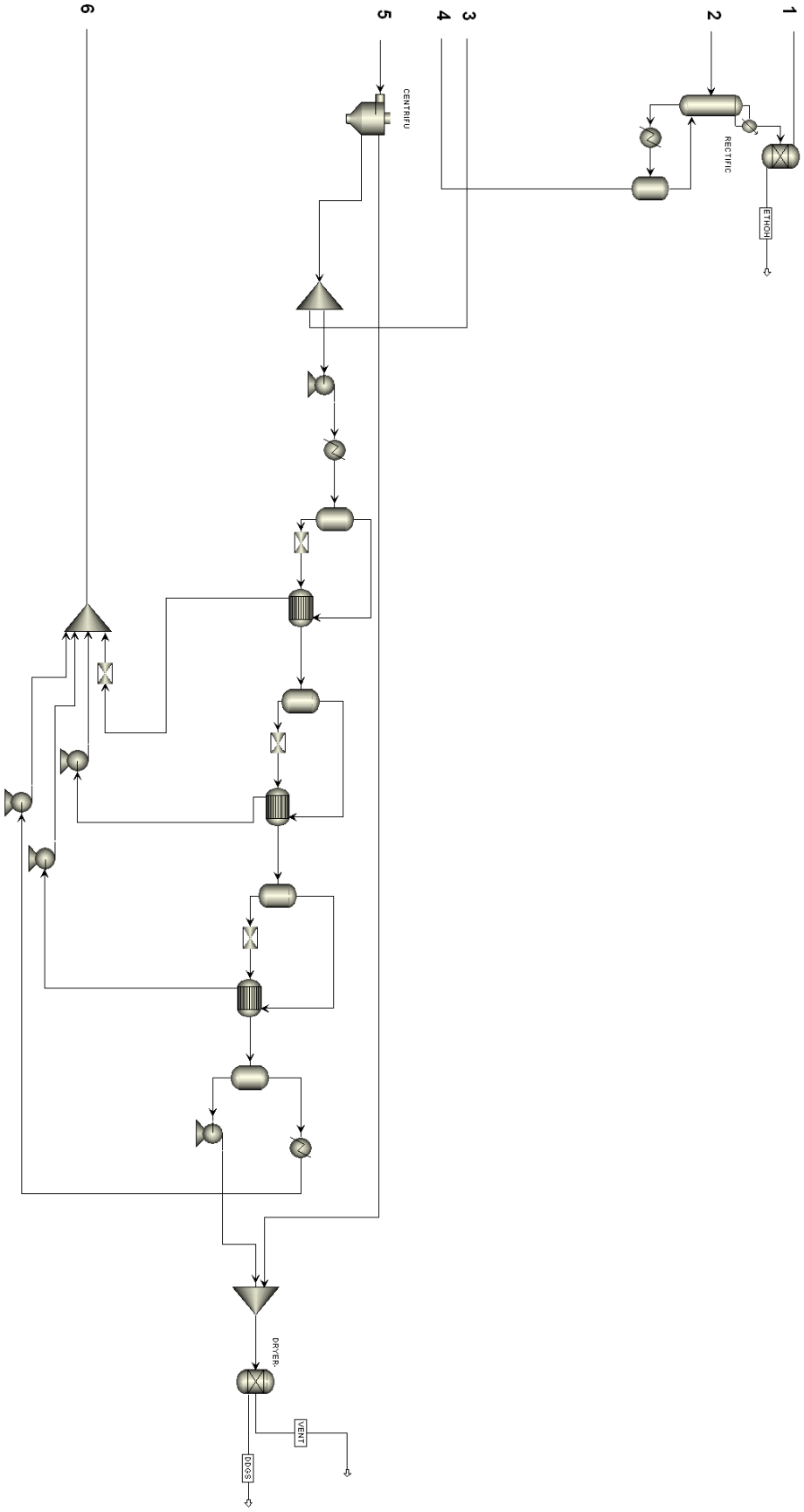


**Figure 2.2** *Aspen Plus™ Flow sheet of the first generation bioethanol plant simulated in this Chapter.*

**Table 2.2** *Input streams.*

| Component | Mass flow [kg/h] | | | | |
|---|---|---|---|---|---|
| | **Corn** | **Water** | **Steam** | **Water abs** | **Enzymes** |
| Water | 6,281 | 708 | 8,400 | 7,400 | 0 |
| Starch | 24,916 | 0 | 0 | 0 | 0 |
| Ethanol | 0 | 0 | 0 | 0 | 0 |
| $CO_2$ | 0 | 0 | 0 | 0 | 0 |
| Acetic acid | 0 | 0 | 0 | 0 | 0 |
| Glycerol | 0 | 0 | 0 | 0 | 0 |
| Non fermentable solids | 10,678 | 0 | 0 | 0 | 68 |

**Table 2.3** *Output streams.*

| Component | Mass flow [kg/h] | | | |
|---|---|---|---|---|
| | **$CO_2$ purge** | **Ethanol** | **DDGS** | **Vent** |
| Water | 412 | 27 | 1,221 | 18,321 |
| Starch | 0 | 0 | 226 | 0 |
| Ethanol | 7 | 13,548 | 0 | 0.14 |
| $CO_2$ | 13,101 | 0 | 0 | 0 |
| Acetic acid | 0 | 0 | 0 | 205 |
| Glycerol | 0 | 0 | 0 | 631 |
| Non fermentable solids | 0 | 0 | 10,746 | 0 |

In general, the DGP needs a large amount of water and, therefore, it is important to recover and recycle as much of it as possible in order to minimise the overall make-up. After this analysis the makeup is a little bit more than 8,000 kg/h of process water and 8,400 kg/h of cooking steam (excluding the water required by cooling towers' and boilers' make-ups, if needed). Figure 2.3 shows the block flow diagram of water recoveries throughout the process while the process overall mass and energy balances are summarised in Table 2.4.

**Table 2.4** *Overall mass balance and energy balance.*

| | | |
|---|---|---|
| **Water** | 8,107 [kg/h] | 0.597 [kg/kg EtOH] |
| **Cooking steam** | 8,400 [kg/h] | 0.619 [kg/kg EtOH] |
| **Corn** | 41,875 [kg/h] | 3.085 [kg/kg EtOH] |
| **Enzymes (db)** | 68.34 [kg/h] | $5.034\ 10^{-3}$ [kg/kg EtOH] |
| | | |
| **Natural gas** | 1.15 [t/h] | 0.085 [kg/kg EtOH] |
| **Electric power** | 7 [MW] | 515 [W/ kg EtOH] |

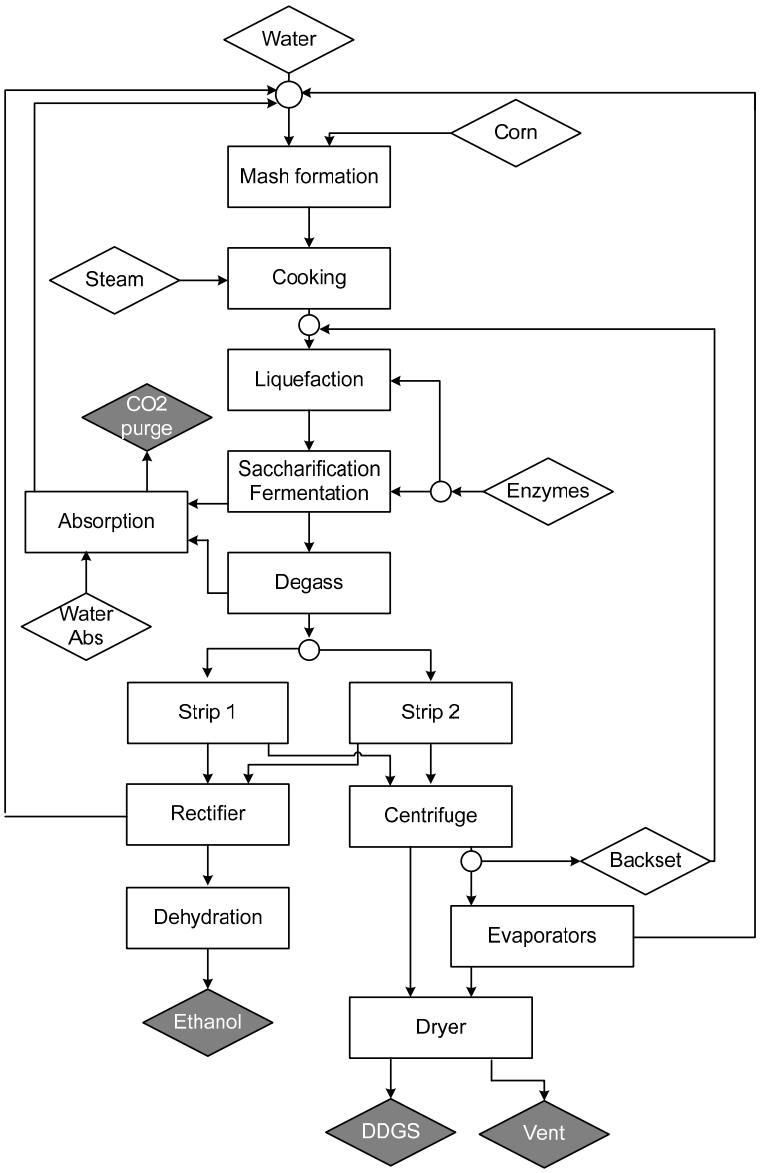


**Figure 2.3** *Block flow diagram of water recoveries, where the white blocks represent streams where water is an input, and the black blocks represent streams where water is an output.*

## 2.3 Thermodynamic model

In order to simulate the DGP with Aspen Plus$^{TM}$ as well as to perform the simulation of all the other processes described in the following Chapters of this thesis a suitable thermodynamic model was developed.

The thermodynamics of the vapour-liquid equilibria were described by using the NRTL model (Renon and Prausnitz, 1968). Carbon dioxide was defined as a Henry component and the capacity of the model to estimate the gas solubilities was checked using literature experimental data (Sukuki and Sue, 1990, Hirohama *et al.*, 2005, Ning *et al.*, 2005, Dalmolin, *et al.,*2006). For the correct use of the thermodynamic model the values of binary parameters

of all the pairs must be known. Binary parameters involving acetic acid were not available in the simulator databank and have been regressed from experimental data (Ito and Yoshida, 1960 and Rius *et al.,* 1958) The physico-chemical properties of the solid components involved were taken from the database specifically created for this purpose by Wooley and Putsche (1996).

### 2.3.1 VLE equilibria

The Aspen Plus™'s NRTL relationship for the calculation of activity coefficient is:

$$\ln \gamma = \frac{\sum_j x_i \tau_{ij} G_{ji}}{\sum_k x_k G_{ki}} + \sum_j \frac{x_j G_{ij}}{\sum_k x_k G_{ki}} \left( \tau_{ij} - \frac{\sum_m x_m \tau_{mj} G_{mj}}{\sum_k x_k G_{kj}} \right) \tag{2.3}$$

where $x$ is the mole fraction of component $i$, while $G$ and $\tau$ are calculated from:

$$G_{ij} = \exp(-a_{ij}\tau_{ij}) \tag{2.4}$$

$$\tau_{ij} = a_{ij} + b_{ij}/T + e_{ij}\ln T + f_{ij}T \tag{2.5}$$

$$a_{ij} = c_{ij} + d_{ij}(T - 273.15\text{K}) \tag{2.6}$$

$$G_{ii} = 0 \tag{2.7}$$

$$\tau_{ii} = 0 \tag{2.8}$$

**Table 2.5** *Matrix of the thermodynamic parameters.*

| | **Ethanol** | **Glycerol** | **Acetic Acid** | **$CO_2$** |
|---|---|---|---|---|
| **Water** | NRTL<br>Aspen database | NRTL<br>Aspen database | NRTL<br>Regressed | HENRY<br>Aspen database |
| **Ethanol** | | NRTL<br>Aspen database | NRTL<br>Regressed | HENRY<br>Aspen database |
| **Glycerol** | | | ---------- | HENRY<br>Aspen database |
| **Acetic Acid** | | | | HENRY<br>Aspen database |

The large part of the binary parameters ($a_{ij}$, $b_{ij}$, $c_{ij}$, $d_{ij}$, $e_{ij}$, $f_{ij}$) of the model are present in the Aspen Plus™ database, the other are regressed from experimental data. Details are given in Table 2.5.

### *2.3.2 Solid definition*

The solids present in the system are not involved in any thermodynamic equilibrium but their properties (like heat of formation, heat capacity and density) are important to simulate the system with Aspen Plus™.

**Table 2.6** *Solid proprieties inserted in the Aspen Plus ™ simulation.*

| Propriety | Cellulose | Hemicellulose | Lignin | Enzymes | Biomass |
|---|---|---|---|---|---|
| Formula | $C_6H_{10}O_5$ | $C_5H_8O_4$ | $C_{7.3}H_{13.9}O_{1.3}$ | - | - |
| Mol. weight | 162.1436 | 132.117 | 122.493 | 22.83983 | 23.238 |
| Solid heat of formation [kJ/kmol] | -976,362.0 | -762,416.0 | -159,265.9 | -74,944.0 | -97,133.8 |
| Solid molar volume [cum/kmol] | 0.106 | 0.0864 | 0.0817 | 0.0152 | 0.01549 |
| Solid heat capacity [J/kmol K] | -11,704+672·T | -529.9+547.25·T | 31,431.7+394.427·T | 35,533 | 38,409 |

In their work Wooley and Putsche (1996) gave all the properties of the solids and explained their implementation in Aspen Plus™. Tables 2.6 and 2.7 summarize the information inserted in Aspen Plus™.

**Table 2.7** *Scalar properties used to represent glucose and xylose in the Aspen Plus ™ simulation.*

| Propriety | Glucose | Xylose |
|---|---|---|
| Formula | $C_6H_{12}O_6$ | $C_5H_{10}O_5$ |
| Mol. Weight | 180.16 | 150.123 |
| Critical Temperature [K] | 1011.1 | 890.42 |
| Critical Pressure [Pa] | 6,200,000 | 6,577,700 |
| Critical Volume [cum/ kmol] | 0.4165 | 0.3425 |
| Acentric factor | 2.5674 | 2.3042 |
| I.G. Heat of formation [MJ/kmol] | -1,256.903 | -1,040.020 |
| Liquid molar volume [cum/ kmol] | 0.35852 | 0.29936 |

Cellulose, hemicelluloses, lignin, enzyme and biomass are defined as solids while glucose and xylose are modelled as liquids component, although they never exist as pure liquid. The vapour pressure is low enough that they never be flashed into the vapour stream.

The temperature dependent properties of glucose are completely described in the Aspen database while the ones for xylose have been inserted. The temperature dependent properties modelled for glucose e xylose are:

The vapour pressure, (PLXANT)

$$\ln p_i^{*l} = C_{1i} + \frac{C_{2i}}{T + C_{3i}} + C_{4i}T + C_{5i}\ln T + C_{6i}T^{C_{7i}} \quad per\ C_{8i} \le T \le C_{9i} \tag{2.9}$$

and the heat of vaporization (DHVLWT)

$$\Delta_{vap}H_i^*(T) = \Delta_{vap}H_i^*(T_1)\left(\frac{1-T/T_{ci}}{1-T_1/T_{ci}}\right)^{a_1+b_1(1-T/Tci)} \quad per\ T > T_{\min} \tag{2.10}$$

with $\Delta_{vap}H^*$($T_1$=298 K) = 4186800 J/(kmol)

$a_i$=0.38

$b_i$=0

$T_{min}$=200

The different coefficients of Eqs. (2.9), (2.11) and (2.12) for xylose are reported in Table 2.8. Finally the I.G. (CPIG) and liquid heat capacities (CPLDIP) are calculated by:

$$C_p^{*ig} = C_{1i} + C_{2i}T + C_{3i}T^2 + C_{4i}T^3 + C_{5i}T^4 + C_{6i}T^5 \quad per\ C_{7i} \le T \le C_{8i} \tag{2.11}$$

$$C_{p,i}^{*l} = C_{1i} + C_{2i}T + C_{3i}T^2 + C_{4i}T^3 + C_{5i}T^4 \quad per\ C_{6i} \le T \le C_{7i} \tag{2.12}$$

**Table 2.8** *Coefficients of Equations ( 2.9), ( 2.11) and ( 2.12).*

| Coefficient | PLXANT | CPIG | CPLDIP |
|---|---|---|---|
| $C_1$ | 481.33 | -4349 | 172857 |
| $C_2$ | -46623 | 832.38 | 0 |
| $C_3$ | 0 | -0.70717 | 0 |
| $C_4$ | 2.10E-02 | 2.352E-4 | 0 |
| $C_5$ | 64.331 | -2.0252E-10 | 0 |
| $C_6$ | 6.22430E-06 | 0 | 250 |
| $C_7$ | 2 | 573.15 | 1000 |
| $C_8$ | 573.15 | 1023.2 | - |
| $C_9$ | 873.15 | - | - |

The starch is inserted as solid an equation fitted from experimental data is used.

$$Cp = 0.7267\ T - 6.8331 \tag{2.13}$$

where *Cp* is the solid heat capacity [J/K mol] and *T* is the temperature [K], and the validity range of the equation is from 8K to 490K.

### 2.3.3 Solubility of $CO_2$: Henry's Law

The behaviour of carbon dioxide was proved to be well represented by using the Henry's law (Franceschin, 2007) so it was defined in Aspen Plus™ like *Henry component*.
The Henry's law is written as:

$$\ln\left(H_i \Big/ \gamma_i^{\infty}\right) = \sum w_A \ln\left(H_{iA} \Big/ \gamma_{iA}^{\infty}\right) \tag{2.14}$$

where

$$w_A = \frac{x_A (V_{CA})^{2/3}}{\sum_B x_B (V_{CB})^{2/3}} \tag{2.15}$$

$$\ln H_{iA}\left(T, p_A^{*l}\right) = a_{iA} + b_{iA}/T + c_{iA} \ln T + d_{iA} T + e_{iA}/T^2 \tag{2.16}$$

Linear extrapolation is taken for ln ($H_{iA}$) versus $T$ outside of bounds.

$$H_{iA}(T,P) = H_{iA}(T,p) \tag{2.17}$$

The parameter $V_{iA}^{\infty}$ is the mole partial volume of component *i* at infinite dilution in solvent *A* and is obtained from the Brelvi-O'Connell model, $p_A^{*l}$ is the vapour pressure of component *A* obtained from the Antoine model, and $\gamma_{iA}^{\infty}$ is the activity coefficient of component *i* at infinite dilution calculated from the appropriate activity coefficient model.
The Henry's constants $a_{iA}$, $b_{iA}$, $c_{iA}$, $d_{iA}$, and $e_{iA}$ are specific to a solute-solvent pair. They can be obtained from regression of gas solubility data, but in the case of interest all the binary parameter of the components of this system were available in the database.

## 2.4 Energy optimization: Pinch technology analysis

The energy optimisation of the bioethanol process has been achieved by using Pinch Technology Analysis (PTA, Linnhoff and Flower, 1978), through the definition of the heat exchangers network, the classification of the hot and cold streams, the determination of the pinch point (by composite curves), and eventually the setting up of the final heat exchangers network.

The hot (i.e. to be cooled) and cold (i.e. to be heated) streams can be represented on a temperature-enthalpy diagram in the form of two composite curves, which are represented in Figure 2.4.

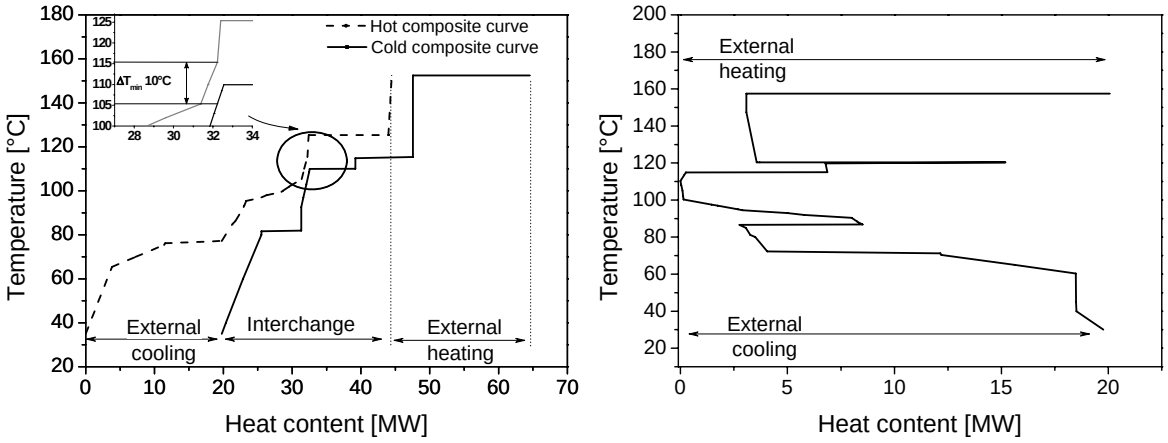


*(a)* *(b)*

**Figure 2.4** *Hot, cold composite curves and pinch point determination (a), grand composite curve (b).*

The $\Delta T_{min}$ represents the minimum temperature difference between the hot and cold sides which is allowed in all the heat exchangers of the process. We selected $\Delta T_{min}$ 10°C. Usually $\Delta T_{min}$ occurs at one point only, which is called the pinch. The enthalpy differences between the cold and hot composite curves represent the minimum amount of external heating and cooling required by the process. A cascade of heat exchangers is defined between hot and cold streams, in order to recover all the heat according to the composite curve construction.

Figure 2.4 b shows the grand composite curve of the bioethanol process: about 20 MW are needed as external heating and about 19.8 MW as external cooling. The pinch temperatures are 95.4 °C for the cold streams and 115.4 °C for the hot ones. The building of the heat exchangers network near the pinch point is carried out according to the usual algorithms (Linnhoff and Flower, 1978).

The results show that the minimum energy demand is achieved by a network of 17 heat exchangers. The utilities' consumptions are reported in Table 2.9.

**Table 2.9** *Utilities demand.*

| | **Without optimization [kg/kg EtOH]** | **PTA [kg/kg EtOH]** |
|---|---|---|
| High pressure steam (7 atm) | 3.26 | 2.18 |
| Low pressure steam (4 atm) | 2.41 | 0.38 |
| Cooling water | 235.10 | 104.30 |

It can be seen that a significant reduction in terms of steam and water requirements can be reached with respect to the base case. According to our experience, present industrial design is already rather good in terms of steam consumption (although our data suggest that some room for improvement may still be possible), but quite poor in terms of the cooling system. Assuming to use cooling towers (and chillers) in the cooling water cycle, the optimisation indicates a possible make-up of about 2.1 kg of fresh water per kg of ethanol (2% of the total demand): that should be set as a technological goal.
Further improvement could be achieved through a more substantial technological change, either by adopting heat integrated distillation columns or membrane technology. The analysis of such technologies is, however, beyond the scope of this work.

## 2.5 Sensitivity on process variables

A sensitivity analysis was carried out to assess the effects of some key process variables. In particular, starch content in the corn and ethanol concentration in the fermentation tanks have been considered evaluated.
The alcohol concentration in a fermenter is limited by the activity inhibition of yeast caused by metabolic by-products. Biotechnological research is currently aiming at increasing the yeasts resistance. Table 2.10 shows some simulation results for different ethanol concentrations in the fermenters.

**Table 2.10** *Fermenters ethanol concentration sensitivity results.*

| | **Base case** | **Case 1** | **Case 2** |
|---|---|---|---|
| Fermenter ethanol fraction (w/w) | 0.109 | 0.154 | 0.210 |
| Water make up [kg/kg EtOH] | 0.597 | 0.773 | 0.838 |
| High pressure steam [kg/kg EtOH] (7 bar) | 2.18 | 2.12 | 2.11 |
| Low pressure steam [kg/kg EtOH] (4 bar) | 0.38 | Not needed | Not needed |
| Cooking steam [kg/kg EtOH] | 0.62 | 0.48 | 0.38 |
| Cooling water [kg/kg EtOH] | 104.3 | 78.3 | 72.6 |

As shown in the Table 2.10, it appears that the higher the ethanol concentration the lower the energy consumption; that is due to an “easier” distillation and to less water recirculation.
Another popular research topic is the quest for new varieties of corn at higher starch content. Although the actual effect of modifying the composition of corn is not so straightforward (Wu *et al.,* 2006), Table 2.11 shows the simulation result for different starch concentration of the corn, assuming that potential side effects can be overcome.

**Table 2.11** *Starch corn content sensitivity results.*

| | Base case | Case 3 |
|---|---|---|
| Kernel starch fraction | 0.595 | 0.695 |
| Fermenter ethanol fraction (weight) | 0.109 | 0.109 |
| Corn consumption [kg/kg EtOH] | 3.08 | 2.64 |
| Water make up [kg/kg EtOH] | 0.597 | 0.241 |
| High pressure steam [kg/kg EtOH] (7 bar) | 2.18 | 2.19 |
| Low pressure steam [kg/kg EtOH] (4 bar) | 0.379 | 0.560 |
| Cooking steam [kg/kg EtOH] | 0.619 | 0.611 |
| Cooling water [kg/kg EtOH] | 104.3 | 114.7 |
| DDGS production[kg/kg EtOH] | 0.281 | 0.181 |

As expected, a higher starch fraction does not affect the energy consumption significantly, but quite obviously the corn consumption is lower.

## 2.6 Concluding remarks

This Chapter has analysed a dry-grind process for the production of bioethanol in Italy. A rigorous process simulation was carried out to assess the overall yield and the energy and water requirements. The process was optimised adopting a pinch technology analysis that demonstrated the possibility of reducing both energy and (particularly) water duties.

Changes on the corn starch content and yeast's ethanol tolerance directly affect the production costs by influencing plant capacity and utilities needs. In fact, the former will increase the alcohol production, whereas the latter will allow higher alcohol percentage in the fermentation tanks and, consequently, lower energy in the distillation.

Similar significant advantages do not seem to be achieved if enrichment in the corn starch content is taken into account.

## 2.7 References

Dalmolin, I., E. Skovroinski, A. Biasi, M.L. Corazza, C. Dariva, J.V. Oliveira (2006). Solubility of Carbon Dioxide in Binary and Ternary Mixtures With Ethanol and Water. *Fluid Phase Equilib.,* **245**, 193-200.

Franceschin, G. (2007). Impianto di Produzione di Bioetanolo da Mais: Simulazione ed Ottimizzazione Energetica. *Tesi di Laurea in Ingegneria Chimica*, DIPIC, Università di Padova.

Hirohama, S., T. Takatsuka, S. Miyamoto, and T. Muto (2005). Measurement and Correletion of Phase Equilibria for the Carbon Dioxide- Ethanol -Water System. *J. Chem. Eng. Jpn.,* **26**, 408-415.

Ito, T. and F. Yoshida (1963). Vapor Liquid Equilibria of Water-Lower Fatty Acid System. *J. Chem. Eng. Data*, **8,** 315-320.

Kwiatkowski, J.R., A.J. McAloon, F. Taylor, and D.B. Johnston (2006). Modeling the Process and Costs of the Production of Fuel Ethanol by the Corn Dry-Grind Process. *Ind. Crops and Products*, **23**, 288-296.

Linnhoff, B. and J.R. Flower (1978). Synthesis of Heat Exchanger Networks: I. Systematic Generation of Energy Optimal Networks. *AIChE J.,* **24**, 633-642.

Morey, R.V., D.G. Tiffany, and D.L. Hatfield (2006). Biomass for Electricity and Process Heat at Ethanol Plants. *Applied Eng. in Agriculture*, **22**, 723-728.

Ning, A., J. Chen, F. Weiyang (2005). Solubility of Carbon Dioxide in Four Mixed Solvents. *J. Chem. Eng. Data*, **50**, 492-496.

Peschel, A., R. Karuppiah, M. Martín, I.E. Grossmann, L. Zullo, and W. Martinson, (2006). A Superstructure Optimization Approach for the Design of Corn-Based Ethanol Plants, *AIChE Annual Meeting*, November 12-17, 2006, San Francisco, U.S.A.

Renon, H. and J.M. Prausnitz (1968). Local Compositions in Thermodynamic Excess Functions for Liquid Mixtures. *AIChE J.*, **14**, 135-144.

Rius, A., J. Otero, and L.A. Macarron (1958). Equilibres Liquide-Vapeur de Mèlanges Binaires Donnant une Rèaction Chimique Mèthanol-Acide Acètique; Ethanol -Acide Acètique; n-Propanol -Acide Acètique; n-Butanol -Acide Acètique. *Chem. Eng. Sci.,* **10**, 105-290.

Suzuki, K. and Sue (1990). Isothermal Vapor-Liquid Equilibrium Data for Binary System at High Pressures: Carbon Dioxide-Methanol, Carbon Dioxide-Ethanol, Carbon Dioxide-1-Propanol, Methane-Ethanol, Methane-1-propanol, Mthane-Ethanol, and Ethane-1-Propanol System. *J. Chem. Eng Data*, **35**, 63-66.

Wooley, R.J., V. Putsche (1996). *Development of an ASPEN PLUS Physical Property Database for Biofuels Components National Renewable Energy Laboratory*. Report: NREL/MP-425-20685.

Wu, X., R. Zhao, D. Wang, S.R. Bean, P.A. Seib, M.R. Tuinstra, M. Campbell, and A. O'Brien (2006). Effect of Amylose, Corn Protein, and Corn Fiber Contents on Production of Ethanol from Starch-Rich Media. *Cereal Chemistry*, **83**, 569-575.

Wyman, C.E. (1996). *Handbook On Bioethanol: Production And Utilization: Production & Utilization.* Taylor & Francis, Washington DC (U.S.A.).

# Chapter 3

# High pressure VLE of the mixture: water, ethanol, $CO_2$

A brief literary review on the ternary equilibrium $CO_2$/ ethanol/ water and on $CO_2$ supercritical (SFE) extraction of ethanol is presented. It was found that previous research works addressed the use of supercritical carbon dioxide for the extraction of ethanol from water mixtures and proposed this application as a way to obtain absolute grade fuel ethanol avoiding azeotropic distillation or molecular sieve purification (Budich and Brunner, 2003 and Zetzl *et. al*, 2007). These authors experimentally proved that the separation is possible, so that the azeotrope can be broken and an ethanol weight fraction of 0.999 can be achieved by supercritical extraction in a single column only. Extraction condition of 333 K and 100 bar was found as the best one (Budich and Brunner, 2003) to obtain pure ethanol. Three attempts to reproduce the experimental thermodynamic data allowed selecting the most suitable model to be used in Aspen Plus™ simulations of the supercritical column.

## 3.1 Phenomenology of ternary system

When a binary mixture is processed with a supercritical fluid in a fractionation or in an extraction process a three–component system is formed. In this system we can recognize a low volatile substance (B) a substance with an intermediate volatility (C) and the supercritical gas (A). The ternary system phase behaviour can be classified in two main groups as shown in Figure 3.1. In Figure 3.1a, both the binary systems B+C and A+B show full miscibility.

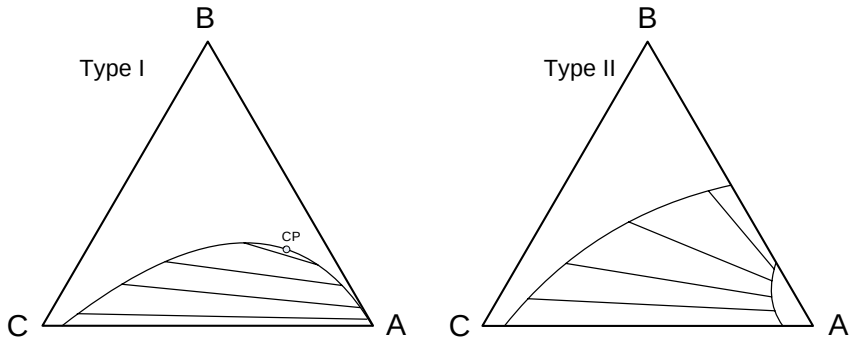


*(a)* *(b)*

**Figure 3.1** *Schematic phase behaviour of the ternary mixtures (adapted from Budich and Brunner, 2003).*

Because the binary system A+C has a miscibility gap and consists of a liquid and vapour phase, there is a two-phase region limited by the liquid and vapour curves and a critical point CP where they merge. This kind of phase behaviour is called type I (Treybal, 1980).
In contrast to type I, a ternary mixture with phase behaviour of type II has two miscibility gaps (Figure 3.1b). Again, the binary feed mixture B+C is completely miscible at any composition.
In the absence of azeotropic behaviour, products of almost pure B and almost pure C can be obtained by a multistage process. On the contrary at azeotropic conditions, the line connecting the pure solvent A and a mixture of B+C is congruent to a tie line, and both phases L and V have exactly the same solvent-free composition. Until the connecting lines and tie lines cross at any point inside the two-phase region different products can be obtained. In order to obtain pure ethanol the supercritical extraction has to be performed at temperature and pressure that allow a type II phase behaviour.

## 3.2 State of the art

Literature data for the vapour liquid equilibria (VLE) of the $CO_2$/ ethanol/ water ternary system are available in a wide range of temperatures and pressures. At the beginning, in order to get a high solubility of ethanol in the vapour phase, many studies were carried out at a type I behaviour. Some experimental results are shown in Figure 3.2 (Gilbert and Paulaitis, 1986).

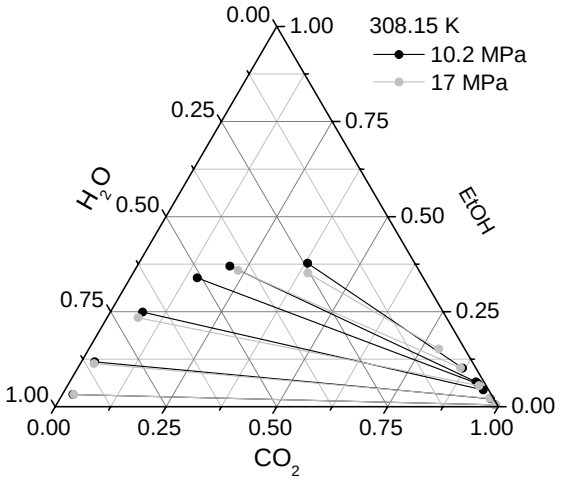


**Figure 3.2** *Phase behaviour of ternary system $CO_2$ Ethanol –Water pressure 10.2 MPa and 17 MPa and at temperature of 308.15 K (Gilbert and Paulaitis, 1986). Compositions are expressed in mole fraction.*

Based on these data, some researchers concluded that it was not possible to break the azeotrope by using supercritical $CO_2$ (Gilbert and Paulaitis, 1986).

One of the first studies reporting the possibility to produce anhydrous ethanol by means of $CO_2$ without adding an entrainer is the one by Nagahama *et al.,* (1988). Unfortunately since water was not detectable in any sample from the vapour phase taken at 313 K and either 3.86 or 5.79 MPa, no separation factors can be derived from this paper.

SFE of ethanol-water mixtures was then studied intensively at the research laboratories of Kobe Steel Ltd in Japan. One of the first publications reported VLE data at 10.1 MPa and 313, 323, and 333 K (Furuta *et al.*, 1989).

At 10.1 MPa and either 313 or 323 K it was not possible to obtain pure. However, selectivity in the region of low ethanol concentration was best at low temperatures. No azeotrope was observed at 10.1 MPa and both 333 and 383 K. In 1994 Lim and Lee hypothesized that it is possible to concentrate ethanol above atmospheric azeotropic composition (89.4% mol/mol) when the system pressure is below the critical pressure of the $CO_2$-$C_2H_5OH$ binary system. This simple statement was truly a surprise after many years of research in breaking the azeotrope. Some results of these authors are proposed in Figure 3.3a and 3.3.b. At 10.1 MPa and 323.2 K the presence of the azeotrope is evidenced while at 333.2 K the azeotrope is broken. The critical pressure ($P_c$) of the binary mixture $CO_2$ - $C_2H_5OH$ at 333.2 K is 10.62 MPa while at 323.2 K is 9.41 MPa and according to the theory working at 10.1 MPa the system pressure is above the $P_c$ at 323.2 K but below the one at 333.2 K. In Figure 3.3a and b the equilibrium changes from type I to type II behaviour are also shown.

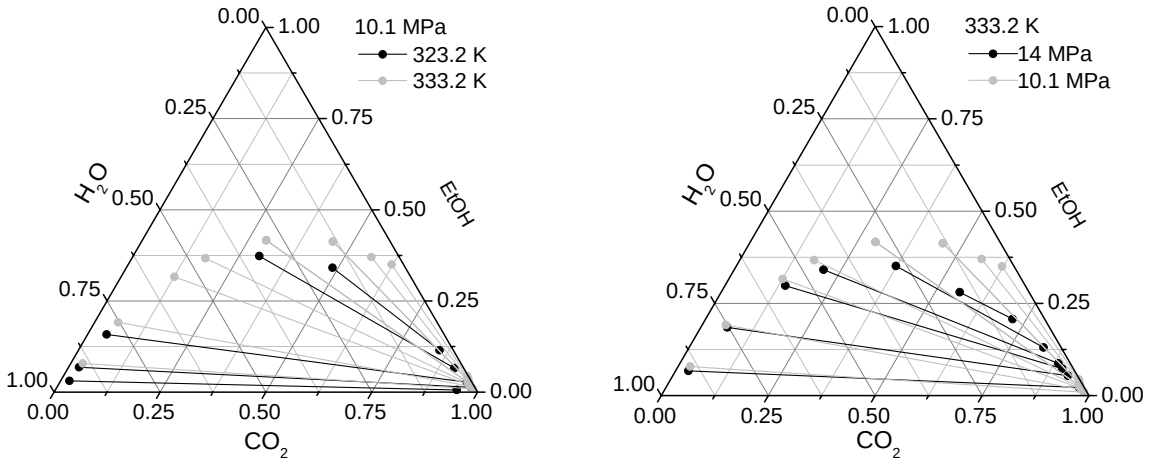


*(a)* *(b)*

**Figure 3.3** *$CO_2$, water, ethanol ternary system data (Lim and Lee, 1994).*

More recently other researches focused their attention on the possibility to obtain pure ethanol by supercritical extraction. Budich and Brunner (2003) recognized the temperature of 333 K as the best one for the separation due to the possibility of product degeneration at higher ones. Considering that for this temperature the critical pressure of the binary system $CO_2$/ ethanol is 10.62 MPa pressures higher than 10.1 MPa, are not recommended.

Due to scattering in published data at 333 K and 10.0 or 10.1 MPa, respectively, and diverging opinions about the existence of an azeotrope, VLE measurements of the ternary mixture $CO_2$/ethanol/water were carried out from Budich and Brunner (2003) and a good representation of the equilibrium was eventually archived. Figure 3.4a and b shows the equilibrium at 333 K and 10.1 MPa. These data are chosen as reference ones for this thesis.

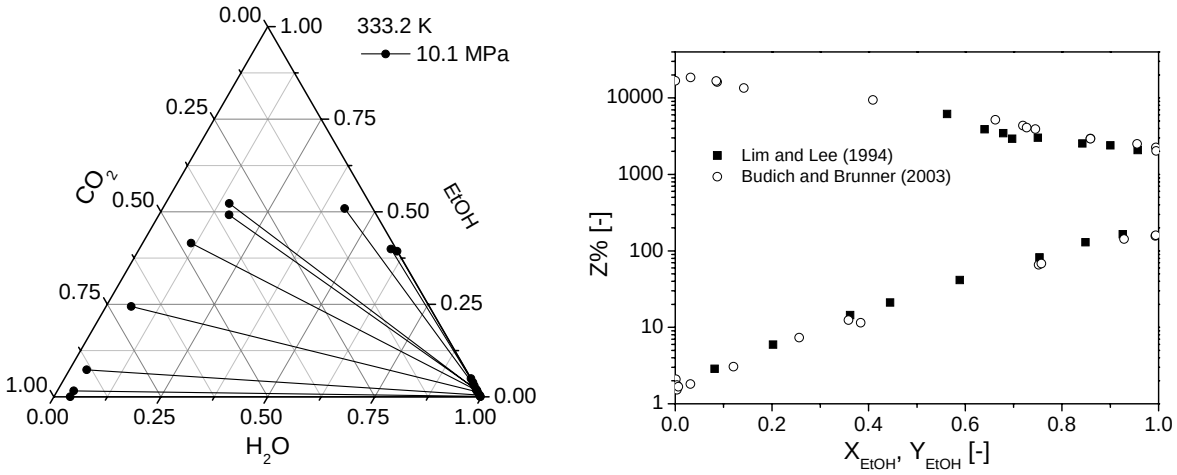


*(a)* *(b)*

**Figure 3.4** *Budich and Brunner (2003) data (mass fractions) at 313 K and 100 bar (a) and comparison with Lim and Lee (1994) data (b) at 333 K and 10.1 MPa (molar base).*

In Figure 3.4b Budich data and Lim ones are compared using a Jänecke diagram. In this graph the *Z* values of the two phases (3.1) are plotted in the y-axis as a function of the respective pseudobinary ($CO_2$-free) fraction (3.2):

$$Z_x = \frac{x_{CO_2}}{x_{H_2O} + x_{EtOH}} \qquad Z_y = \frac{y_{CO_2}}{y_{H_2O} + y_{EtOH}} \tag{3.1}$$

$$X_{EtOH} = \frac{x_{EtOH}}{x_{EtOH} + x_{H_2O}} \quad Y_{EtOH} = \frac{y_{EtOH}}{y_{EtOH} + y_{H_2O}} \tag{3.2}$$

where $x_i$ and $y_i$ are the mole fractions of the component *i* in the liquid phase and in the supercritical phase respectively.

Once the experimental equilibrium data were obtained Budich and Brunner (2003) performed some experiments with a countercurrent column and compared them with theoretical calculation of equilibrium stages (Figure 3.5a). The study of the flooding point of a packaging column equipped with Sulzer EX packing with 25 mm ID allowed determining the relation between maximum cross-section capacity and ethanol content of the solvent free liquid phase (Figure 3.5b).

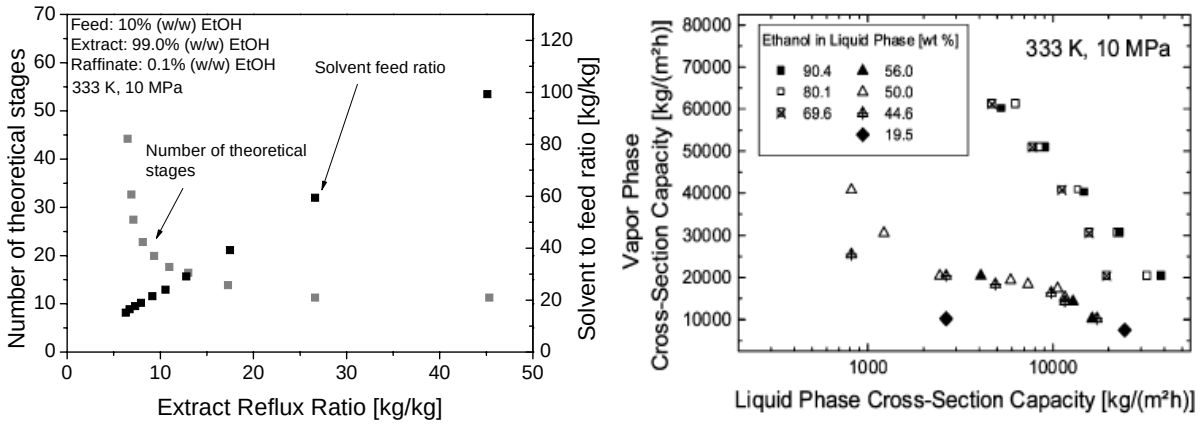


*(a)* *(b)*

**Figure 3.5** *Number of theoretical stages and solvent to feed ratio as function of the extract and reflux ratio (Budich and Brunner, 2003) (a) and cross section capacity experimental results (Zetzl et al., 2007) (b).*

In another work Zetzl *et al.,* (2007), underline that, in order to recover all the ethanol from the liquid stream, in the bottom of the column the ethanol concentration has to be lower than 19.5% and, as shown in Figure 3.5 b, the vapour phase cross section capacity must be as low as 10,000 kg/m$^3$h. In this case the column diameter at the bottom should be greater than at the top to avoid flooding. An alternative to mass transfer in falling droplets can be the use of a-mixer settler system. Additionally, in this way, operative conditions different from those of the column can be fixed.

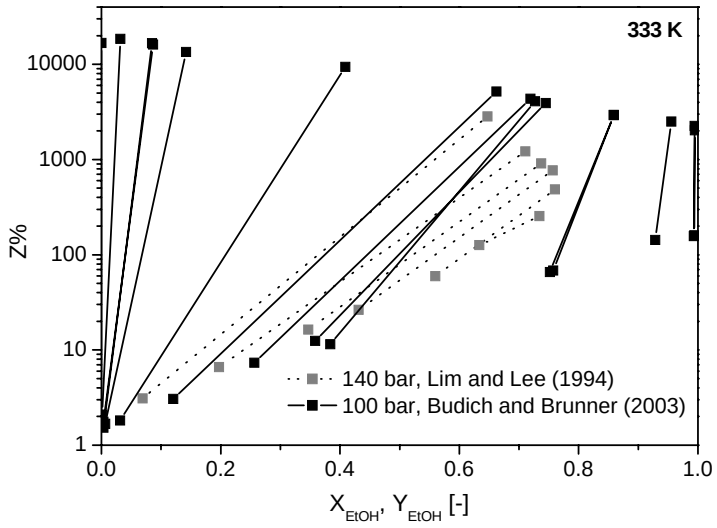


**Figure 3.6** *Jänecke diagram at 333 K for both 100 bar and 140 bar.*

As shown in Figure 3.6, at 140 bar the phase equilibrium lens closes at maximum ethanol concentration of about 90% (so this pressure is not suitable to obtain pure ethanol) but the

slope of tie lines is much smaller than in the case of 100 bar. This means that the ethanol at the bottom can be stripped out with less equilibrium steps.
For binary and ternary mixtures of $CO_2$/ ethanol/ and water many papers about modelling the equilibrium data by equations of state can be found. Of course while most of the well-known EOS and mixing rules enable a good representation of the mixtures $CO_2$ + ethanol and ethanol + water, more sophisticated mixing rules are required to model the $CO_2$ + water mixture (Lim and Lee, 1994). Even with a successful fit for all binary systems, the ternary mixture is not represented well enough, as reported by Lim and Lee (1994).
Recently, the good suitability of the Wong-Sandler mixing rule was demonstrated for $CO_2$ + water (Shyu *et al.*, 1997 and Durling *et al.*, 2007).

## 3.3 Thermodynamic model

Reliable process simulation results need a suitable identification of the system components and the choice of a suitable thermodynamic model.
Experimental equilibrium data have to be compared with simulated ones, to be sure that thermodynamic is represented correctly and, if necessary, have to be regressed to find the best parameter values to correlate them. The NTRL model and Henry's law for $CO_2$ were chosen for the low pressure part of the system (§ Chapter 2) while for the high pressure part some model have been tested in order to find the best one in Aspen Plus $^{TM}$.
In the event that simulation problem involves high pressure operations the use of equations of state is mandatory instead of activity coefficient models. The Peng Robinson equation of state has been used to model a large number of systems at supercritical conditions; if polar components are present the mixing rule must be linked to an activity coefficient model ($g^E$ EOS models). In their work Durling *at al.,* (2007) utilised a flow experimental method for determining phase equilibrium data for $CO_2$/ EtOH/ $H_2O$ ternary system at high pressure and then modelled their data using the PR EOS with Wong Sandler mixing rules. For this reason in this thesis the first attempt was done using PRWS models, than different K-models were investigated.

### *3.3.1 High pressure model: PRWS*

First, as proposed by Durling *et al.,* (2007), an attempt to use the Peng Robinson equation of state with Wong Sandler mixing rule was done. The Aspen Plus$^{TM}$ property method based on the Peng Robinson Wong Sandler equation of state model is named PRWS. In this method the default model used to calculate excess Helmholtz energy is UNIFAC, but we selected the NRTL. Wong Sandler mixing rules use a relationship between the excess Helmholtz energy and equation-of-state. These authors (Wong and Sandler, 1992a, b) did not use a relationship between equation-of-state properties and excess Gibbs energy, as in the Huron-Vidal mixing

rules. The pressure-explicit expression for the equation-of-state is substituted in the thermodynamic equation:

$$p = -\left(\frac{\partial A}{\partial V}\right)_T \tag{3.3}$$

The Helmholtz energy $A_m$ is obtained by integration of Eq. (3.3), $A^E$ is calculated by:

$$A_m^E = A_m - \sum_i x_i A_i^* - RT \sum_i x_i \ln x_i \tag{3.4}$$

Where also $A_i^*$ is obtained by using Eq. (3.3). $A_i^*$ and $A_m$ are written in terms of equation of state parameters. Like in the procedure by Huron and Vidal (1975), the limiting case of infinite pressure is used. This simplifies the expressions. Equation (3.4) becomes:

$$\frac{a}{b} = \sum_i x_i \frac{a_i}{b_i} - \frac{1}{\Lambda} A_m^E (p = \infty) \tag{3.5}$$

where:

$$\Lambda = \frac{1}{\lambda_1 - \lambda_2} \ln\left(\frac{1+\lambda_1}{1+\lambda_2}\right) \tag{3.6}$$

The parameters $\lambda_1$ and $\lambda_2$ depend on the equation of state used. For the Peng Robinson case $\lambda_1 = (1-\sqrt{2})$ and $\lambda_2 = (1+\sqrt{2})$.

Eq. (3.5) is similar to the Huron-Vidal mixing rule for the excess Gibbs energy at infinite pressure. The excess Helmholtz energy can be approximated by the excess Gibbs energy at low pressure through any liquid activity coefficient model. Using the Helmholtz energy permits another mixing rule for *b* than the linear one. The mixing rule for *b* is derived staring from the point that the second virial coefficient must depend quadratically on the mole fraction:

$$B(T) = \sum\sum x_i x_j B_{ij} \tag{3.7}$$

with:

$$B_{ij} = \frac{\left(B_{ii} + B_{jj}\right)}{2}\left(1 - k_{ij}\right) \tag{3.8}$$

The relationship between the equation-of-state at low pressure and the virial coefficient is:

$$B = b - \frac{a}{RT} \tag{3.9}$$

$$B_{ii} = b_i - \frac{a_i}{RT} \tag{3.10}$$

Wong and Sandler (1992 a, b) derived the following mixing rule to satisfy Eq. (3.5) (using Eqs. 3.9 and 3.10):

$$b = \frac{\sum_i \sum_j x_i x_j B_{ij}}{1 - \frac{A_m^E(p=\infty)}{\Lambda RT} - \sum_i x_i B_i} \tag{3.11}$$

The excess Helmholtz energy is almost independent of pressure. It can be approximated by the Gibbs energy at low pressure. The difference between the two functions is corrected by fitting $k_{ij}$ until the excess Gibbs energy from the equation-of-state (using the mixing rules 3.5 and 3.10) is equal to the excess Gibbs energy computed by an activity coefficient model (at low pressure). This mixing rule accurately predicts the VLE of polar mixtures at high pressures. UNIFAC or other activity coefficient models and parameters from the literature can be used. Gas solubilities are not predicted and must be regressed from experimental data.
Unlike other (modified) Huron-Vidal mixing rules, the Wong and Sandler mixing rule meets the theoretical limit at low pressure (i.e. Eq. 3.7). For calculations in which densities are important, it must be checked whether they are realistic. These parameters are identified in the program as follows:

**Table 3.1** *Parameter identification in Aspen Plus.*

| Parameter | Symbol | Default | Units |
|---|---|---|---|
| **NRTL/1** | $a_{ij}$ | 0 | - |
| **NRTL/2** | $b_{ij}$ | 0 | Temperature |
| **NRTL/3** | $c_{ij}$ | 0.3 | - |
| **NRTL/4** | $d_{ij}$ | 0 | Temperature |
| **NRTL/5** | $e_{ij}$ | 0 | Temperature |
| **NRTL/6** | $f_{ij}$ | 0 | Temperature |

First of all equilibrium data for the $CO_2$-EtOH binary system were fitted (Day *et al.,* 1999), Table 3.1 summarises NRTL parameters in Aspen Plus$^{TM}$, while Table 3.2 shows the regressed parameters. Figures 3.7a, b and c compare the experimental and simulated Pxy diagram for this binary system.

**Table 3.2** *Parameters regressed from CO2-EtOH equilibrium data.*

| ***Parameter*** | *i\j* | ***ethanol*** | ***$CO_2$*** |
|---|---|---|---|
| **NRTL/2** [K] | **ethanol** | | 1892.76 |
| | **$CO_2$** | 216.91 | |

This fitting problem, as the following ones, is solved choosing the K-value (3.12) as the objective function.

$$K_{EtOH} = \frac{y_{EtOH}}{x_{EtOH}} \tag{3.12}$$

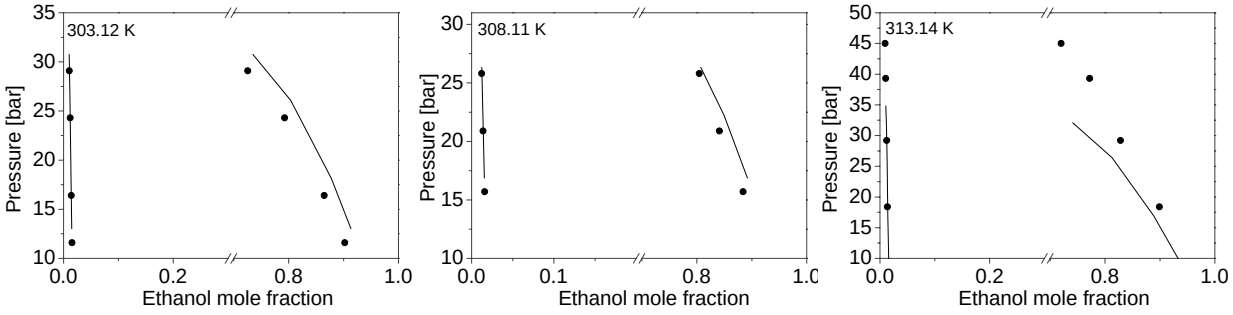


*(a)* *(b)* *(c)*

**Figure 3.7** *Spots represent the experimental Pxy diagram and lines the estimated ones. The data temperatures of graph (a), (b) and (c) are respectively 303.12 K 313.14 K and 308.11 K.*

Figure 3.8 shows a graphical representation of the experimental EtOH-$H_2O$ binary system data at 101.32 kPa (Arce *et al*., 1996) compared with the estimated equilibrium. Table 3.3 reports the NRTL binary parameter regressed for this binary system.

**Table 3.3** *Parameters regressed from Table EtOH-$H_2O$ equilibrium data.*

| **Parameter** | i\j | **ethanol** | **Water** |
|---|---|---|---|
| **NRTL/2** [K] | **ethanol** | | 869.399 |
| | **Water** | 68.990 | |

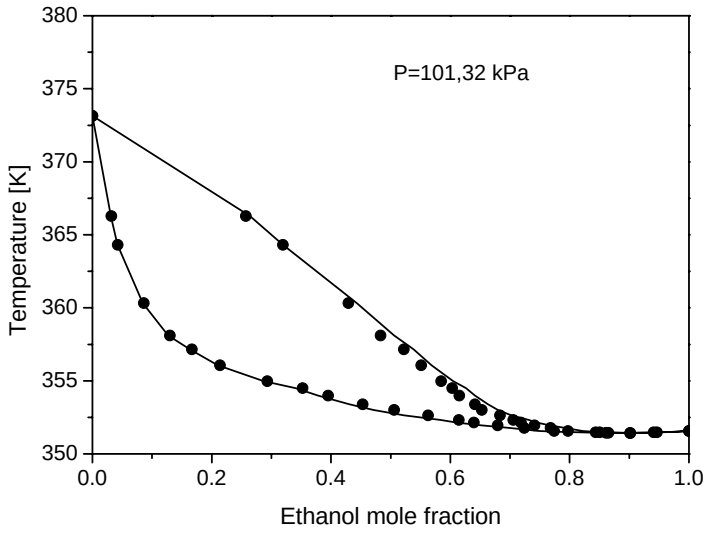


**Figure 3.8** *Txy diagram of water ethanol system. Spots represent the experimental data while lines the estimated VLE curve.*

Once EtOH-$CO_2$ and EtOH-$H_2O$ binary systems NRTL parameter has been calculated, the NRTL parameter for the $H_2O$– $CO_2$ binary system and the PRSWK parameter (one for each of the three pairs) are regressed. To do that Table 3.4 data and ternary equilibrium data (Durling *et al.*, 2007) were used.

**Table 3.4** *Equilibrium data (Budich and Brunner, 2003) at 100 bar and 333.15 K.*

| **Pressure** | **Temperature** | **Liquid phase** | | **Gaseous phase** | |
|---|---|---|---|---|---|
| [bar] | [K] | **$CO_2$** | **Water** | **$CO_2$** | **Water** |
| 100 | 333.15 | 0.03821 | 0.96179 | 0.99757 | 0.00243 |

**Table 3.5** *Calculated parameters from Table 3.4 and ternary equilibrium data.*

| **Parameter** | *i\j* | **water** | **$CO_2$** |
|---|---|---|---|
| **NRTL/2** | **water** | | 4455.82 |
| | **$CO_2$** | 665.95 | |
| **PRWSK** | **water** | | 0.479 |
| | **Ethanol** | -0.2677 | 0.0896 |

The ethanol partition coefficients, $K_{EtOH}$, between the $CO_2$ rich phase and the water rich phase were calculated using Eq. (3.12), where $y_{EtOH}$ and $x_{EtOH}$ are the mole fractions of ethanol in the supercritical and liquid phases, respectively.

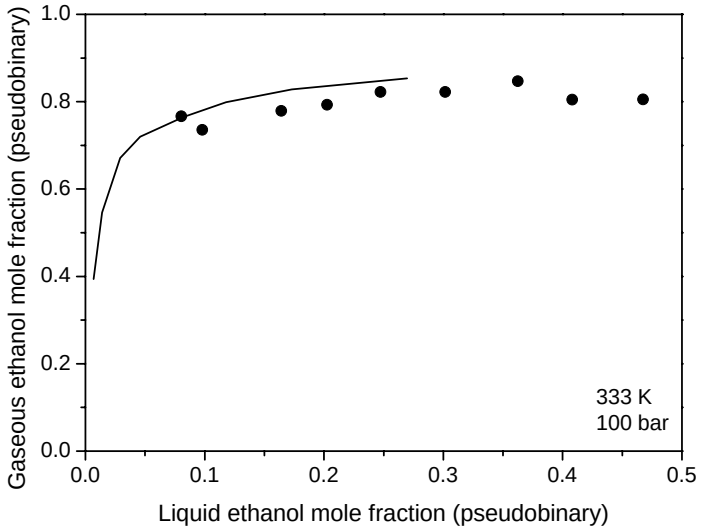


**Figure 3.9** *X vs Y diagram. Spots represent experimental data (Brunner et al., 2003) while lines the simulated ones.*

In Figure 3.9 the pseudobinary simulated liquid and vapour ethanol mole fraction are compared with the experimental data.

For a separation process the ethanol selectivity with respect to water and the ethanol loading in the extract (supercritical) phase are of key importance.

The selectivity of ethanol ($S_{EtOH,W}$) is given by the ratio of the partition coefficients of ethanol and water:

$$S_{EtOH,W} = \frac{K_{EtOH}}{K_{H_2O}} \tag{3.13}$$

The ethanol loading ($L_{EtOH}$) of gas phase (g/100 g supercritical phase) is obtained from the mass ratio of ethanol and $CO_2$:

$$L_{EtOH} = 104.55\left(\frac{y_{EtOH}}{y_{CO_2}}\right) \tag{3.14}$$

From Eqs. (3.13) and (3.14) the loading of water in the vapour phase can be easily derived:

$$L_{H_2O} = 40.93\left(\frac{y_{H_2O}}{y_{CO_2}}\right) \tag{3.15}$$

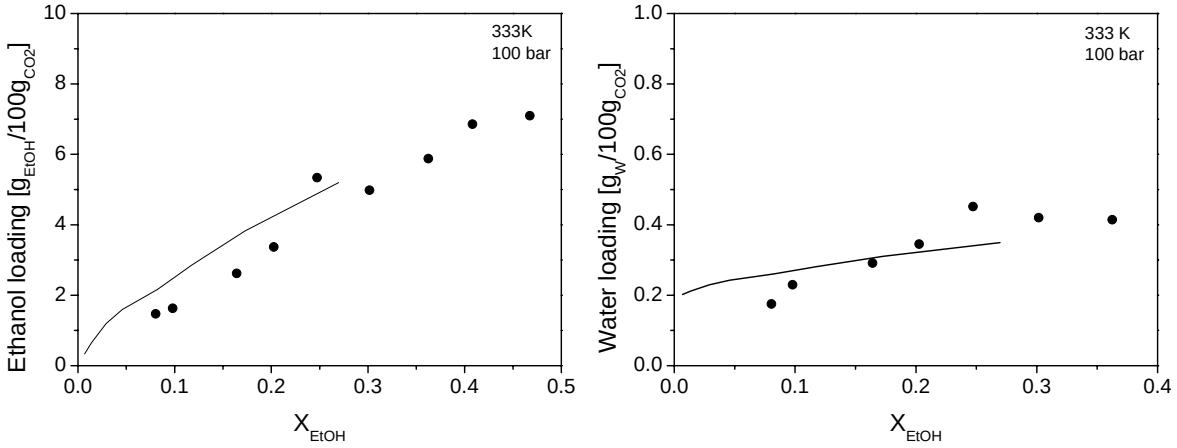


**Figure 3.10** *Ethanol loading (a) and water loading (b) vs X. Spots represent experimental data (Brunner et al., 2003) while lines the simulated ones.*

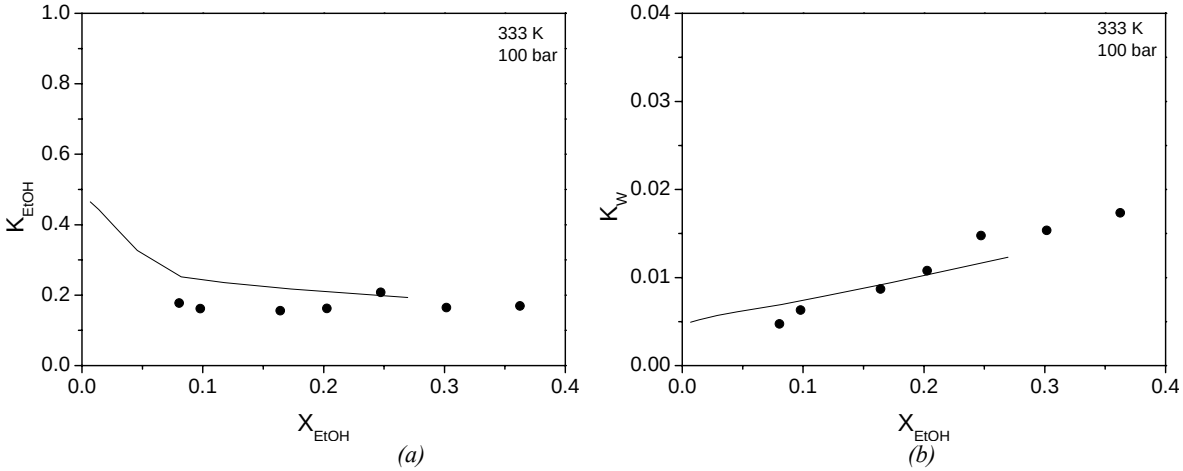


**Figure 3.11** *$K_{EtOH}$ (a) and $K_w$ (b) vs $X_{EtOH,w}$. Spots represent experimental data (Brunner et al., 2003) while lines the simulated ones.*

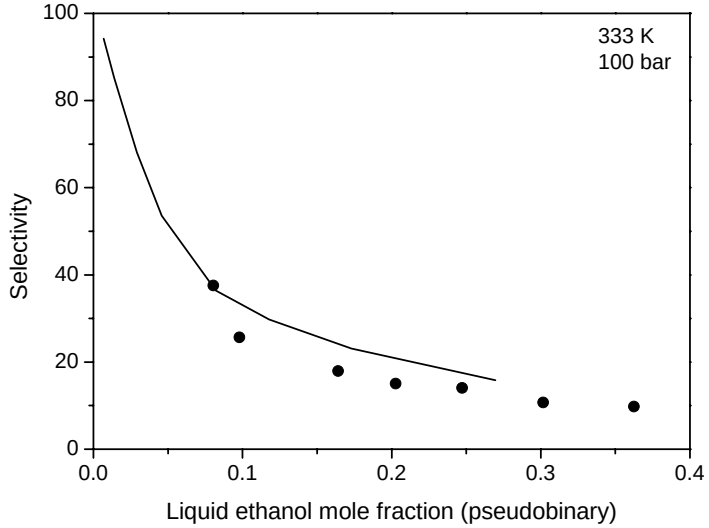


**Figure 3.12** *Selectivity vs $X_{EtOH,w}$. Spots represent experimental data (Brunner et al., 2003) while lines the simulated ones.*

Figures 3.10, 3.11, and 3.12 show the difference between the coefficients calculated from experimental data (Loading, K, selectivity) and the simulated ones. In all of this graphs the liquid mole fraction of ethanol (for the pseudobinary system ethanol -water Eq. 3.2) is represented on the x-axis. In this way it can be easily checked that experimental data agree with the simulated ones especially for concentrations similar to fermentation ones (low values).

The fit of high polar components like those of this system is difficult although the number of estimated parameters is large. The use of an equation of state is useful because allows the equilibrium determination at different temperatures and pressures. In this case, data at 333 K and 100 bar are well predicted but the model is not able to describe changes occurring when, for example, temperature is 313 K and the equilibrium turns from type II to type I (Figure 3.1). Moreover, during the simulation of the extraction column, this model resulted to be not flexible, so that also the small temperature changes that occur from top to bottom of the column caused convergence problem.

### *3.3.2 High pressure model: K-value approach*

Another possibility is to set up a correlation between the component K-value (Eq. 3.12) and the liquid phase composition; in this way the simulation program has less convergence problems but the dependence from temperature and pressure is lost.
Two different Fortran subroutines were written to enable Aspen Plus™ to use this correlation; all data points were taken from Budich and Brunner (2003).

#### 3.3.2.1 1st correlation

The Fortran subroutine have to supply Aspen Plus ™ the components' K –values and, if the system is simplified as a ternary one of ethanol, water, and $CO_2$, the easiest way to obtain a correlation for the K-value is to find its dependence with the composition of the liquid phase.
In Figure 3.13 a and b the K-values of water and ethanol are represented against the molar fraction of water in liquid phase. The correlations obtained from this graphs are:

$$K_{EtOH} = 0.9112x_{H_2O}^4 - 1.987x_{H_2O}^3 + 1.7758x_{H_2O}^2 - 0.6584x_{H_2O} + 0.125 \quad (3.16)$$

$$K_{H_2O} = -0.0165 \ln(x_{H_2O}) + 0.0002 \quad (3.17)$$

For $x_{H2O} \leq 0.2002$ while the $K_{H2O}$ for $x_{H2O} > 0.2002$

$$K_{H_2O} = 0.0058x_{H_2O}^{-0.9037} \quad (3.18)$$

with $x_{H2O}$ water molar fraction.

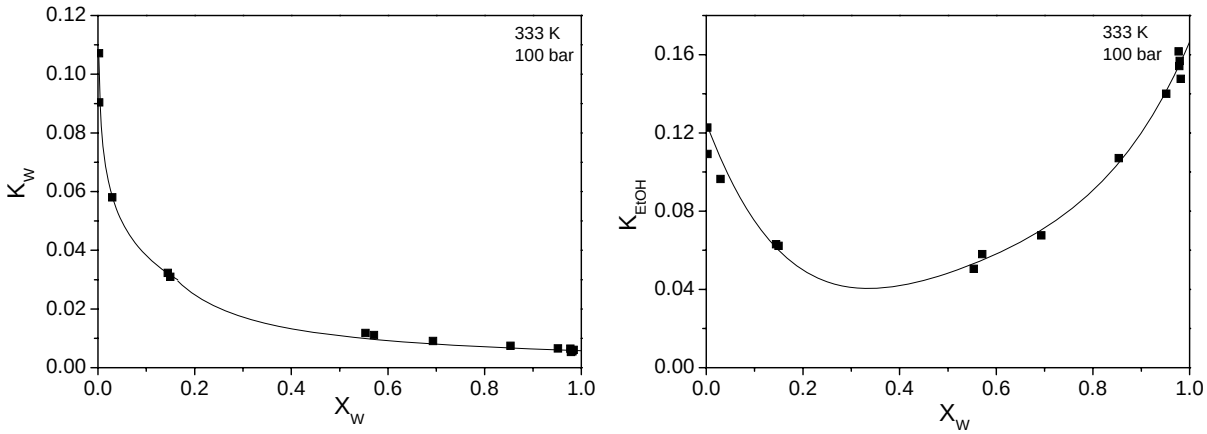


*(a)* *(b)*

**Figure 3.13** *K- value of water (a) and ethanol (b) as function of pseudobinary molar fraction of water in the liquid phase.*

In order to avoid convergence problems the K-values of $CO_2$ were set in an indirect way. First two different relations (3.20 and 3.21) were obtained for $Z_y$ and $Z_x$ fitting the equilibrium data (see Figure 3.14) then remembering the definition of K-value (3.12) the relation (3.21) can be achieved.

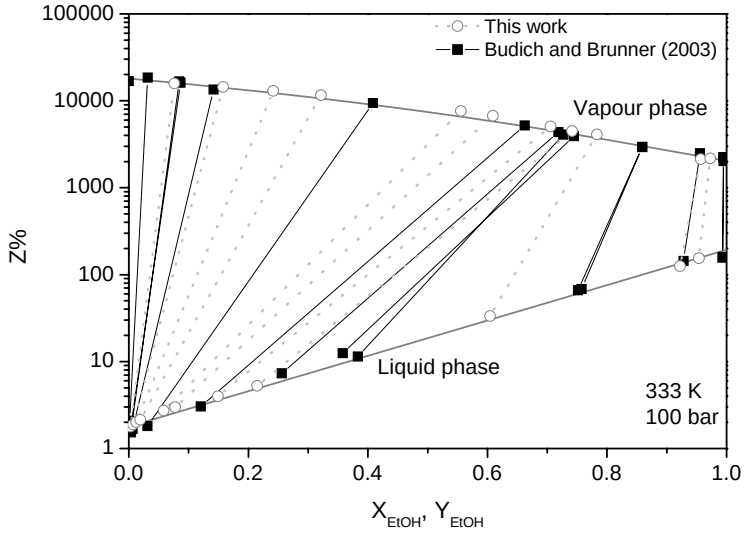


**Figure 3.14** *Jänecke diagram for the ternary system water ethanol $CO_2$. Square symbols (black tie line) represent experimental data while gray continues lines the interpolation curves of Eqs. (3.19) and ( 3.20). The circles and dashed tie line are simulation results.*

$$Z_x = 0.0179 \exp(4.6824 X_{EtOH}) \tag{3.19}$$

$$Z_y = 105.88 Y_{EtOH}^2 - 266.4 Y_{EtOH} + 180.94 \tag{3.20}$$

$$K_{CO_2} = \frac{Z_y}{Z_x}\frac{(y_{EtOH} + y_{H_2O})}{(x_{EtOH} + x_{H_2O})} \tag{3.21}$$

In Figure 3.15 the experimental data are compared with some equilibrium data obtained in simulation using this model. Accordingly to Figure 3.14 no azeotrope is present. As can be seen the simulated equilibrium is similar to the experimental one.

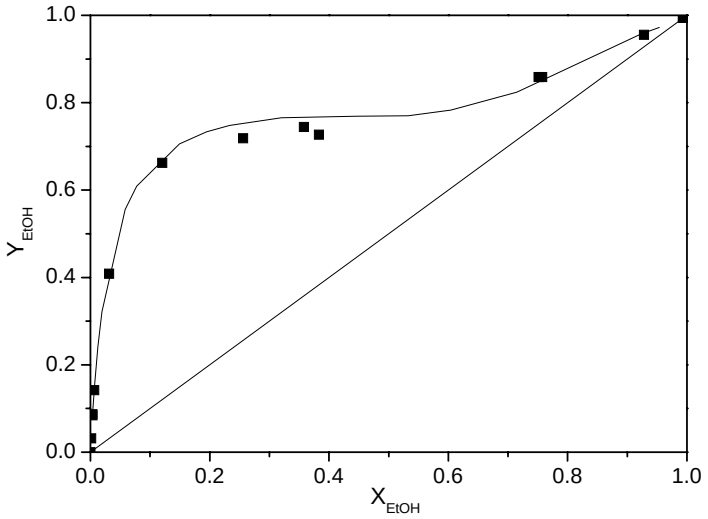


**Figure 3.15** *Pseudobinary diagram ($CO_2$ free). Square symbols represent experimental data while the continuous line the simulation ones.*

In the same way the K-value relations for equilibrium at 140 bar were obtained (ternary equilibrium data of Lim and Lee (2004) were used).
The relations implemented in the Fortran subroutine are:

$$K_{EtOH} = -36.66x_{H_2O}{}^5 + 106.9x_{H_2O}^4 - 122.5x_{H_2O}^3 + 69.92x_{H_2O}^2 - 20.15x_{H_2O} + 2.62 \tag{3.22}$$

$$K_{H_2O} = 0.0125x_{H_2O}{}^{-1.9669} \tag{3.23}$$

for values of water molar fraction ($x_w$) lower than 0.5610 while for $x_w$> 0.5610

$$K_{H_2O} = -0.07\ln\left(x_{H_2O}\right) + 0.007 \tag{3.24}$$

$$K_{EtOH} = -0.003\,x_{H_2O}^2 + 0.249\,x_{H_2O} + 0.106 \tag{3.25}$$

and finally for $K_{CO2,\ the}$ correlation of Eq. (3.21) is used but with $Z_x$ and $Z_y$ calculated by means of:

$$Z_x = 0.0179 \exp(6.2753 X_{EtOH}) \tag{3.26}$$

$$Z_y = -53.653\, Y_{EtOH}^2 - 119.92\, Y_{EtOH} + 127.1 \tag{3.27}$$

where $X_{EtOH}$ is the ethanol pseudobinary molar fraction ($CO_2$ free) calculated by means of Eq. (3.12). The simulation of the equilibrium is compared with literature data in Figure 3.16 a and b.

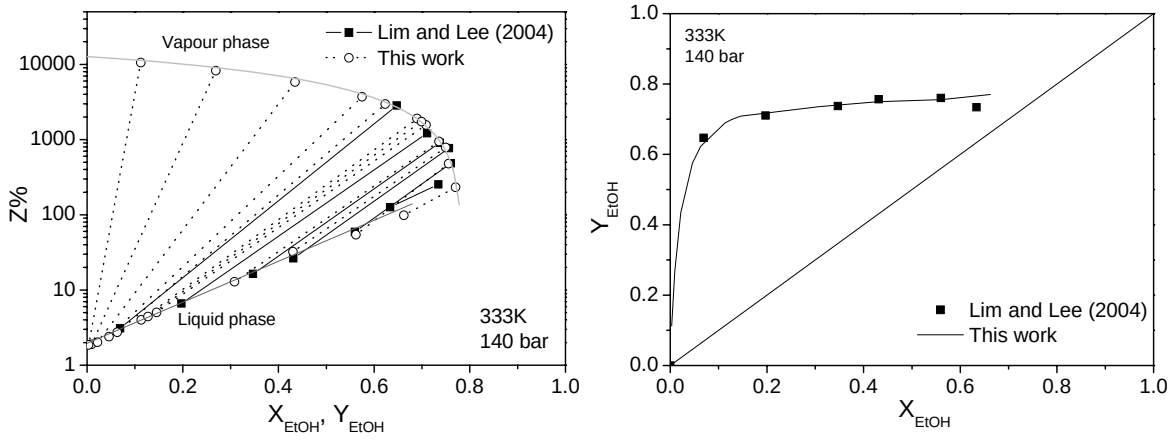


*(a)* *(b)*

**Figure 3.16** *Jänecke diagram for the ternary system water ethanol $CO_2$ (a). Square symbols and continue line represent experimental data while circles and dashed line the simulation ones. The gray lines are the plot of Eqs. (3.26) and (3.27). Pseudobinary diagram ($CO_2$ free) (b).*

As shown from the previous figures the equilibrium seem to be well represented both at 100 bar and at 140 bar, but during the simulation of the whole extraction column a discontinuity was encountered. The reason is that the K-values cannot be fixed independently because the relation 3.28.

$$1 = \sum_i x_i K_i \tag{3.28}$$

has to be respected otherwise the model becomes thermodynamically inconsistent. However this fact is marginally important because Aspen Plus $^{TM}$ itself is able to correct the value keeping the system thermodynamically consistent. But when simulating the extraction column for high recovery and purity of ethanol this correction leads to a discontinuity in the simulation results.

Even the combination of the water and ethanol K-value to calculate the $CO_2$ K–value (by means of Eq. 3.28) was investigated, but the results obtained were not satisfying.

### 3.3.2.2 2nd correlation

In order to avoid the problem outlined above a thermodynamically consistent K-value model was developed.

First, as shown in Figure 3.17, the correlation between the ethanol mole fraction in the liquid phase and its pseudobinary mole fraction in the same phase was obtained.

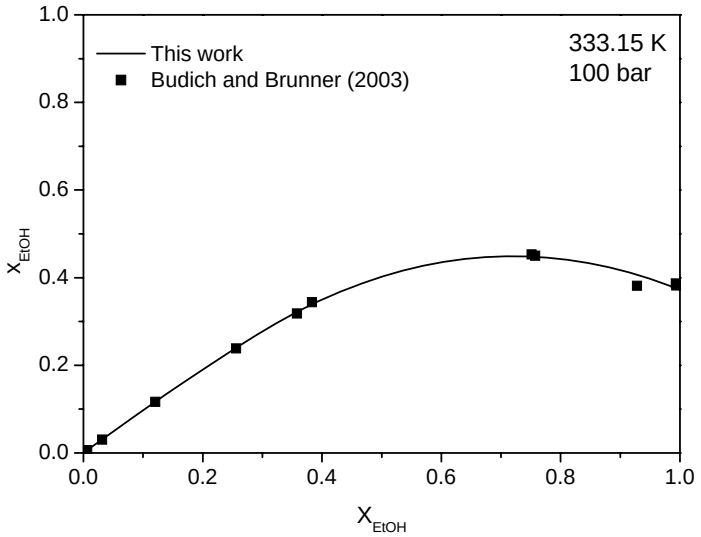


**Figure 3.17** *Fitting of ethanol mole fraction in the liquid phase as function of the pseudobinary mole fraction of ethanol in the liquid phase.*

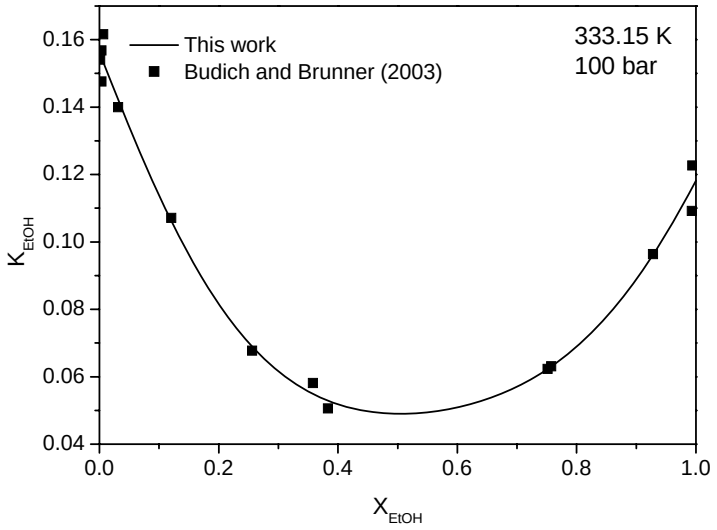


**Figure 3.18** *Fitting of ethanol K value (mole basis) as function of the pseudobinary mole fraction of ethanol in the liquid phase.*

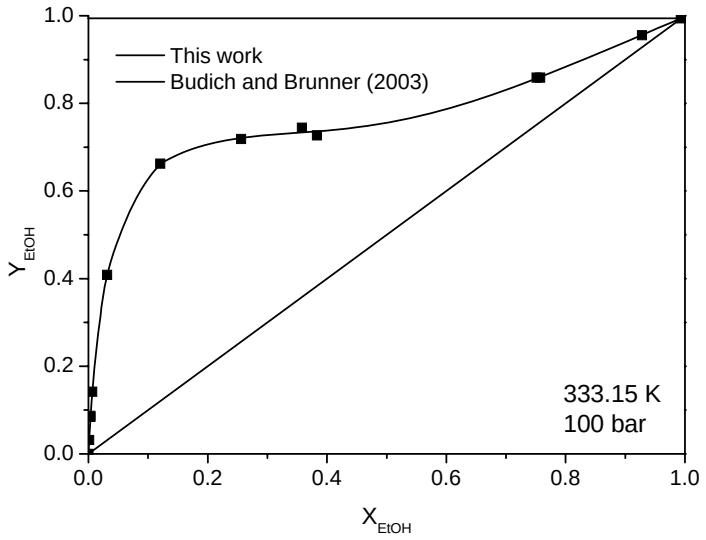


**Figure 3.19** *Fitting of the pseudobinary mole fraction of ethanol in the supercritical phase as function of the pseudobinary mole fraction of ethanol in the liquid phase.*

Second, also the relation between the ethanol K- value and the pseudobinary ethanol mole fraction in the liquid phase, as well as the relation between the pseudobinary ethanol mole fraction in the supercritical phase and that in the liquid phase were obtained (Figures 3.18 and 3.19).

The first correlation allows determining the composition of the liquid phase once $X_{EtOH}$ is known, by means of:

$$x_{H_2O} = \frac{1 - X_{EtOH}}{X_{EtOH}} \cdot x_{EtOH} \tag{3.29}$$

$$x_{CO_2} = 1 - x_{EtOH} - x_{H_2O} \tag{3.30}$$

where $x_i$ is the molar fraction of component $i$ in the liquid phase.

On the base of the correlation of Figures 3.18 and 3.19 is then possible to calculate also the composition of the vapour phase with the equations:

$$y_{EtOH} = K_{EtOH} \cdot x_{EtOH} \tag{3.31}$$

while water and $CO_2$ mole fraction, in the supercritical phase can be obtained by:

$$y_{H_2O} = \frac{1 - Y_{EtOH}}{Y_{EtOH}} \cdot y_{EtOH} \tag{3.32}$$

$$y_{CO_2} = 1 - y_{EtOH} - y_{H_2O} \tag{3.33}$$

It was difficult to fit the data of the Figure 3.17 and 3.18 with a unique equation. So the interpolating equations for the ethanol mole fraction are:

$$x_{EtOH} = -0.6812 X_{EtOH}^2 + 0.0301 X_{EtOH}^2 + 0.9838 X_{EtOH} \tag{3.34}$$

$$x_{EtOH} = -0.972615 X_{EtOH}^2 + 1.39964 X_{EtOH} - 0.05463 \tag{3.35}$$

The first one applied when $0 \leq X_{EtOH} \leq 0.236344$ and the second one when $0.236344 \leq X_{EtOH} \leq 1$.

The same happens for the correlation between $Y_{EtOH}$ and $X_{EtOH}$ and the interpolating curves are:

$$Y_{EtOH} = 3333218 X_{EtOH}^5 - 404802 X_{EtOH}^4 + 24977 X_{EtOH}^3 - 921. X_{EtOH}^2 + 26 X_{EtOH} \tag{3.36}$$

in the range of $0 \leq X_{EtOH} \leq 0.030260$,

$$Y_{EtOH} = 42.12 X_{EtOH}^5 - 97.31 X_{EtOH}^4 + 85.08 X_{EtOH}^3 - 34.60 X_{EtOH}^2 + 6.65 X_{EtOH} + 0.233 \tag{3.37}$$

for $0.030260 \leq X_{EtOH} \leq 0.12237$ and

$$Y_{EtOH} = 2.87345 X_{EtOH}^5 - 10.20116 X_{EtOH}^4 + 13.5792 X_{EtOH}^3 - 7.95137 X_{EtOH}^2 + 2.20857 X_{EtOH} + 0.48961 \tag{3.38}$$

for $0.122370 \leq X_{EtOH} \leq 0.9939$ and finally

$$Y_{EtOH} = 0.87391 X_{EtOH} + 0.12609 \tag{3.39}$$

for $X_{EtOH} > 0.9939$. The interpolating curve chosen in order to represent the $K_{EtOH}$ value as a function of the pseudobinary mole fraction is:

$$Y_{EtOH} = -1.3829 X_{EtOH}^6 + 4.5638 X_{EtOH}^5 - 5.3712 X_{EtOH}^4 + 2.5428 X_{EtOH}^3 + 0.0604 X_{EtOH}^2 + 0.4510 X_{EtOH} + 0.15623 \tag{3.40}$$

Using these correlations the resulting curves of $Z_y$ and $Z_x$ are well represented (Figures 3.20).

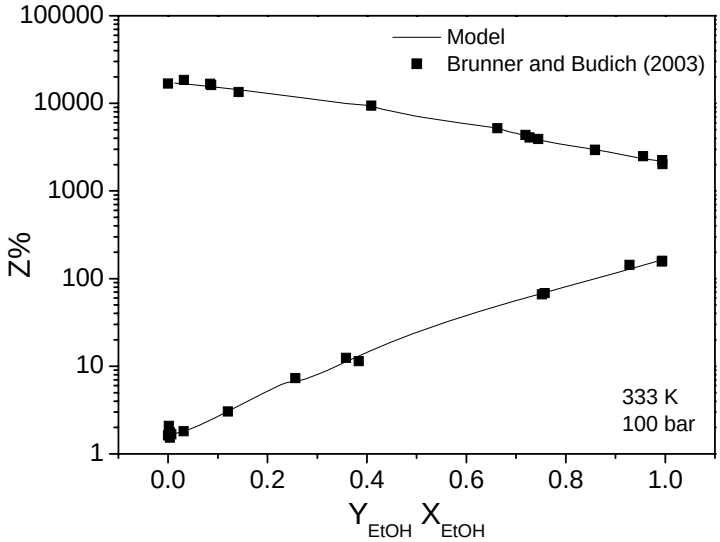


**Figure 3.20** *Zy and Zx curves calculated starting from the correlations from Eq. (3.36) to Eq. (3.40).*

The Fortran subroutines used to simulate the supercritical extraction of ethanol with supercritical $CO_2$ are reported in appendix A.

### *3.3.3 Pure $CO_2$: Benedict-Webb-Rubin-Starling*

The supercritical extraction of ethanol with $CO_2$ involves compressors and pumps and these units cover a significant share of the process energy demand. It is important to have a thermodynamic model that allows a precise determination of entropy, enthalpy changes and, consequently, a reliable calculation of the energy needs.

Different Aspen thermodynamic models were tested in order to recognize the best one.

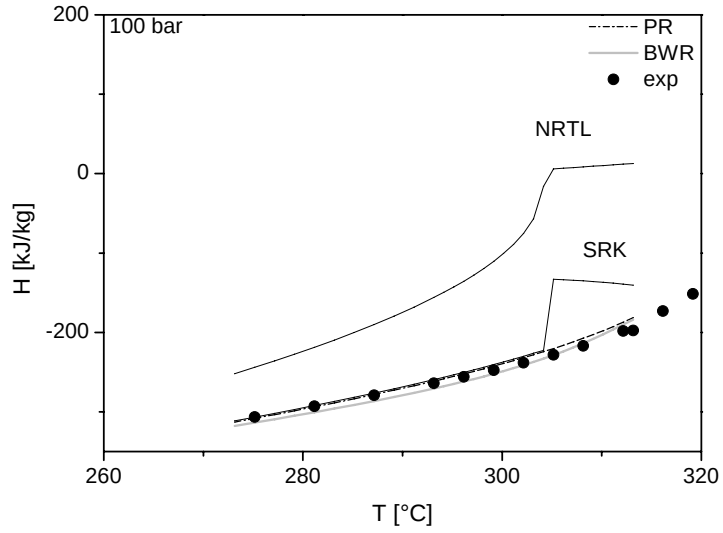


**Figure 3.21** *Enthalpy changes with temperature at 100 bar. The enthalpy values are referred at T 298.15 K and 1 bar.*

Four different models were checked and compared with the results of a $CO_2$ specific literature model (Sievers, 1984). At pressure of 1 bar all the models give similar results while when the pressure is raised up to 100 bar the NRTL (non random two liquid) model and the SRK (Soave-Redlich-Kwong) equation of state give wrong results. Figure 3.21 shows the enthalpy changes with temperature at pressure of 100 bar.
In Figures 3.22 the entropy changes of $CO_2$ at 100 bar as a function of temperatures are reported. In this case all the models tested gave good results at 1 bar, but when the pressure is 100 bar NRTL and SRK were not able to represent the system, while PR and BWRS gave good results.

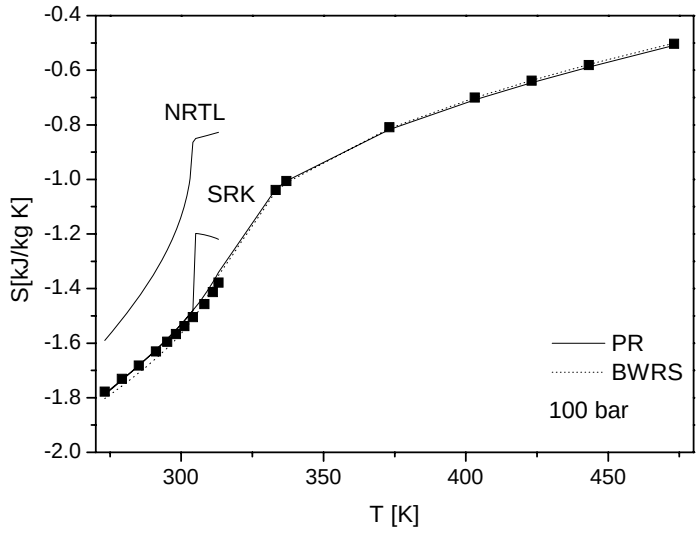


**Figure 3.22** *Entropy changes with temperature at 100 bar. Comparison of different models. The entropies are referred at T 298.15 K and 1 bar.*

For all the reason above the BWRS model was chosen to represent the system when almost pure $CO_2$ is involved. The Benedict-Webb-Rubin-Starling equation-of-state (Benedict *et al.,* 1940, Han and Starling, 1972, Starling, 1973) is the basis of the Aspen's BWRS property method.

## 3.4 Extraction column simulation

In order to perform the simulation the extraction column was conveniently split into a cascade of theoretical stages, and Aspen Plus$^{TM}$ was used to solve their mass balances, while energy balances were neglected. The model at 100 bar and 333.15 K was validated comparing the results obtained with the simulation of the countercurrent extraction column with calculations presented by Budich and Brunner (2003) by means of the Ponchon / Savarit method. Figure 3.23 shows simulation results compared with literature one.

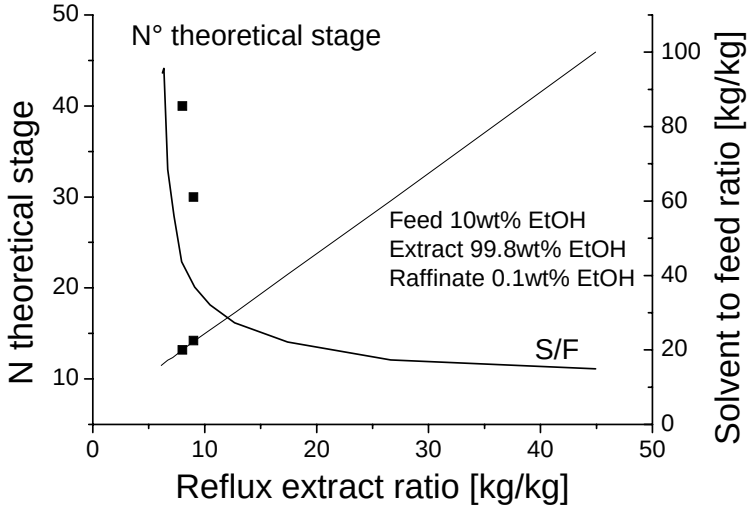


**Figure 3.23** *Comparison between the simulation results of column with 30 and 40 theoretical stage (point) and literature results (lines) obtained with the Ponchon savarit method (Budich and Brunner, 2003).*

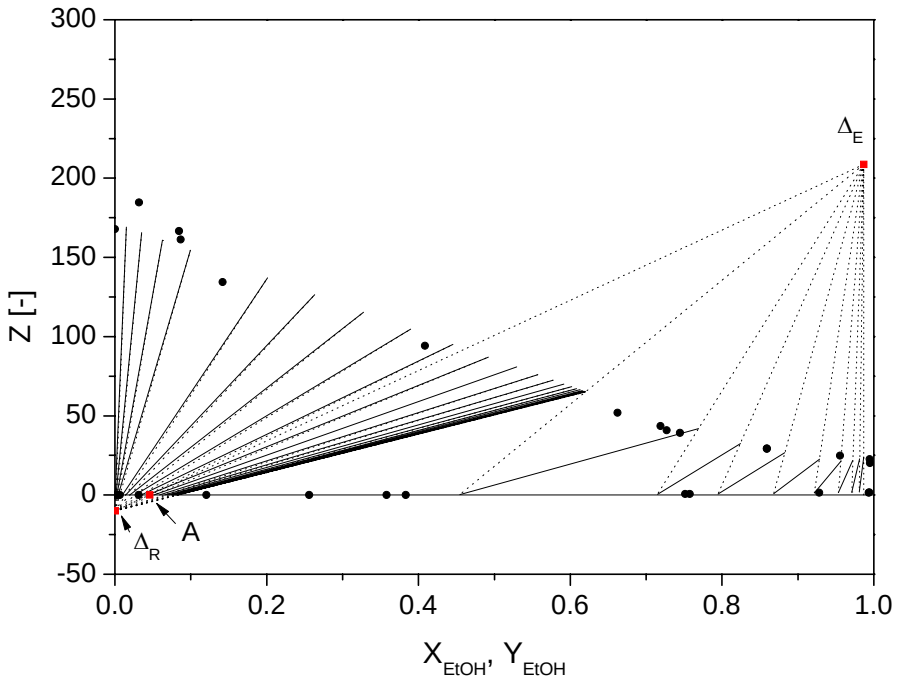


**Figure 3.24** *Plot of the composition of the theoretical stage. The points are the experimental equilibrium by Budich and Brunner (2003). The tie lines are continuous while the operating lines are dotted.*

Figure 3.24 shows the simulation results of a supercritical extraction column of 30 theoretical stages. The feed stage is the 15$^{th}$ from the top, the solvent to feed ratio is equal to 22.5 and the reflux ratio is 9 in mass basis. With these conditions at the top of the column an ethanol pseudobinary concentration of 99.81% (w/w) is achieved while at the bottom 0.146 % (w/w) is obtained. The symbols are the experimental equilibrium points by Budich and Brunner

(2003), the continuous lines represent liquid and vapour phases of every tray (simulated), while the dotted segments the operating lines. The plot of these lines shows that the system respects the Jänecke construction. Looking at the sensitivity of Figure 3.23 it is clear that an increase in the number of theoretical stage over 40 does not lead to a substantial decrease of the solvent usage. For this reason in all the following technical options investigated a number of 40stages was used.

## 3.5 Nomenclature

$x_i$ = molar fraction of component *i* in the liquid phase (-)
$y_i$ = molar fraction of component *i* in the vapour phase (-)
$Z_x$ = solvent molar fraction in the liquid phase (solvent free basis) (-)
$Z_y$ = solvent molar fraction in the vapour phase (solvent free basis) (-)
$X_i$ = pseudobinary molar fraction of component *i* ($CO_2$ free) in the liquid phase (-)
$Y_i$ = pseudobinary molar fraction of component *i* ($CO_2$ free) in the vapour phase (-)
$A_i$ = Helmholtz energy
$T$ = temperature (K)
$K_i$ = K-value of component *i* (-)
$S_{i,j}$ = selectivity of component *i* (-)
$L_i$ = loading of component *i* (g/100g)

Subscripts:
m = mixture
EtOH = ethanol
$H_2O$ = water
$CO_2$ = carbon dioxide

## 3.6 References

Arce, A., J. Martinez-Ageitos, and A. Soto (1996). VLE for Water + Ethanol + 1-Octanol Mixtures. Experimental Measurements and Correlations. *Fluid Phase Equilib.*, **122,** 117-129.

Benedict, M., G.B. Webb, and L.C. Rubin (1940). An Empirical Equation for Thermodynamic Properties of Light Hydrocarbons and Their Mixtures I. Methane, Ethane, Propane and n-Butane. *J. Chem. Phys*., **8**, 334-345.

Budich, M. and G. Brunner (2003). Supercritical Fluid Extraction of Ethanol from Aqueous Solution. *J. of Supercr. Fluid*, **25,** 45-55.

Day, C.Y., C.J. Chang, and C.Y Chen (1999). Phase Equilibrium of Ethanol + $CO_2$ and Acetone at Elevated Pressures. *J.Chem. Eng. Data,* **44***, 365.*

Durling, N.E., O.J. Catchpole, S.J. Tallon, and J.B. Grey (2007). Measurement of the Ternary Phase Equilibria for High Pressure Carbon Dioxide- Ethanol- Water Mixtures. *Fluid Phase Equilib.*, **252,** 103-113.

Furuta, S., N. Ikawa, R. Fukuzato, and N. Imanshi (1989). Extraction of Ethanol from Aqueous Solutions Using Supercritical Carbon dDioxide. *Kagaku Kogaku Ronbunshu*, **15**, 519–525.

Gilbert, M.L. and M.E. Paulaitis (1986). Gas-Liquid Equilibrium for Ethanol-Water-Carbon Dioxide Mixtures at Elevated Pressures. *J. Chem. Eng. Data*, **31**, 296-298.

Han, M.S. and K.E. Starling (1972). Thermo Data Refined for LPG. Part 14: Mixtures, *Hydrocarbon Process.*, **51**, 129-132.

Huron, M.J. and J. Vidal (1979). New Mixing Rules in Simple Equations of State for Representing Vapour-Liquid Equilibria of Strongly Non-Ideal Mixtures. *Fluid Phase Equilib*., **3**, 255-271.

Lim, S.J. and Y.Y. Lee (1994). Phase Equilibria for Carbon Dioxide- Ethanol – Water System at Elevated Pressures. *J. of Supercritical Fluid*, **7**, 219-23.

Nagahama, K., J. Suzuki, and T. Suzuki (1988). High pressure vapor–liquid equilibria for the supercritical $CO_2$ + ethanol + water system. In M. Perrut (Ed.), *Proceedings of the 1st International Symposium on Supercritical Fluids*, Nice, France.

Shyu, G.S., N.S.M. Hanif, K.R. Hall, and P.T. Eubank (1996). Carbon dioxide-water phase equilibria results from the Wong-Sandler combining rules. *Fluid Phase Equilib.*, **130**, 73-85.

Sievers, U. (1984). *Die thermodynamischen Eigenschaften von Kohlendioxid.* VDI- Verlag GmbH Düsseldorf, Dusseldorf (Germany).

Starling, K.E. (1973). *Fluid Themodynamic Properties for Light Petroleum Systems*. Gulf Publishing Co., Houston, Texas (U.S.A.).

Wong, D.S. and S.I. Sandler (1992a). A Theoretically Correct New Mixing Rule for Cubic Equations of State for Both Highly and Slightly Non-ideal Mixtures. *AIChE J.*, **38**, 671–680.

Wong, D.S. and S.I. Sandler (1992b). Equation-of-state Mixing Rule for Non-ideal Mixtures Using Available Activity Coefficient Model Parameters and That Allows Extrapolation over Large Ranges of Temperature and Pressure. *Ind. Eng. Chem. Res.*, **31**, 2033–2039.

Zetzl, C., V. Patil, M. Budich, and G. Brunner (2007). One Step Purification to Absolute Alcohol from Sugar Cane Molasse by Means of Supercritical $CO_2$. In Proceedings of: *Prosciba, I Iberoamerican Conference on Supercritical Fluids*, Iguassu Falls (Brasil). April 10-13, paper SC-017.

# Chapter 4

# Supercritical $CO_2$ extraction of ethanol[2]

Previous research works addressed the use of supercritical carbon dioxide for the extraction of ethanol from water mixtures (Budich and Brunner, 2003 and Ikawa *et al.*, 1993) and proposed this application as a way to obtain absolute grade fuel ethanol avoiding azeotropic distillation or molecular sieve purification (Zetzl *et al.,* 2007). These authors experimentally proved that the separation is possible, so that the azeotrope can be broken and an ethanol weight fraction of 0.999 (w/w) can be achieved by supercritical extraction only. However, the consequences of the choice of this alternative to distillation on the economy of a large scale plant have not been studied yet.

The aim of this part of the thesis is to study the effect of the integration of supercritical $CO_2$ extraction of ethanol in a medium scale bioethanol plant from corn, and the comparison of capital costs and operating costs of different technical options with the current process.

The thermodynamic models described in Chapter 3 were used in order to simulate the process and the obtained results allowed estimating the number and the size of the required equipment as well as the utilities needs. This lead to the determination of capital investment and operating costs of the new process. The two different technical options investigated differ in the way ethanol is recovered from supercritical $CO_2$. The first option considers the use of molecular sieves, while the second one employs a second distillation column.

## 4.1 Column simulation

The overall capacity of the plant considered is 109,700 t/y of bio-ethanol, starting from approximately 41,900 kg/h of corn grain (a medium size plant).

**Table 4.1** *Composition of the feed stream.*

| | **Weight fraction %** |
|---|---|
| **Water** | 88.043 |
| **Ethanol** | 11.817 |
| **$CO_2$** | 0.140 |
| **Total flow [t/h]** | 115.4 |

[2] Part of this Chapter has been published in proceedings of: *11th European Meeting on Supercritical Fluids* (see Page XVI).

In all the simulations the composition of the extraction column feed stream was the one of Table 4.1 (data from Franceschin *et al.,* 2007). Minor components (glycerol, acetic acid) that are usually present in the beer were not accounted for, because of the lack of thermodynamic data in supercritical $CO_2$. The possibility that corn oil can be extracted from the corn residue using supercritical $CO_2$ was not taken into account as well. The solids were not simulated because it was hypothesized that they do not influence the extraction equilibria. The simulation of the 100 bar and 333 K SFE was accomplished by means of the correlation showed in Chapter 3.3.2.2.

The number of theoretical trays for both the options was set at 40 with the feed stage at the 34$^{th}$ tray from the top. The reflux ratio and the amount of $CO_2$ at the bottom were adjusted in order to obtain an extract with an ethanol pseudobinary mass fraction ($W_{EtOH}$) of 99.8% and a raffinate with only 0.1% (w/w) of ethanol in water.

## 4.2 1$^{st}$ technical option simulation and design

In this case the supercritical extraction is carried out at 100 bar and 333.15 K while the recovery of the ethanol from the extract (top) is achieved by using an activated carbon system as proposed by Hagen and Hartwig (1985).

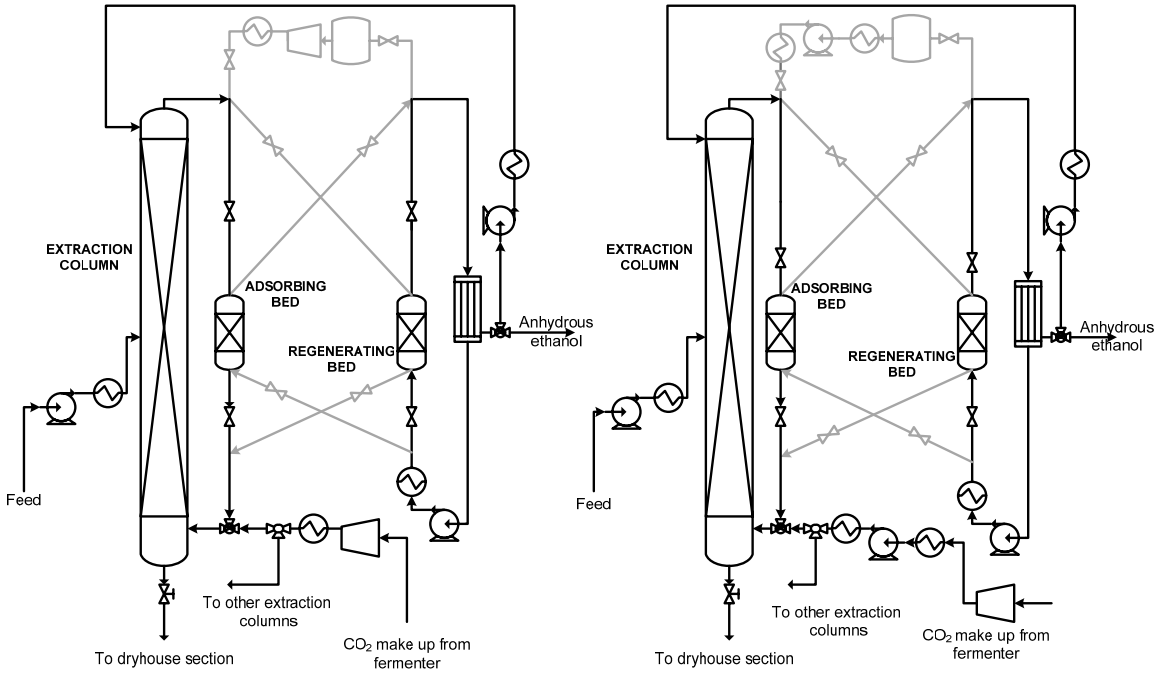


*(a)* *(b)*

**Figure 4.1** *Schemes of the 1$^{st}$/a option (a) and of the 1$^{st}$/b option (b).*

As clear from Figures 4.1a and 4.1b the $CO_2$ is fed at the bottom of the extraction column, the stream from the fermenter (Feed) at tray 34 from the top, and anhydrous ethanol is fed at the top as reflux. The column achieves the ethanol water separation: anhydrous ethanol in

$CO_2$ is obtained ($w_{CO_2}$ = 95.42% w/w, $w_{EtOH}$ = 4.57% w/w) at the top and the water is extracted from the bottom. In order to separate ethanol from this very large amount of $CO_2$ the stream is passed thorough to an activated carbon bed where anhydrous ethanol is absorbed ($W_{H_2O}$ = 0.2% w/w). The recovered $CO_2$ is recycled back to the extraction unit without pressure changes except for the friction loss. Once the adsorbing bed is saturated the ethanol has to be recovered. A part of the obtained ethanol is used as column reflux while the remaining is stored and sold.

The regeneration of the activated carbon bed (removal of alcohol) is achieved by stripping with $CO_2$ at 473.15 K and 10 bar (Hagen and Hartwig, 1985). In this way the ratio between the extraction and the regeneration $CO_2$ flow rates is around 1.28.

In order to separate ethanol from $CO_2$ the stream is cooled down to 308.15 K. This last temperature was chosen after a sensitivity analysis. Figure 4.2 shows that working at 308.15 K the recovery of the ethanol present by means of condensation is around the 80%. The remaining 20% is recycled back with the $CO_2$ stream.

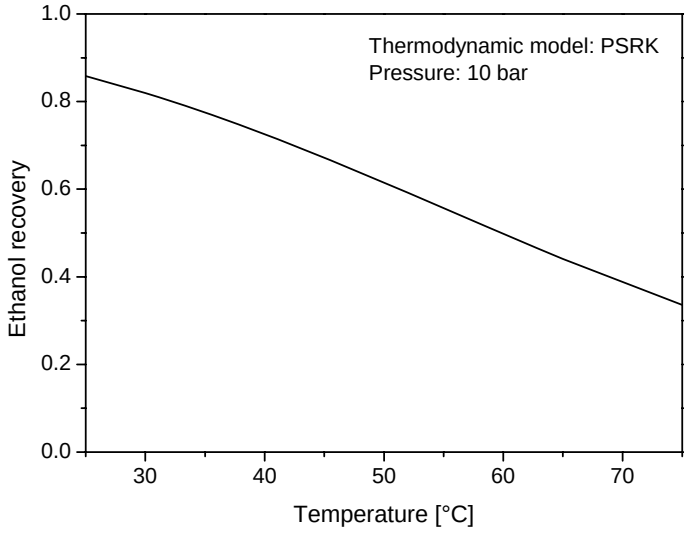


**Figure 4.2** *Ethanol recovery as function of the cooling temperature.*

The first technical option is then subdivided into two cases that differ in the way the $CO_2$ from the regenerating bed is pumped back to the extraction pressure.

This can be done by direct compression of the gas up to 100 bar (with a compressor) or in two steps: by compressing the gas up to 50 bar with a compressor and then, after condensation, pumping the liquid $CO_2$ from 50 bar to 100 bar. We have identified as $1^{st}$/a option the use of compressors up to 100 bar (for both make up and holdup compression) whereas $1^{st}$/b indicates the compressors/pumps coupled system.

### 4.2.1 Extraction column

Table 4.2 shows the results obtained from the simulation of an extraction column of 40 theoretical stages that work at 333.15 K and 100 bar.

**Table 4.2** *Simulation results for the 1st technical option columns.*

| Reflux ratio [kg/kg] | S/F ratio [kg/kg] |
|---|---|
| 7.2 | 19.9 |

The column diameter is calculated starting from the flooding relationship measured by Stockfleth and Brunner (1999) and reported in Figure 4.3.

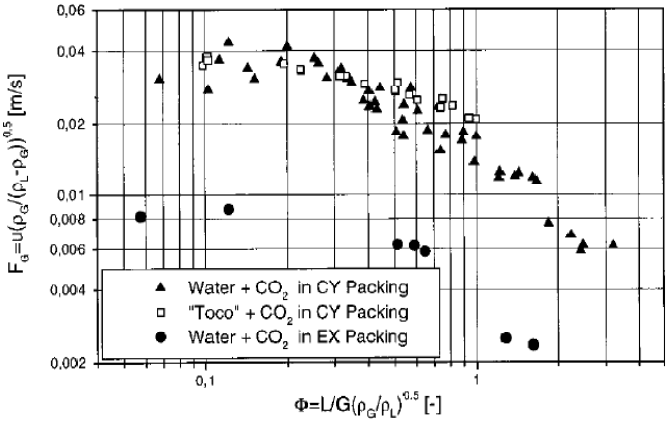


**Figure 4.3** *Flooding diagram for pure water and supercritical $CO_2$ (Stockfleth and Brunner, 1999).*

This relationship links together the flow parameter Φ [-]

$$\Phi = \frac{L}{G}\left(\frac{\rho_G}{\rho_L}\right)^{0.5} \tag{4.1}$$

with the gas capacity factor $F_G$ [m/s]

$$F_G = u\left(\frac{\rho_G}{\rho_L - \rho_G}\right)^{0.5} \tag{4.2}$$

In Eqs. (4.1) and (4.2) $L$ and $G$ are the mass flow rates of liquid and supercritical phase [kg/h m$^2$], ρ is the density [kg/m$^3$] and $u$ is the velocity of the supercritical phase [m/s]. This relation allows determining the flooding diameter of the column in case Sulzer CX package is used and the liquid phase is pure water. Diameter calculation were performed by means of the relationship of Figure 4.3 even though ethanol is present in the liquid phase, because the

vapour phase cross section capacity decrease significantly increasing the water content of the liquid phase. This is shown in the experiments performed by Budich and Brunner (2003). Due to the large amount of $CO_2$ a unique extraction column cannot be used, as the resulting diameter would be technically infeasible. A maximum diameter of 1.8 meter was chosen as technical limit because of the Sulzer CX package.

**Table 4.3** *Sizing of the 1st option extraction columns.*

| | **1st option** |
|---|---|
| **Φ [–]** | 0.0249 |
| **Number of column in parallel** | 19 |
| **Column diameter [m]** | 1.77 |
| **Column high[m]** | 13.2 |

Table 4.3 reports the extraction column design results. The columns height is calculated assuming an HETS of 0.33 as reported from Budich and Brunner (2003). The resulting value is underestimated because if also the solids are sent to the column, the structured package cannot be used and have to be replaced with "disc and donuts" tray. Hypothesizing that it is possible to perform the extraction with this type of trays, surely the tray efficiency decreases and this leads to higher column heights.

### *4.2.2 Activated carbon system*

The activated carbon system is sized using the data from Hagen and Hartwig (1985). An activated carbon system for every column was designed in order to keep the dimension of this system low. It was assumed a bed density of 500 kg/m$^3$, an internal porosity of 0.6 (Perry *et al.,* 1999), and finally an absorption capacity of 417 $g_{EtOH}/kg_{carbon}$ (Hagen and Hartwig, 1985). With a working time of 1 hour there is the need of 2 beds with a diameter of 2 meters and 8 meters high that working in parallel so, when one is used in adsorption the other can be regenerated, making the process continuous.

### *4.2.3 Pumps, compressors and heat exchangers*

The supercritical extraction columns work at 100 bar, so from both the capital investment and the energetic point of view, it is important to consider the compression phase. The first stream that has to be raised up to 100 bar is the column feed. The total flow rate of the ethanol and water mixture coming from the fermenters is 115.42 t/h and it is available at 1 bar. The $CO_2$ make up is another stream that is available at 1 bar and has to be raised up to the extraction pressure. In this process the main $CO_2$ losses are at the bottom of the columns with the liquid output (overall amount 4,100 kg/h of $CO_2$) and at the top with the anhydrous ethanol streams (overall amount 780 kg/h). The amount of $CO_2$ produced at 1 bar during the

fermentation (13,100 kg/h) is enough to supply the required makeup for the extraction. A third stream, that has to be pumped or compressed from 10 bar to 100 bar, is the activated carbon system hold up, in fact every hour the regenerated bed is switched with the saturated one and about 5,380 kg/h of $CO_2$ have to be compressed back from the bed working at 100 bar (and has to be depressurized to 10 bar) to the one that was under regeneration at 10 bar and has to be pressurized to 100 bar. Finally the reflux streams (5,394 kg/h for each column) has to be pumped from 10 bar (pressure of the regenerating bed) to 100 bar and of course heated up to the extraction temperature. In the other cases, like for example the pumps located in the cycle of the carbon absorber regeneration, only the friction loss have to be supplied. These units are not taken into account because negligible if compared with the other for both operating costs and capital investment. The thermal utilities usage and the sizing of the heat exchangers are tightly connected with the choice of the technical option. As already explained, in the 1st/a option only compressors are used while in the 1st/b option the gas is first compressed to 50 bar and then condensed through two steps. The first one involves cooling water and the second one needs the use of a refrigeration system due to the lower temperature. Once a liquid phase is obtained, a pump is used to reach 100 bar, and finally the temperature is raised up to the extraction temperature again. The requirement of energy of pumps and compressors are estimated by means of Aspen Plus ™ simulations as well as the heat exchangers duties. These units are then roughly sized assuming an overall heat transfer coefficients $U$ of 850 W/m$^2$K for condensers and 200 W/m$^2$K in case of cooling or heating of gas without change of physical state. The overall efficiency of compressors was set at 70% while the one of pumps at 90%.

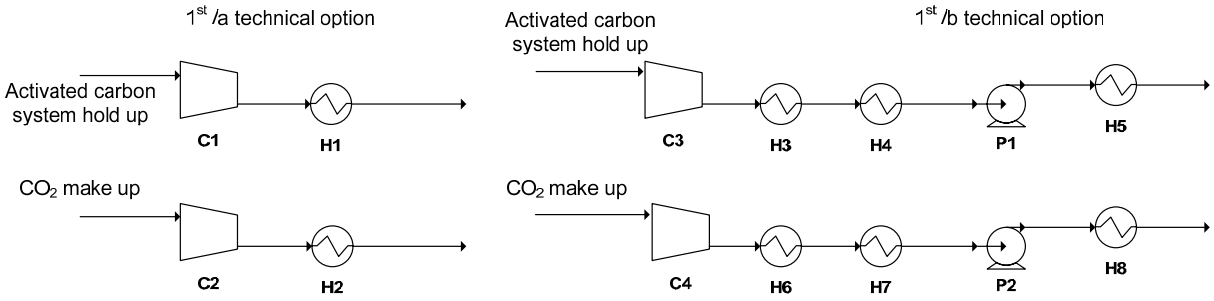


**Figure 4.4** *Identification of pumps, compressors and heat exchangers of the 1st/a option and 1st/b one.*

Figure 4.4 shows the units of the 1st/a and 1st/b options while Tables 4.4 and 4.5 the utilities usage and the size of the equipment. The energy required to pump the liquid feed of the extraction column from 1 bar to 100 bar is equal to 368.5 kW (for the whole fermenter output stream) and is the same for both the options as well as the energy to pump the reflux from 10 bar to 100 bar (432 kW).

**Table 4.4** *Utilities usage and the size of the equipment for 1st/a option of Figure 4.4.*

| Unit | in | out | Total units N° | | value |
|---|---|---|---|---|---|
| **C1** | 10 bar | 100 bar | 19 | Elect. Energy [kW] | 506.7 |
| **H1** | 491 °C | 60 °C | 19 | Cooling water [t/h] | 47.5 |
| | | | | Exchanger area [$m^2$] | 24.2 |
| **C2** | 1 bar | 100 bar | 1 | Elect. Energy [kW] | 843.7 |
| **H2** | 627 °C | 60°C | 1 | Cooling water [t/h] | 55.8 |
| | | | | Exchanger area [$m^2$] | 23.7 |

**Table 4.5** *Utilities usage and the size of the equipment for 1st b option of Figure 4.4.*

| Unit | in | out | Total units N° | | value |
|---|---|---|---|---|---|
| **C3** | 10 bar | 50 bar | 19 | Elect. Energy [kW] | 330.2 |
| **H3** | 383 °C | 40 °C | 19 | Cooling water [t/h] | 33.4 |
| | | | | Exchanger area [$m^2$] | 25.3 |
| **H4** | 40 °C | 14.5°C | 19 | Refrigeration [kW] | 348.1 |
| | | | | Exchanger area [$m^2$] | 19.1 |
| **P1** | 50 bar | 100 bar | 19 | Elect. Energy [kW] | 8.9 |
| **H5** | 21 °C | 60 °C | 19 | Steam [kg/h] | 467.6 |
| | | | | Exchanger area [$m^2$] | 11.8 |
| **C4** | 1 bar | 50 bar | 1 | Elect. Energy [kW] | 665.8 |
| **H6** | 514 °C | 40 °C | 1 | Cooling water [t/h] | 42.1 |
| | | | | Exchanger area [$m^2$] | 25.3 |
| **H7** | 40 °C | 14.5 °C | 1 | Refrigeration [kW] | 316.0 |
| | | | | Exchanger area [$m^2$] | 17.3 |
| **P2** | 50 bar | 100 bar | 1 | Elect. Energy [kW] | 9.9 |
| **H8** | 21 °C | 60 °C | 1 | Steam [kg/h] | 424.4 |
| | | | | Exchanger area [$m^2$] | 10.7 |

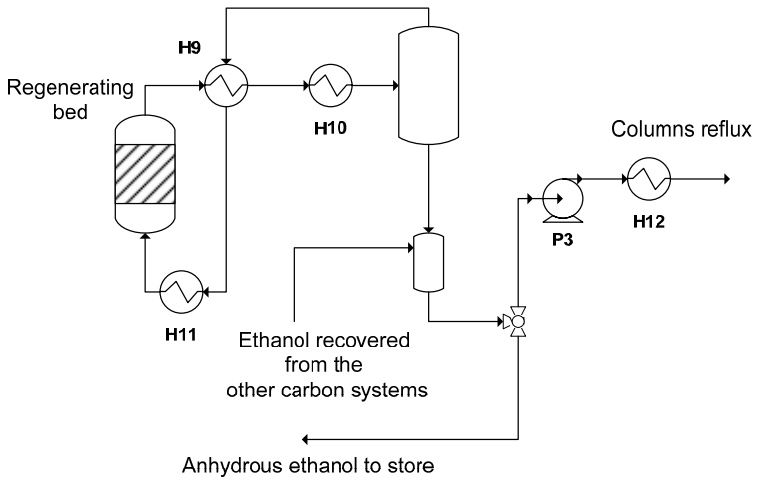


**Figure 4.5** *Units involved in the regeneration of the activated carbon bed.*

The number of the equipment is kept as low as possible and is clearly shown from the tables. So, the whole $CO_2$ make up is compressed by means of a unique compressor and then the flow is split between the columns. The same happens for the compression of the reflux stream. The pumps and heat exchangers involved in the carbon regeneration cycle are shown in Figure 4.5. Table 4.6 reports the utilities usage and the size of the equipment depicted in Figure 4.5.

**Table 4.6** *Utilities usage and the size of the equipment involved in the regeneration of the activated carbon bed for both the 1st/a option and the 1st/b option.*

| Unit | in | out | Total units N° | | value |
|---|---|---|---|---|---|
| **H9** | 200 °C | 62 °C | 19 | Utilities [t/h] | 0.0 |
| | 35 °C | 190 °C | | Exchanger area [$m^2$] | 301.0 |
| **H10** | 62 °C | 35 °C | 19 | Cooling water [t/h] | 128.5 |
| | | | | Exchanger area [$m^2$] | 129.0 |
| **H11** | 190 °C | 200 °C | 19 | Steam [kg/h] | 547.4 |
| | | | | Exchanger area [$m^2$] | 85.0 |
| **P3** | 10 bar | 100 bar | 1 | Elect. Energy [kW] | 432.0 |
| **H12** | 37 °C | 60 °C | 1 | Steam [kg/h] | 3054.0 |
| | | | | Exchanger area [$m^2$] | 21.3 |

## 4.3 2nd technical option simulation and design

According to this option the supercritical extraction is carried out at 100 bar and 333.15 K (as in the first one) while the recovery of ethanol is done by a second distillation column running at 50 bar.

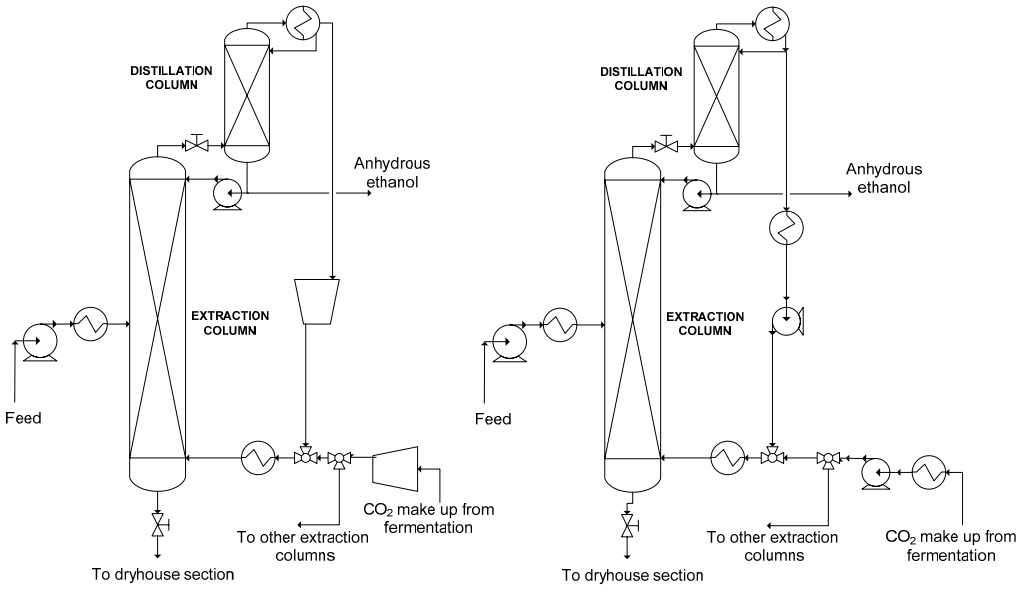


*(a)* *(b)*

**Figure 4.6** *Scheme of the 2nd/a technical option (a) and of the 2nd/b (b) option.*

This idea has been proposed by both Ikawa *et al.,* (1993) and Budich and Brunner (2003).
The distillation is necessary because the depressurization to 50 bar does not allow the recovering of enough ethanol to permit the required reflux flow for the extraction unit.
The process is schematically depicted in Figure 4.6. The compression of the $CO_2$ make up from 1 bar to 100 bar can be done as previously outlined, by using a compressor up to 100 bar or by using a compressor up to 50 bar, followed by condensation and a pump up to 100 bar. At the same time the recovery of the $CO_2$ at the top of the column can be done either using a pump if the total condenser is used, or a compressor if the condenser is a partial one. We have identified as 2nd/a option the one which refers to the use of compressor up to 100 bar for both make up and recovery of $CO_2$, instead the 2nd/b option indicates the use of the coupled system compressor-pump, and of a total condenser in the distillation column.

### *4.3.1 Extraction column*

The column was simulated and then was sized using correlations (4.1) and (4.2), hypothesizing HETS 0.33. The only difference with the first option is the composition of the extraction column reflux.

**Table 4.7** *Simulation results for the technical option 2nd.*

| Reflux ratio [kg/kg] | S/F ratio [kg/kg] |
|---|---|
| 7.3 | 20.1 |

In the 1st option this is the one in equilibrium at the operating condition of the flash (H10) in the carbon regeneration cycle (i.e. 35°C and 10 bar corresponding to about 5.16 % w/w of $CO_2$) while for the 2nd option it is the one in equilibrium at the condition at the bottom of the distillation column (i.e. 61.4 °C and 50 bar corresponding to about 21.2 % w/w of $CO_2$). Table 4.7 shows the reflux ratio of the extraction column and the solvent ($CO_2$) feed ratio obtained from the simulation.

**Table 4.8** *Sizing of the extraction column in the case of 2nd option.*

| | 2nd option |
|---|---|
| **Φ [–]** | 0.0260 |
| **Number of column** | 19 |
| **Column diameter [m]** | 1.78 |
| **Column high[m]** | 13.2 |

These results show that there is no difference between the two cases. In both 1st and 2nd case 19 extraction column 13.2 meters high and with a diameter of 1.8 meters are needed.

### 4.3.2 Distillation column

The Aspen Plus™ simulation of the distillation column used to recover the ethanol from supercritical $CO_2$ showed that only few theoretical stages are needed for the complete recovery of ethanol. But of course the whole amount of supercritical $CO_2$ has to be treated and this leads to very large diameters. Setting a number of 6 theoretical stages (total height of 2 meters), in order to have a column diameter of 1.4 m it is necessary to use two distillation columns for each extraction columns (38 in the whole process). Table 4.9 shows the simulation results of one of the 38 columns at 50 bar with a mole reflux ratio of 0.11.

**Table 4.9** *Simulation results for the distillation columns. Flow rates are referred to each one of the 38 columns.*

| % (w/w) | Feed | Bottom | Top |
|---|---|---|---|
| **$CO_2$** | 95.42 | 21.15 | 99.97 |
| **Ethanol** | 4.57 | 78.73 | 0.0284 |
| **Water** | $7.4559\ 10^{-3}$ | 0.12 | $5.1567\ 10^{-4}$ |
| **Total flow [t/h]** | 64.575 | 3.728 | 60.847 |

The temperature at the top of the column is 287.8 K, and as shown in Table 4.9 the $CO_2$ is quite pure while at the bottom the temperature is 334.58 K. The energy requirement in terms of cooling utilities is huge. Moreover because of the low temperature at the top a refrigerator system have to be used. In each condenser 12.95 GJ/h have to be removed if the condenser is total ($2^{nd}$/b technical option) while only 1.68 GJ/h if the condenser is partial ($2^{nd}$/a technical option).

### 4.3.3 Pumps, compressors and heat exchangers

In the $2^{nd}$ technical option the streams that are mainly involved in pressure changes are: the extraction column feed (from the fermenters), the reflux stream, the $CO_2$ make up and the distillate stream of the distillation column. In Figure 4.7 the units involved in the make up and in the recovery of $CO_2$ are identified.

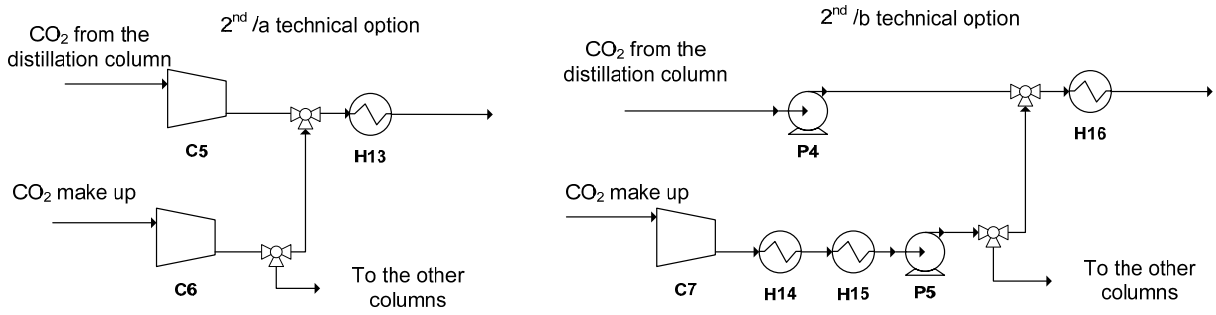


**Figure 4.7** *Units involved in the compression of the system make up and in the recovery of the $CO_2$ from the top of the distillation column to the bottom of the extraction column.*

Table 4.10 and 4.11 reports sizes and the utility consumptions of these units.

**Table 4.10** *Size and utilities consumption of the units reported in Figure 4.7 for 2nd/a option. COND= distillation column condenser.*

| Unit | in | out | Total units N° | | value |
|---|---|---|---|---|---|
| **C5** | 50 bar | 100 bar | 19 | Elect. Energy [kW] | 1164.1 |
| **H13** | 73 °C | 60 °C | 19 | Cooling water [t/h] | 65.5 |
| | | | | Exchanger area [$m^2$] | 145.6 |
| **C6** | 1 bar | 100 bar | 1 | Elect. Energy [kW] | 1308.0 |
| **COND** | 14.9 °C | 14.3 °C | 38 | Refrigeration [GJ/h] | 1.7 |

**Table 4.11** *Size and utilities consumption of the units reported in Figure 4.7 for 2nd b option. COND= distillation column condenser.*

| Unit | in | out | Total units N° | | value |
|---|---|---|---|---|---|
| **C7** | 1 | 50 | 1 | Elect. Energy [kW] | 1032.2<br>950.8 |
| **H14** | 514 °C | 40 °C | 1 | Cooling water [t/h] | 65.29 |
| | | | | Exchanger area [$m^2$] | 33.7 |
| **H15** | 40 °C | 14.5°C | 1 | Refrigeration [kW] | 489.9 |
| | | | | Exchanger area [$m^2$] | 28.2 |
| **P4** | 50 bar | 100 bar | 19 | Elect. Energy [kW] | 223.9 |
| **P5** | 50 bar | 100 bar | 1 | Elect. Energy [kW] | 13.9 |
| **H16** | 21°C | 60°C | 19 | Steam [t/h] | 10.6 |
| | | | | Exchanger area [$m^2$] | 267 |
| **COND** | 14.9 °C | 14.3 °C | 38 | Refrigeration [GJ/h] | 12.9 |

The energy necessary to pump the column feed from 1 bar to 100 bar is 368.5 kW (for the whole fermenters output stream) while the one of reflux pumps (from 50 bar to 100 bar) is 342.1 kW (in total), for both 2nd/a and 2nd/b options.

## 4.4 Economical analysis

In order to compare the two technical options considered from the economical point of view the capital investment and the operating costs were calculated using the simulation results and the calculated equipment size. The equipment purchase and installation costs were calculated starting from literature correlations (Ulrich and Vasudevan, 2006). In Table 4.12 the parameters and data used in the financial model are shown.

**Table 4.12** *Summary of the financial model parameters and data.*

| Data | Value | Reference |
|---|---|---|
| **Prices** | | |
| **Denaturated Ethanol** | 0.58 €/l | European Ethanol Market Report, 2007 |
| **DDGS** | 300 €/t | Industrial survey |
| **Corn** | 200 €/t | |
| **Water** | 0.041 €/t | Average industrial data |
| **Denaturant** | 0.26 €/l | Industrial data |
| **Yeasts** | 0.516 €/kg | Industrial information |
| **Enzymes** | 5€/kg (α amylase); 3.5 €/kg (β amylase) | Industrial data |
| **Urea** | 132.74 €/t | Industrial data |
| **Sulphuric acid** | 69.32 €/t | Industrial data |
| **Lime** | 51.62 €/t | Industrial data |
| **Utilities** | | |
| **Steam** | 15.97€ /t | Average industrial data |
| **Natural gas** | 0.268 €/kg | http://epp.eurostat.ec.europa.eu, May 2007 |
| **Electricity** | 0.1027€/kWh | http://epp.eurostat.ec.europa.eu, May 2007 |
| **Refrigeration** | 20$/GJ | |
| **Other costs** | | |
| **Labour** | 33,500€ / labour | Average industrial data |
| **Maintenance** | 3% TCI | Average industrial data |
| **Administration** | 2% Total revenue | Average industrial data |
| **Start up** | 10% TCI | Average industrial data |

In Figure 4.8a and b the different equipment contribution to the extraction section capital investment are shown for both the 1st/a and 1st/b technical option.

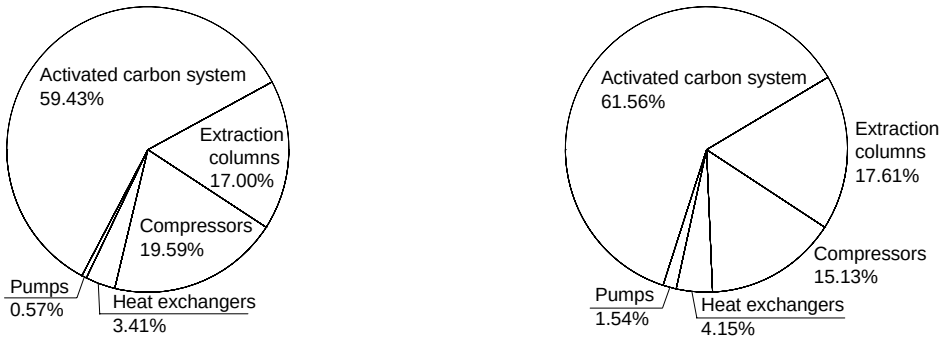


*(a)* *(b)*

**Figure 4.8** *Capital investment distribution for the supercritical extraction section of the 1st/a technical option (a) and the 1st/b one (b).*

It is clear that the largest part of the capital investment related to the supercritical extraction section depends on the activated carbon system. This is due to the low capacity of the

activated carbon to absorb ethanol (417g of ethanol for kg of activated carbon) leading to huge volumes (25 $m^3$ each bed). A large number of vessels is needed (38) and they have to resist to high pressure. For these reasons their contribution to the capital investment is noteworthy. A second major contribution is the one of the extraction columns, followed by the compressors. To calculate the total capital investment of the considered plant first the cost of the extraction section was calculated as sum of all the equipment installed costs, than this capital was added to the one of a traditional first generation ethanol plant of the same size to which the distillation section was excluded. It was assumed a total capital investment for the whole traditional first generation ethanol process of 70,000,000 € (Kranz and Worrell, 2001) of which a 13.45% is due to the distillation section (Krishnan *et al.*, 2000). The economic analysis results for the 1st/a and 1st/b technical options are reported in Table 4.13.

**Table 4.13** *Economic analysis results (the entry "thermal utilities" is referred to the sum of cooling water, steam and refrigeration costs).*

| | **1st/a option** | **1st/b option** |
|---|---|---|
| **Extraction section capital investment [M€]** | 162.86 | 157.21 |
| **Total capital investment [M€]** | 223.44 | 217.79 |
| **Electrical energy [M€/y]** | 15.29 | 12.52 |
| **Thermal utilities [M€/y]** | 3.47 | 6.78 |
| **Production cost [€/kg EtOH]** | 0.887 | 0.885 |

When using the compressors plus pumps coupled system, as expected, lower electricity usage and capital investment where found, but the thermal duty increases because of the needs of a refrigeration system to condensate the $CO_2$. The final production cost is similar for both of the options. In Figure 4.9 the different contributions to the ethanol production cost are shown.

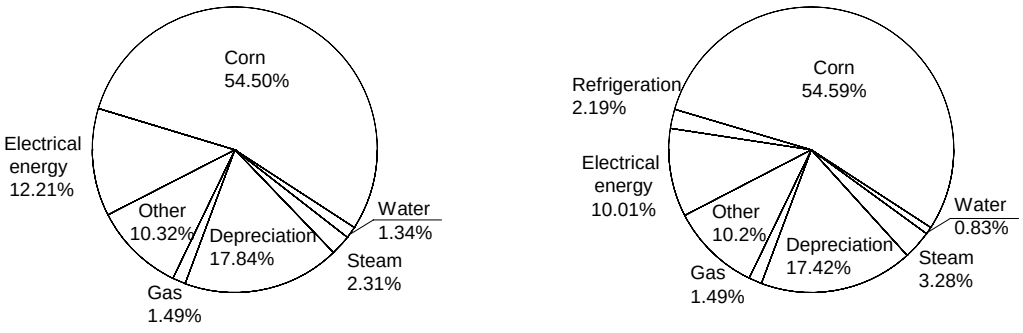


*(a)* *(b)*

**Figure 4.9** *Cost distribution for both the 1st/a option (a) and the 1st/b (b) one.*

In order to calculate the depreciation quote the capital annualizing was done by means of a straight line method distributed in a 10-year plant life time. In these pie charts "other" includes: labour, maintenance, yeasts, enzymes, process water and cost of other chemicals used.

Clearly the major contribution is given by the feed material, as for the traditional process (without SFE). Depreciation and electrical energy account also for a large percentage due to the additional capital and operating costs due to the SFE units. The results from the calculations about the supercritical extraction capital investment for the 2nd technical options are shown in Figure 4.10a and b.

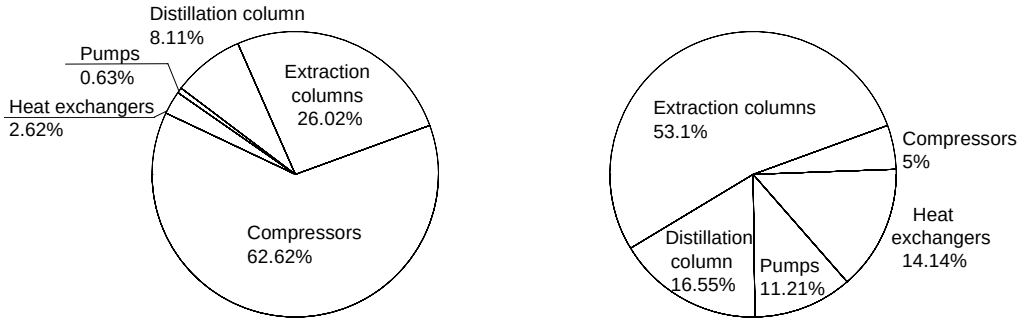


*(a)* *(b)*

**Figure 4.10** *Capital investment distribution for the supercritical extraction section of the 2nd a technical option (a) and 2ndt b one (b).*

In this case the difference between option a and b is greater than for the 1st option. This occurs mainly for two reasons. First, in the 1st technical option the amount of $CO_2$ that has to be compressed is lower than for the 2nd option. In fact the $CO_2$ make up is similar, but with the activated carbon system only the activated carbon hold up (102.22 t/h) has to be compressed from 10 bar to 100 bar, while in the 2nd option the whole amount of extraction $CO_2$ (2,300 t/h) have to be compressed from 50 bar to 100 bar. Accordingly the capital investment saving obtained replacing compressors with pumps is larger. The second reason is that the distillation pressure (50 bar) is high enough to allow condensing the $CO_2$ so that in option 2nd b the only compressor is the make up one (the percent of the extraction capital cost due to the compressors drops from 62.62% of 2nd/a option to 5% of 2nd/b option. For the same reasons there is a large difference between the thermal utilities usage of option 2nd/a and 2nd/b. The ethanol production cost distributions for the two options are reported in Figure 4.11. Considering the results of Tables 4.13 and 4.14 the lowest production cost is the one of the 1st technical option. It has to be specified that in those analysis the costs are allocated only to the ethanol production and not to the DDGS production.

**Table 4.14** *Economic analysis results.*

| | 2nd a option | 2nd b option |
|---|---|---|
| **Extraction section capital investment [M€]** | 106.39 | 52.14 |
| **Total capital investment [M€]** | 166.97 | 112.72 |
| **Electrical energy [M€/y]** | 26.06 | 10.82 |
| **Thermal utilities [M€/y]** | 7.40 | 80.99 |
| **Production cost [€/l EtOH]** | 0.919 | 1.469 |

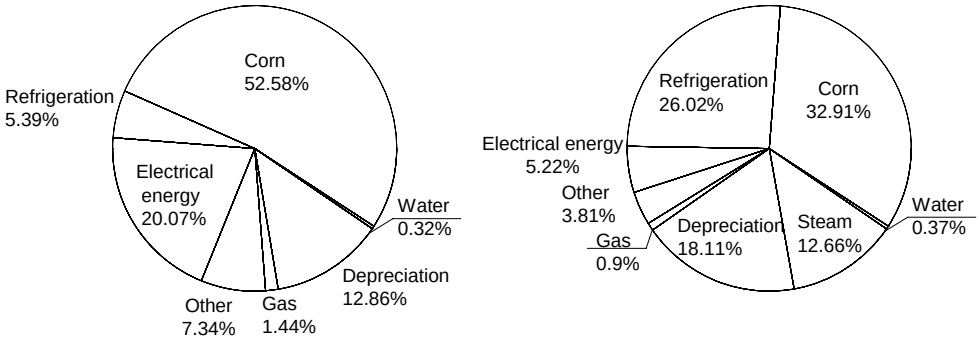


*(a)* *(b)*

**Figure 4.11** *Cost distribution for the 2nd/a option (a) and the 2nd/b (b) one.*

Referring to the traditional process economical analysis Table 4.15 shows the results, while Figure 4.12 the different contribution to the total ethanol production cost. The traditional process is definitively more economic than the one where distillation is replaced with the supercritical extraction. Moreover it has to be pointed out that the distillation section in the traditional process consists in 3 different distillation columns (under 5 bar), while the supercritical extraction needs 19 extraction columns.

**Table 4.15** *Traditional process economical analysis results (Franceschin et al., 2007).*

| | Traditional process |
|---|---|
| **Total capital investment [M€]** | 70.00 |
| **Electrical energy [M€/y]** | 5.86 |
| **Thermal utilities [M€/y]** | 5.06 |
| **Not allocated production cost [€/l EtOH]** | 0.670 |

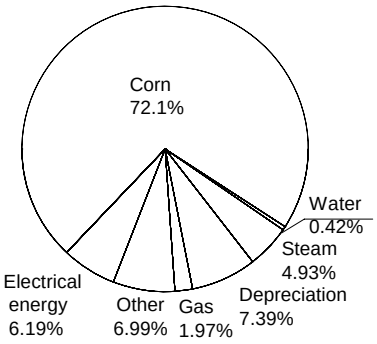


**Figure 4.12** *Cost distribution for the traditional process.*

Furthermore on the one hand the 1st option needs a large volume of activated carbon that means a large number of absorption columns and each one of these has to be double because of the batch working condition. On the other hand the 2nd option, requires distillation columns in order to recover the ethanol but these columns have to treat all the amount of $CO_2$ and so, because of flooding problem, they are roughly double in number with respect to the extraction columns. This large number of pieces of equipment obviously requires more space and more workers in comparison to the traditional process. Finally even though a relatively safe gas like $CO_2$ is involved the operating pressures are quite high, so special safety solution and specialized staff would be required. All these points, which were not taken into account in the previous economical analysis, would lead to a further increment of capital investment (bigger occupied space) and operating costs (larger number and more specialized staff).

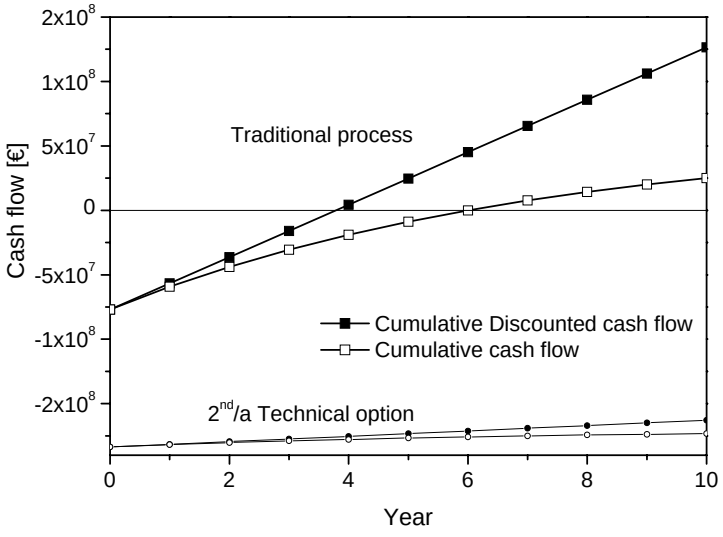


**Figure 4.13** *Cumulative cash flow for the 2nd/a option and the traditional process.*

Figure 4.13 shows the cumulative cash flow the 2nd/a option and the one of the traditional process. In the first case the payback period is of 6 years, but in the second case even after 10 years the cumulative cash flow is negative. The pay back time calculated by means of the cumulative cash flow is 140 years which is completely unrealistic.

## 4.5 Conclusions

Two different technical options for the recovery of ethanol by means of supercritical $CO_2$ were analysed. Results showed that the production of anhydrous ethanol by means of $CO_2$ extraction is technically possible and the amount of $CO_2$ obtained in the fermenter (13,109 kg/h) is enough to supply the required makeup for all the technical options considered. However, due to the low ethanol loading of $CO_2$, a large amount of $CO_2$ is needed and this leads to a large number of extraction columns and particularly high operating costs and capital investment.

In summary, at present the integration of supercritical $CO_2$ extraction into existing bioethanol production is attractive, technically feasible, but definitively not economic.

## 4.6 Nomenclature

| | | |
|---|---|---|
| $F_G$ | = | gas capacity factor (m/s) |
| $G$ | = | mass flow rates of the supercritical phase (kg/h $m^2$) |
| $L$ | = | mass flow rates of the liquid phase (kg/h $m^2$) |
| $u$ | = | velocity of the supercritical phase (m/s) |

Greek letters:

| | | |
|---|---|---|
| $\Phi$ | = | flow parameter (-) |
| $\rho$ | = | density (kg/$m^3$) |

Subscripts

| | | |
|---|---|---|
| G | = | supercritical phase |
| L | = | liquid phase |

## 4.7 References

Budich, M. and G. Brunner (2003). Supercritical Fluid Extraction of Ethanol From Aqueous Solution. *J. of Supercrit. Fluid*, **25,** 45-55.

Franceschin, G., A. Zamboni, F. Bezzo, and A. Bertucco (2007). Ethanol from Corn: a Technical and Economical Assessment Based on Different Scenarios. *Chem. Eng. Res. Des.,* **86**, 488-498.

Hagen, R. and J. Hartwig (1985). *Method for Separating Ethanol from an Ethanol Containing Solution.* United States Patent Number 4492808.

Ikawa, N., Y. Nagase, T. Tada, S. Furuta, and R. Fukuzato (1993). Separation Process of Ethanol from Aqueous Solutions Using Supercritical Carbon Dioxide. *Fluid Phase Equilib.*, **83**, 167-74.

Kranz, N. and E. Worrell, (2001). *Effect of a Shortened Depreciation Schedule on The Investment Costs for Combined Heat and Power Systems.* Ernest Orlando Lawrence Berkeley National Laboratory Technical Report (LBNL-49518).

Krishnan, M.S., F. Taylor, B.H. Davison, and N.P. Nghiem, (2000). Economic Analysis of Fuel Ethanol Production from Corn Starch Using Fluidized-bed Bioreactors. *Bioresour. Technol*., **75**, 99-105

Perry, H.R. et al. (1999). *Perry's Chemical Engineers' Handbook* ($7^{th}$ ed.) McGraw-Hill Book Co., New York (U.S.A.).

Stockfleth, R. and G. Brunner (1999). Hydrodynamics of a Packed Countercurrent Column for the Gas Extraction. *Ind. Eng. Chem. Res.,* **38**, 4000-4006.

Ulrich, G.D. P.T. and Vasudevan (2006). *Process Design and Economics. A Practical Guide*. Process Publishing, Lee (U.S.A.).

Zetzl, C., V. Patil, M. Budich, and G. Brunner (2007). One Step Purification to Absolute Alcohol from Sugar Cane Molasse by Means of Supercritical $CO_2$. In Proceedings of *Prosciba, I Iberoamerican Conference on Supercritical Fluids*, Iguassu Falls (Brasil). April 10-13, paper SC-017.

# Chapter 5

# Second generation ethanol: a technical and energetic assessment of an industrial process[3]

In this Chapter a second generation ethanol process is modelled and simulated by the software Aspen Plus™. This allowed comparing two different configurations for the distillation section, calculating exactly the energy consumption of the process, and verifying the possibility of an energy recovery from the solid residue in order to assess the technical and energetic sustainability of the process at the industrial scale. In processes based on starchy raw materials the largest part of the operating costs is due to the feedstock and only a fraction between 10% and 14% of the final ethanol production cost is related to energy demands. On the other end the lignocellulosic plants the cost of the raw material is negligible, as it is a waste product. For this reason, and due to the lower concentration of ethanol after the fermentation, the portion of total ethanol production cost due to steam and cooling water usage is higher. Therefore energy optimization results become a key factor for the economy of lignocellulosic processes and particularly if the liquid hot water pretreatment is performed, which involves a relatively high temperature. Experimental data about the pretreatment and enzymatic hydrolysis steps were used to achieve a realistic process model. Energy and mass balances were solved for different plant configurations and the pinch technology analysis was carried out in order to optimize the energy consumption. The possibility to produce steam and electric power was investigated in order to recover energy from solid residues of the process and to make it energetically self-sufficient.

## 5.1 Introduction

Owing to the rise of environmental concerns and to the periodic crises in oil exporting Countries followed by the threat of a permanent increase of the oil price, bioethanol has become a viable and realistic alternative in the fuel market. Corn and wheat are the common raw materials to obtain bioethanol in U.S.A. and Europe. However, in the last years, due to the competition with food production, the experimental research has focused on

[3] Part of this Chapter has been submitted for publication in *Renewable Energy* (See Page XV).

lignocellulosic materials. These substrates, differently from starchy ones, that need only a fast cooking as pre-treatment, require more complex steps before proceeding with the enzymatic hydrolysis. Only in this way the amount of sugars recovered can be maximized without using too many enzymes and too long saccharification time. On the other hand, the pre-treatment is expensive and may be relevant in determining the overall bioethanol production cost of the process. So, a careful consideration and minimization of operating costs, especially those due to energy duties, is essential in view of achieving a process energetically efficient and economically sustainable at the industrial level. Process modelling and simulation based on reliable laboratory data is the correct way to address this issue and to evaluate quantitatively the solutions proposed (Cardona and Sánchez, 2007).

We have investigated the case of rye straw as raw material. Rye straw 2007 world production is estimated to be around 14.7 million tons, 91.5% of which is in Europe, where Germany has the largest share: in 2006 and 2007 its amounts exceeded 2.64 and 2.70 million of metric tons, respectively (FAO, 2008). In general, the residue generation ratio for straw to cereal grain is around 1.3 (Ericsson and Nilsson, 2006) and, if it is assumed that one quarter of these residues can be harvested and roughly one third of the harvested straw is used in animal husbandry the results lead to 0.22 ton of straw per ton of cereal. Therefore, rye straw in Europe can be a real potential source of lignocellulosic material for energy purposes.

Among other pre-treatment types suitable to achieve the targets listed above, liquid hot water (LHW), steam explosion, dilute acid, lime and ammonia processing have potential as cost effective ones (Mosier *et al.,* 2005).

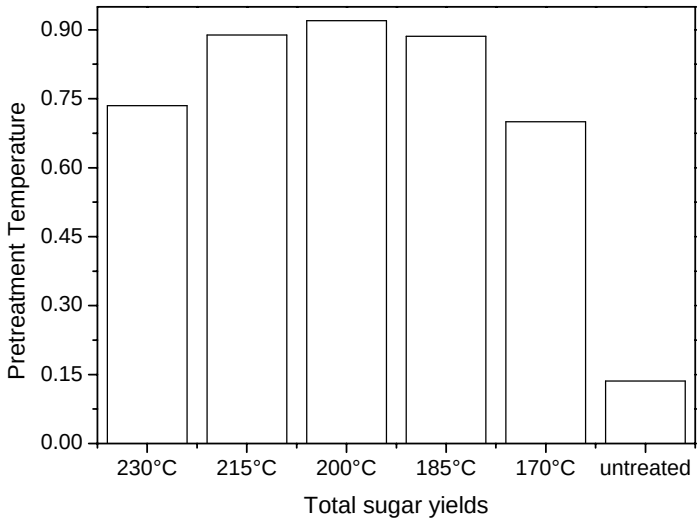


**Figure 5.1** *Sugar yield after enzymatic treatment, with pretreatment at different conditions and without pretreatment (adapted from Ingram et al., 2008).*

In this Chapter we have referred to the LHW pre-treatment, which is most promising due to its simplicity, low generation of inhibiting products, use of no chemicals and consequently no production of process residues, low cost of material of construction and the possibility to avoid the particle size reduction step (Lynd, 1996).
The LHW effect on different raw materials was studied thoroughly by Schacht *et al.,* (2008), Rogalinski *et al.,* (2008), Ingram *et al.,* (2008) and Albrecht (2006).
Figure 5.1 shows the experimental results obtained treating rye straw with hot liquid water at different temperatures in a semi-batch reactor (Ingram *et al.*, 2009), a clear indication that an economic sugar recovery can be achieved using the combination of pre-treatment and enzymatic hydrolysis only.
In our investigation we have used the referenced experimental data to obtain a realistic Aspen Plus™ model of the process producing ethanol from rye straw, with the aims of minimizing the energy duties of the process and of comparing different technical alternatives. Up to our knowledge no specific energy analysis on processes which include LHW as pretreatment has been done yet.

## 5.2 Process description and flowsheet

A process to convert lignocellulosic materials to ethanol generally includes five main steps:

1. Feedstock handling
2. Pre-treatment
3. Saccharification and fermentation
4. Ethanol recovery
5. Solid residue recovery and disposal

The lignocellulosic process shown in the block flow diagram of Figure 5.2 was simulated with Aspen Plus™.
Table 5.1 shows the composition of the raw material (rye straw) used in simulation.

**Table 5.1** *Rye straw dry composition used in simulation.*

| Component | Mass fraction |
|---|---|
| Hemicellulose | 0.235 |
| Cellulose | 0.436 |
| Lignin | 0.186 |
| Ash | 0.034 |
| Other | 0.109 |

This composition was calculated assuming that all the glucose present in the solid sample is coming from cellulose, while hemicellulose provides xylose and other sugars. Calculations

were based on the analysis performed to estimate monomeric sugar composition, lignin, moisture and ash content (Ingram, 2008). The moisture content was 5.45% by weight.

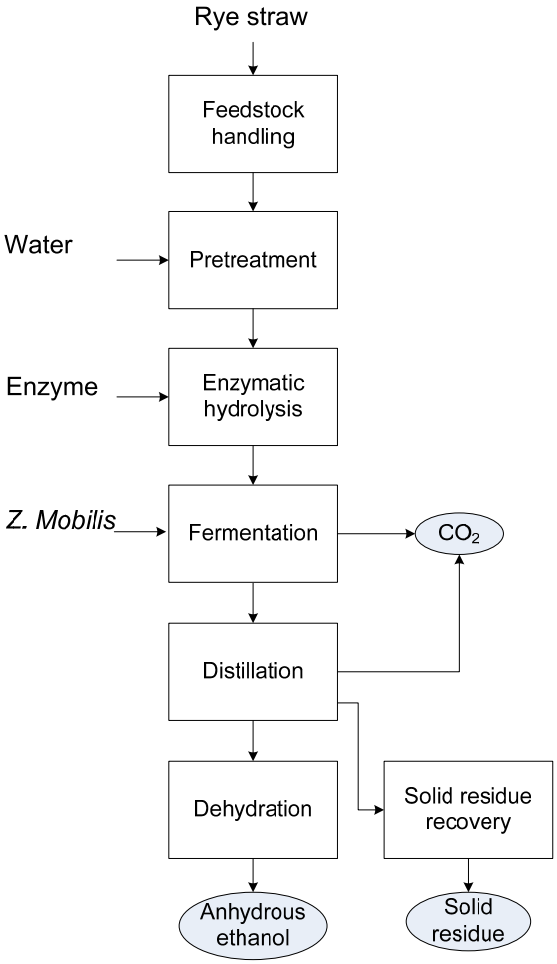


**Figure 5.2** *Process block flow diagram.*

The thermodynamic properties of the components involved in the simulation were the same presented in Chapter 2 (§2.3.1, §2.3.2, §2.3.3).

In the first plant section the raw material is collected, milled to the suitable size and washed. In the subsequent step three pre-treatment reactor types can be used: a batch reactor, a continuous (PFR) and a semibatch one. Experimental data (Ingram, 2008) proved that the semibatch arrangement is the best one thanks to the possibility to control the residence time of the liquid phase, and therefore of the hydrolysate, at high temperature. In this way it is possible to avoid the degradation of the monomeric sugars into products like HMF (Hydro Methyl Furfural) and furfural, which inhibit the fermentation downstream. For instance, it was shown (Ingram *et al.,* 2009) that with a residence time of 9 minutes furfural is not detected in the hydrolysate, and only 1.6% of the xylose is degraded to HMF. Different pre-treatment temperatures were studied by these authors: the final monomeric sugars recoveries after enzymatic treatment were compared and the optimal pre-treatment temperature was

found to be 200 °C. The amount of water used in this process section is around 4 times the solid content of the reactors.

After the pre-treatment, the hydrolysate fraction and the solids are mixed together and undergo an enzymatic hydrolysis, which is carried out at 50 °C for 24 h. The yields of glucose and xylose (defined as the ratios between the amount of recovered monomeric sugars and the amount contained in the raw material) are 92% and 82%, respectively. An amount of 12 FPU enzymatic complex per kg of cellulose (Aden *et al.,* 2002) was used.

The fermentation step is carried out at 41 °C by the bacteria *Z. Mobilis*, which is able to transform both hexoses and pentoses. The 10% of the hydrolysate from the enzymatic step was used for the inoculum preparation. Table 5.2 shows the reactions modelled in the simulation of both the inoculum and fermentation reactors. Only the formation of glycerol and acetic acid were taken into account as the secondary products. Conversions of glucose and xylose to ethanol and bacteria are referred to a fermentation time of 36 hours and are taken from literature data (Aden *et al.,* 2002), as well as those of glycerol and acetic acid.

**Table 5.2** *Modelled reactions and conversion.*

| **Reaction** | **Mass fraction** | |
|---|---|---|
| | **Seed reactor** | **Fermenter** |
| Glucose → 2 Ethanol + 2 $CO_2$ | 0.90 | 0.95 |
| 3 Xylose → 5 Ethanol+ 2 $CO_2$ | 0.80 | 0.85 |
| Glucose+ 0.018 DAP→ 6 *Z. Mobilis* +0.3505 Oxygen + 1.77 Water | 0.04 | 0.02 |
| Xylose + 0.015 DAP → 5 Z. Mobilis + 0.278 Oxygen+ 1.5 Water | 0.04 | 0.019 |
| 2 Glucose +Water → Ethanol + 2 Glycerol + Acetic acid + 2$CO_2$ | 0.027 | 0.03 |
| 2 Xylose → 5 Acetic acid | 0.037 | 0.0385 |
| 3 Xylose + 5 Water → 5 Glycerol + 2.5 Oxygen | 0.037 | 0.0385 |

DAP: Diammonium Phosphate

During the fermentation a large amount of $CO_2$ is produced, the 98.4% of which is removed as vent from the reactor, the 1% after heating before distillation, while the rest is distilled. An ethanol concentration of 6.37% (w/w) resulted from the simulation in the outlet stream from the fermenter.

Two distillation arrangements were simulated, as depicted in Figures 3a, 3b. The first one involves three columns at different pressures in order to recover as much heat as possible. Accordingly, the feed stream is split and sent to two beer columns operated at 1.75 bar and 0.49 bar, respectively. The heat duty of the top condenser of the first column is used in the reboiler of the second one. Both of them are without reflux. The top products are sent to a rectifying column (operating at 5.2 bar) where an ethanol concentration of 92% (w/w) is achieved. The specifications on ethanol recovery of the beer and rectifier columns are set to 99.8% and 99.99%, respectively. The heating power available from the condenser of the last

column is enough to boil the 1.75 bar beer column. After degassing, the main part of $CO_2$ is recovered from the two condensers and this stream is sent to a scrubbing tower.

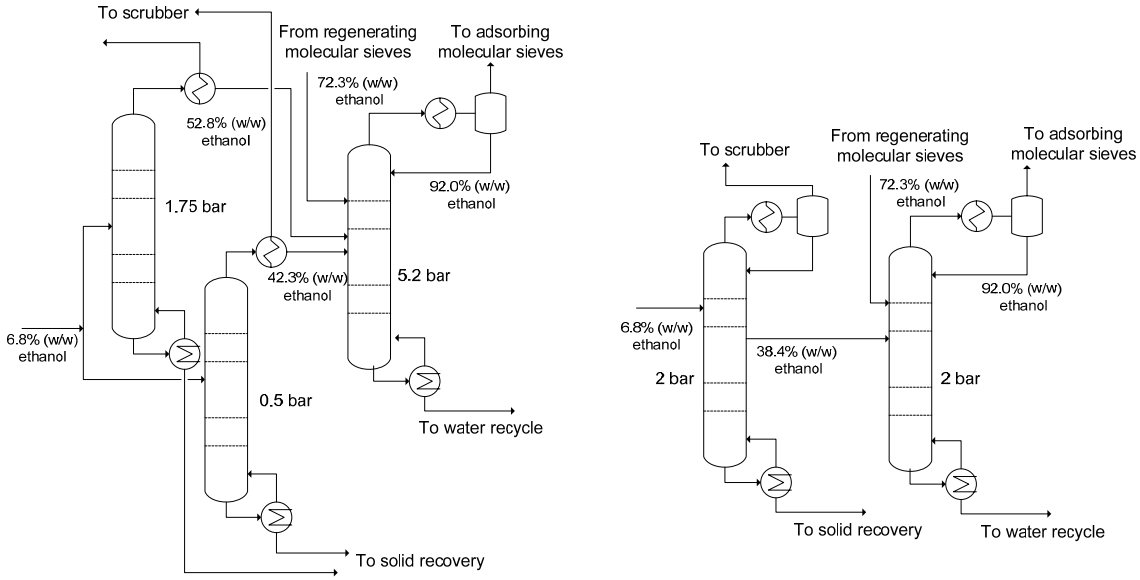


**Figure 5.3** *Distillation section options.*

In the second arrangement only two columns are used: the beer and the rectifying ones. The beer column works at 2 bar and the ethanol is collected as a side product ($4^{th}$ tray from the top); the condenser product is a gas stream mainly composed of $CO_2$ (68.3% $CO_2$, 24.7% EtOH and 7% water), while water and solids are extracted from the bottom. The gas stream is sent to a scrubbing tower, working with fresh water that is recycled to the process before the pre-treatment step. Also in this case the ethanol is concentrated in a rectifying column, which is now operated at 2 bar.

In both distillation options 99.8% (w/w) of ethanol purity is reached by means of molecular sieve columns downstream. Here the superheated vapour from the top of the rectifier column is fed alternately to one or the other of two adsorption columns, which remove the water and a small portion of ethanol. The 99.8% pure ethanol vapour is cooled, condensed and pumped to storage. While one bed is adsorbing water, the other is being regenerated by pure ethanol vapour, which strips the water off the adsorbent, so that a mixture with an ethanol content of 72.3% (w/w) is condensed and returned to the rectifier.

The recovery of solids from the beer column bottom stream is performed by a multiple evaporator system and a press filer, as depicted in Figure 5.4. The evaporators work at 0.6, 0.4, and 0.2 atm, respectively. A stream called backset is recycled back to the pre-treatment step, in order to improve the performances or the conversion efficiency, together with the make-up and other water recycling streams. The solids obtained have a moisture content of 55% by weight.

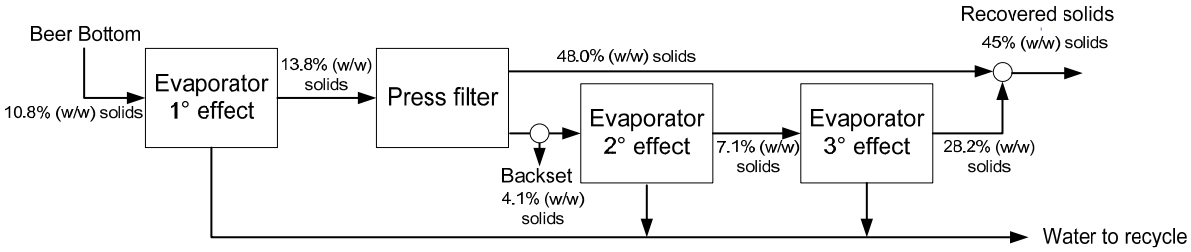


**Figure 5.4** *Solid recovery section.*

Some possible options are drying and sending them to disposal, or using them to produce energy for the process. Three possibilities have been investigated in this respect, in order to check if enough steam and electrical energy for the process can be obtained.

## 5.3 Simulation results and equipment design

The plant size (2000 dry t/d of feed) was chosen to be as close as possible to the one studied by the National Renewable Energy Laboratory (Aden *et al.*, 2002), to which our results can be compared. Wooley *et al.,* (1999a) investigated the effect of the plant capacity on the economy of the process and showed that for a size like the one considered, even if some equipment like fermenter and pre-treatment vessels have reached their maximum volumes, there are still economies of scale available in other parts of the process. Clearly one should account also for the increase of feedstock collection costs, an effect which is tightly correlated to the feedstock type, and is site specific, but this is not the focus of the present work.

In order to perform the pre-treatment in a semi-batch mode, and to be able to treat continuously 83.3 kg/h of dry solids, five tubular reactors working in parallel were used. If a time of 5 min is supposed to be necessary for the reactors load/unload between two batch cycles, and if the solid reaction time is set to 30 min, then each reactor has to treat 9,722 kg/h of solids. Accordingly, these tubular vessels have a diameter of 2.5 m and a length of 4 m. The water flow rate to be pumped at 40 bar and 205 °C through each reactor is 345.0 kg/h, while the solid residence time is 25 min.

Other reactors needed are those for enzymatic hydrolysis and for fermentation. Both of these options were carried out in a train of 5 parallel vessels with the size of 2,400 $m^3$ and of 3,493 $m^3$ volume each, respectively. From the fermentation 25,300 kg/h of $CO_2$ and 27,000 kg/h of ethanol are produced. Figure 5.5 summarizes the main inlet and outlet process streams with the respective mass flow rates.

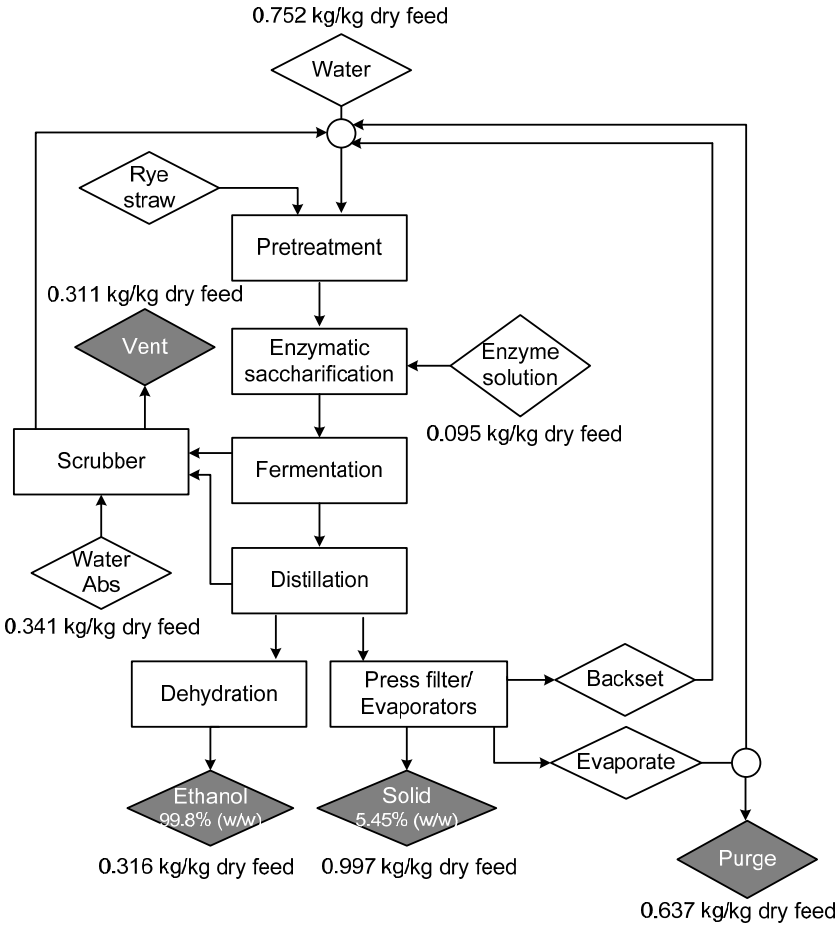


**Figure 5.5** *Principal inlet and outlet process streams.*

Table 5.3 shows the distillation columns details for both of the arrangements proposed. We have assumed Nutter V-grid trays for the beer and rectifying columns and a random packing in the scrubbing tower.

**Table 5.3** *Columns details.*

| | Diameter [m] | High [m] | Theoretical tray number | Trays efficiency | Mass reflux ratio |
|---|---|---|---|---|---|
| **1st configuration** | | | | | |
| Scrubber | 2.4 | 7.6 | 4 | Pack column | - |
| Beer columns | 3.0 | 19.5 | 15 | 48% | - |
| Rectifier column | 3.3 | 36.6 | 35 | 52% | 3.59 |
| **2nd configuration** | | | | | |
| Scrubber | 2.3 | 7.6 | 4 | Pack column | - |
| Beer column | 4.3 | 19.5 | 15 | 48% | 2.80 |
| Rectifier column | 1.3 above tray 26/3.9 below | 36.6 | 35 | 52% | 2.68 |

It is noteworthy that the lignocellulosic to ethanol processes need large amounts of water. For this reason it is important to recover and recycle as much water as possible and to minimize the make up required. Our analysis showed that setting a purge flow of 53 t/h in order to avoid the build up of secondary products, and using 28.4 t/h of water in the scrubbing tower, a water make up of around 62.7 t/h is necessary. This means a water consumption of 3.45 kg per kg of 99.8% purity ethanol produced.

## 5.4 Pinch analysis

In bioethanol processes based on starchy raw materials the larger part of the operating costs is due to the feedstock and only a fraction between 10% and 14% of the final ethanol production cost is related to energy demands (Franceschin *et al.,* 2008). In lignocellulosic processes the cost of the raw material is really negligible, as long as it can be considered a waste product. For this reason, and because of the lower ethanol concentration in the fermentation broth, the portion of the total ethanol production cost due to steam and cooling water usage is higher. Therefore energy optimization results to be a key factor for the economy of lignocellulosic processes. This is even more important if a LHW pre-treatment is performed, owing to the relatively high temperature involved.

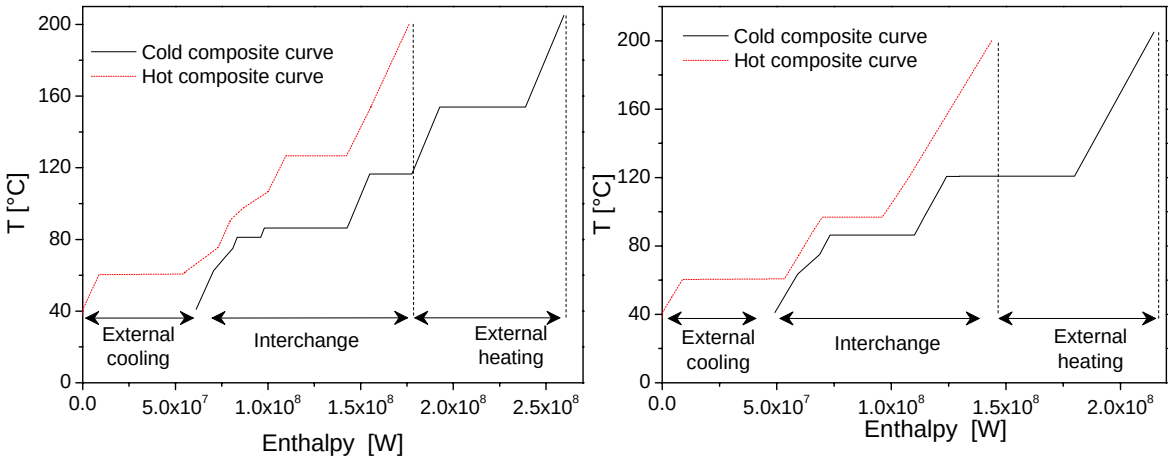


**Figure 5.6** *Hot stream and cold stream cumulative curves for the three columns configuration (a) and the two columns configuration (b).*

Pinch Technology Analysis (PTA) is one of the most widely applied approaches for heat integration in process industry, as it allows the determination of the minimum energy needs of the process. A simplified PTA based on the procedures developed by Linnhoff and Flower (1978) was performed and the minimum amount of steam and cooling water required were calculated, assuming $\Delta T_{min}$ =10 °C. The results for both the distillation options are shown in Figure 5.6.

If three columns are used the primary energy to be supplied to the process is 90.0 MW and the one that has to be removed is 60.0 MW. With only two columns the energy to be supplied/removed is reduced to 73.2 MW and 48.6 MW, respectively (see Table 5.4).
Note that the pre-treatment reactor heating has not been taken into account. If heat losses are neglected, heating up the solids requires around 5 MW, which cannot be recovered from other streams due to the high temperature needed. Regarding electric power requirements, they amount is roughly to 8.1 MW, corresponding to a consumption of 0.288 kWh/L ethanol produced (Morey *et al.,* 2006).

**Table 5.4** *Energy requirements of the plant: steam and electrical power.*

| | 1° configuration | 2° configuration |
|---|---|---|
| **Electrical power [MWe]** | 8.1 | 8.1 |
| **Steam 21 bar [MWth]** | 6.3 | 6.3 |
| **Steam 6.83 bar [MWth]** | 68.9 | 55.8 |
| **Steam 1.74/1.1 bar [MWth]** | 14.8 | 11.1 |

Table 5.4 reports details about the energy duties of the plant for the two different arrangements of the distillation section.

## 5.5 Energy recovery from solid residues

Solid residues from the process could be used to produce the energy required by the process itself, in terms of electric power and steam. A combined heat and power (CHP) plant can be envisaged, in which residues are burnt and the heat of flue gas is used to produce high pressure steam for both the plant and for the production of electric power by a steam turbine.
Burning the solid residue of the process to generate steam and electricity allows the plant to be self sufficient in energy (Aden *et al.*, 2002) and we have verified this in our case. In addition, it reduces solid waste disposal costs and generates additional revenues through sales of excess electricity (Aden *et al.*, 2002).
Solids are sent directly from the solid recovery section to the combustion chamber for burning. Moisture content is about 55%, which is reasonably acceptable: according to Aden *et al.*, (2002), maximum feed moisture should be 60%. Treated water enters the heat exchanger circuit in the combustor and is evaporated and superheated to 650 °C and 86 atm (Aden *et al.*, 2002) to produce around 181,300 kg/h of steam. The boiler efficiency, defined as the percentage of the feed heat that is converted to steam heat, is around 68%, while the electric power efficiency, defined as the percent of the feed heat that is converted to electricity, is about 15% (Wooley *et al.,* 1999b). After generating high pressure steam, the

remaining heat content in the flue gas is used to preheat the entering combustion air, then the gas is treated by a purification system to remove contaminants before being exhausted. A multistage turbine and generator produce electricity. After each decompression stage a part of the steam is extracted from the turbine to supply the plant energy requirements while the rest is decompressed to the lower stage. This is done at 21, 6.83 and 1.74/1.1 bar according to the two distillation arrangements (Table 5.4). The steam obtained is sufficient to fulfil all the process duties. Values used in the simulation for the efficiencies of turbines and compressors are reported in Table 5.5 and are taken from Ong'iro *et al.*, 1995 for gas turbine, and from Donatini *et al.,* (2007) for steam turbine and compressors.

**Table 5.5** *Efficiency of the power plant equipment.*

| Component | Gas turbine | Steam turbine | Compressor |
|---|---|---|---|
| $\eta_{isoentropic}$ | 0.92 | 0.88 | 0.85 |
| $\eta_{mechanical}$ | 0.99 | 0.975 | 0.9 |

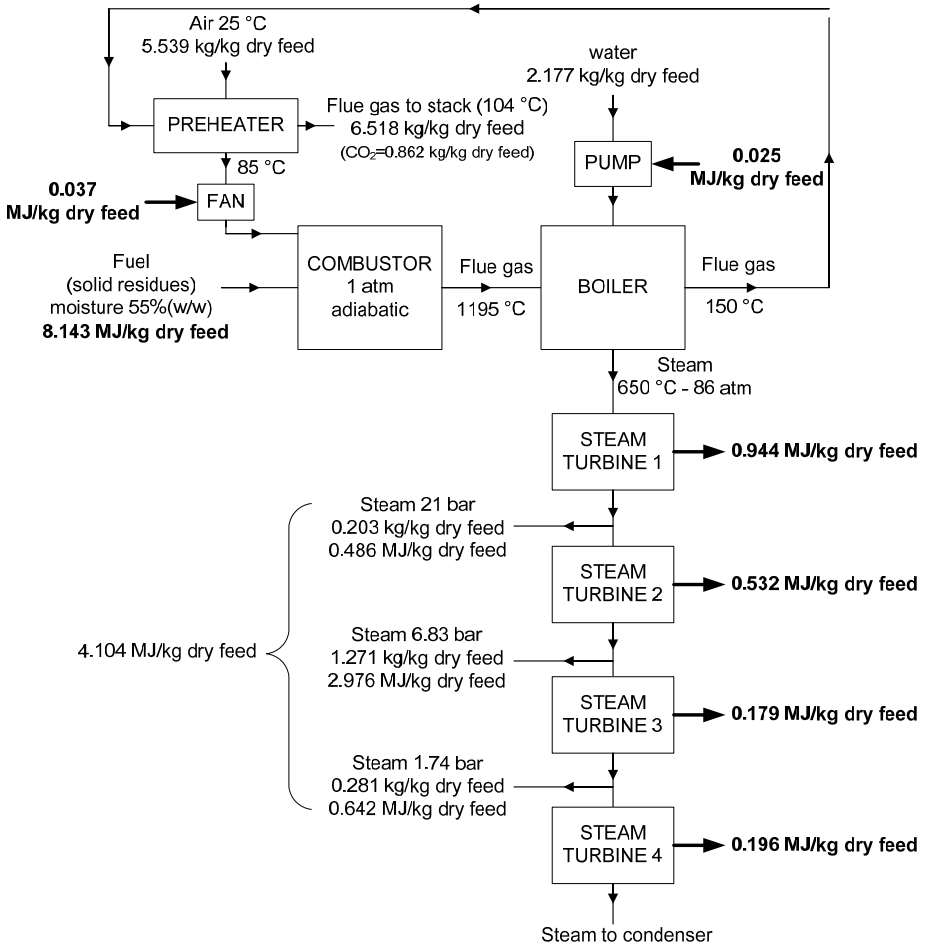


**Figure 5.7** *Block flow diagram of the CHP plant simulated, with all main results and mass flow rates of the input streams (energy needs of bioethanol plant with 1° distillation configuration).*

Figure 5.7 shows a block flow diagram of the CHP plant simulated, with all main mass flow rates of the input and output streams (results refer to the energy requirements with the first distillation arrangement). Finally, the calculated process performances are summarized in Table 5.6, for both the distillation configurations.
As main performance parameters we have chosen those commonly used in industrial practice, and reported by the literature (Ståhl *et al*., 1999):

$$Net\ electrical\ efficiency\ [\%] = \frac{Net\ power\ produced\ [MWe]}{Fuel\ energy\ input\ [MW]} \times 100 \quad (5.1)$$

$$Total\ en.efficiency\ [\%] = \frac{Net\ power\ produced\ [MWe] + Steam\ heat\ [MWth]}{Fuel\ energy\ input\ [MW]} \times 100 \quad (5.2)$$

**Table 5.6** *Energy requirements of the plant: steam and electrical power.*

| | **1° configuration** | **2° configuration** |
|---|---|---|
| **Power/Heat generation** | 40.5 MWe/90.7 MWth | 44.6 MWe/73.9 MWth |
| **Solid residue energy** | 188.5 MW | 188.5 MW |
| **Net electrical efficiency** | 22.2% | 26.8% |
| **Total energy efficiency** | 72.6% | 68.3% |
| **kg $CO_2$/MWh produced** | 1720.8 | 1424.5 |

Values obtained for net electrical efficiency and total energy efficiency are in agreement with those reported by (Aden *et al.*, 2002), which are 14.7% and 68.2%, respectively; according to another source (Wooley *et al.,* 1999b) they are 15.0% and 65.0%.

## 5.6 Conclusions

A rigorous and realistic simulation of the process producing ethanol from rye straw was carried out on the basis of experimental data about the pretreatment and enzymatic hydrolysis steps. Two different arrangements concerning the distillation section were investigated. Pinch technology analysis was applied to optimize the energy consumptions.
It was shown that steam and electric power required by the plant can be recovered from the solid residues of the process, i.e. the whole process can be made energetically self-sufficient even though an energy intensive pretreatment like the LHW is performed.

## 5.7 References

Aden, A., Ruth M., K. Ibsen, Jechura J., Neeves K., Sheehan J., Wallace B., Montague L., Slayton A., and Lukas J. (2002). *Lignocellulosic Biomass to Ethanol Process Design and Economics Utilizing Co-Current Dilute Acid Prehydrolysis and Enzymatic Hydrolysis for Corn Stover.* National Renewable Energy Laboratory report TP-510-32438.

Albrecht, T. (2006). Conversion of Lignocellulosic Materials and Model Compounds in Sub- and Supercritical Water. *PhD thesis*, TU Hamburg-Harburg (Germany).

Cardona, C.A. and Ó.J. Sánchez (2007). Fuel Ethanol Production: Process Design Trends and Integration Opportunities. *Bioresour. Technol.,* **98**, 2415–2457.

Donatini, F., G. Gigliucci, J. Riccardi, M. Schiavetti, R. Gabbrielli, and S. Briola (2007). Supercritical Water Oxidation of Coal in Power Plants with Low $CO_2$ Emissions. In Proceedings of: *ECOS07 20th International Conference on Efficiency, Cost, Optimization, Simulation and Environment Impact of Energy Systems*, Padova (Italy), June 25-28, Volume II, 1315-1322.

Ericsson K. and L.J. Nilsson (2006). Assessment of the Potential Biomass Supply in Europe Using a Resource-Focused Approach. *Biomass and Bioenergy,* **30**, 1–15.

FAO (2009). *Statistics*. Available at: http://faostat.fao.org/site/567/default.aspx#ancor [Accessed September 2009].

Franceschin, G., A. Zamboni, F. Bezzo, and A. Bertucco (2008). Ethanol from Corn: a Technical and Economical Assessment Based on Different Scenarios. *Chem. Eng. Res. Des.,* **86**, 488–498.

Ingram, T. (2008). Thermal and Thermal-Enzymatic Hydrolysis of Ligno- cellulosic Biomass for the Production of Bioethanol. *Master thesis*, TU Hamburg-Harburg (Germany).

Ingram, T., T. Rogalinski, V. Bockemühl, G. Antranikian, G. Brunner (2009). Semi-Continuous Liquid Hot Water Pre-treatment of Rye Straw for Bioethanol Production. *J. Supercrit. Fluids,* **48,** 238-246.

Lynd, R.L. (1996). Overview and Evaluation of Fuel Ethanol from Cellulosic Biomass: Technology, Economics, the Environment, and Policy. *Annu. Rev. Energy Environ*., **21** 403-465.

Linnhoff, B. and J.R. Flower (1978). Synthesis of Heat Exchanger Networks: I. Systematic Generation of Energy Optimal Networks. *AIChE J.,* **24**, 633-642.

Ong'iro, A.O., V.I. Ugursal, A.M. Al Taweel, and D.K. Blamire (1995). Simulation of Combined Cycle Power Plants using the Aspen Plus Shell. *Heat Recov. Syst. CHP,* **15**, 105-113.

Rogalinski, T., T. Ingram, and G. Brunner (2008). Hydrolysis of Lignocellulosic Biomass in Water Under Elevated Temperatures and Pressures. *J. Supercrit. Fluids*, **47**, 54-63.

Schacht, C., C. Zetzl, and G. Brunner (2008). From Plant Materials to Ethanol by Means of Supercritical Fluid Technology. *J. Supercrit. Fluids*, **46**, 299-321.

Ståhl, K., M. Neergaard, and J. Nieminen, (1999). Progress Report: Värnamo Biomass Gasification Plant. Presented at *Gasification Technologies Conference*, San Francisco, California (U.S.A.), October 17-20.

Wooley, R., M. Ruth, D. Glassner, and J. Sheehan (1999a). Process Design and Costing of Bioethanol Technology: A Tool for Determining the Status and Direction of Research and Development. *Biotechnol. Prog*, **15**, 794-803.

Wooley, R., M. Ruth, J. Sheehan, K. Ibsen, H. Majdeski, and A. Galvez (1999b). *Lignocellulosic biomass to ethanol process design and economics utilizing co-current dilute acid prehydrolysis and enzymatic hydrolysis current and futuristic scenarios*. National Renewable Energy Laboratory Technical Report TP-580-26157.

Wooley, R. J. and V. Pusche (1996). *Development of an ASPEN PLUS Physical Property Database for Biofuels Components*. National Renewable Energy Laboratory report MP-425-20685.

# Chapter 6

# Conversion of rye straw into fuel and xylitol: a technical and economical assessment based on experimental data[4]

In this Chapter a contribution to the development of economically sustainable processes to obtain lignocellulosic bioethanol is presented. The simultaneous production of bioethanol and xylitol from rye straw is investigated, as this compound can become a realistic alternative to the transformation of xylose into ethanol. A complete process from the raw material to the end products is developed and simulated with respect to all major operations: hot liquid water pretreatment, fermentation of glucose to ethanol, fermentation of xylose to xylitol, separation and purification of both products. Calculations are based on experimental as well as on literature data. In particular, experimental data about the pretreatment and enzymatic hydrolysis steps previously obtained (Ingram *et al.*, 2009) are used in order to achieve a realistic model that has been implemented using the software Aspen Plus™. The optimization of the process energy duties is carried out by means of the pinch technology analysis. Mass balances from the simulation are used in order to size the equipment and calculate the capital investment. Finally production costs and some financial indexes are estimated by a simple economical analysis.

## 6.1 Introduction

By now bioethanol, in Europe and U.S.A., is made mostly from corn and wheat, but the true alternative raw materials are the lignocellulosic ones. In this case a far greater source of biomass could be used for bioethanol production in more areas of the world than for sugar or cereal ethanol feedstock crops and, importantly, the competition of biofuels for land with food crops would be reduced or better be eliminated. Although "Second Generation bioethanol" is nowadays receiving much attention by politicians, especially in the EU, as a more $CO_2$ friendly alternative to fossil transport fuels than corn, wheat or sugar beet bioethanol, its exploitation at a large industrial scale is not developed yet. At the moment the main issue with bioethanol from lignocellulosic biomass is that it is by far more

[4] Part of this Chapter has been submitted for publication in *Chemical Engineering Research and Design* (See Page XV)

expensive than ethanol obtained by traditional feedstock based processes, due to the additional treatment required and to costly enzymes involved in plant operation (Balat and Balat, 2009). Another problem when processing these raw materials comes from the difficult fermentation of the hemicellulose fraction. In fact, while hexoses can be easily converted to glucose by *Saccharomyces cerevisiae* by a well-known technology, pentoses, i.e. the main constituents of hemicellulose, are more cumbersome to ferment. Yeasts and bacteria able to ferment simultaneously hexoses and pentoses are currently under development (Hägerdal *et al.,* 2007), as conventional organisms are not suitable to this scope. Several economic evaluations have illustrated that an efficient utilization of pentoses is important for the overall economy of ethanol production from lignocellulosic materials (Sassner *et al.,* 2008). The average content of pentoses in lignocelluosic biomass ranges between 23 and 32% (w/w) so that, if this fraction is not used, a significant loss of potential revenue can be expected. Besides, this fraction of the feedstock must anyway be transported to the plant and would further add substantial costs for waste disposal.

A simple alternative to the transformation of xylose into ethanol could be the conversion of this sugar into xylitol, which would become another valuable product of the process. Xylitol is equivalent to sucrose in sweetness, but unlike sucrose it is anticariogenic and is metabolized by an insulin-independent pathway, so it can be used as a sucrose substitute in clinical diabetic foods (Leathers, 2003). Also, it can be promoted for oral health and caries prevention; therefore, the bulk of its production is consumed in various food products such as chewing gums, sweets, soft drinks and ice-creams (Nigam and Singh, 1995). For the reasons mentioned above, the production of xylitol from xylose is a relevant alternative to the fermentation of pentoses to ethanol, which is actually a major obstacle to the development of industrial scale bioethanol processes from lignocellulosic material. The revenue from selling xylitol could improve the profitability of the plant, making also relatively small facilities economically valuable. This could knock down another obstacle in the diffusion of lignocellulosic bioethanol plants, for which NREL evaluated the suitable size by looking at the trade off between economies of scale and increased cost of delivering feedstock: results showed that the optimal minimum plant size is in the 2,000 to 4,000 MT per day range. Obviously this involves a quite high capital investment (197,400,000$ for the 2,000 MT/day plant) associated to remarkably high risk, especially in this period of instable economy (Aden *et al.*, 2002).

Today, xylitol is produced from hardwood or maize and the largest manufacturer in the world is the Danish company Danisco, with several other suppliers from China. Xylitol is obtained by hydrogenation of xylose, which converts this sugar into a primary alcohol. In 2000/2001 sales of all polyols amounted to 1.4 million tonnes with a market value of US$1.3 billion. Sorbitol had the largest share of the market (48%), followed by xylitol (12%), mannitol (11%) and maltitol (10%) (Business Communications Co. Inc., 2002). The

xylitol market continues to see strong demand and rapid growth worldwide due to an increasingly health conscious consumer and fast growth in chewing gum sales.
A crucial issue in the effective utilization of the lignocellulosic materials is, without doubts, the pretreatment step. Accordingly, a relevant part of the research in the fields is concentrated on this topic (the other one being the biotechnological research for the fermentation step, as recalled above). Several pretreatments may be appropriate: liquid hot water, steam explosion, dilute acid, lime and ammonia processing have all a potential as cost effective ones (Mosier *et al.,* 2005). However, the hot liquid water pretreatment, apart from the advantages to be simple, to produce low amounts of inhibiting products and to avoid any further chemicals (Lynd, 1996), is particularly suitable for the purpose of producing xylitol. In fact it permits a simple and massive separation between C5 and C6, especially if carried out in a fixed bed reactor (Ingram *et al.,* 2009).

Our aim was to investigate the economical value of a process that simultaneously produces xylitol and bioethanol from rye straw. Experimental data about the pretreatment and enzymatic hydrolysis steps previously obtained (Ingram *et al.,* 2009) were used in order to develop a realistic model that was then implemented using the software Aspen Plus$^{TM}$ to simulate the process. Then, pinch technology analysis was performed and the configuration of the heat exchangers to recover the maximum thermal power was found. Based on simulation results and equipment cost data, the costs for the simultaneous production of xylitol and bioethanol were calculated and a financial analysis was carried out.

## 6.2 Process description and flowsheet

Figure 6.1 shows a simplified block flow diagram of the process to convert lignocellulosic materials into ethanol and xylitol presently developed, while in Figure 6.2 a more complete scheme reporting the most important streams is shown. The first two steps are common for both of these products:

1. Feedstock handling (Area 100)
2. LHW pretreatment (Area 200)

Downstream, the two fractions obtained with the pretreatment (hydrolysate and solid residue) are collected separately and the process splits into the two corresponding production lines. The destiny of the solid residue (stream 201) is equal to the one of a common bioethanol process:

3. Saccharification and fermentation of C6 sugars to ethanol (Area 300)
4. Ethanol recovery (Area 400)
5. Water recycle

On the other hand, the liquid fraction called hydrolysate (stream 202) is processed in a different way:

6. Saccharification and fermentation of C5 sugars to xylitol (Area 500)
7. Recovery of xylitol (Area 600)
8. Water recycle

Finally, common to both the product lines is also:

9. Solid residue recovery (Area 700)

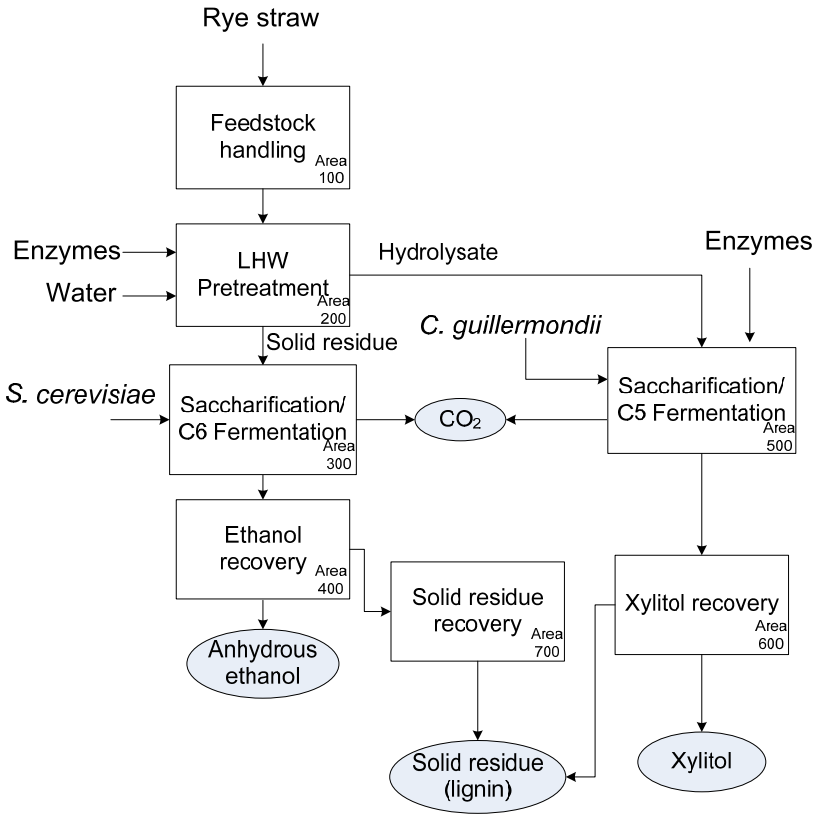


**Figure 6.1** *Simplified process block flow diagram.*

In the first plant section the raw material is collected and washed. The subsequent step consists in the LHW pretreatment of the biomass in fixed bed reactors. In a previous work (Ingram, 2008) it was shown that the semibatch reactor is the best one for pretreating the feedstock, due to the possibility to control the residence time of the hydrolysate, at high temperature. In this way the degradation of the monomeric sugars into products like HMF (Hydromethylfurfural) and furfural can be limited. The pressurized hot water flows through the solid bed in the reactor, so that two intermediate streams are produced: the liquid fraction, named hydrolysate, which consists in the feed water with part of the solid, mostly the hemicellulose, solubilised and hydrolysed, and the solid fraction, remaining in the reactor after the pretreatment, which is called solid residue and is mainly made of the cellulose and the insoluble lignin.

Experimental results showed an optimal pretreatment temperature of 200 °C (50 bar). The two fractions were treated separately in enzymatic reactors at 50 °C for 36 h. All in all, it was possible to recover 91.8% of the initial xylose and 4% of the initial glucose from the liquid hydrolysate. Whereas 88.9% of the feed glucose could be recovered from the solid residue (Bockemühl *et al.,* 2009).

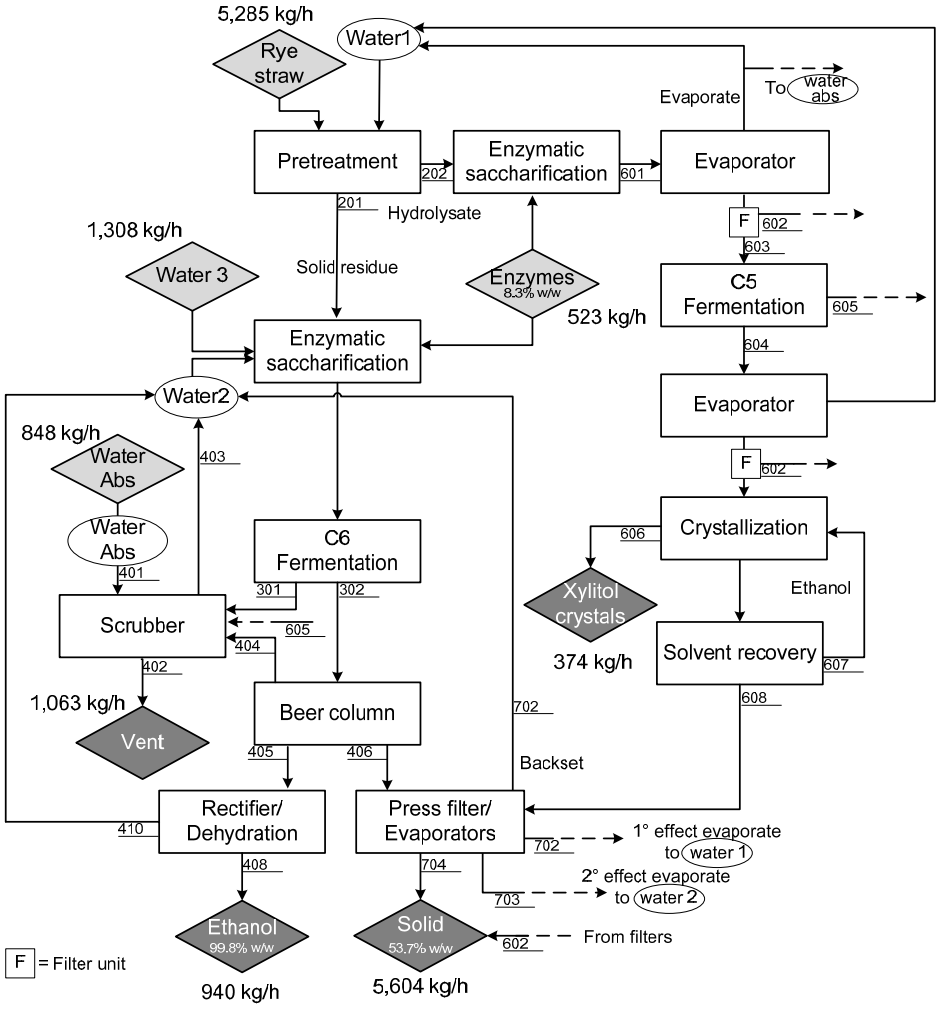


**Figure 6.2** *Principal inlet, outlet and internal streams of the process (mass balance is not completely satisfied due to other minor inlet stream like DAP and oxygen).*

With reference to the ethanol production line, after the enzymatic treatment, the 10% of the saccharified stream is used for the inoculum preparation, which is afterwards added again to the other 90% in the fermentation reactor. Fermentation is carried out at 41 °C for 36 h by the yeast *Saccharomices cerevisiae*. Table 6.1 shows the reactions used in simulation for both the inoculum and fermentation reactors. Conversion of glucose to ethanol and yeasts requires a fermentation time of 36 hours (these data as well as the secondary products are taken from literature, Aden *et al.,* 2002). Even though these conversions are referred to

fermentation by bacteria, other papers confirmed that they can be achieved with *Saccharomyces cerevisiae* as well (Zhisheng and Hongxun, 2004, Kádár *et al.,* 2007).

**Table 6.1** *Modelled reactions and conversion.*

| Reaction | Sugar conversion | |
|---|---|---|
| | Seed reactor | Fermenter |
| Glucose → 2Ethanol+2 $CO_2$ | 0.9 | 0.95 |
| Glucose+ 0.018 DAP → 6 Yeast+ 0.3505 $O_2$+ 1.77 $H_2O$ | 0.04 | 0.02 |
| 2 Glucose+ $H_2O$ → Ethanol+2 Glycerol+ Acetic ac.+ 2$CO_2$ | 0.027 | 0.03 |

Note that, in order to simplify the model without losing significant information, only the formation of glycerol and acetic acid as secondary products is taken into account.

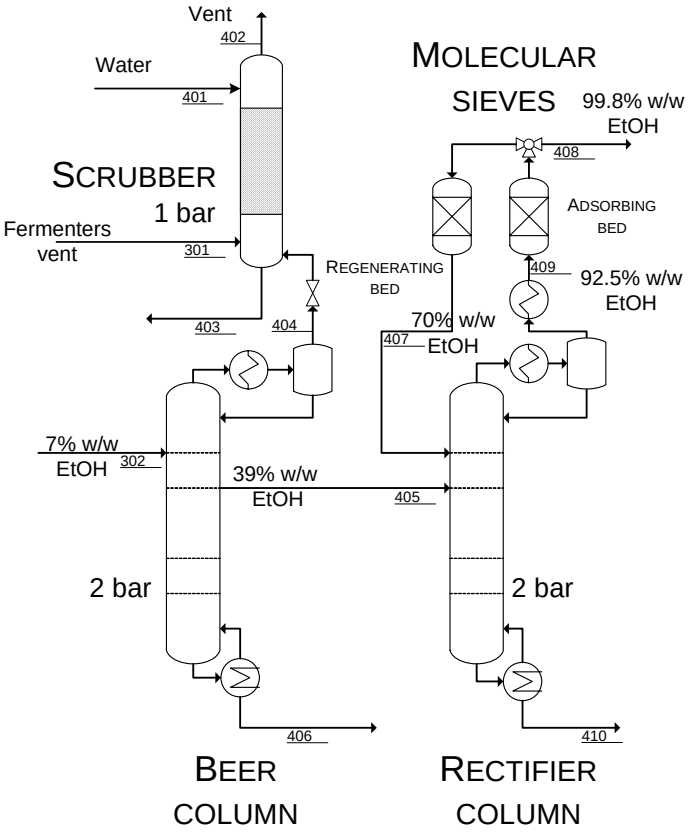


**Figure 6.3** *Ethanol recovery (Area 400) details.*

In the distillation section (Figure 6.3) the ethanol recovery is achieved by means of two columns: the beer and the rectifier ones. The beer column works at 2 bar and ethanol (39% w/w) is collected as the side product from the 4$^{th}$ theoretical tray from top (stream 405); at the top a gas stream (stream 404) mainly composed 95.0% w/w $CO_2$, 4.1% w/w EtOH and 0.9% (w/w) water is collected, while water and solids are extracted from the bottom (stream 406). The stream exiting from the top is sent, with the purge from the

fermenter (stream 301), to a scrubbing tower. This last column works with fresh water that is recycled and fed back to the process before the enzymatic treatment of the solid residue (stream 403). The side stream (stream 405) of the beer column is sent to the rectifier column (2 bar) that reaches an ethanol concentration of 92.5% (w/w) at the top. Molecular sieve columns are used downstream to reach the 99.8% (w/w) of ethanol purity (stream 408). The superheated vapour (stream 409) from the top of the rectifier is fed alternately to one or the other of two adsorption columns, which remove the water and a small portion of ethanol. The 99.8% (w/w) pure ethanol vapour is cooled, condensed and pumped to storage. While one bed is adsorbing water, the other is regenerated. Pure ethanol vapour is applied back through the loaded bed to do that. The de-adsorbed water is stripped off, and the mixture, which is condensed and returned to the rectification column has an ethanol content of 70.0% (w/w) (stream 407). When the adsorbing bed is saturated with water the system is switched, so that the other bed is used in adsorbing mode while the first one is regenerated.

Two evaporators working at 0.6 and 0.4 atm and a press filter are used in order to recover the solid residues of the process (from both the process lines). The 25% of the stillage from the filter press (named backset, stream 702) is sent to the solid residue enzymatic treatment, together with the make up and other recovered streams. The stream obtained (stream 704), which has a solids content of 36.1% (w/w), is then added to the other solid recovered by filtering the xylitol process line.

In a parallel process line the hydrolysate from the pretreatment, after saccharification, is fermented in order to produce xylitol. The saccharified stream (stream 601), mainly consisting of xylose and water, is first sent to a preliminary concentration stage (up to 88 g/l of xylose, according to Martinez *et al.*, 2009) and to a subsequent filtration in order to separate the cellulose and hemicellulose fractions not hydrolysed, the lignin, and the enzymes from sugars and water. Note that the product must be purified from compounds which are inhibitors for the successive fermentation; in fact the presence of inhibitors derived from sugar degradation in the hemicellulosic hydrolysate, originated during the hydrolysis of the raw material, negatively influences the bioconversion of xylose to xylitol. Therefore, their removal must be ensured before the fermentation reactor (Canilha *et al.,* 2008). The treatment of the hydrolysate can be done by active charcoal adsorption, which offers a high efficiency associated to a lower cost (Canilha *et al.,* 2008).

A common feature of yeasts producing xylitol is that they are subject to glucose repression. *Pichia* and *Candida* yeasts convert xylose to xylitol, or a mixture of xylose and arabinose to xylitol and arabitol (Leathers, 2003). However, if glucose is also present, as in rye straw hydrolysate, the strain preferentially utilizes glucose and metabolizes xylose and arabinose only slowly, with little accumulation of sugar alcohol (Leathers, 2003). Yeasts produce ethanol until the glucose is totally consumed and then they start to ferment xylose and arabinose (Leathers, 2003).

The fermentation is performed at a temperature between 30 °C (Nigam and Singh, 1995) and 34 °C (Saha and Bothast, 1996), i.e. within a range suitable for these yeasts.
In the simulation model we have assumed: a fermentation time of 92 h, complete conversion of glucose into ethanol, and 99.1% of xylose assimilation with a yield factor of 0.7024 g/g for xylitol and of 0.078 g/g for the biomass, according to Martìnez *et al.,* 2009. In order to take into account the presence of arabinoxylan a conversion of 0.54 g arabitol/g arabinose in arabitol was considered (Saha and Bothast, 1996).
After fermentation, the recovery of xylitol from other compounds (i.e. xylose, arabinose, arabitol), can be done by crystallization, as widely proposed in literature (Rivas *et al.,* 2006, Martìnez *et al.,* 2009, Sampaio *et al.,* 2006). According to Rivas *et al.,* (2006) first the separation of coloured substance is done by charcoal adsorption (1 kg/15 kg liquor), then, after filtration to remove yeast and other solids, the liquor (stream 604) is concentrated by vacuum evaporation at 30-40 °C to reach a NVC (non volatile compounds) content of 0.4 kg/kg (corresponding to a xylitol concentration of 0.28 kg/kg of liquor). At this point ethanol is added in order to perform the precipitation of a part of the NVC (proteins, uronic acids, ashes). After separation of the precipitate, a second evaporation stage brings the concentration of NVC up to 0.68 kg/kg. Finally the crystallization is performed in ethanol medium (60% v/v) cooling down to -5 °C in 72 hours, so that the xylitol solubility is reduced in the presence of ethanol. The xylitol crystals (98 % w/w) are washed and dried, and an overall recovery yield of 50% is obtained. Xylitol is sold as valuable co-product of the process, together with ethanol; thanks to its several applications in the food and health care industries its market price is quite high (7 $/kg, Leathers, 2003).
The ethanol used in the xylitol separation section is recovered at 83% (w/w) (stream 607) by means of a distillation column with 8 theoretical trays and mass reflux ratio of 2.58.
After the separation, the solids of mother liquid (stream 608) can be recovered and the obtained product contains about 55% (w/w) of xylitol, 20% (w/w) of xylose and other minor compounds (ash, arabitol, arabinose). There is no market for this low purity xylitol, so in our study the mother liquid is sent to the evaporation section, and recovered with the other solid residues of the process, for possible energy production.

## 6.3 Simulation results and equipment design

Although other works dealing with simulation and economical analysis of corn stover processes refer to a capacity of 2,000 tons of raw material per day (i.e. Aden *et al.,* 2002, Wooley *et al.,* 1999a), in this work a more realistic value of 120 tons of rye straw per day was assumed, taking into account the problems related to the collection and the logistic of larger amounts of rye straw, and to the risk of investment associated with large plants, at least for the situation typical for Germany, to which we are referring.

Table 6.2 shows the composition of the lignocellulosic material (rye straw) used in simulation. The moisture content is 5.4% (w/w). Calculations were based on the analysis performed to evaluate monomeric sugars composition, lignin, moisture and ash content (Ingram, 2008).

**Table 6.2** *Rye straw dry composition used in simulation.*

| Component | Mass fraction |
|---|---|
| Hemicellulose | 0.235 |
| Cellulose | 0.436 |
| Lignin | 0.186 |
| Ash | 0.034 |
| Other | 0.109 |

The physico-chemical properties of the components involved were taken from the database specifically created for this purpose by Wooley and Putsche (1996). The thermodynamic properties and binary coefficients necessary to implement the NRTL thermodynamic model were either available in Aspen Plus$^{TM}$ database or regressed from literature experimental data.

Figure 6.2 summarizes the principal inlet and outlet streams of the process with the corresponding mass flow rate values. The total water consumption is 2.29 kg per kg of 99.8% w/w ethanol produced.

The fixed-bed reactors, where the pretreatment is carried out, maintain features of a batch operation: so, in order to process 5,285 kg/h of solids five parallel tubular reactors able to load 625 kg each were used. The diameter of such reactors is 0.75 m and their length is 3.5 m, if we assume 10 min as the time needed to load/unload them between two subsequent batch cycles. The solid reaction time is set at 25.5 min. A total flow rate of 21,200 kg/h of water is pumped at 40 bar and 205 °C through the (already preheated) solids in the reactors.

In the ethanol production line reactors for both the enzymatic hydrolysis and the fermentation are present. These two operations are carried out in trains of 2 vessels with the size of respectively 287 $m^3$ volume each (hydrolysis) and 237 $m^3$ volume each (fermentation). The enzyme consumption is 12 FPU (filter paper unit) of cellulase per kg of cellulose (Aden *et al.,* 2002). The flow rate of water added to the solid is 10,370 kg/h, so that the ethanol concentration at the end of the fermentation (stream 302) turns to be around 7% (w/w). The inoculum for the fermenters is obtained in 3 batch reactors with a volume of 0.53, 5.3 and 53 $m^3$, respectively. The batch time for each step is 24 hr and the turn-around time for each seed fermenter is 12 hr. In this way it is possible to obtain 1330 kg of inoculum every hour. During the fermentation 932 kg/h of ethanol and 899 kg/h of $CO_2$ are produced. The 98.8% of the total $CO_2$ is removed as vent from the reactors (stream 301),

and the rest from the top stream of the beer column (stream 404). Both of these streams are sent to a scrubber column where the 99.3% of the ethanol in the vents is recovered.
Table 6.3 shows the columns details. As suggested by the literature, Nutter V-grid trays are used for the beer and rectifier columns due to their good performance with solid suspensions and their relatively high efficiency. The scrubbing tower is a random packed column (Aden *et al.,* 2002).

**Table 6.3** *Columns details.*

| | **Diameter [m]** | **Tot High [m]** | **Theoretical trays** | **Trays efficiency[1]** | **Mass reflux ratio** |
|---|---|---|---|---|---|
| Scrubber | 0.80 | 3.8 | 2 | Pack col. | - |
| Beer column | 0.74 | 19.5 | 13 | 48% | - |
| Rectifier column | 0.64 | 36.6 | 34 | 52% | 2.58 |
| Solvent recycle column | 1.96 | 8.4 | 8 | 52% | 2.58 |

The hydrolysate coming out from the pretreatment undergoes enzymatic hydrolysis, for which two reactors are used with a volume of 460 $m^3$ each. The outlet stream flow rate (stream 601) is 23,104 kg/h, of which 1,048 kg/h are xylose. The saccharified stream is concentrated up to 88 g/L of xylose and subject to a preliminary filtration stage and an active charcoal adsorption treatment to separate inhibitors for the following fermentation of xylose to xylitol, which is carried out in four fermenters (332 $m^3$ volume each). As a result, 736 kg/h of xylitol, 82 kg/h of cells, 52 kg/h of ethanol are obtained (stream 604); in the product also arabitol, $CO_2$, unreacted xylose and arabinose are present, according to the yields reported in section 6.2.

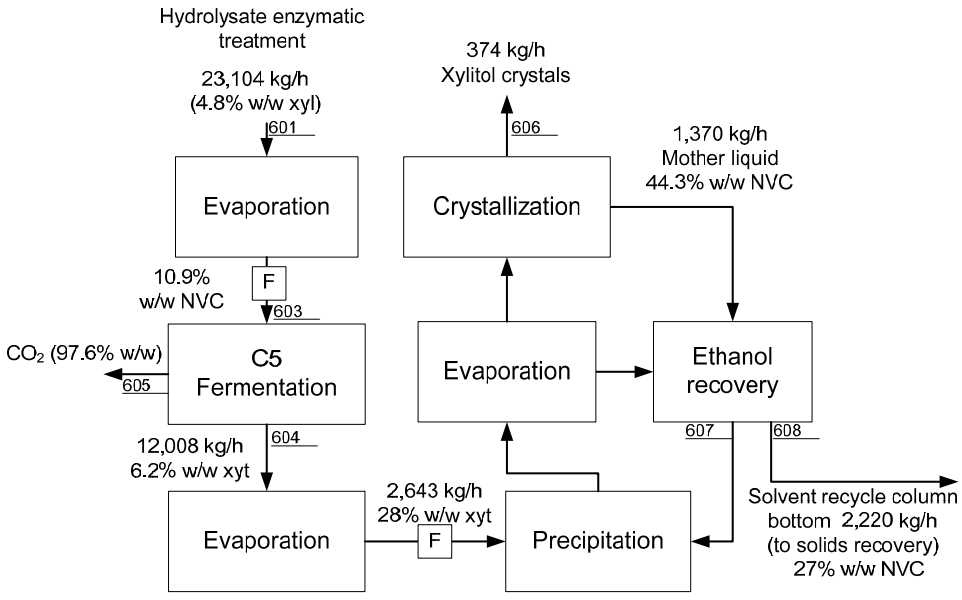


**Figure 6.4** *Recovery of xylitol (Area 600) details.*

By means of the crystallization 374 kg/h of xylitol of 98.94 % (w/w) purity can be recovered (stream 606); although this value could be improved by further processing of the mother liquid, the following calculations are based on this value, in order to be as close as possible to existing literature experimental data (Rivas *et al.,* 2006).
Figure 6.4 shows the simulation results obtained for the process line to obtain xylitol, while in Figure 6.5 the solid recovery section results are reported.

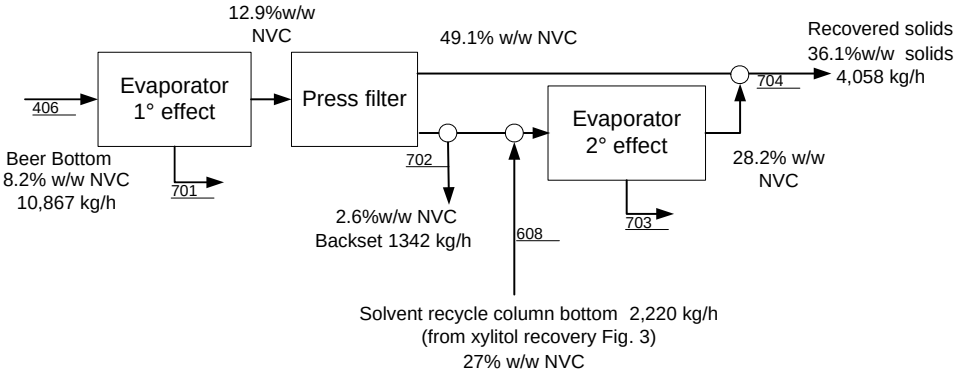


**Figure 6.5** *Solid residue recovery (Area 700) details.*

A Lower Heating Value (LHV) of 8,650 kJ/kg was calculated for these two solid streams mixed together, which can then be directly fed to a burner (we recall that, according to Wooley *et al.,* (1999b), a minimum value of 4,644-5,800 kJ/kg is required to sustain combustion. The higher value we found is mainly due to the lignin). In our work the production of energy from the solids was not simulated nor included in the economical analysis, but it was estimated that about 85% of all the process energy requirements could be obtained and supplied in this way. In fact according to Wooley *et al.,* (1999b) with a combined heat and power generation plant (CHP) approximately 50% of boiler feed can be recovered as steam and 15% as electricity, so that calculations using this data showed that in our case 7.6 MW as steam and 2.28 MW as electricity could be produced.

## 6.4 Energy balance and pinch analysis

The hot liquid water pretreatment is an energy intensive operation because of the high temperature and the large water flow rate involved. Therefore, energy optimization results to be a key factor for the overall economy of the process. Heat integration in the process was performed by applying the Pinch Technology Analysis (PTA), originally proposed by Linnhoff and Flower (1978), to design heat exchanger networks.
According to PTA, the thermodynamic analysis of the process streams is carried out first, in order to find the maximum theoretical heating power that can be recovered and exchanged between hot and cold streams of the process. The hot and cold composite curves obtained

are displayed in Figure 6.6a, while Figure 6.6b shows the grand composite one. The resulting pinch point is at 96.36 °C for the hot streams and 86.36 °C for the cold ones (a $\Delta T_{min}$ of 10 °C was assumed).

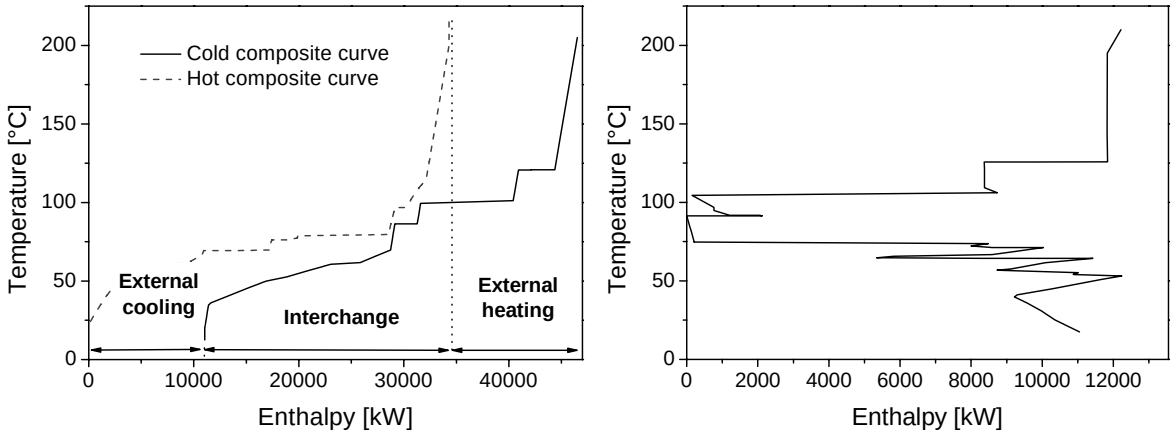


*(a)* *(b)*

**Figure 6.6** *Pinch analysis results. Hot and cold composite curves (a) and grand composite curve (b).*

From these figures the minimum energy to be supplied (12,216 kW) and to be removed (11,047 kW) by external sources can be calculated. This information was then used to build up the exchanger network that was eventually simulated. The exchange areas were calculated with an overall coefficient of 850 W/m$^2$K for single-phase fluids, and of 1500 W/m$^2$K when steam is used for heating. The resulting network consists in 14 regenerative heat exchangers that allow obtaining a theoretical energy saving equal to 68.9% (as steam) of and a reduction of cooling water consumption of 64.4%.

These data do not include the amount of power required to heat up the solid, part of which was provided from the water itself (heated up to 205 °C instead than to 200 °C), while the rest (i.e. 264 kW) was supposed to be supplied directly by steam at high temperature (200 °C). This option was chosen in order to be conservative. In practice, the solids can be preheated using the steam produced depressurizing the other pretreatment reactors.

## 6.5 Economical and financial analysis

To carry out an economic analysis all the capital and operating costs must be known. To this purpose, the process was divided in 7 sections, listed in Table 6.4. The capital investment was estimated mostly using the relationships developed by Ulrich and Vasudervan (2004), and the results are shown in Table 6.4. Other costs are: operating ones (natural gas, electric power, high and low pressure steam, refrigerant and cooling water), maintenance cost,

labour cost and feedstock cost. Raw materials are rye straw, enzymes, chemicals, process water and denaturant.

**Table 6.4** *Total capital investment and contribution of the different areas.*

| | Installed cost [€] | Contingency [€] | Auxiliary Facilities [€] | Total grass root [€] |
|---|---|---|---|---|
| **Feedstock storage/handling, area 100** | 1,049,000 | 188,800 | 371,300 | 1,609,100 |
| **Pretreatment, area 200** | 945,000 | 170,100 | 334,500 | 1,449,600 |
| **Enzymatic hydrolysis and fermentation (solid residue), area 300** | 4,797,000 | 863,500 | 1,698,200 | 7,358,700 |
| **Ethanol and solid recovery, area 400/700** | 2,693,000 | 484,700 | 953,300 | 4,131,000 |
| **Saccharification hydrolysate, area500** | 2,455,000 | 441,900 | 869,100 | 3,766,000 |
| **Xylitol production and recovery, area500/600** | 5,524,000 | 994,300 | 1,955,500 | 8,473,800 |
| **Heat exchanger network** | 1,517,000 | 273,000 | 537,000 | 2,327,000 |
| **Total** | | | | 29,115,200 |

Main parameters and data used in the calculations are reported in Table 6.5. These values were retrieved from literature and from data of industrial plants. Note that the enzymes costs are not known because industrial cellulosic ethanol plants are not in operation yet. For this reason, we have assumed an additional cost of 0.17 $/gal ethanol to take into account the use of cellulase, according to current ethanol financial models (e.g. Aden *et al.*, 2002).

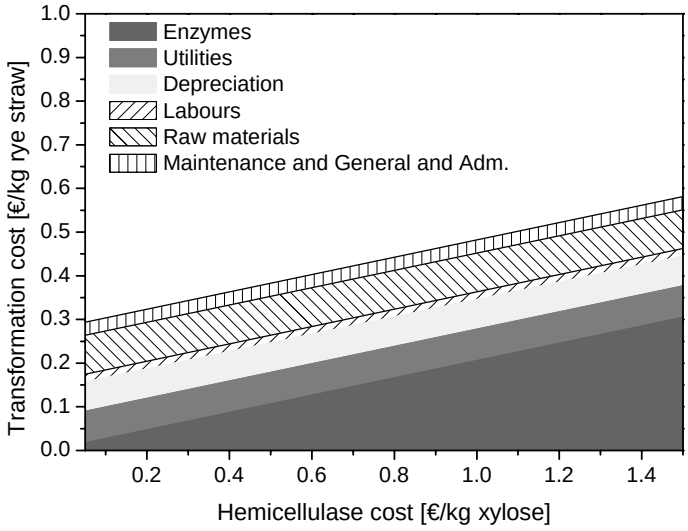


**Figure 6.7** *Cost per tons of raw material processed as a function of the hemicellulose cost.*

Due to the lack of data it is almost impossible to estimate the costs of enzymes like xylosidase and xylanase, used to break down the hemicellulose. Therefore a sensitivity analysis was performed, whose results are shown in Figure 6.7.

**Table 6.5** *Main parameters used in the analysis.*

| | Value | Reference |
|---|---|---|
| **Prices** | | |
| Ethanol denaturated [€/L] | 0.56 | European ethanol price report (October 2008) |
| Xylitol [€/kg] | 5.18 | Leathers, 2003 |
| Rye Straw [€/tonne] | 87 | Leieble *et al*., 2008 |
| Process water [€/tonne] | 0.041 | Average industrial data |
| **Utilities** | | |
| Steam 10 bar [€ /tonnes] | 12.9 | Ulrich and Vasudervan (2004) |
| Steam 25 bar [€ /tonnes] | 63.0 | |
| Refrigerant [€/GJ] | 2.49 | |
| Cooling water [€ /tonnes] | 0.041 | Average industrial data |
| Electricity [€/100 kWh] | 12.72 | Eurostat, 2009 |
| Natural gas [€/GJ] | 3.85 | Bloomberg, 2009 |
| **Other costs** | | |
| Labours [€/operator/yr] | 33,300 | Average industrial data |
| Maintenance | 3% TCI | Average industrial data |
| General and Administrative | 2% T.R. | Average industrial data |
| **Tax rate** | 40% | Average industrial data |
| **Discount rate** | 12% | Average industrial data |

Unknown are also the costs for rye straw, because they depend on a number of parameters. In general they should include the collection and bare costs as well as the transport cost, a premium paid to the farmer and finally a part due to the use of fertilizer (Aden *et al.,* 2002). Some literature estimates include no net payment to the farmer, while others account for premiums, but assume that the cost of fertilizer is hidden in the premium payment. The transport costs depend on the plant size and location, so a correct estimate should be based on a supply chain analysis aimed to find out their optimal values. Among other literature works about this topic, we recall the one by Leible *et al.,* (2007), who estimated a cost of 87 €/ton for the preparation and supply of straw when the transport distance is 100 km. Our simulation is based on the situation in Germany, which is one of the biggest world rye producers: in 2006 the amount exceeded 2.64 million of metric tons, and it reached 3.319 million in 2007 (FAO, 2009). Ericsson and Nilsson (2006) propose a residue generation ratio for straw to cereal grain equal to 1.3; so, if it is assumed that one quarter of these residues can be harvested and roughly one third of the harvested straw is used in animal

husbandry, it can be obtained 0.22 ton of straw per ton of cereal. This means that all the rye straw needed to feed our process has to be harvested in an area with a radius of about 80 km: note that the calculation is conservative because the yield of rye production takes into account the whole area of the Country, while conceivably the plant will be placed in a region where the rye is cultivated more intensively.

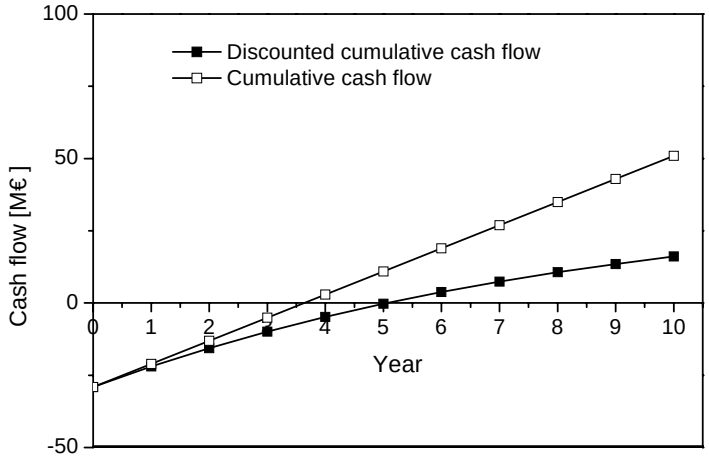


**Figure 6.8** *Process discounted and cumulative cash flow in case of hemicellulase cost contribution of 0.1$ every kg of xylose processed.*

For the quantification in terms of cost savings and returns in a short-term time horizon has been conducted by means of a financial analysis. A payback time of 5 years was obtained (Figure 6.8), a value in the range of the standard requirements by the financial market, if we assume a hemicellulase contribution to the total operating cost of 54.7 € per ton of xylose produced from saccharification.

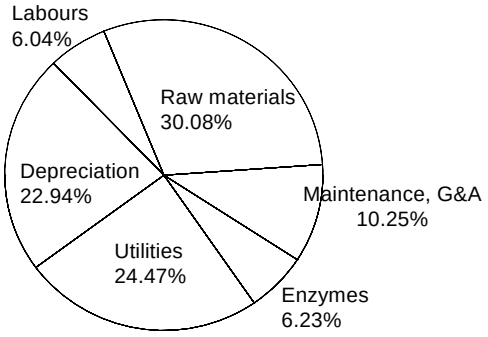


**Figure 6.9** *Allocation of the process costs in case of hemicellulase cost contribution of 0.1$ every kg of xylose processed.*

The resulting cost allocation is the one reported in Figure 6.9. The "Net Present Value" (NPV) at the 10th year, is about 21.75 M€, while the calculated "Return On Investment" (ROI) is equal to 0.255, and the internal rate of return (IRR) after 10 years is 24.78%.

## 6.6 Concluding remarks

This chapter addressed the possibility to integrate the classical production of bioethanol from cellulose with an alternative utilization of the hemicellulosic part of the biomass to produce xylitol. The problem was considered from both the technical and economical points of view.

The analysis was based on a rigorous process simulation that was carried out to assess the mass and energy balances of all the sections of the process. The minimum energy and water consumptions were determined. The capital investment and operating costs were estimated according to up-to-date information, and finally a financial analysis was implemented and carried out to highlight costs and profitability.

It was found out that, if a substantial portion of hemicellulose is transformed to xylitol, this product significantly contributes to the total revenue of the process, thus making it profitable to build also smaller plants like the one presently considered.

## 6.7 References

Aden, A., M. Ruth, K. Ibsen, J. Jechura, K. Neeves, J. Sheehan, B. Wallace, L. Montague, A. Slayton, and J. Lukas (2002). *Lignocellulosic Biomass to Ethanol Process Design and Economics Utilizing Co-Current Dilute Acid Prehydrolysis and Enzymatic Hydrolysis for Corn Stover.* National Renewable Energy Laboratory Technical Report, TP-510-32438.

Balat, M. and H. Balat (2009). Recent Trends in Global Production and Utilization of Bio-Ethanol Fuel. *Appl. Energy*, **86**, 2273-2282.

Bloomberg (2009). *Energy Prices*. Available at: www.bloomberg.com [Accessed September 2009].

Bockemühl, V., T. Ingram, T. Rogalinski, L. Popper, G. Brunner, and G. Antranikian (2009). Bioconversion of Rye Straw at Elevated Temperatures. Presented at: *Biorefinica 2009*, DBU Osnabrück (Germany), January 27-28.

Business Communications Co. Inc., ETATS-UNIS (2002). The Global Market for Polyols. *Int. Sugar J.*, **104**, 352-354.

Canilha, L., W. Carvalho, M. Das Graças Almeida Felipe, and J.B. De Almeida e Silvia (2008). Xylitol Production from Wheat Straw Hemicellulosic Hydrolizate: Hydrolizate Detoxification and Carbon Source used for Inoculum Preparation. *Braz. J. of Microbiol.*, **39**, 333–336.

Ericsson, K. and L.J. Nilsson (2006). Assessment of the Potential Biomass Supply in Europe using a Resource-Focused Approach. *Biomass and Bioenergy*, **30**, 1–15.

Eurostat (2009). *Electricity Prices for First Semester 2009* Available at: http://epp.eurostat.ec.europa.eu/cache/ITY_OFFPUB/KS-QA-09-048/EN/KS-QA-09-048-EN.PDF [Accessed Sempember 2009].

FAO (2009). *Statistics*. Available at: http://faostat.fao.org/site/567/default.aspx#ancor [Accessed September 2009].

Hägerdal, B.H., K. Karhumaa, C. Fonseca, I. Spencer-Martins, and M.F. Gorwa-Grauslund (2007). Towards Industrial Pentose-Fermenting Yeast Strains. *Appl. Microbiol. Biotechnol.*, **74**, 937-953.

Ingram, T. (2008). Thermal and Thermal-Enzymatic Hydrolysis of Ligno-cellulosic Biomass for the Production of Bioethanol. *Master thesis*, TU Hamburg-Harburg (Germany).

Ingram, T., T. Rogalinski, V. Bockemühl, G. Antranikian, and G. Brunner (2009). Semi-Continuous Liquid Hot Water Pre-treatment of Rye Straw for Bioethanol Production. *J. of Supercrit. Fluids*, **48**, 238-246.

Kádár, Z., S.F. Maltha, Z. Szengyel, K. Réczey, and W. De Laat (2007). Ethanol Fermentation of Various Pretreated and Hydrolyzed Substrates at Low Initial pH. *Appl. Biochem. Biotechnol.,* **137-140**, 847-858.

Leathers, T.D. (2003). Bioconversion of Maize Residues to Value-added Coproducts Using Yeast-like Fungi. *FEMS Yeast Res*., **3**, 133-140.

Leible, L., S. Kälber, G. Kappler, S. Lange, E. Nieke, and B. Fürniss (2007). Fischer-Tropsch Synfuels from Cereal Straw via Fast Pyrolysis and Gasification – Costs and Benefits. Presented at: *15th European Biomass Conference & Exhibition 2007*, Berlin, (Germany), May 7-11.

Linnhoff, B. and J.R. Flower (1978). Synthesis of Heat Exchanger Networks: I. Systematic Generation of Energy Optimal Networks. *AIChE J.,* **24**, 633-642.

Lynd, R.L. (1996). Overview and Evaluation of Fuel Ethanol from Cellulosic Biomass: Technology, Economics, the Environment, and Policy. *Annu. Rev. Energy Environ*., **21**, 403-465.

Martínez, E.A., M. Giulietti, J.B. de Almedia e Silva, S. Derenzo, and M. das Graças Almeida Felipe (2009). Batch Cooling Crystallization of Xylitol Produced by Biotechnological Route. *J. Chem. Technol. Biotechnol.*, **84,** 376-381.

Mosier, N., C. Wymann, B. Dale, R. Elander, Y.Y. Lee, M. Holtzapple, and M. Ladish (2005). Features of Promising Technologies for Pretreatment of Lignocellulosic Biomass. *Bioresour. Technol*., **96**,673-686.

Nigam, P., and D., Singh (1995). Processes for Fermentative Production of Xylitol – a Sugar Substitute. *Process Biochemistry*, **30**, 117-124.

Rivas, B., P. Torre, J.M. Domínguez, A. Converti, and J.C. Parajó (2006). Purification of Xylitol Obtained by Fermentation of Corncob Hydrolysates. *J. Agric. Food. Chem.,* **54**, 4430-4435.

Saha, B.C. and R.J. Bothast (1996). Production of L-Arabitol from L-Arabinose by Candida Entomaea and Pichia Guillermondii. *Appl. Microbiol. Biotechnol.,* **45**, 299-306.

Sampaio, F.C., F.M. Lopes Passos, F.J. Vieira Passos, D. De Faveri, P. Perego, and A. Converti (2006). Xylitol Crystallization from Culture Media Fermented by Yeasts. *Chem. Eng. Process.,* **45**, 1041-1046.

Sassner, P., M. Galbe, G. Zacchi (2008). Techno-Economic Evaluation of Bioethanol Production from Three Different Lignocellulosic Materials. *Biomass and Bioenergy*, **32**, 422-430.

Ulrich, G.D. and P.T. Vasudevan (2006). *Process Design and Economics. A Practical Guide*. Process Publishing, Lee (U.S.A.).

Wooley, R., M. Ruth, D. Glassner, and J. Sheehan (1999a). Process Design and Costing of Bioethanol Technology: A Tool for Determining the Status and Direction of Research and Development. *Biotechnol. Prog.,* **15**, 794-803.

Wooley, R., M. Ruth, J. Sheehan, K Ibsen, H. Majdeski, and A. Galvez (1999b) *Lignocellulosic Biomass to Ethanol Process Design and Economics Utilizing Co-Current Dilute Acid Prehydrolysis and Enzymatic Hydrolysis Current and Futuristic Scenarios*. National Renewable Energy Laboratory report, NREL/TP-580-26157

Wooley, R.J. and V. Pusche (1996). *Development of an ASPEN PLUS Physical Property Database for Biofuels Components*. National Renewable Energy Laboratory report, MP-425-20685.

Zhisheng, Y. and Z. Hongxun, (2004). Ethanol Fermentation of Acid-hydrolyzed Cellulosic Pyrolysate with Saccharomyces Cerevisiae. *Bioresour. Technol.*, **93**, 199–204.

# Chapter 7

# LHW pretreatment of wheat bran[5]

This Chapter deals with the experimental pretreatment of lignocellulosic material with the liquid hot water (LHW) pretreatment. The experiments were performed at the TUHH University of Hamburg (Germany). The objective of this investigation was to determine the best pretreatment conditions (temperature and total reaction time) for the hot liquid treatment of wheat bran in order to obtain the maximum amount of fermentable sugars after the enzymatic hydrolysis. The LHW pretreatment of wheat bran was studied in both batch and fixed-bed reactor, in order to understand the behaviour of this material and its different polymers. Solid, carbon, and protein solubilization were measured after the treatment at different temperatures and for different total reaction times. It was demonstrated that, with a fixed bed reactor, the amount of degradation products is significantly lower compared to the treatment in the batch reactor. The enzymatic hydrolysis was performed only for the hydrolysates obtained after pretreatment with the fixed bed reactor. Cellulases and xylanases from *Penicillium janthinellum* were used and it was demonstrated that the sugar recovery from the liquid hydrolysate increases with the increasing reaction temperature, while the sugar recovery from the solid residue decreases.
To our best knowledge, experimental data on the pretreatment of the whole wheat bran with liquid hot water finalised to ethanol production are not available in the literature, as so far the research in this field was focused on destarched wheat bran (Chotěborská *et al.,* 2004, Palmarola-Adrados *et al.,* 2005). Wheat bran was chosen as a lignocellulosic material because it is a by-product of the wheat milling industry in large quantities, and so it represents a significant and underutilized source of sugars that could be exploited to produce bioethanol.

## 7.1 Introduction

It is well known that by now lignocellulosic ethanol is not economic and still under study (Saxena *et al.,* 2009). The current research is mainly focused on two issues: the use of the pentose part of the biomass and the development of the pretreatment step (Hendriks and Zeeman, 2009). On the one hand natural yeasts are able to ferment only C6 monomeric

[5] Part of this Chapter has been submitted for publication to *Biomass and Bioenergy,* (See Page XV).

sugars, while the portion of C5 sugars in lignocellulosic materials may be relevant, on the other hand sugars in the biomass are present as polysaccharides (cellulose for C6, hemicellulose for C5), so that their hydrolysis must be performed first. The pretreatment is the first step of the transformation of the biomass, through which, in general, the highly crystalline structure of the cellulose and the hydrophobic seal due to the lignin fraction of the biomass can be broken down (Mosier *et al.,* 2005b). In Figure 7.1 the structure of the biomass is shown. Cellulose and hemicelluloses are present in the plant cell wall in a complex and compact structure.

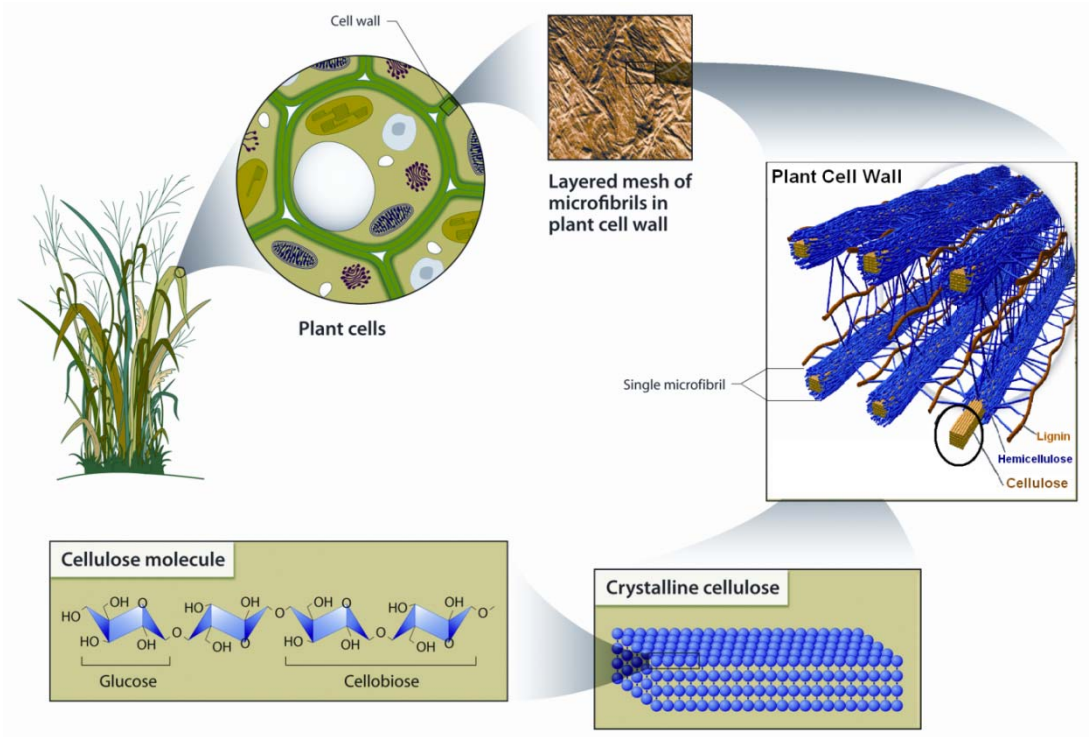


**Figure 7.1** *Structure of a lignocellulosic biomass (U.S. Department of Energy Genome Programs, 2009).*

The pretreatment is really an important step, as it strongly affects the enzymatic treatment and fermentation steps downstream. The influence on the structure of the biomass and the partial hydrolysis of polymeric sugars usually achieved by a suitable pretreatment allow the enzymes to hydrolyse more efficiently these polymers (Yu *et al.*, 2008, Balat *et al.,* 2008). However the pretreatment has to be carefully balanced, because if it is too strong both higher production of monomeric sugars and degradation into compounds toxic for yeasts are obtained. It is noteworthy to remind that the task of this step is not to obtain monomeric sugars but to prepare the biomass to the following enzymatic hydrolysis and fermentation, in order to maximize the ethanol production. For these reasons a key factor of the use of lignocellulosic materials to produce bioethanol is definitively the pre-treatment. A wide range of pretreatments have been proposed and are under current investigation: steam, $CO_2$,

and ammonia fiber explosion as well as ozonolysis, acid, and alkaline hydrolysis, or organosolv process, and also biological pretreatments (Sun and Cheng, 2002).

Among other methods the liquid hot water pretreatment (LHW) seems to be promising. This pretreatment has several potential advantages if compared with others: simplicity, no use of additional chemicals and consequently no production of process residues, low generation of inhibiting products, low cost of material of construction (Lynd, 1996). The LHW method has been broadly investigated in the past on a wide range of biomass and using different reactor types: batch (Laser *et al.,* 2002), continuous (Mosier *et al.,* 2005a, Rogalinski *et al.,* 2008), and fixed bed (Sasaki *et al.,* 2003, Liu and Wyman, 2005, Ingram *et al.,* 2009). We think that use a semi-continuous fixed-bed reactor allows obtaining high solid-to-water-ratios and to save energy because no biomass comminution is necessary. In addition, by controlling the residence time of the hydrolysate it is also possible to prevent the degradation of the sugars. A pioneer of the use of compressed-hot water through a stationary bed of biomass in order to accelerate solubilization of hemicellulose and lignin was Bobleter (Bobleter *et al.,* 1980; Bobleter, 1994; Hormeyer *et al.,* 1988). In this Chapter the LHW of wheat bran is addressed by performing experiments in both a batch and in semi-continuous reactor. Wheat bran was chosen as lignocellulosic material because it is a by-product of the wheat milling industry in large quantities, and so it represents a significant and underutilized source of sugars that could be exploited to produce bioethanol.

## 7.2 Properties of LHW, and mechanism of action

LHW can be generally described as a treatment of biomass with water at temperature above 120 °C and under various pressures. In Figure 7.2a the water VLE diagram of water is shown: the critical point is at 22.1 MPa and 647 K.

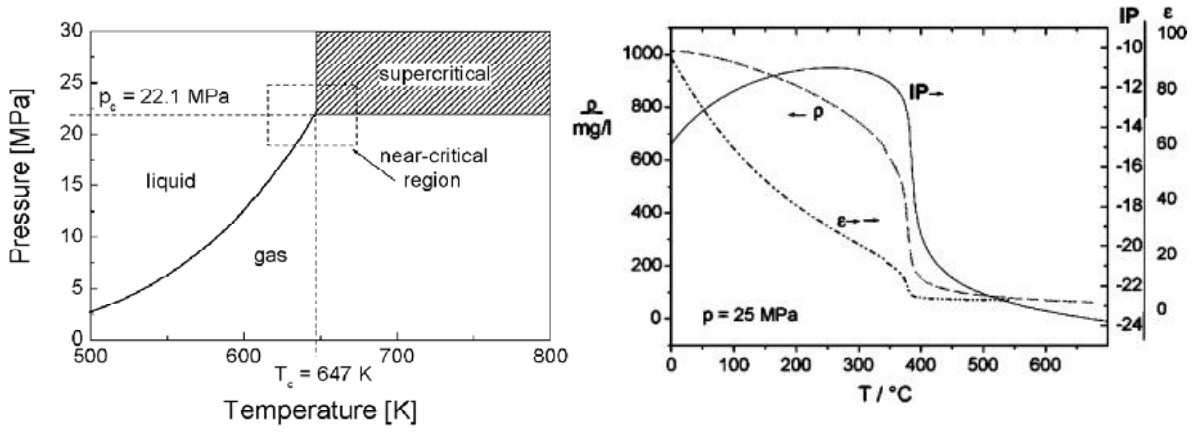


*(a)* *(b)*

**Figure 7.2** *Water VLE diagram (a) and selected properties of water at high temperature and high pressure (b). IP: ionic product, expressed as log[$H_3O^+$][$OH^-$]; ε: relative dielectric constant; ρ: density (Yu et al., 2008).*

Compared to ambient conditions the thermodynamic properties of sub- and supercritical water change dramatically. One important property with respect to the polarity of water is its dielectric constant $\varepsilon$ (Figure 7.2b), that is a function of temperature and density.
The drop of the dielectric constant with the temperature clarifies the significant increase of the solvent power for most organic compounds in sub- or supercritical water. Moreover a higher ε reduces the activation energy of reactions with a transition state of higher polarity compared to the initial state. Another propriety that changes with temperature is the ionic product that rises from a value of $10^{-14}$ up to $10^{-11}$ in the subcritical region. Due to the associated increase in the activity of hydronium and hydroxyl ions, subcritical water itself promotes acid and base catalysed reactions without any additional catalysts like mineral acids. In contrast, the ionic product drops at near- and supercritical conditions as a result of the strong decrease in water density. It should be noted, that the pressure does not noticeably affect the ionic product at temperatures below 300 °C. A suitable explanation is the incompressibility of water at these conditions (Yu *et al.,* 2008). Depending upon the temperature and pressure, LHW supports either free radical or ionic reactions. At high densities below the critical temperature or in supercritical water at very high pressures, ionic reactions dominate; at high temperatures and low densities, free-radical reactions are superior.
At temperatures in the range of 150-230 °C, and in presence of liquid water the lignocellulosic materials undergo hydrolysis reactions. Different are the theories proposed in literature about the reaction mechanism, some of them which presented in Chapter 9. Garrote *et al.*, (1999) asserted that these hydrolysis reactions are catalyzed by the presence of the hydronium ions generated by water autoionization. The hemicellulose, which is made mostly of xylose, is the part of the biomass most susceptible to this type of reactions because of its heterocyclic ether bonds. Both generation of oligosaccharides and splitting of the acetyl groups from the hemicellulosic fraction of the raw materials occur. These authors suggested that in further reaction stages, the hydronium ions generated from acetic acid autoionization also act as catalysts in the degradation of polysaccharides.
Other researchers proposed that, under the operational conditions usually employed in hydrothermal treatments, the formation of hydronium ions from acetic acid is more important than from water (Heitz *et al.,* 1986, Nabarlatz, 2004), the role of water autoionization being limited to the initial reaction stages. Uronic acids can also contribute to the generation of hydronium ions, but their effects are not well established (Conner and Lorenz, 1986). Depending on the operational conditions used in experiments, polysaccharides (mainly hemicelluloses) are depolymerised to oligomers and monomers, and the correspondent sugars (pentoses and hexoses) can be dehydrated to furfural and hydroxymethylfurfural, respectively. Other fractions of the lignocellulosic material different from hemicelluloses can also react in the presence of water: for example, cellulose and

lignin can be partially depolymerised by similar hydrolysis reactions. Additional condensation reactions involving furfural, lignin and/or reaction intermediates have been reported (Li *et al.,* 2007, Kim and Lee 2006, Sun *et al.,* 2004), and Garrote *et al.,* (1999) found that $CO_2$ was generated from uronic acids by decomposition of the carbonyl groups. In autohydrolysis, the depolymerised lignin fragments remain in the proximity of condensation sites in the biomass matrix, and are more liable to recondense than in acidolysis, where degradation products go into solution.

## 7.3 Materials

### *7.3.1 Wheat bran*

Bran is the hard outer layer of the kernel and consists of combined aleurone and pericarp. Along with germ, it is an integral part of whole grain, and is often obtained as a by-product of milling in the production of refined grains. Bran is present in and may be milled from any cereal grain, including rice, wheat, oats, and millet. Industrial wheat bran usually accounts for 14-19% (w/w) of the grain and comprises the outer covering, the aulerone layer and part of the starchy endosperm (Figure 7.3a and b).

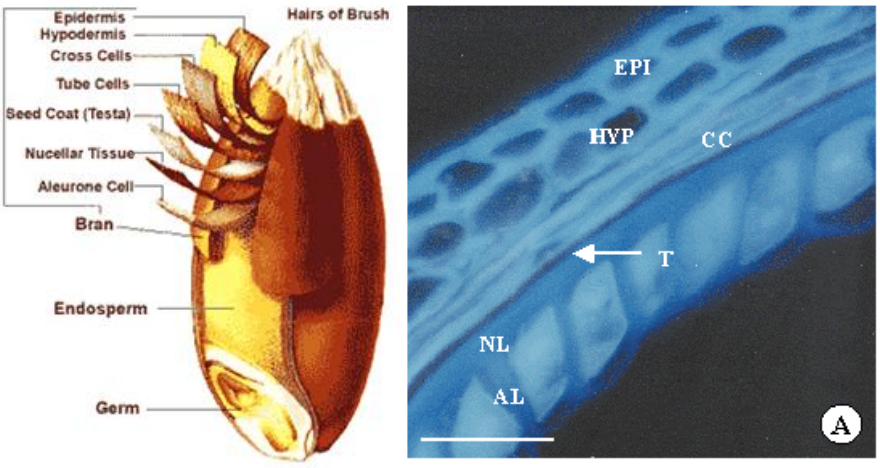


*(a)* *(b)*

**Figure 7.3** *Wheat kernel (a) and autofluorescence pictures of wheat bran (b) AL: Aleurone layer, NL: Nucellus, S: Seed coat, CC: Cross cells, EPI: Epidermis, HYP: Hypodermis (Benamrouche et al., 2002).*

Table 7.1 shows the carbon and nitrogen content of the wheat we have used. The amount of proteins was calculated using a nitrogen factor of 6.25. In order to determine the carbohydrates amount, the starting material was analyzed according to the two steps acid hydrolysis method (NERL, 2009) in the laboratories of the Institute of Wood Technology

and Wood Biology (Hamburg, Germany). Results are reported in Table 7.2 and compared with some literature values.

**Table 7.1** *Carbon (C), nitrogen (N), protein, and ash content of wheat bran.*

| C [g/kg] | N % (w/w) | Protein % (w/w) | Ash % (w/w) |
|---|---|---|---|
| 470 | 2.55 | 15.9 | 6.4 |

**Table 7.2** *Two steps acid hydrolysis results. Amount of monomeric carbohydrates obtained from 100 g of dry matter.*

| | D-Xylose | D-Glucose | L-Arabinose | D-Galactose | Mannose | Rhamnose |
|---|---|---|---|---|---|---|
| **This work** | 16.4 | 31.1 | 9.88 | 1.2 | 0.33 | 0.11 |
| **Swennen *et al.*, 2006** | 18.5 | 37.3 | 10.2 | 1.3 | 0.5 | n.a. |
| **Maes and Delcour, 2002** | 16.9 | 28.5 (16.7)[1] | 10.1 | 1.9 | n.a. | n.a. |

1-Starch
n.a.: not analyzed

Wheat bran is a kind of "special" lignocellulosic material because of the presence of starch, proteins and fats. The two steps acid hydrolysis is optimized for less complex raw materials made mainly of cellulose, hemicellulose and lignin. The behaviour of the other components is not exactly known and this could lead to errors in the results of the analysis

It can be interesting to briefly describe the wheat bran arabinoxylane (AX) as it is different from hemicellulose usually present in the lignocellulosic biomass. AX and its extraction from wheat bran have been studied because of AX important role in the preparation of dough, its bread making properties and its application as food additive (Maes and Delcour, 2002, Bergmans *et al.*, 1996). This polymer consists of a backbone of (1→4)-β-linked D-xylopyranosyl units to which α-L-arabinofuranosyl units are linked at positions C-(O)-2 and/or C-(O)-3, and uronic acids (mostly glucuronic acid or its 4-methyl ether derivative) at the C-(O)-2 position (Figure 7.4).

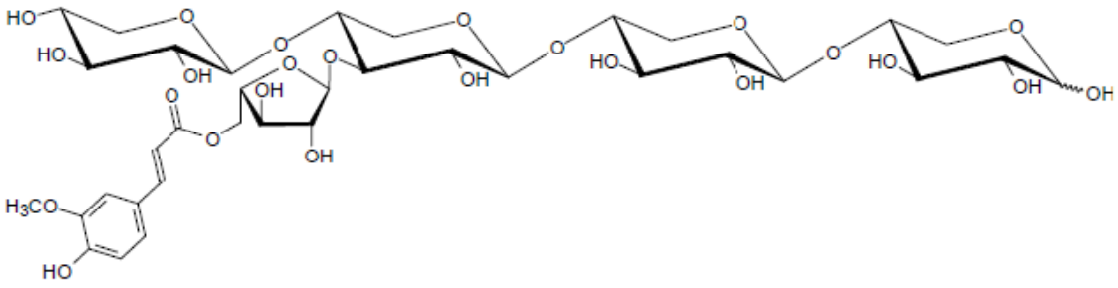


**Figure 7.4** *Arabinoxylan oligosaccharide.*

Additionally, phenolic acids, such as ferulic and p-coumaric acids, are esterified to some of the arabinose in the chain. In general, wheat pericarp AX is highly substituted with an arabinose-to-xylose ratio, further expressed as degree of substitution (DS), of approximately 1.0, while AX of the aleurone layer shows a relatively low DS (0.2–0.4) (Bergmans *et al.*,

1996). The fairly linear structure of arabinoxylans results in a rod-like conformation, as a consequence of which these polysaccharides form viscous solutions upon hydration. Because AX of wheat bran contains ca. 3% uronic acid residues, they are referred to as glucuronoarabinoxylan (GAX) and their levels are calculated by (Maes and Delcour, 2001):

$$GAX\% = 0.88 \cdot (\%Ara + \%Xyl) + 3\% \quad (7.1)$$

Where *Ara* and *Xyl* represent respectively the arabinose and xylose mass content of wheat bran, 0.88 is the factor introduced for the conversion of free sugar residues to anhydrous sugars as present in polysaccharides, and 3% is added in order to take into account the uronic acid residues.

Table 7.3 reports the composition of the wheat bran we have used. For cellulose and starch the conversion factor of free sugars to polysaccharides monomers is 0.9.

**Table 7.3** *Wheat bran composition. Value in %( w/w).*

| GAX | Cellulul. + starch | Other sugars | Lignin | Protein | Ash | Other |
|---|---|---|---|---|---|---|
| 26.1 | 28 | 1.4 | 10.6 | 15.9 | 6.4 | 11.5 |

Under the hypothesis that the fats account for the 5-6% of the biomass (Maes and Delcour) there is still a 5-6% of material which is unknown. This amount could include water soluble lignin and probably some sugars that are not detected during the analysis because degraded. This last assumption is supported by the fact that the carbohydrates content reported by other literature sources is larger (Table 7.4).

**Table 7.4** *Literature compositions of wheat bran. The composition is expressed as gram content in 100 g of dry matter while the moisture is g of water in 100 g of material.*

| | This work | Palmarola Adrados *et al.*,2005 | USDA, 2008 | Maes and Delcour, 2002 | Bergmans *et al.*, 1996 | Saxholt *et al.*, 2008 |
|---|---|---|---|---|---|---|
| **Carbohydrates** | 49.8 | 74 (34[2]) | 71.59[(1)] | 61.7 (17.1[2]) | 66.8 (11.8[2]) | 70.92[(1)] |
| **Lignin** | 10.6 | 5 | n.m. | n.m. | 9.8 | n.m. |
| **Proteins** | 15.9 | 13.5 | 17.26 | 17.0 | 15.9 | 17.54 |
| **Ash** | 6.4 | n.m | 6.42 | 5.9 | n.m. | 5.77 |
| **Fats** | n.m | n.m | 4.72 | 6 | n.m. | 5.77 |
| **Others** | 17.3[(1)] | 7.5 | | | | |
| **Moisture** | 6.7 | n.m. | 9.89 | n.m | n.m. | 8.2 |

(1) Determined as difference
(2) Starch
n.m.: Not measured

Proteins are an important part of wheat bran. Approximately 22% w/w of the nitrogen of the wheat kernel resides in the seed coats or bran (Jones and Gersdorff, 1925). The bran

proteins, in contrast to the endosperm proteins, are strikingly high in their content of the basic diaminoacids. They contain much larger quantities of the so called nutritionally essential aminoacids than are contained in the endosperm proteins.
The quantity of basic amino acids in the bran globulin, particularly that of arginine and lysine, exceeds that found in most vegetable proteins. The bran albumin also contains unusually large quantities of tryptophane, tyrosine, and cystine. Bran prolamin, the protein corresponding to gliadin of the endosperm, contains as much of these aminoacids as is present in most seed proteins, and much more than is found in gliadin. Wheat endosperm, which comprises practically the whole of the white wheat flour of commerce, contains approximately 11% w/w of protein, about 80% of which consists of gliadin and glutenin, which are present in approximately the same quantities (Murphy and Jones, 1926). Table 7.5 reports the type and the amount of aminoacids present in wheat bran and the comparison with the endosperm amounts.

**Table 7.5** *Aminoacids in 100 gm of wheat bran and of wheat endosperm (Murphy and Jones, 1926).*

| | Cystine | Arginine | Histidine | Lysine | Tryptophane |
|---|---|---|---|---|---|
| **Wheat bran** | 0.25 | 0.85 | 0.18 | 0.54 | 0.28 |
| **Wheat endosperm** | 0.14 | 0.36 | 0.20 | 0.23 | 0.12 |

In the biorefinery optic it could be interesting to recover these proteins. In order to extract rice bran proteins Jiamyangyuen *et al.,* (2005) proposed to perform first a defatting procedure: the bran is defatted twice using hexane in bran to solvent ratio of 1:3 at a setting of 250 rpm in a lab stirrer for 30 min and centrifuge at 5000 g for 10 min at room temperature. After air-drying an alkaline extraction followed by isoelectric precipitation is used to prepare rice bran extract.

### 7.3.2 Triton X1004

Triton X1004 was purchased from Merck. This tenside decreases the surface tension between water and the suspended bran. It increases the solubility of hydrophobic substances. Due to the hydrophobic character of lignin the addition of Triton X is assumed to affect the suspension and wettability of the solid biomass. 0.05 g Triton X was added to all experiments performed with the batch autoclave.

### 7.3.3 Enzymes

Solid residues and liquid hydrolysates resulting from the hydrothermal pretreatment were converted to monomeric sugars using appropriate enzyme systems (V16 and V39) from *Penicillium janthinellum* and *T. lanuginosus*. Table 7.6 gives the optimal working

conditions of the enzymes used in this work and the type of organisms used for their production.

**Table 7.6** *Enzymes used in this work.*

| | Organism | Opt. condition |
|---|---|---|
| **V16 Complex** | *P. janthinellum* | pH 5, 50 °C |
| **V39 Complex** | *P. janthinellum* | pH 5, 50 °C |
| **Xylanase** | *T. lanuginosus* | pH 4-6, 75 °C |

The V16 and V39 complexes contain endoglucanase, exoglucanase, and β-glucosidase activities for a total of 600 FPU/g at pH 4.0 and 50 °C (Ghose, 1984) as well as endoxylanase and β-xylosidase activities for a total of 4794 U/g (V16) and 3985 U/g (V39). BCA assay: 1% beechwood xylan, pH 4.0, 20 min, 50 °C (Kenealy and Jeffries, 2003). The extracellular enzyme systems were extracted from the filamentous fungi by lyophilisation of the supernatant.

## 7.4 Analytical methods

### *7.4.1 Determination of the DOC*

The liquid fractions obtained from the hydrothermal pretreatment of the biomass were analyzed in the Central Analytical Laboratory of the TUHH. Their carbon content was determined with a fully automated analyser (Elementar HighTOC + TNb). For the determination of the dissolved organic carbon (DOC), eluent samples were filtered with a 0.45 µm filter prior to injection, in order to retain suspended particles. The samples were first treated with phosphoric acid to remove any inorganic carbon and afterward subjected to catalytic incineration. The carbon bound was oxidized at two different temperatures (950 °C, 1050 °C). The resulting $CO_2$ was quantified and converted into DOC concentration.

### *7.4.2 Sugar analysis*

The determination of glucose, xylose, arabinose, furfural, and HMF concentration in the liquid hydrolysates were carried out via HPLC with a ligand exchange chromatography column in the Central Analytical Laboratory of the TU-Hamburg-Harburg. The samples were first centrifuged at 13000 rpm to separate solid impurities. Prior to injection the supernatant was passed through a 0.2 µm filter unit. 20 µL of the liquid samples were injected into the eluent flow (demineralised and degasified water, $\dot{V}$ = 0.5 mL/min) and separated with a Nucleogel Sugar (Macherey Nagel) column packed with a cation exchange

polymer at 80 °C. The different substances were quantified with a refractive index detector (RI-IV LCD Analytical, Agilent 1100). The hydrolysate consisted of both oligomers and monomers. Some analyses were repeated twice using another column specifically designed for carbohydrates (Aminex 42A) and using water as liquid phase with a flow rate of 0.6 mL/min and an oven temperature of 70 °C. The quantification was done with a refractive index detector (LaChrom® L-7490).

### 7.4.3 Moisture and ash

The moisture content of the biomass was measured by weighting the samples before and after heating at 105 °C until constant weight according to the standards given by NREL (Sluiter *et al.*, 2008). The samples were transferred into a desiccator for 1h, before the final weight was noted. The dried bran was incinerated in the Central Analytical Laboratory of the TUHH at 550 °C for 2 h and the final ash content weighed.

### 7.4.4 Protein determination

The protein content was measured by means of the Kjeldahl Method. The Nitrogen containing organic compounds were digested with sulphuric acid. The thereby formed Ammoniumsulphate was, after neutralization with NaOH, separated as ammonia by steam distillation and trapped in boric acid. The amount was finally determined by back titration with hydrochloric acid. Empirical factors allow the conversion of the total N in the proteins content.

### 7.4.5 Raw material and solid residues composition

This procedure uses a two steps acid hydrolysis to fractionate the biomass into forms that are more easily quantified. Samples of 10.0 mg of solid material were added to 0.01 mL of 72% sulphuric acid and, after mixing, placed in a water bath set at 30 ± 3 °C, and incubated for 60 ± 5 min. Using a stir rod, the samples were stirred every five to ten minutes without removing them from the bath. Stirring is essential to ensure acid to particle contact and uniform hydrolysis. Upon completion of the 60 min hydrolysis, the tubes were removed from the water bath. The samples were then diluted to an acid concentration of 4% by adding 84.00 ± 0.04 mL deionized water. The tubes were placed in an autoclave for one hour at 121 °C. Finally the samples were neutralized with $CaCO_3$ and the sugar content was determined by HPLC. The solid residue after this two step hydrolysis is referred to as acid insoluble Klason lignin.

## 7.5 Experimental apparatus and procedures

### 7.5.1 Batch reactor

Figure 7.5 shows the reactor scheme. The batch autoclave had a total volume of 250 mL. An electrical jacket heater allowed increasing the temperature up to 240 °C. The reactor content was homogenised with a magnetic stirrer. The pressure (max. 100 bar) was adjusted with nitrogen from a gas tank. The reactor was first loaded with demineralized water (100 mL) and 0.05 g/L Triton X, then wheat bran was added up to the desired concentration. The reactor lid was closed and the temperature of the control unit adjusted. The pressure was regulated depending on the experimental conditions. In order to remove the $O_2$ dissolved in water the reactor was first filled with $N_2$ up to a pressure of 50 bar and then, after some minutes, the gas was purged. Heat up times varied between 20 to 40 min.

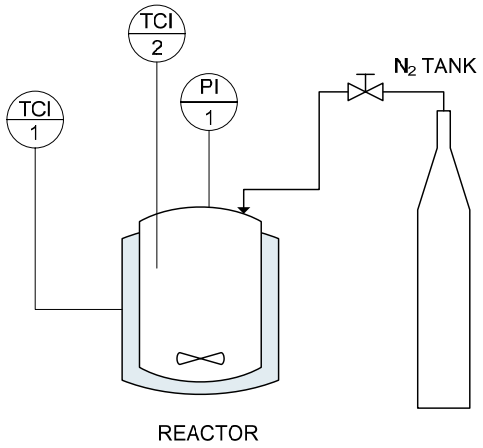


**Figure 7.5** *Batch reactor.*

At the end of the reaction time, the reactor was removed from the jacket heater and quenched into a water bath. At temperatures below 90 °C the reactor was depressurized and opened. Samples were taken and stored in a freezer, until they were analyzed.

### 7.5.2 Fixed bed reactor

This apparatus that was initially designed for supercritical fluid extraction (Speed SFE, Applied Separations) is represented in Figure 7.6. First the reactor (50 mL) was filled with solid material in the reactor then a layer of glass wool at the inlet and a layer of glass wool and a metallic filter at the exit were used in order to avoid entrainment of wheat bran from the reactor. At this point the reactor was placed in an oven preheated at the desired reaction temperature. After 15 min of preheating the HPLC pump was switched on and the water was started to flow through the system. The temperature of water was increased up to the reaction temperature by an adequate inlet pipe length within the oven before the reactor.

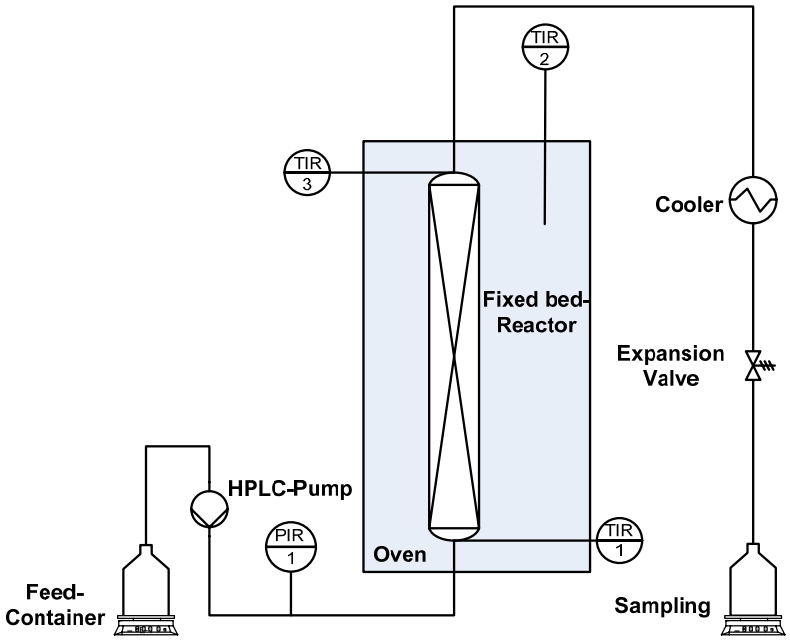


**Figure 7.6** *Fixed bed reactor.*

Temperature and pressure were measured and controlled during the whole reaction time. The hydrolysis reaction was stopped simply by opening the exit valve to ambient conditions and quenching the reactor in a water bath.

### *7.5.3 Enzymatic hydrolysis*

The solid residues and the liquid hydrolysates obtained were treated with enzymes in order to recover the monomeric sugars. 1 mL of hydrolysate sample was treated adding 100 μL of enzyme complex V16 or V39 and 100 μL of β-xylosidase. Initially the solid residues were treated by suspending a quantity of 0.01 g in 1 mL of deionized water and adding 100 μL of enzyme complex V16 or V39 and 100 μL of β-xylosidase. Due to the small amount of solid treated and the methodology used (0.1 g were first suspended in 10 mL and then a pipette used to collect 1 mL of suspension) the amount of solid was not constant. For this reason the treatment was repeated with 0.1g of solid in 10 mL of water and adding 1 mL of enzyme complex V16 or V39 and 1 mL of β-xylosidase. The solutions of V16 and V39 were prepared solubilising 0.1 g of lyophilized enzyme in 1 mL of deionized water. The samples were incubated in a thermo stirrer for 24 h at 50 °C and subsequently analyzed in order to determine their monomeric sugar contents.

## 7.6 Results

### 7.6.1 Batch reactor

Initially the biomass was treated in a batch reactor in order to study its behaviour as a function of temperature and reaction time. After the treatment the hydrolysate was analyzed and the following concentrations measured: monomeric sugars, degradation products, DOC, and proteins. A preliminary investigation about the capacity of the magnetic stirrer to work with different solid concentrations showed that the stirring is possible up to a solids concentration of 10% (w/w). In order to avoid any stirring problem and maintain homogeneous conditions all the experiments were carried out with a solid concentration of 7% (w/w) corresponding to 6.6% (w/w) in a dry basis.
Note one of the limitations of using a batch reactor is the relatively high time to reach the reaction temperature (Figure 7.7).

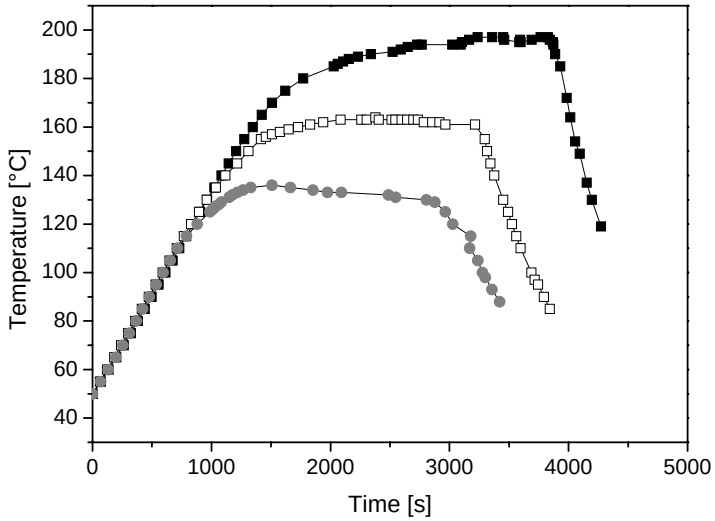


**Figure 7.7** *Temperature profile during batch experiments of 30 min at different temperatures.*

In the following when results are shown as function of the reaction time, this has to be intended as the time elapsed since the internal temperature equals the reaction temperature minus 5 °C. As shown in Figure 7.7, considering as time zero the one corresponding to a temperature of 50 °C, the preheating time is between 17 and 35 minutes and turns to be of the same order of magnitude of the reaction time. All the experiments were carried out trying to have heating curves similar as much as possible. In order to understand the extension of the reaction during the preheating time some experiments were carried out by heating the mixture at 120 and 145 °C and cooling down as soon as these temperatures were reached.

### 7.6.1.1 Carbon solubilization and monomeric sugars concentration

The degree of carbon solubilization ($f$) of the solid substrate was calculated as:

$$f = \frac{DOC}{TOC_{in}} \tag{7.2}$$

where the $TOC_{in}$ [g] denotes the total organic carbon of the starting material initially loaded in the reactor and $DOC$ [g] the dissolved organic carbon in the hydrolysate. Figure 7.8a shows the carbon solubilization as a function of time for experiments carried out at different reaction temperatures. In this case the error bars values were calculated by means of the error propagation theory (Taylor, 1997). Negative times refer to the preheating step. Clearly for the experiments at 200 °C and 160 °C the carbon solubilization, during the preheating time, is not relevant with respect to its maximum value. For the experiments at 130 °C the maximum $f$ is quite low, as the hydrolysis of the biomass starts at higher temperature and in this case half of the solubilization is already reached during the preheating step.

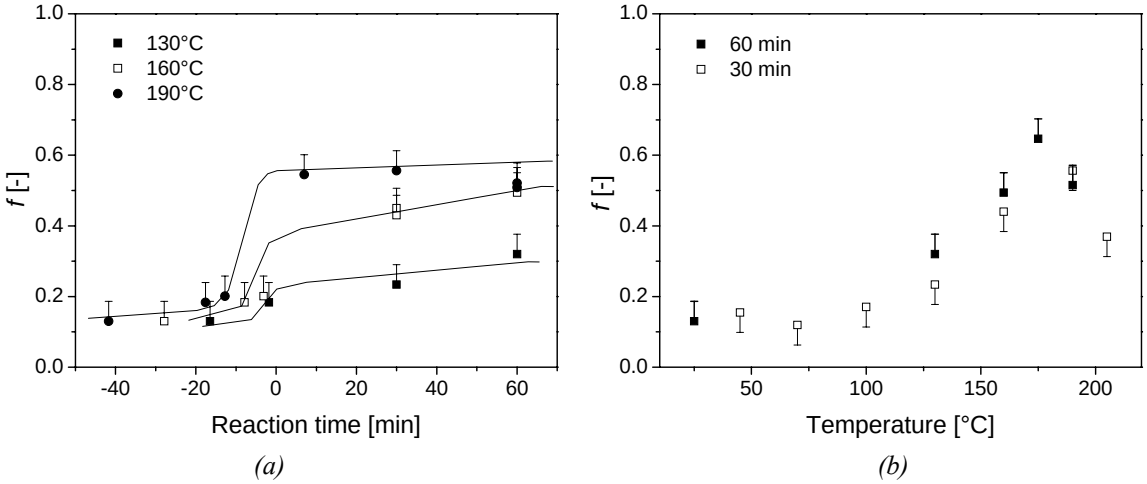


**Figure 7.8** *Carbon solubilization as a function of reaction time (a) and temperature (b). Lines show possible trends only.*

Due to the impossibility to perform a statistically significant number of experiments for every reaction condition investigated, the standard deviation was measured for the set of experiments at 130 °C, 30 minutes, and assumed to be independent of temperature and reaction time. Some of the other experiments were performed twice. Figure 7.8b shows the carbon solubilization as a function of the temperature for the runs with a reaction time of 30 min and 60 min. Note that after 30 min of reaction $f$ is already closed to the maximum value.

To evaluate the treatment intensity in batch LHW processes Overend and Chornet (1987) defined the severity factor $R_0$ as:

$$R_0 = t \cdot \exp\left(\frac{T-100}{14.75}\right) \tag{7.3}$$

where $t$ is the residence time [min] and $T$ the temperature [°C].
Using this factor it is possible to account for the influence of the preheating and cooling times. Accordingly we have modified the definition of $R_0$ in order to take into account the changes of temperature with time:

$$R_0 = \int_0^{t_{tot}} \exp\left(\frac{T(t)-100}{14.75}\right) dt \tag{7.4}$$

where $T$ [°C] is the temperature and time $t$ is expressed in minutes. In this case $t$ = 0 identifies the beginning of the experiment and $t_{tot}$ denotes the total time (heating and cooling included).

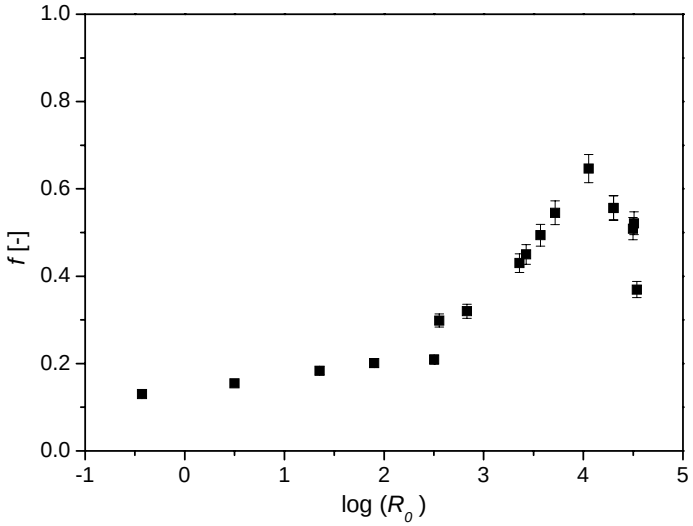


**Figure 7.9** *Carbon solubilization as function of the log($R_0$) calculated with Eq. (7.4).*

The carbon solubilization, reported in Figure 7.9 gives important information about the effects of the pretreatment on the complex structure of the biomass. Clearly at 25 °C about 12% (w/w) of the total carbon is solubilized corresponding to the soluble fraction of the starting material. Increasing the temperature the *f* factor increases first slowly (at 100 °C *f* is only 0.2) and then sharply, reaching the value of 55.6% at the maximum temperature investigated (200 °C), At this conditions the biomass starts to lose its compact structure and the hydrolysis reactions start. The carbon solubilization decreases for values of log ($R_0$) higher than 4, corresponding to the formation of carbon residues in the hydrolysate; this

phenomenon could be explained with the recondensation of lignin and degradation products that occurs at high temperature (Kim and Lee 2006, Sun *et al.,* 2004).

Figure 7.10a reports the concentrations of the monomeric sugars: glucose, xylose, and arabinose after treatment at 190 °C, while Figure 7.10b shows those of the main degradation products: HMF and furfural. The production of monomeric sugars starting from the polymers can be represented using different models (see Chapter 9), but in any case the polymers are first hydrolysated, producing the monomeric sugars, and then the monomeric sugars are degraded to products like HMF and furfural.

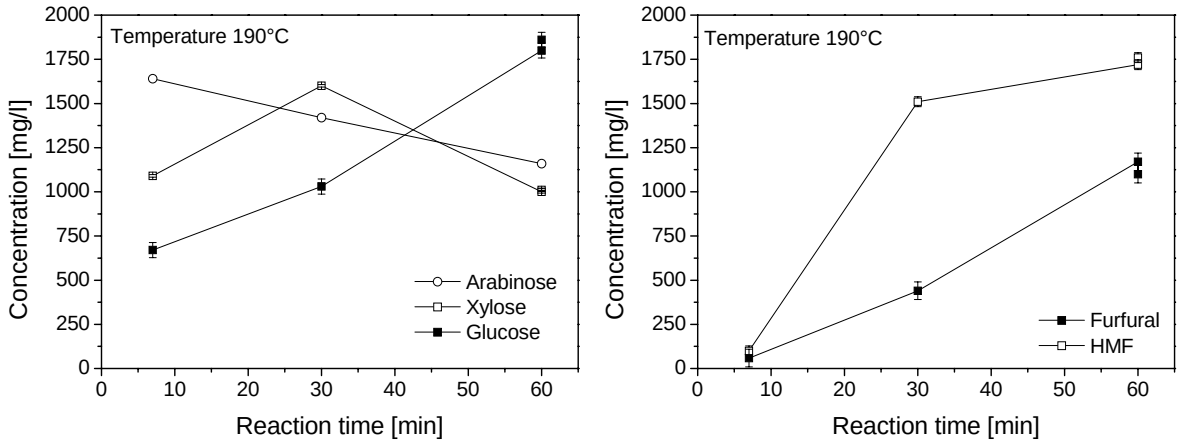


*(a)* *(b)*

**Figure 7.10** *Monomeric sugars (a) and degradation products (b) concentration after hydrolysis at 190 °C for different reaction times.*

In Figure 7.10a it can be noticed that for glucose and arabinose the concentration has a monotonic trend with the reaction time, therefore the dominant reaction is always one (production reaction for glucose and degradation one for arabinose). Xylose behaves differently: for small reaction times the production reaction is faster than the degradation one but due to the increasing xylose concentration with time, the degradation becomes faster and the concentration decreases. This does not happen at lower temperatures (160 °C and 130 °C), as shown in Figure 7.11a and b: in these cases, the production reaction is faster than the degradation ones. It was found that the maximum monomeric sugars recovery can be obtained treating the raw material at 190 °C. The corresponding value for glucose was 8.4% of the total glucose presents in the starting material, and was obtained with a treatment of 60 min. With a treatment of 30 min at the same temperature 13.8% of xylose was recovered while with a very short treatment (7 min) 23.4% of the starting arabinose was detected in the hydrolysate. It is also evident that the fermentation of the hydrolysates obtained after the pretreatment would lead to a low production of bioethanol, so that an enzymatic treatment is needed.

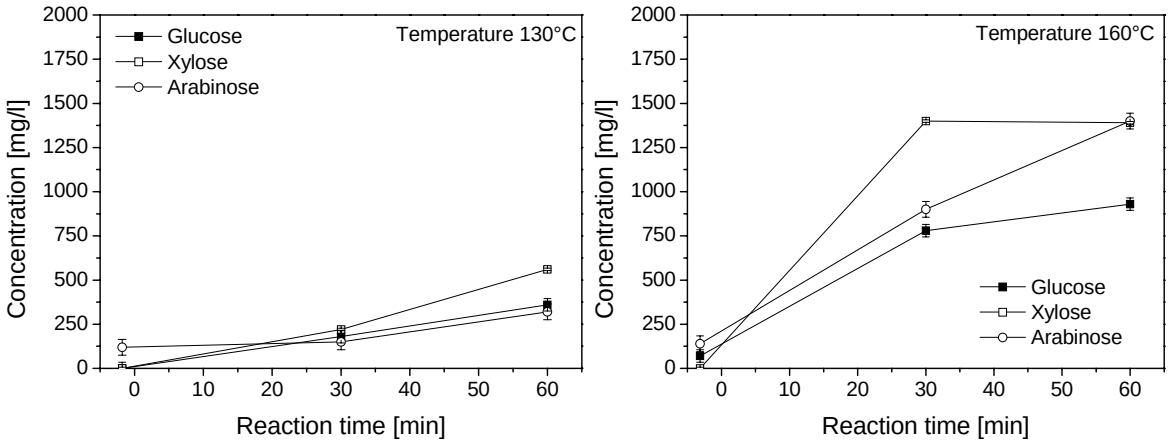


*(a)* *(b)*

**Figure 7.11** *Monomeric sugars concentrations after hydrolysis at 130 °C (a) and 160 °C (b) for different times.*

Error bars for Figures 7.10 and 7.11 were calculated by means of a set of 30 min experiments for treatments at 130 and 160 °C, and with a set of 60 min experiments for the treatment at 190 °C and then the errors were supposed to independent of the reaction time.

### 7.6.1.2 Proteins recovery

The proteins recovery in the hydrolysate was calculated as the ratio between the amount of proteins present in the hydrolysate after the treatment and the amount of proteins of the starting wheat bran. Different temperatures different reaction times were investigated.

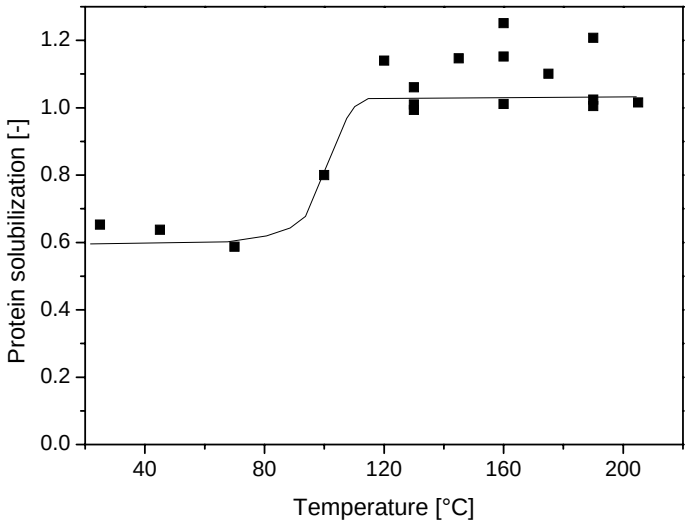


**Figure 7.12** *Proteins recovery for different reaction temperatures. The line represents only a possible trend.*

No relationship between the recovery of proteins and the reaction time was observed. By only heating up to 120 °C and cooling down immediately 100% of protein recovery was observed. This indicates that proteins are released very fast once an adequate temperature is reached. At ambient conditions 64.7% of proteins are water soluble. With reference to Figure 7.12, we note that a recovery larger than 100% may indicate wrong determination of the starting material proteins content or errors in the analysis. Anyway it is possible to observe that a consistent amount of proteins (60%) are water soluble and between 80 °C and 120 °C the solubilization of the insoluble proteins at ambient conditions starts.

### 7.6.2 Fixed bed reactor

All the experiments in the fixed bed reactor were carried out at a constant flow rate of 4 mL/min and at the same pressure of 40 bar. The influence of flow rate and the pressure were not investigated. The reactor was always filled with 10 g of solids (9.32 g dry base). Plugging problems were detected with higher solid amounts.
The use of a fixed bed reactor allows the separation between liquid hydrolysate and solid residue.


**Figure 7.13** *Liquid hydrolysates and solid residue collected after the treatment at different temperatures.*

In Figure 7.13 some pictures of these two fractions are shown. The first test tubes on the left contain the dry solid residue obtained with the pretreatment (165 and 190 °C). The liquid

samples were collected sequentially during the reaction time. The first hydrolysate coming out (left test tubes) was viscous, then it became less concentrated and transparent (right test tubes). The higher is the reaction temperature the darker are the samples. In the Petri dish the wet solid residue obtained after the pretreatment are shown.

### 7.6.2.1 Temperature profiles during the reaction time

The temperature during the reaction time was not constant even thought the reactor was placed in the hot oven and a preheating time of 15 min was set before starting to pump the water.

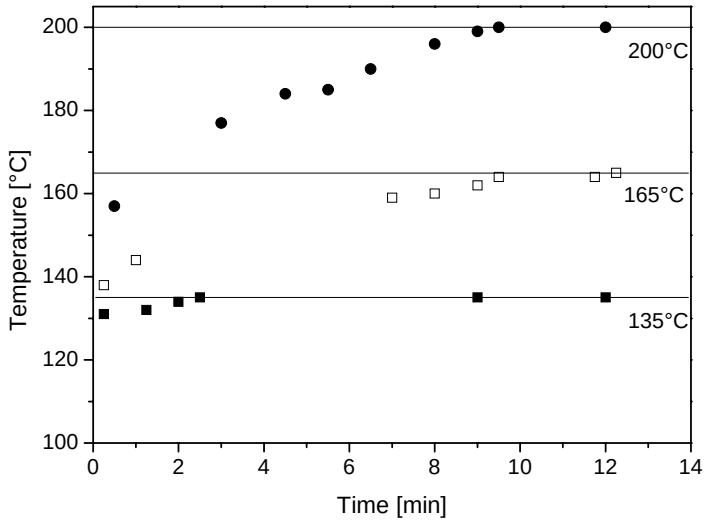


**Figure 7.14** *Temperature of the inlet water. Time zero is referred to the pump switch on. The hydrolysate starts to come out after between 10 and 11 minutes.*

In Figure 7.14 the temperatures measured at the reactor inlet is shown as a function of the reaction time. A temperature drop was recorded when switching the pump on as the first drops of water introduced in the hot system were vaporized, then the temperature increased with the increasing pressure.

For every temperature investigated the selected reaction temperature was reached before the hydrolysate started to exit from the system. With a flow rate of 4 mL/min a time between 10 to 11 minutes was necessary in order to fill the reactor and to start the collection of the liquid hydrolysate. For this reason the results are presented as a function of the hydrolysate collected at the reactor outlet. This amount includes both the water flowed during the reaction time and the one collected by opening the expansion valve at the end of the reaction. It was clear that, above all in the shorter experiments, the contribution of the hydrolysate presents in the reactor at the end of the experiment was not negligible (from 10 to 15 mL, depending on biomass solubilization).

### 7.6.2.2 Total solids solubilization

The degree of solubilization of the biomass was defined as:

$$\text{Degree of solub.} = 1 - \frac{\text{Solid residue [g]}}{\text{Starting material[g]}} \tag{7.4}$$

where *Solid residue* is the amount of dry solids still present in the reactor after the treatment while *Starting material* denotes the amount of dry solid loaded in the reactor before the treatment. Figure 7.15 shows this factor for different treatment temperatures and volumes of hydrolysate collected. The hydrolysis reactions start at temperatures near 130 °C and for this reason the solubilization increases sharply. At 200 °C there is a plateau correspondent to the 80% of solubilization, and finally after 225 °C there is another solubilization increase probably due to the hydrolysis of cellulose. The hydrolysis kinetics and consequently the solubilization kinetics seem to be quite fast. For all the temperatures investigated, using 60 mL of water to treat the solids, the value of the solubilized biomass was closed to the maximum: as shown in Figure 7.15 there is a further increment for treatments with 120 mL, but then the value remains constant. The data of this figure comprise all the experiment performed in the semibatch apparatus, errors were calculated by means of the error analysis theory but were not plotted due to graphical reasons. The maximum error value found was 0.018.

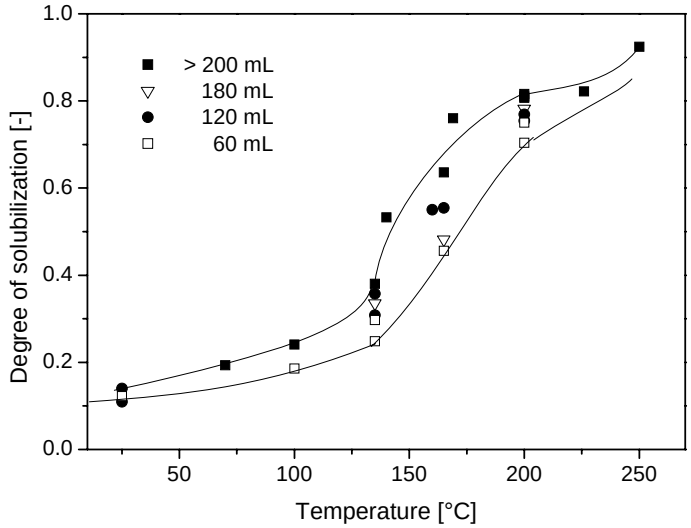


**Figure 7.15** *Degree of solubilization of the biomass as function of the temperature for different amounts of water used. Lines show only trends.*

These results were also plotted as function of the logarithm of the $R_0$ factor (Figure 7.16).

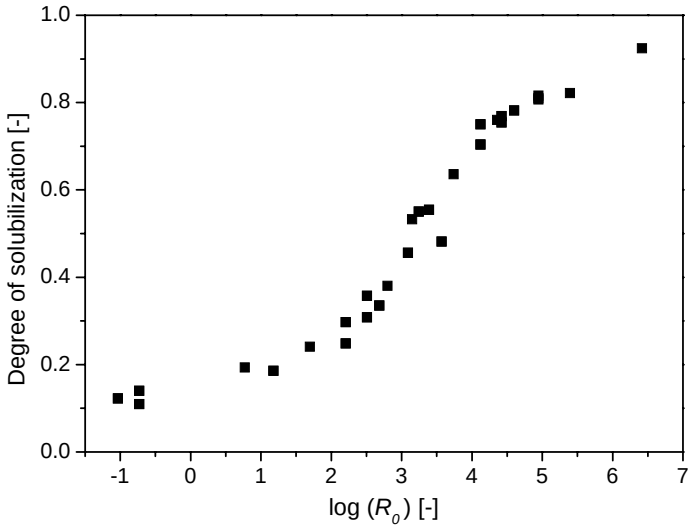


**Figure 7.16** *Degree of solubilization as function of the logarithm of the $R_0$ factor.*

We have modified the definition of the $R_0$ factor (Eq. 7.3) in order to take into account the reactor filling time with water. If the axial coordinate is named as $z$ and a plug flow behaviour is assumed, it is reasonable to write:

$$R_0(z) = \int_{t_{in}}^{t_{fin}} \exp\left(\frac{T(t)-100}{14.75}\right) dt \tag{7.4}$$

where the reaction time ($t_{in}$) of a given axial coordinate starts when the water reaches the corresponding reactor point, so it can be calculated as:

$$t_{in} = \frac{z \cdot A}{\dot{V}} \varepsilon \tag{7.5}$$

In Eq. 7.5 $A$ [m$^2$] is the cross sectional reactor area, $\dot{V}$ [m$^3$/min] the water volumetric flow rate and ε the bed porosity [-]. Eventually, the averaged $R_0$ factor along the reactor is determined as:

$$< R_0 >= \frac{\int_{\cdots 0}^{z_{tot}} (R_0(z))\, dz}{z_{tot}} \tag{7.6}$$

where $z_{tot}$ is the total bed length.

### 7.6.2.3 Carbon solubilization

The instantaneous value of DOC concentration helps to understand the hydrolysis kinetics. Figure 7.17 shows the DOC concentration [g/L] for experiments carried out at 135 °C and 165 °C. The hydrolysis and the solubilization of the biomass are occurring in the first minutes for all the temperatures investigated (the zero time is set when the first drop of hydrolysate comes out). It can be concluded that the solubilization of the biomass is almost totally achieved in the first 20 min.

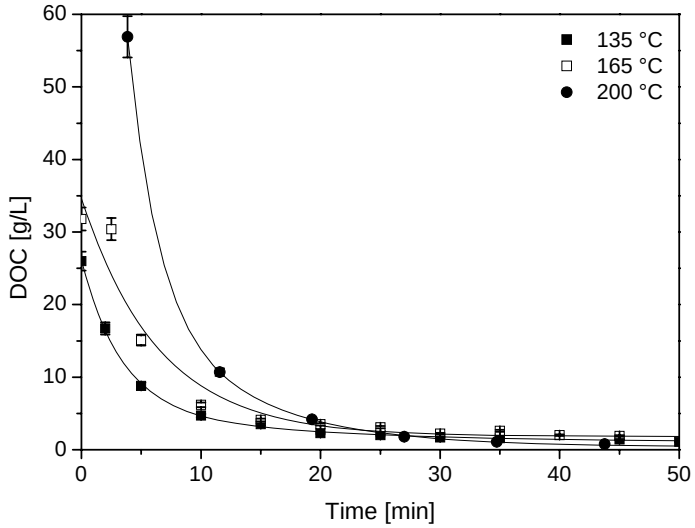


**Figure 7.17** *DOC concentrations as function of the time for experiments at 200, 165, and 135 °C. Error bars were calculated by means of the error propagation theory (Taylor, 1997).*

In the same figure also the values related to a pretreatment temperature of 200 °C are represented. In this case the DOC concentration is not an instantaneous value but that of subsequent samples of 30 mL collected during the reaction time. In order to plot the data in the same graph the concentration of these samples was related to the average time between the start and the end of the collection of the sample itself.

As in the case of the batch autoclave the final degree of carbon solubilization ( $f$ ) was studied for different temperatures and reaction times (Figure 7.18a and b) and calculated from the DOC analysis with Equation (7.7).

$$f = \frac{DOC}{TOC_{in}} \tag{7.7}$$

In this case parameter $f$ is defined as the ratio between the $DOC$ [g] of the total hydrolysate collected at the end of the reaction time and the $TOC$ [g] (total organic carbon) of the starting biomass filled in the reactor.

In Figure 7.18a the comparison between the carbon solubilization and the solid solubilization (Eq. 7.4) is shown. At 200 °C after a treatment of 15 min (60 mL of total hydrolysate amount collected) the carbon solubilization is about 60% while the solid solubilization is near 80%. This means that the solid residue, which remains in the reactor after the pretreatment, is more concentrated in carbon than the starting wheat bran, a clear index that the component with the larger content of carbon (lignin) remains in the solid residue. In fact the carbon content of proteins is 0.53 g/g the one of carbohydrates is 0.44 g/g (Rouwenhorst *et al.*, 1991) while the phenol one is 0.76 g/g.

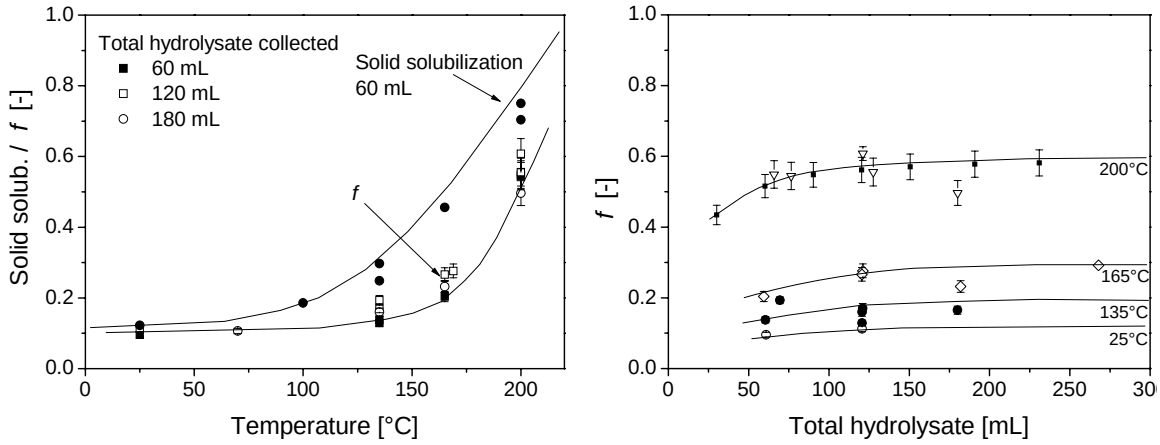


**Figure 7.18** *Carbon solubilization as function of temperature (a) and the total hydrolysate collected (b). Lines represent only the trend.*

The filled points at 200 °C (Figure 7.18b) represent the cumulated value of carbon solubilization calculated analyzing the DOC concentration of subsequent samples of 30 mL collected during the same experiment, while all the other points represent the results of single experiments.

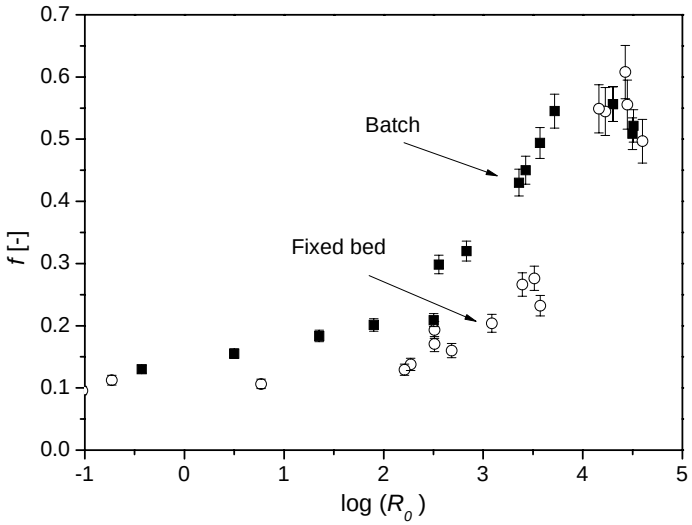


**Figure 7.19** *Carbon solubilization as function of logarithm of the $R_0$ factor.*

The calculation of the $R_0$ factor allow comparing batch experiment with semi batch ones. Figure 7.19 shows the carbon solubilization as a function of the $R_0$ factor for both batch and fixed-bed experiments. From these results it is clear that batch experiments allow higher carbon solubilization.

### 7.6.2.4 Protein and ash solubilization

The liquid hydrolysates and the solid residues were analysed in order to measure the proteins partition after the treatment. Figure 7.20a and b shows the fraction of proteins that is possible to recover from the hydrolysate.

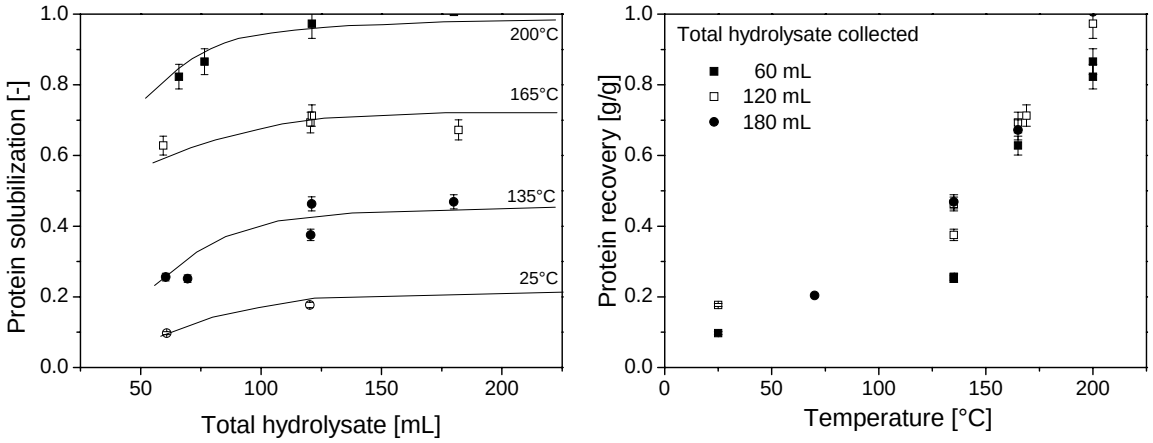


*(a)* *(b)*

**Figure 7.20** *Proteins solubilization as function of the total hydrolysate collected (a) and the temperature (b). Lines represent only the trend.*

In this case the performances of the fixed bed reactor are significantly lower than those of the batch. The total protein balance was confirmed by the analysis of the protein content of the solid residues.

**Table 7.7** *Proteins balance.*

| Pretreatment Temp. [°C] | Tot. hydrolysate [mL] | Dissolved proteins % | Protein in the solids residues % w/w | ∑ |
|---|---|---|---|---|
| 200 | 30 | 86.5 | 25.2 | 111.7 |
| 165 | 30 | 62.8 | 48.2 | 111.0 |
| 135 | 30 | 25.1 | 82.1 | 107.2 |

Table 7.7 presents the total proteins balance related to three different experiments. Deviations from 100% are due to analytical errors.

### 7.6.2.5 Solid residue analysis

The solid residues obtained with the pretreatment carried out at temperatures of 140 and 200 °C were analyzed in order to determine their composition. The reaction time was quite long (more than one hour) for both the experiments so the hydrolysis reactions are supposed to be completely concluded and the maximum amount of solubilized biomass reached. Table 7.8 reports the compositions of these solid residues.

**Table 7.8** *Solid residue composition.*

| Pretreatment Temp. [°C] | Arabinose | Galactose | Mannose | Xylose | Glucose | Kl. lignin |
|---|---|---|---|---|---|---|
| | | | % w/w | | | |
| 140 | 15.30 | 0.00 | 0.41 | 21.90 | 20.20 | 18.3 |
| 200 | 0.1 | 0.1 | 0.3 | 0.9 | 29.3 | 62.1 |

The quantity of lignin present in the solid residue after the treatment at 200 °C is the 106% of the lignin present in the starting raw material while for the after treatment at 140 °C the 99% was measured. This confirms the raw material analysis. The "klason lignin" is, by definition, the residue that is still solid after the double step acid hydrolysis (§ 7.3.5) performed to determine the carbohydrates content, because for the most common lignocellulosic materials it is completely made up of lignin.

Table 7.9 shows the fraction of the starting material sugars that is still present after the treatment. From this table interesting information can be obtained. Clearly after treatment at 140 °C a large fraction of glucose is solubilized, whereas the other sugars are mostly still present in the solid residues. At 200 °C the sugars form the hemicellulose are completely solubilized while some glucose is still in the solid (95.4% of the sugars are glucose). These results lead to the conclusion that at low temperature (140 °C) basically only the starch is solubilized while the cellulose and the hemicellulose are mostly in the solid residue. If the solids are treated at high temperature all the hemicellulose is hydrolyzed and extracted with the liquid and only the cellulose is present in the solid residue.

**Table 7.9** *% of the carbohydrates still present in the solid residues.*

| Pretreatment Temp. [°C] | Arabinose | Galactose | Mannose | Xylose | Glucose |
|---|---|---|---|---|---|
| | | % of the starting material | | | |
| 140 | 93.7 | 0 | 72.87 | 81.07 | 38.47 |
| 200 | 0.2 | 1.6 | 17.8 | 1.1 | 18.6 |

This gives an idea about the quantity of starch and cellulose of the starting material: probably the starch account for more than 60% of the glucose and the cellulose amount near 20%.

**Table 7.10** *Ash not solubilized after the pretreatment.*

| Pretreat. Temp. [°C] | Total hydrolysate [mL] | Not solubilized ash % |
|---|---|---|
| 200 | 60 | 21.4 |
| 165 | 60 | 47.6 |
| 135 | 60 | 58.2 |

Also the ash content of the residues was measured. Results presented in Table 7.10 confirm that the ash solubilization, as the other component, dependents from the reaction temperature.

### 7.6.2.6 Monomeric sugar recovery

The pretreatment causes the solubilization of the polymeric sugars and their partial hydrolysis to oligomers and then to monomeric sugars.

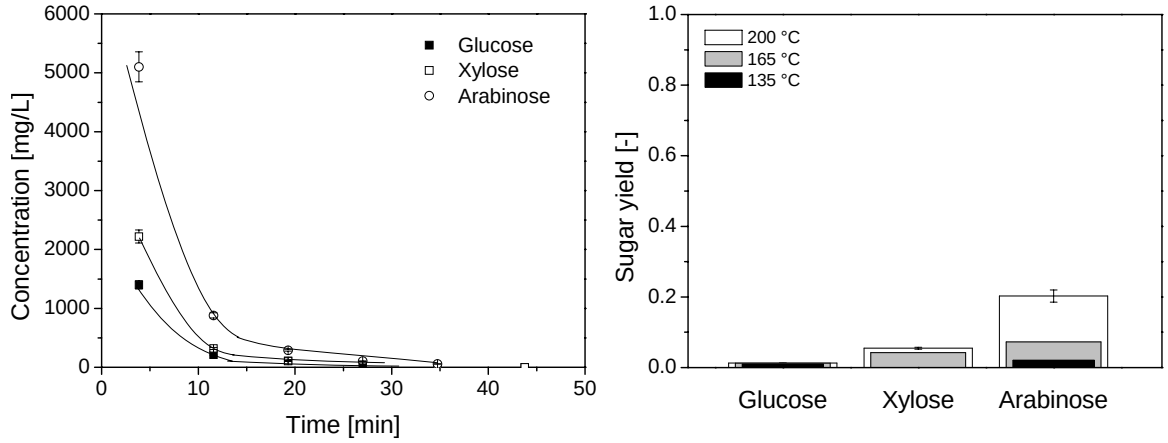


*(a)* *(b)*

**Figure 7.21** *Instantaneous monomeric sugars concentrations as function of the reaction time (a) and monomeric sugars recoveries (b) after treatment with 60 mL of water at 200 °C.*

Figure 7.21a shows the monomeric sugars concentration of subsequent samples of 30 mL collected during the same experiment (200 °C), while Figure 7.21b the fraction of the feed material monomeric sugars recovered after the pretreatment with hot liquid water at 200 °C and 135 °C using 180 mL of water. Due to the impossibility to have a statistical number of values for each pretreatment temperature and reaction time the reproducibility of the measurements was investigated for the temperatures of 200 °C and 135 °C, and using 180 mL of water. In Figure 7.21b the error bars represents a confidential range of 90%.

While the monomeric sugar yields are influenced from the LHW treatment temperature, results (not shown) confirmed that the amount of water used for the pretreatment has irrelevant influence: after 60 mL the maximum monomeric sugars yield has already been reached. In Figure 7.21a the instantaneous monomeric sugars concentrations are shown as a

function of the reaction time for treatment at 200 °C (time 0 correspond to the first drop of hydrolysate) it is clear that after 30 min the hydrolysate content of monomeric sugars is near zero.

### 7.6.2.7 Degradation product and pH

Compared with the batch treatment of the biomass the amount of degradation products is low and detectable in the total hydrolysate only for the experiments carried out at temperature above 200 °C. Table 7.11 reports the results of HMF and furfural produced in the fixed bed reactor.

**Table 7.11** *Hydrolysate amount of degradation products after pretreatment.*

| | HMF [mg] | Furfural [mg] |
|---|---|---|
| 120 mL | 52.3 | 14.0 |
| 60 mL | 55.3 | 14.8 |

Clearly this amount does not change in a significant way with the total reaction time. This because the monomeric sugar concentration is not constant during time, but is higher at the beginning and then decreases fast. Figure 7.22 shows the concentration of HMF in subsequent samples of 40 mL collected during the treatment at 200 °C, furfural was detected only in the first sample with a concentration of 76 g/L.

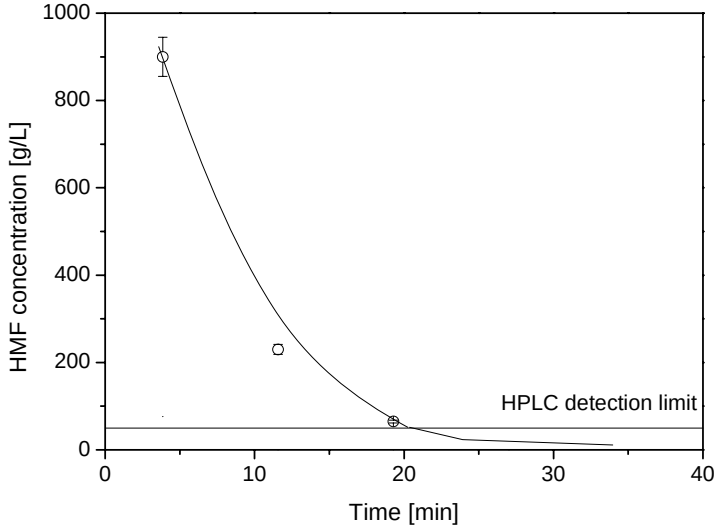


**Figure 7.22** *Concentration of HMF in subsequent sample collected during the HLW treatment. The line shows only a trend.*

The higher hydrolysate concentrations of HMF and Furfural detected in the cumulate amount of hydrolysate obtained at the end of the pretreatment were respectively 921.6 mg/L

and 246.7 mg/L, obtained treating the biomass at the higher temperature (200 °C) and with lower amount of water (60 mL). It is interesting to look at the literature values of typical inhibiting concentrations for the fermentation step as reported in Table 7.12. It can be concluded that even with "short" pretreatment (60 mL) in which concentrations are higher the values are lower the limits of Table 7.12 and should not create problems at the fermentation step.

**Table 7.12** *Literature values of fermentation inhibition Saccharomyces cerevisiae (glucose) and Pichia stipitis (xylose) (Gong et al., 1999).*

| | Concentration [g/L] | Glucose inhibition % EtOH | Xylose inhibition % EtOH |
|---|---|---|---|
| **HMF** | 5.0 | 95.0 | 91.4 |
| **Furfural** | 2.0 | 89.0 | 95.0 |

It is difficult to compare batch treatments with fixed bed ones but if two similar water / solids ratios and two similar temperatures are chosen is possible to see that the concentration of degradation products in the fixed bed reactor is compared to a very short treatment in the batch one (Table 7.13).

**Table 7.13** *Comparison between batch experiments and fixed bed reactor experiments.*

| | Batch 7 min | Batch 30 min | Fixed bed |
|---|---|---|---|
| **Reaction Temp. [°C]** | 190 | 190 | 200 |
| **Water/ In.solid [-]** | 14.2 | 14.2 | 12.9 |
| **HMF [mg/L]** | 100 | 1510 | 436 |
| **Furfural [mg/L]** | 59 | 440 | 117 |

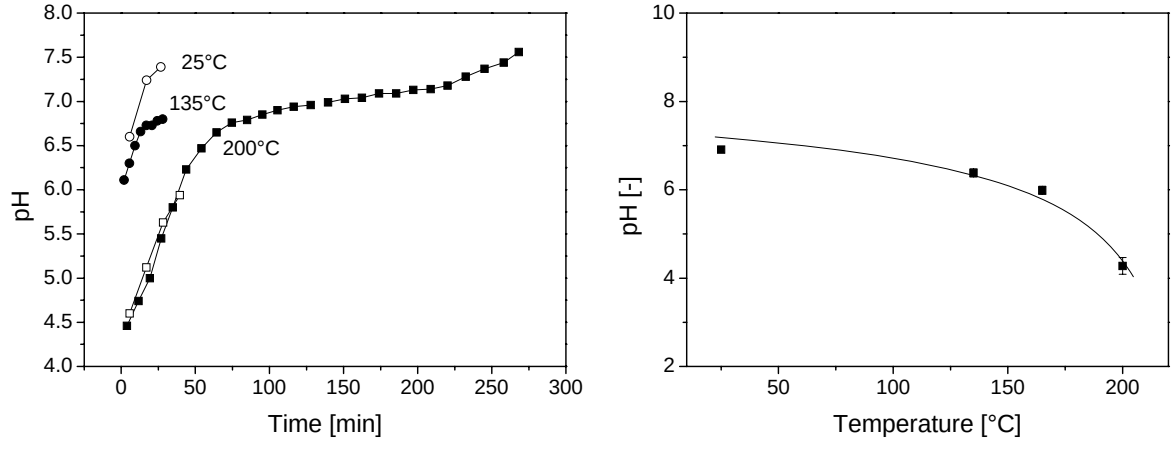


*(a)* *(b)*

**Figure 7.23** *pH of subsequent samples collected during the HLW treatment (a) and pH of the total hydrolysates collected after the pretreatment at different temperatures.*

The pH value is an important factor because usually the enzymes, that perform the hydrolysis of the sugars, prefer an acid environment. Figure 7.23a shows the pH of subsequent samples collected during the LHW pretreatment.
Clearly the treatment causes a decrease of the pH of the total cumulated hydrolysate. The reasons are mainly two: the formation of degradation products and the hydrolysis itself. In the first case acids like formic and levulinic acid are produced from the further degradation of the principal degradation products of the process: HMF and furfural. In the second case the hydrolysis of the arabinoxylan causes the release of the bonded acids like the glucuronic one. Lower pH values correspond to more severe pretreatment condition, but the values were independent from the water amount used, probably because of the formation of weak acids with buffer properties. It can be interesting to observe that in this case the pH reaches a neutral value (7) after 80 min while all the other instantaneous properties reach the asymptote after 45 min.
Figure 7.23b shows the pH of the total amount of hydrolysate that is collected at the end of the reaction time and will be use for the enzymatic hydrolysis. There are substantial changes in the pH only for pretreatment at 200 °C.
These values are a mean obtained from all the runs performed using 60, 120, and 180 mL of water; from the error bars in this range the pH value is not a function of the volume of water used.

### 7.6.2.8 Hydrolysate enzymatic treatment

The experimental procedure to obtain monomeric sugars includes a number of steps so that the sources of errors are plenty.
First of all we considerate the LHW pretreatment. In this step the errors are mostly due the plugging problems of the wheat bran. Sometimes the top layer of the reactor was bypassed with the consequence that a part of the solids could not react. Moreover, when the reaction was stopped the exit valve was opened to the ambient in order to collect the water contained in the reactor: usually it was not possible to reach the pressure of 1 bar, so some of the hydrolysate was lost as steam. In case of short experiments (60 mL) the vent was more concentrated in substances than for of longer experiments, resulting in a larger error.
Also the enzymatic treatment step was a source of errors (sampling of the amount to treat, adding of the enzyme etc.) and the HPLC measurements as well.
Due to the impossibility to repeat the whole procedure (from the HLW treatment to the enzymatic hydrolysis) for a statistical number of times for all temperatures, all amounts of water used, and the two enzyme complexes, it was chosen to study the reproducibility of the results for the temperature of 135 °C and 200 °C and with an amount of hydrolysate of 60 mL (“short experiments”). For each of those temperatures the whole experiment was

repeated four times, and then two of the hydrolysates obtained were treated with an enzyme complex and two with the other.

The results (Figure 7.24a) show that the complex V16 seems to be better, but the difference is so small that the errors bar overlap. It is clear, from Figure 7.24b that also considering together the results obtained with different enzymes the error bars corresponding to 95.4% of confidence is small. For this reason, it was concluded that the two enzymes behave similarly and the results were analysed without distinction in the enzyme system used.

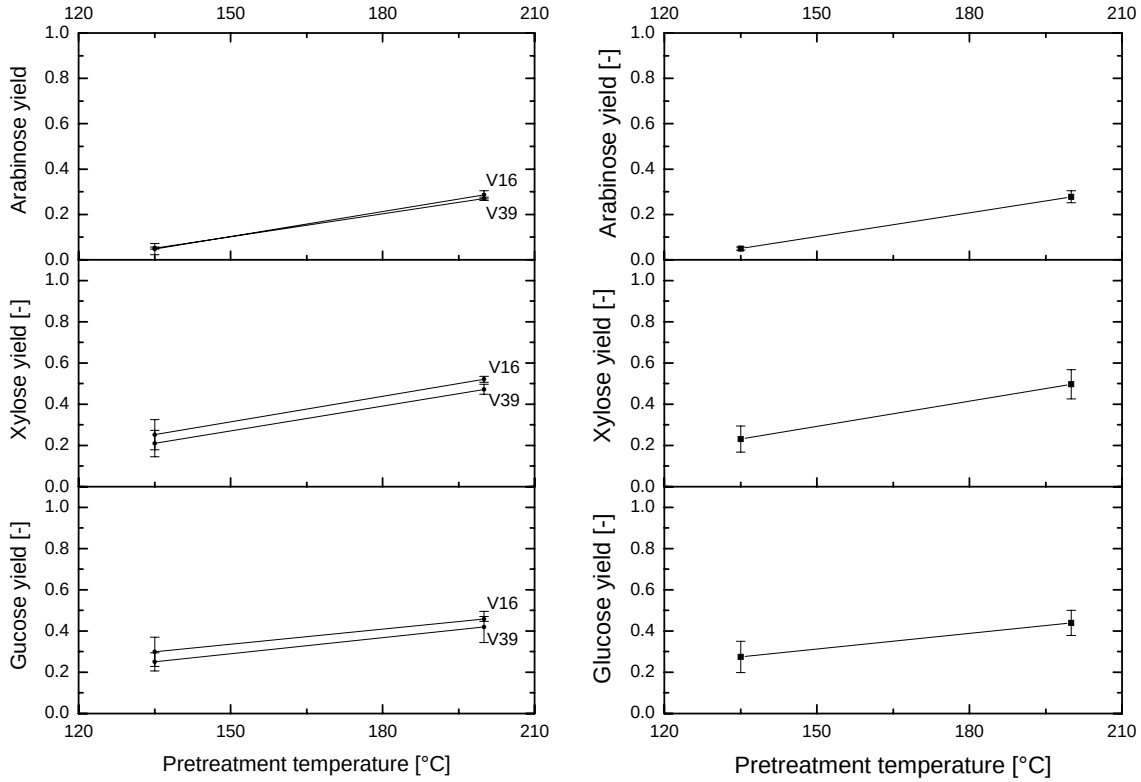


*(a)* *(b)*

**Figure 7.24** *Sugars yields after treatment with HLW followed by enzymatic hydrolysis. Results of treatment with two different enzymatic complexes (a) and mean values (b).*

At the other conditions considered the whole experiments was repeated only twice and the hydrolysate treated with the two different enzymes, if the difference between the results was lower than the errors bars calculated for the treatments with 60 mL of water, the experiments were not repeated further.

Figure 7.25 reports the glucose xylose, and arabinose recoveries defined as fractions of the feed material monomeric sugars detectable after the enzymatic treatment. The comparison between the Figure 7.25 with Figure 7.21 shows that the enzymes are able to increase in a significant way the monomeric sugar yields. It is clear that increasing the reaction temperature a larger amount of sugars is solubilized and consequently recovered after the

enzymatic treatment. There is a small appreciable increment (larger than the calculated errors bars) from treatment with 60 mL of water to treatment of 120 mL of water. Higher values have no influence. The remaining sugars (to reach yields equal to 1) are still present in the solid residue.

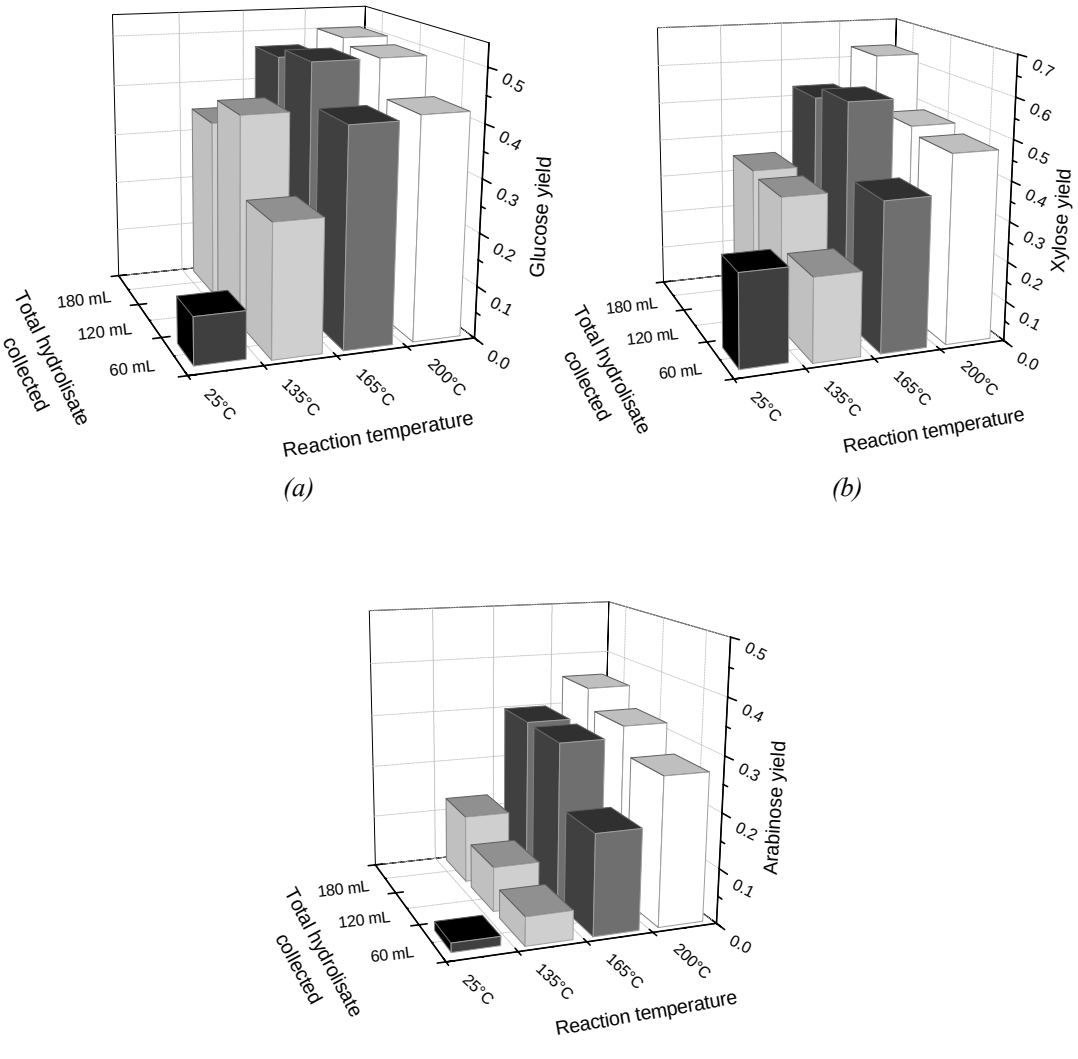


**Figure 7.25** *Glucose (a), xylose (b), and arabinose (c) recovery after enzymatic hydrolysis of the hydrolysate obtained after the pretreatment.*

### 7.6.2.9 Solid residues enzymatic treatment

The enzymatic treatment of the solid residue led to not reproducible results, which are shown in Figure 7.26. The more likely sources of errors were indentified in:

- the treating procedure commonly utilized at the TUHH for the enzymatic hydrolysis. First 0.1 g of solids were mixed with 10 mL of water and then a pipette was used to take 1 mL (the quantity of solid is not exactly 0.01 g);

- inhomogeneous solid composition. Due to the small amounts used for the enzymatic treatment it is possible that the sample does not reproduce the total solid residues;
- unreliable HPLC analysis.

Of course the errors are strongly amplified because of the small amount of solids treated (0.01 g) and this error is even larger when increasing the amount of solid residue after the pretreatment.

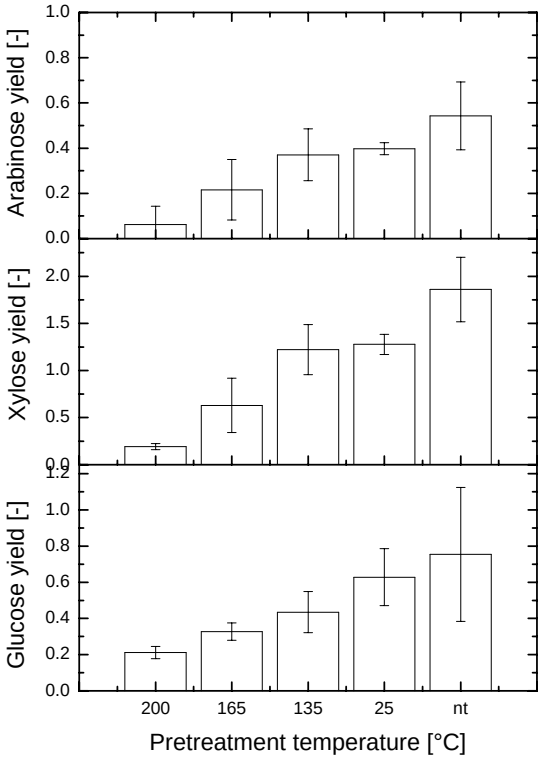


**Figure 7.26** *Glucose, xylose, and arabinose yield after enzymatic treatment of the solid residue fraction obtained with the pretreatment. nt= not treated.*

Considering that the sources of errors have a stronger influence on the results than the type of enzymes used and the reaction time, a statistical analysis was done considering all the results about the enzymatic treatment of solids obtained at the same pretreating temperature (the pretreatment temperature is the only variable that makes the difference). From Figure 7.26 a trend is clearly evidenced, but it was not possible to conclude if the pretreatment is helpful or not.

## 7.7 Conclusions

In this Chapter the liquid hot water pretreatment of wheat bran was investigated experimentally.

The reaction behaviour of this biomass in liquid hot water is considerably more complex than a common lignocellulosic material because of the presence of proteins and fats.
Batch experiments allowed a preliminary study of the behaviour of the biomass and showed that the temperature, more than the time, has the bigger influence.
Further experiments were performed in a fixed bed reactor. The solubilization of the biomass was extensively studied as a function of the temperature and for different water/solid ratios.
Only small differences in the solubilization of the biomass and its components were found when shifting from water/solid ratio of 6.4 to 12.8. Longer experiments did not lead to better performances. It was moreover discovered that temperatures above 200 °C lead to the formation of degradation products, which negatively influence the final fermentation step. As far as proteins are concerned, a recovery of 100% was reached with a treatment at 200 °C. Both the hydrolysate and the solid residue obtained from the pretreatment were treated with enzymes. Two systems of cellulases and xylanases from *Penicillium janthinellum* were used without any significant difference in performances. It was demonstrated that the sugar recovery from the liquid hydrolysate increases with the increasing reaction temperature while the sugar recovery from the solid residue decreases.

## 7.8 Nomenclature

| | | |
|---|---|---|
| $Ara$ | = | arabinose in wheat bran (g/100g) |
| $DOC$ | = | dissolved organic carbon in the hydrolysate (g) |
| $f$ | = | degree of carbon solubilization (-) |
| Gax | = | glucuronoarabinoxylan in wheat bran (g/100g) |
| $T$ | = | temperature (°C) |
| $t$ | = | time (min) |
| $TOC_{in}$ | = | total organic carbon of the starting material (g) |
| $\dot{V}$ | = | volumetric flow rate ($m^3$/min) |
| $Xyl$ | = | xylose in wheat bran (g/100g) |
| $z_{tot}$ | = | fixed bed length (m) |

Greek letters:

| | | |
|---|---|---|
| ε | = | bed porosity (-) |

## 7.9 References

Balat, M., H. Balat, and C. Öz (2008). Progress in Bioethanol Processing. *Prog. Energy Combust. Sci.*, **34**, 551–573.

Benamrouche, S., D. Crônier, P. Debeire, and B. Chabbert (2002). A Chemical and Histological Study on the Effect of (1→4)-β-endo-xylanase Treatment on Wheat Bran. *J. Cereal Sci.*, **36,** 253–260.

Bergmans, M.E.F., G. Beldman, H. Gruppen, and A.G.J. Voragen (1996). Optimisation of the Selective Extraction of (Glucurono) Arabinoxylans from Wheat Bran: Use of Barium and Calcium Hydroxide Solution at Elevated Temperatures. *J. Cereal Sci.*, **23**, 235–245.

Bobleter, O. (1994). Hydrothermal Degradation of Polymers Derived from Plants. *Prog. Polym. Sci.,* **19**, 797–841.

Bobleter, O., G. Bonn, and R. Concin (1980). Hydrothermolysis of Biomass-Production of Raw Material for Alcohol Fermentation and Other Motor Fuels. *Alt. Energy Sources,* **3**, 323–32.

Chotěborská, P, B. Palmarola-Adrados, M. Galbe, G. Zacchi, K. Melzoch, M. Rychtera (2004). Processing of Wheat Bran to Sugar Solution. *J Food Eng*, **61**,561–565.

Conner, A.H. and L.F. Lorenz (1986). Kinetic Modeling of Hardwood Prehydrolysis. Part III: Water and Dilute Acetic Acid Prehydrolysis of Southern Red Oak. *Wood Fiber Sci.,* **18**, 248-263.

Garrote, G., H. Domínguez, and J.C. Parajó (1999). Hydrothermal Processing of Lignocellulosic Materials. *Holz als Roh- und Werkstoff,* **57,** 191-202.

Ghose, T.K. (1984). Measurement of Cellulose Activity, Commission on Biotechnology, International Union of Pure and Applied Chemistry, New Delhi, India.

Gong, C.S., N.J. Cao, J. Du, and G.T. Tsao (1999). Ethanol Production from Renewable Resources. *Adv. Biochem. Eng. Biotechnol*., **65**, 207-241.

Heitz, M., F. Carrasco, M. Rubio, G. Chauvette, E. Chornet, L. Jaulin, and R.P. Overend (1986). Generalized Correlations for the Aqueous Liquefaction of Lignocellulosics. *Can. J. Chem. Eng*., **64**, 647-650.

Hendriks, A.T.W.M. and G. Zeeman (2009). Pretreatments to Enhance the Digestibility of Lignocellulosic Biomass. *Bioresour. Technol*., **100**, 10-18.

Hormeyer, H.F., W. Schwald, G. Bonn, and O. Bobleter (1988). Hydrothermolysis of Birch Wood as Pretreatment for Enzymatic Saccharification. *Holzforschung,* **42**, 95–8.

Ingram, T, T. Rogalinski, V. Bockemühl, G. Antranikian and G.Brunner (2009). Semi-continuous Liquid Hot Water Pretreatment of Rye Straw. *J. Supercrit. Fluids,* **48**, 238–46.

Jiamyangyuen, S., V. Srijesdaruk, and W.J. Harper (2005). Extraction of Rice Bran Protein Concentrate and its Application in Bread. *J. Sci. Technol*., **27**, 55-64.

Jones, B.D. and C.E.F. Gersdorf (1925). Proteins of Wheat Bran II. Distribution of Nitrogen, Percentages of Amino Acids and of Free Amino Nitrogen. *J. Biol. Chem.,* **64,** 241-251.

Kenealy, W.R. and T. Jeffries (2003). Rapid 2,2´-Bicinchoninic-Based Xylanase Assay Compatible with High Throughput Screening. *Biotechnol. Lett*., **25,** 1619-1623.

Kim, T.H. and Y.Y. Lee (2006). Fractionation of Corn Stover by Hot-Water and Aqueous Ammonia Treatment. *Bioresour. Technol*., **97**, 224–232.

Laser, M., D. Schulman, S.G. Allem, J. Lichwa, M.J. Antal, and L.R. Lynd (2002). A Comparison of Hot Liquid Water and Steam Pretreatments of Sugar Cane Bagasse for Bioconversion to Ethanol. *Bioresour. Technol.,* **81**, 33-44.

Li, J., G. Henriksson, and G. Gellerstedt (2007). Lignin Depolymerization/ Repolymerization and its Critical Role for Delignification of Aspen Wood by Steam Explosion. *Bioresour. Technol.,* **98**, 3061–3068.

Liu, C. and C.E. Wyman (2005). Partial Flow of Compressed-Hot Water Through Corn Stover to Enhance Hemicellulose Sugar Recovery and Enzymatic Digestibility of Cellulose. *Bioresour. Technol*., **96**, 1978–85.

Lynd, R.L. (1996). Overview and Evaluation of Fuel Ethanol from Cellulosic Biomass: Technology, Economics, the Environment, and Policy, *Annu. Rev. Energy Environ.*, **21**, 403-465.

Maes, C. and J.A. Delcour (2001). Alkaline Hydrogen Peroxide Extraction of Wheat Bran Non-starch Polysaccharides. *J. Cereal Sci.*, **34**, 29–35.

Maes, C. and J.A. Delcour (2002). Structural Characterisation of Water-extractable and Water-unextractable Arabinoxylans in Wheat Bran. *J. Cereal Sci.*, **35**, 315–326.

Mosier, N., C. Wyman, B. Dale, R. Elander, Y.Y. Lee, M. Holtzapple, and M. Ladisch (2005a). Features of Promising Technologies for Pretreatment of Lignocellulosic Biomass. *Bioresour. Technol.*, **96**, 673–686.

Mosier, N., R. Hendrickson, N. Ho, M. Sedlak, and R.L. Michael (2005b).Optimization of pH Controlled Liquid Hot Water Pretreatment of Corn Stover. *Bioresour. Technol.,* **96,** 1986-1993.

Murphy, J.C. and D.B. Jones (1926). Proteins of Wheat Bran III. The Nutritive Properties of the Proteins of Wheat Bran. *J. Biol. Chem*., **69,** 85-99.

Nabarlatz, D., X. Farriol, and D. Montané (2004). Kinetic Modeling of the Autohydrolysis of Lignocellulosic Biomass for the Production of Hemicellulose-Derived Oligosaccharides. *Ind. Eng. Chem. Res.,* **43**, 4124-4131.

Overend, R.P. and E. Chornet (1987). Fractionation of Lignocellulosics by Steam–Aqueous Pretreatments. *Philos. Trans. R. Soc. Lond*., **321**, 523-536.

Palmarola-Adrados, B., P. Chotěborská, M. Galbe, and G. Zacchi (2005). Ethanol Production From Non-starch Carbohydrates of Wheat Bran. *Bioresour. Technol.*, **96**, 843–850.

Rogalinski, T., T. Ingram, G. Brunner (2008). Hydrolysis of Lignocellulosic Biomass in Water Under Elevated Temperatures and Pressures. *J. Supercrit. Fluids,* **47**, 54-63.

Rouwenhorst, R.J., J.F. Jzn, W.A. Scheffers, and J.P. van Dijken (1991). Determination of Protein Concentration by Total Organic Carbon Analysis. *J. Biochem. Biophys. Methods*., **22,** 119-128.

Sasaki, M., T Adschiri, and K Arai (2003). Fractionation of Sugarcane Bagasse by Hydrothermal Treatment. *Bioresour. Technol*., **86**, 301–304.

Saxena, R.C., D.K. Adhikari, and H.B. Goyal (2009). Biomass-based Energy Fuel Through Biochemical Routes: A review. *Renew. Sust. Energ. Rev*., **13**, 167–78.

Saxholt E., A.T. Christensen, A. Møller, H.B. Hartkopp, K. Hess Ygil, and O.H. Hels (2008). *Danish Food Composition Databank, revision 6.0.Food Informatics*, Available at: http://www.foodcomp.dk/ [Accessed December 2008].

Sluiter, A., B. Hames, D. Hyman, C. Payne, R. Ruiz, C. Scarlata, J. Sluiter, D. Templeton, and J. Wolfe (2008). *Determination of Total Solids in Biomass and Total Dissolved Solids in Liquid Process Samples*. Technical Report NREL/TP-510-42617 January.

Sun, X.F., F. Xu , R.C. Sun, Y.X. Wang, P. Fowler, and M.S. Baird (2004). Characteristics of Degraded Lignins Obtained from Steam Exploded Wheat Straw. *Polym. Degrad. Stab.,* **86**, 245-256.

Sun, Y., and J. Cheng (2002). Hydrolysis of Lignocellulosic Materials for Ethanol Production: a Review. *Bioresour. Technol.,* **83**, 1–11.

Swennen, K., C.M. Courtin, G.C.J.E. Lindemans, and J.A. Delcour (2006). Large-scale Production and Characterisation of Wheat Bran Arabinoxylo-Oligosaccharides. *J. Sci. Food Agric.*, **86**, 722–731.

Taylor, J.R. (1997). *An Introduction to Error Analysis: The Study of Uncertainties in Physical Measurements (2nd edition)*. University of science books. Sausalito (U.S.A.).

U.S. Department of Energy Genome Programs, (2009). Available at: http://genomics.energy.gov [Accessed November 2009].

USDA, U.S. Department of Agriculture, Agricultural Research Service (2008). *National Nutrient Database for Standard Reference*, *Release 21*. Available at: http://www.ars.usda.gov/ba/bhnrc/ndl [Accessed December 2008]

Yu, Y., X. Lou, and H. Wu (2008). Some Recent Advances in Hydrolysis of Biomass in Hot-Compressed Water and Its Comparisons with Other Hydrolysis Methods. *Energy Fuels*, **22**, 46-60.

# Chapter 8

# LHW pretreatment of paper

An experimental apparatus for the liquid hot water pretreatment (LHW) of biomass with and without addition of $CO_2$ was developed. Once the apparatus was built and the experimental procedures were defined, some preliminary experiments were performed. In this Chapter the apparatus is first described then the results of LHW pretreatment of white office paper without $CO_2$ additions in a fixed-bed reactor are presented. Different temperatures and reaction times were investigated in order to understand the behaviour of this material and its different polymeric constituents. The enzymatic hydrolysis of the two fractions obtained from the pretreatment (the liquid hydrolysate and the solid residues) was performed using cellulases and xylanases available from the market. The aim was to determine the best pretreatment conditions (temperature and total reaction time) for the LHW of paper in order to obtain the maximum amount of fermentable sugars after the enzymatic hydrolysis.

## 8.1 Introduction

The advantages of LHW among the other pretreatment presented in Chapter 1 and Chapter 7 can be possibly improved by using $CO_2$ to catalyze the process. $CO_2$ is an acidifying agent which can overcome the common disadvantage emerging when using mineral acids: Corrosiveness can be reduced, no waste products are created (e.g. gypsum), $CO_2$ can be easily removed by depressurization and is a green process component. If pre-treatment of lignocellulose with $CO_2$ could be applied at lower temperatures than a similar process without $CO_2$ addition, xylose degradation could be avoided and yield enhanced (Schacht *et al.,* 2008).

On the other hand, carbonic acid is relatively mild and hence does not offer the same hydrolytic capability of sulphuric acid. However, van Walsum (2001) demonstrated that at temperatures on between 170-230 °C, carbonic acid does exhibit a catalytic effect on the hydrolysis of xylan. Similarly van Walsum and Shi (2004) observed an enhanced release of xylose and low degree of polymerization of xylan oligomers compared to pretreatment using hot water alone.

However so far, the effect of $CO_2$-LHW pretreatment on biomass have not been investigated deeply, and even fewer are the study on the sugar yield obtained after enzymatic treatment of the biomass treated in this way. Both Yourchisin and van Walsum (2004) and Schacht *et*

*al.,* (2008) found that the use of $CO_2$ did not enhance enzymes performances. Due to the lack of experimental data about this type of pretreatment an experimental investigation turns to be interesting.
White office paper was chosen as raw material to test the experimental LHW apparatus, to determine the experimental procedure for both pretreatment and enzymatic hydrolysis and to start this experimental investigation. In fact, waste paper constitutes a considerable share of municipal and industrial wastes even though recycling efforts have been strengthened in recent years by legal provisions like the Packaging Directive. Although the actual European recycling ratio (66.6% CEPI, 2008) is relatively high, it has not reached yet a satisfactory level. Moreover, when paper materials are recycled, they are usually turned into lower grade paper products. With further recycling of paper, fibres length in the paper becomes shorter. Since the shortening of paper fibres decreases the quality of paper, the maximum ratio of paper-to-paper recycling is said to be 65% (Ikeda, 2006). This means that a certain fraction of paper would always been sent to disposal. This fraction could be converted to ethanol and used for energetic proposal achieving both environmental and energy benefits. Previous research works were focused on enzymatic conversion of waste paper to monomeric sugars using enzymes (Yamashita *et al.,* 2008; Vynios *et al.,* 2009; Dale and Musgrove, 2004).
Up to our knowledge there are still no data about the effect of LHW pretreatment to office paper, especially if a semibatch reactor is used.

## 8.2 Experimental apparatus and LHW pretreatment procedure

### *8.2.1 Plug flow reactor design*

The reactor is a 304 stainless steel welded cylinder with an internal diameter of 21 mm and an external one of 25 mm. Considering a maximum operation temperature of 250 °C the maximum operation pressure ($P_{max}$) was calculated by the Von Mises criteria:

$$P_{\max} = \frac{\sigma_{adm}\left(K^2 - 1\right)}{\sqrt{3}K^2} \tag{8.1}$$

where $K=d_e/d_i$ [-] is the ratio between external diameter ($d_e$) and internal one ($d_i$) and $\sigma_{adm}$ is the maximum allowable stress, calculated as:

$$\sigma_{\text{adm}} = \frac{\sigma_{s(250°C)} \cdot z}{f_s} \tag{8.2}$$

the welding efficiency ($z$) was assumed to be 0.80 (Guarise, 2007), the safety factor is $f_s$=1.5 while the yield strength of stainless steel AISI 304 at 250 °C ($\sigma_{s,250°C}$) was calculated using the correlation (Guarise, 2007):

$$\sigma_{s,T} = \sigma_{s,20} \cdot \left[1 - 0.0015 \cdot \left(T - 20\right)\right] \tag{8.3}$$

that expresses the temperature dependence of the yield strength starting from the yield strength at 20 °C ($\sigma_{s,20}$= 18 kgf/mm$^2$).

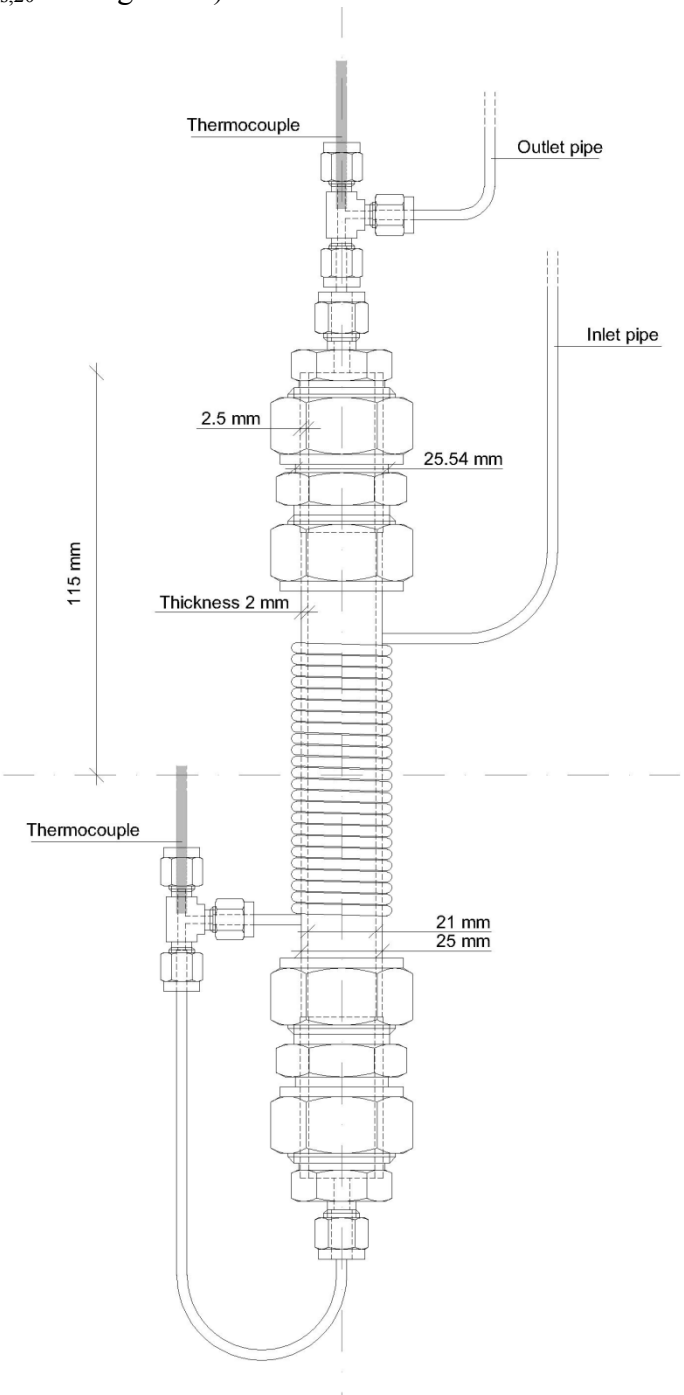


**Figure 8.1** *Reactor technical details.*

The resulting maximum working pressure was 104.1 bar. Swagelock fittings were connected (Figure 8.1) to this cylinder (150 mm length), in order to reduce the nominal diameter to the one of inlet and outlet pipes. The final reactor length results to be 230 mm while the total volume about 79.7 $cm^3$.

## 8.2.2 LHW Process

The reactor was filled with the solid material and a layer of glass wool and a metal filter (1 mm mash size) were placed in the outlet section in order to retain the paper inside.
In all experiments the same amount of paper was treated (28 g) in order to work with the same solid apparent density. The water was first pumped into the inlet pipe then, when it reached the inlet section, the loaded reactor was connected and placed into the oven. The desired reaction pressure (60 bar) was obtained by pressurizing with nitrogen, and the reactor was preheated for 15 minutes. As shown in Figure 8.2a the nitrogen tank is connected to the reactor outlet pipe. This allows avoiding the formation of air sac in the inlet pipe, that could cause negative effects during the depressurising procedure. When the HPLC pump was switched on water started to be pumped through the reactor. All the experiments in the fixed bed reactor were carried out at a constant flow rate of 5 mL/min and at the pressure of 60 bar. The water temperature was increased up to the reaction temperature first by an electrical resistor and then by an adequate heat exchange in the inlet pipe inside the oven (12 cm of pipe are wrapped around the reactor).

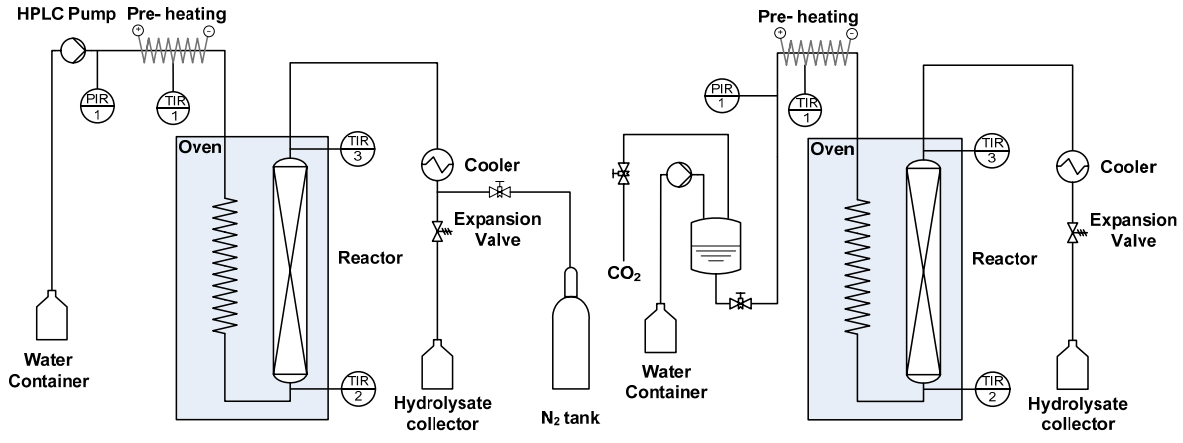


**Figure 8.2** *Scheme of the apparatus for LHW of biomass (a) and adaption for the use of the $CO_2$ (b).*

Water enters the reactor from the bottom. By means of T-fittings two thermocouples are placed in the inlet and outlet pipes to measure the water temperature. At the oven exit the hydrolysate was cooled down by an ice bath and collected. When the suitable reaction time is reached, the hydrolysis reaction was stopped by depressurizing the system: the exit valve

was opened to ambient conditions and the reactor was disconnected and immediately placed in a water bath. Two fractions were obtained: the liquid ones (hydrolysate) collected during the whole reaction time, and the solids retained in the reactor (solid residue). In Figure 8.2b the apparatus that permits the use of $CO_2$ as catalyst is shown. In this case first the whole system is pressurized with $CO_2$, then water is pumped into a mixing vessel in order to solubilise $CO_2$ and finally the water $CO_2$ liquid mixture flows through the reactor.

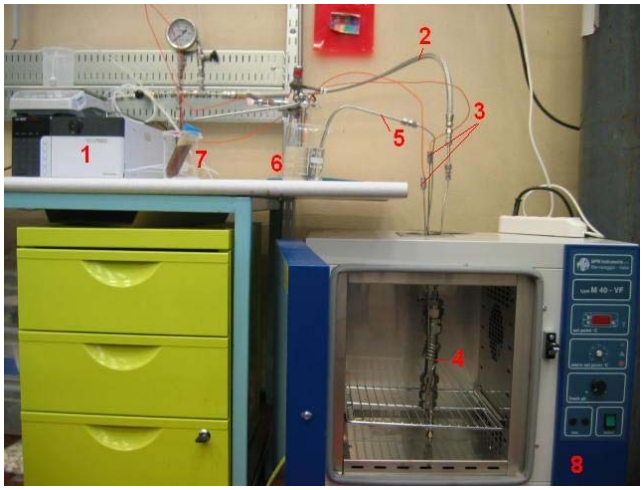


**Figure 8.3** *LHW apparatus: 1 HPLC pump, 2 inlet pipe, 3 thermocouples, 4 reactor, 5 exit pipe, 6 cooler, 7 sample, 8 oven.*

In Figure 8.3 a picture of the apparatus for the LHW of lignocellulosic biomass is reported.

### 8.2.3 Enzymatic hydrolysis

The hydrolysate fraction as well as the solid residue obtained from the LHW treatment were treated with enzymes to determine the maximum monomeric sugars yield. Hydrolysis was carried out at temperature of 55 °C. Enzymatic reaction time, enzyme amount, and solid concentration were varied in order to understand the different contribution on the final sugar yield.

## 8.3 Materials

### 8.3.1 Raw material: paper

The treated material was standard white office paper (80 g each sheet) commercially available (DiEM).

### 8.3.2 Enzyme system

The enzyme complex (Accellerase™ 1000) used for the treatment of both hydrolysate and solid residues from the pretreatment was kindly provided from Genecor®. This enzyme complex is produced using a genetically modified strain derived from *Trichoderma reesei* and is specifically developed for the treatment of lignocellulosic biomass. The multiple enzyme activities include: exoglucanase, endoglucanase, hemicellulose and betaglucosidase. The endo-1,4-β-D-glucanases (EGs) cleave cellulose in its internal non-terminal regions, yielding oligosaccharides (the minimum activity guarantee in the enzyme complex is 2500 CMC U/g). A carboxymethhy cellulose activity unit (CMCU) is equal to the μmol of reducing sugars (expressed as glucose equivalents) liberate in one minute under specific assay conditions of 50°C and pH 4.8. The enzyme β-Glucosidase is an exo-hydrolase that yields glucose monosaccharides from soluble oligosaccharaides such as cellobiose. The β-Glucosidase activity in the complex is 400 pNPG U/g minimum. One pNPG unit denotes 1 μmol of Nitrophenol liberated from para-nitrophenyl-B-D-glucopyranoside in 10 min at 50°C and pH 4.8. A dosage rate of 0.1 to 0.5 g per g of cellulose or roughly 0.05 to 0.25 mL per g of biomass is suggested.

## 8.4 Analytical methods

### 8.4.1 Sugar analysis

D-Glucose and D-xylose were determined in the liquid hydrolysate after the HLW treatment and after the enzymatic hydrolysis using the Glucose and the Xylose enzyme kits purchased from Megazyme. These kits do not allow the determination of polysaccharides, but of monomeric sugars only.

During glucose determination first the monosaccharide is phosphorylated to glucose-6-phosphate (G-6-P) by reacting with adenosine-5'-triphosphate (ATP). The hexokinase (HK) enzyme catalyzes the reaction:

$$\text{D-Glucose} + \text{ATP} \rightarrow \text{G-6-P} + \text{ADP} \qquad (8.4)$$

In the presence of the enzyme glucose-6-phosphate dehydrogenase (G6P-DH), G-6-P can be oxidised by nicotinamide-adenine dinucleotide phosphate ($NADP^+$) to gluconate-6-phosphate with the formation of reduced nicotinamide-adenine dinucleotide phosphate (NADPH).

$$\text{G-6-P} + NADP^+ \rightarrow \text{gluconate-6-phosphate} + \text{NADPH} + \text{H} \qquad (8.5)$$

The amount of NADPH formed in this reaction is stoichiometric with the amount of the initial D-glucose. Finally the NADPH causes an increase in absorbance at 340 nm.

Also the xylose determination kit is based on the increased absorbance due to the NADH formation. In this case first the interconversion of the α- and β-anomeric forms of D-xylose is catalysed by xylose mutarotase (XMR)

$$\alpha\text{-D-Xylose} \rightarrow \beta\text{-D-xylose} \tag{8.6}$$

Then the β-D-xylose is oxidised by $NAD^+$ to D-xylonic acid in the presence of β-xylose dehydrogenase (β-XDH) at pH 7.5

$$\beta\text{-D-Xylose} + NAD^+ \rightarrow \text{D-xylonic acid} + NADH + H+ \tag{8.7}$$

As for the glucose kit the amount of NADH formed in this reaction is stoichiometric with the amount of D-xylose.

### *8.4.2 Moisture and pH*

The dry matter content of treated solid samples, as well as those of raw material and hydrolysate samples, was determined by weighting the samples before and after heating at 105 °C until constant weight, according to the standards given by NREL (Sluiter *et al.,* 2008). The measurement of the moisture of the raw material was done before each experiment, as it depends from the ambient humidity. The pH of the hydrolysate was measured with a Delta OHM pH meter.

## 8.5 Results

### *8.5.1 Hydrolysate instantaneous dissolved solid concentration*

Figure 8.4 shows the instantaneous solid concentration of the hydrolysate. In this way it is possible to monitor the time dependence of the treatment. The concentration of solid in the hydrolysate increases with the temperature, a clear sign that dissolution kinetics are faster at higher temperatures. But while for low temperatures the dissolution is over after 30 minutes, increasing the temperature, the dissolution continues for longer times.

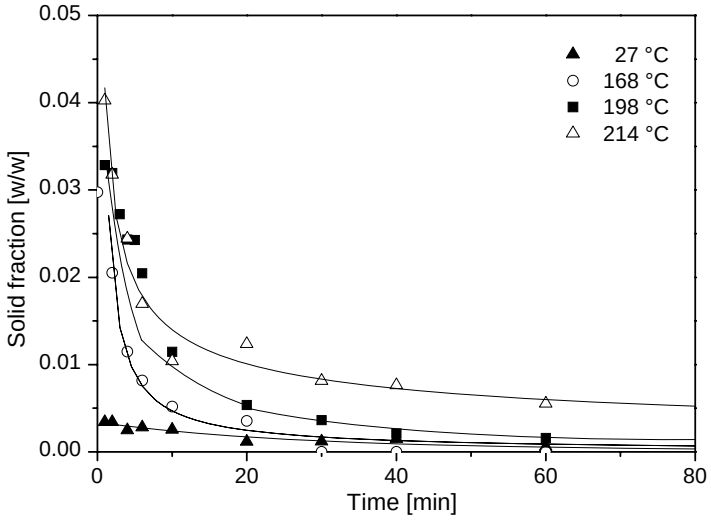


**Figure 8.4** *Instantaneous concentrations of solid in the hydrolysate during the reaction time. Every curve represents a different experiment. Lines show only trends.*

## 8.5.2 Total solids dissolution and hydrolysate pH

Figure 8.5 shows the maximum amount of dissolved solid as a function of the pretreatment temperature. The experiments (empty circles) were carried out for 3 hours. Paper, unlike other biomasses, has already been subject to mechanical and chemical treatments so, when pretreated with LHW, it behaves differently. For instance at temperatures above 214 °C the pieces of paper are not recognizable anymore and the treated material is present, in the reactor, as a fine powder.

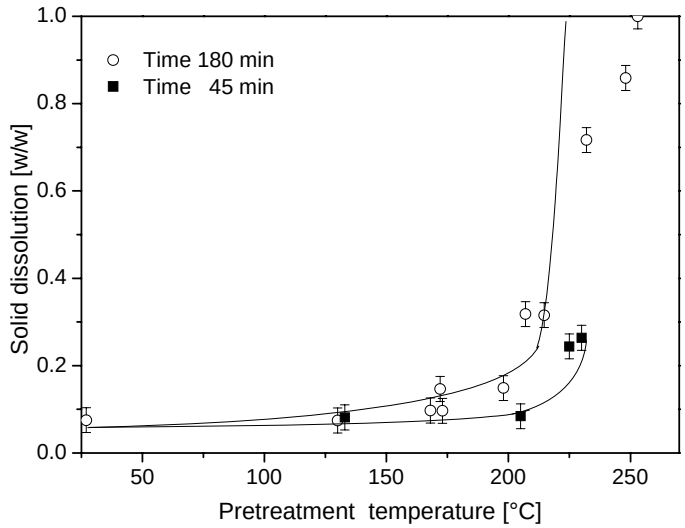


**Figure 8.5** *Solid dissolution after a treatment 3h long (empty circles) and dissolution after treatment for 45 min (square). Every point is a different experiment. Lines represent only trends.*

A sheet of paper is, in fact, made of milled wood fibres; the hot water breaks the bonds between the fibres and the material loses its compactness. For this reason a total solid dissolution for the points above 214 °C can be assumed.
In Figure 8.5 some of the points above this temperature display a value below 1. This is only due to the fact that after 3 hours not all the fibres have already reached the size of the metal filter. Increasing the reaction time all the fibres would have left the reactor.
In Figure 8.5 the solids dissolved after a treatment of 45 minutes are also shown. Clearly the values are lower.
Figure 8.6 shows the pH values of the total hydrolysates collected during experiments at different temperatures. When increasing the severity of the treatment a decrease of the pH value was observed. This happens owing both to the formation of degradation products and the release of the acids contained in the hemicellulose. Clearly the pH values are not influenced by the total amount of water utilized for the hydrolysis, probably because some weak acids with buffer properties are produced.

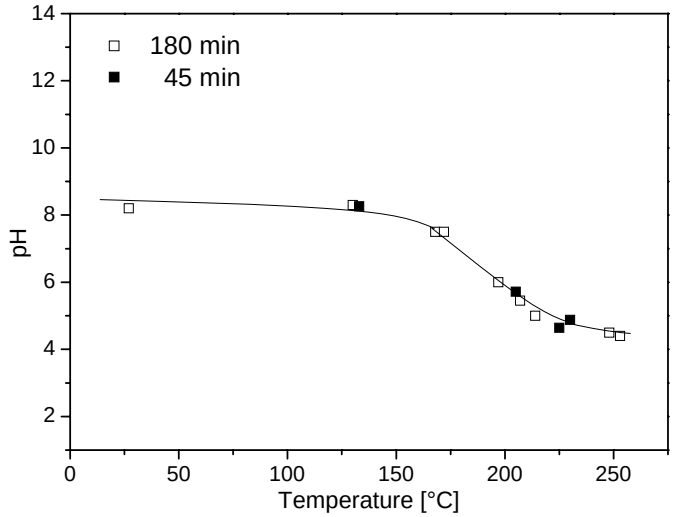


**Figure 8.6** *Total hydrolysate pH after treatment at different temperatures. Empty squares: 180 min treatments. Filled squares: 45 minutes treatment.*

## 8.5.3 Enzymatic hydrolysis

Enzymes performances are influence by different factors, first of all the ratio between the enzyme used and the biomass treated. More importantly, enzymes are inhibited by their own reaction products (monosaccharide sugars). For these reasons the solid and liquid phases produced by the LHW process were treated with a very large amount of enzymes (solid residue: 14 mL/g solid; liquid hydrolysate: 0.4 mL/mL hydrolysate). 3 mL of buffer were added to perform both the treatments in order to keep the final sugar concentration low and to regulate the pH at its optimum value. Finally the enzymatic treatment was performed for long time (72 h).

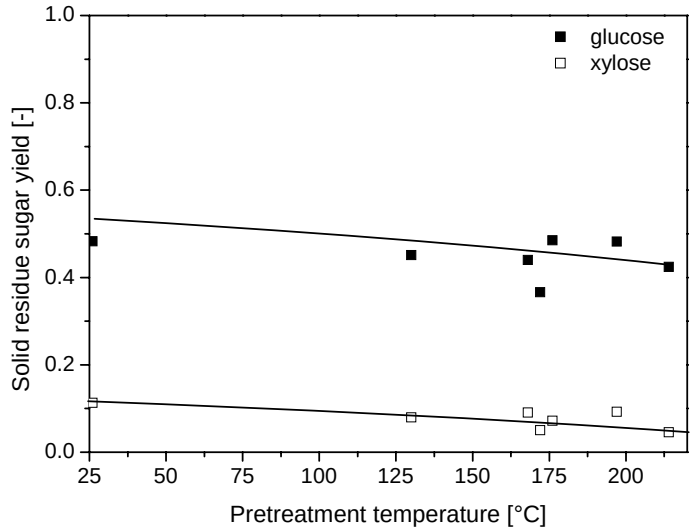


**Figure 8.7** *Sugar yields obtained after enzymatic treatment of the solid residue.*

In this way the maximum amount of sugars obtainable from both of the fractions by the enzymatic treatment was determined. In Figure 8.7 the sugar yield from the solid residue is shown while in Figure 8.8 the one from the liquid hydrolysate. This factor is calculated as the ratio between the obtained monomeric sugar [g] and the paper treated in with the semibatch reactor [g].

From Figure 8.7 and 8.8 it can be concluded that the amount of sugar hydrolysed by LHW at the investigated temperature is really low. Almost the total amount of sugar can be found in the solid residue.

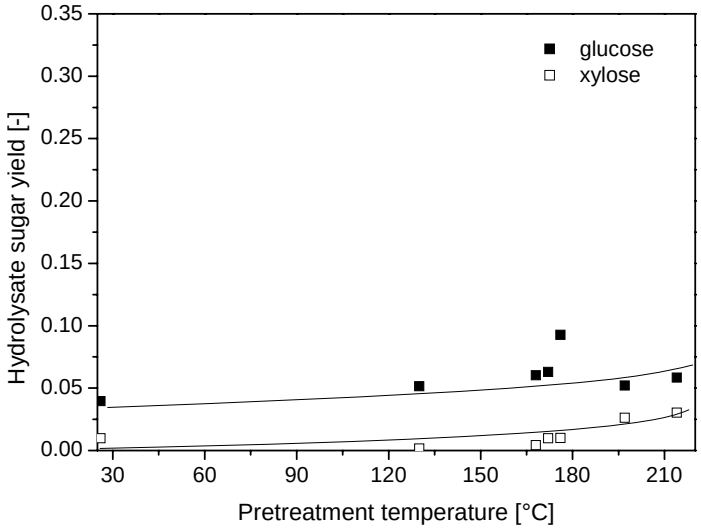


**Figure 8.8** *Sugar yields obtained after enzymatic treatment of the liquid hydrolysate.*

As expected there is no influence of the pretreatment on the enzymes performances, as the enzyme were used in excess to hydrolyse all the sugars present in the biomass. It has to be taken into account that the data of the Figures were obtained after: pretreatment of paper, enzymatic treatment of a small fraction of the solid residue (there is the possibility that the sample does not respect the feature of the whole amount) and determination of monosaccharides with the sugar kits. All these passages increase the experimental error of the data, so that the values of Figure 8.7 and 8.8 can be considered as constant.

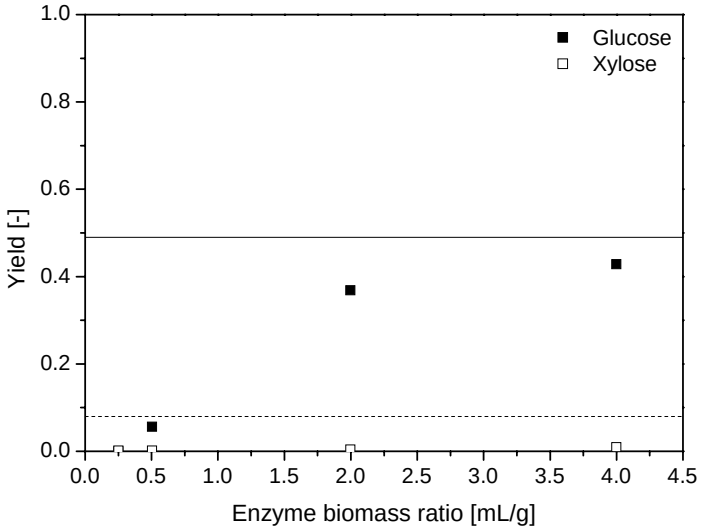


**Figure 8.9** *Sensitivity analyses on the enzyme biomass ratio. Lines show the maximum amount of sugar yield.*

In order to test if the LHW pretreatment is really able to enhance the sugar yield, lower (and more economic in a large scale plant) enzyme – biomass ratio should be used. A sensitivity analysis (Figure 8.9) has been carried out on the solid sample obtained after LHW treatment at 200 °C for 45 minutes in order choose the suitable amount of enzymes. With 4 mL of enzyme every grams of solid treated almost the maximum yield of glucose can be obtained. The enzymes are less efficient on the hydrolysis of the xylan due to the fact that they were developed and optimized for the cellulose hydrolysis.

## 8.6 Concluding remarks and future work

An experimental set up was built to study the LHW pretreatment of lignocellulosic materials with and without addition of $CO_2$. Samples of white office paper were treated in a semibatch reactor. Increasing the temperature the solid dissolution increased. Above 214 °C the complete degradation of the biological material occurred. Similarly the pH of the hydrolysate decreased as a consequence of the release of acids from the hemicelluloses, and to the formation of degradation products. The treatments of the hydrolysate and solid

residue with enzymes showed that it is possible to obtain monomeric sugars from paper for a further possible fermentation to ethanol.
Clearly the results obtained are still of preliminary nature. The tests performed with a huge enzymes- biomass ratio permitted to have the maximum possible sugar yield after enzymatic hydrolysis while the sensitivity on the amount of enzyme to identify a suitable value. In order to understand the real potential of the LHW pretreatment further investigations with samples treated at different temperatures and for different times using intermediate amounts of enzymes are needed. Moreover a statistical number of test has to be performed to identify the experimental errors.
The functionality of the apparatus that permits the use of $CO_2$ has been tested, but no experimental results are available yet. A study on the effect of $CO_2$-LHW treatment on the biomass is in progress and also the difference on the enzymatic digestibility between treatment with and without $CO_2$ has to be determined.

## 8.7 Nomenclature

| | | |
|---|---|---|
| $d$ | = | diameter (m) |
| $f_s$ | = | safety factor (-) |
| $K$ | = | diameter ratio (-) |
| $P_{max}$ | = | maximum operation pressure (kgf/mm$^2$) |
| $T$ | = | Temperature (°C) |
| $z$ | = | weld efficiency (-) |

Greek letters:

| | | |
|---|---|---|
| $\sigma_{adm}$ | = | maximum allowable stress (kgf/mm$^2$) |
| $\sigma_{s,T}$ | = | yield strength at temperature T (kgf/mm$^2$) |

## 8.8 References

CEPI (Confederation of European Paper Industries) (2008). *Key Statistics 2008 European Pulp and Paper Industry*. Available at: http://www.cepi.org/Content/Default.asp?pageid=12 [Accessed August 2009].

Dale M.C. and D. Musgrove (2004). Continuous Conversion of MSW-derived Waste Paper to Bio-ethanol Using a 100 L 6-stage Continuous Stirred Reactor Separator. In proceeding of: *AIChE Annual Meeting*, 8237–8242.

Guarise G.B. (2007). *Lezioni di impianti chimici ad alta pressione*. Cleup, Padova (Italia).

Ikeda, Y., E.Y. Park, and O. Naoyuki (2006). Bioconversion of Waste Office Paper to Gluconic Acid in a Turbine Blade Reactor by the Filamentous Fungus Aspergillus niger. *Bioresour. Technol.*, **97**, 1030-1035.

Schacht C., C. Zetzl, and G. Brunner (2008). From Plant Materials to Ethanol by Means of Supercritical fluid Technology. *J. of Supercrit. Fluids*, **46**, 299-321.

van Walsum, G.P. (2001). Severity Function Describing the Hydrolysis of Xylan Using Carbonic Acid. *Appl. Biochem. Biotechnol.,* **91–93**, 317-329.

van Walsum, G.P. and H. Shi (2004). Carbonic Acid Enhancement of Hydrolysis in Aqueous Pretreatment of Corn Stover. *Bioresour. Technol.,* **93**, 217–226.

Vynios, D.H., D.A. Papaioannou, G. Filos, G. Karigiannis, T. Tziala, G. Lagios (2009). Enzymatic Production of Glucose from Waste Paper. *BioRes.*, **4**, 509-521.

Yamashita, Y., A. Kurosumi, C. Sasaki, and Y. Nakamura (2008). Ethanol Production from Paper Sludge by Immobilized Zymomonas mobilis. *Biochem. Eng. J.*, **42**, 314-319.

Yourchisin, D.M. and van Walsum (2004). Comparison of Microbial Inhibition and Enzymatic Hydrolysis Rates of Liquid and Solid Fractions Produced from Pretreatment of Biomass with Carbonic Acid and Liquid Hot Water. *Appl. Biochem. Biotechnol.,* **113–116***,* 1073-1086.

# Chapter 9

# Semi continuous LHW reactor model

In order to simulate the semicontinuous LHW process a mathematical model of the reactor was developed and solved with gPROMS$^{TM}$. The model accounts for the solubilization of the biomass, the formation of monomeric sugars, and the degradation product reactions, under different experimental conditions. The core driver of this Chapter was the lack in literature models about LHW pretreatment if a semibatch reactor is used. This specific problem was addressed only twice: by Ingram *et al.,* (2009) and by Ji *et al.,* (2009). In both cases the filling time of the reactor is not accounted for, and in the first one the model is focused especially on the solid solubilization only. In this Chapter data from Ingram *et al.,* (2009) are used to fit the kinetic parameters values for the solid solubilization, and the results obtained are compared to those of the model by Ingram *et al.,* (2009).

## 9.1 Literature models

So far, mathematical models based on pseudo-first order kinetics have been successfully employed for modelling the autohydrolysis (without any catalyst), acid prehydrolysis, and acid hydrolysis of lignocellulosic material. In fact, all these cases are characterized by hydronium-catalysed reactions of polysaccharide heterocyclic ethers, so that the interpretation of data has been carried out by closely related methods. For this reason pretreatement models are available in the literature since the beginning of the 80s (Garrote *et al.,* 1999).

On the other hand, a rigorous kinetic study of the polysaccharide hydrolysis by the catalytic action of hydronium ions is quite a difficult problem involving at least five sequential steps (Carrasco and Roy, 1992; Gámez *et al.*, 2006 cited in Vázquez *et al.,* 2007):

i) diffusion of the catalyst in the polysaccharide heterogeneous matrix;
ii) protonation of the heterocyclic ether;
iii) breakage of the ether bond with generation of a carbonium ion and a new polymer, oligomer or monomer (depending on the position of the broken bond on the polymer chain);
iv) regeneration of the hydronium ion by hydrolysis of water, to produce saccharide with a polymerization degree dependent on the position of the broken bond;
v) diffusion of the reaction products through the solid matrix into the liquid phase.

Other aspects affecting the hydrolysis of polysaccharides in lignocellulosic material include:

- interferences caused by different components present in wood;
- simultaneous reactions of other fractions present in the raw material, as lignin;
- limitations in the accessibility of hydronium ions to ether bonds caused by the presence of lignin and by the structure of cell walls;
- variations in specific surface, available surface area and substrate accessibility during reaction;
- time-dependence of the effective concentration of hydronium ions.

In order to reduce the problem of the kinetic modelling to a practical limit, the following simplifications are commonly accepted (Garrote *et al.,* 1999):

i) the polysaccharide hydrolysis and related reactions are assumed to follow irreversible, pseudohomogeneous, first-order kinetics, as proposed by Saeman (1945) for wood processing with dilute, aqueous solutions of sulphuric acid;

ii) the apparent kinetic coefficients are calculated from experimental data, and their temperature dependence is assumed to follow the Arrhenius equation;

iii) hemicellulose hydrolysis is considered to be independent of other reactions (involving cellulose and lignin) occurring in the medium;

iv) the effects derived from the time dependence of parameters such as particle size and acidity are neglected.

The simplified models based on these assumptions do not describe the elementary reaction steps and cannot be used to predict reaction rates, but are useful for interpreting the experimental results obtained under a wide variety of operational conditions and provide all the information necessary for comparative studies and design purposes.

There are several literature models describing the hydrolysis of lignocellulosic material, but most of them present common features. Basically, they consider a homogeneous phase system with pseudo-first-order reactions. This assumption allows a fair description of the process because the kinetic parameters are not really referred to simple reactions but to all the phenomena previously cited, transport mechanisms included, i.e. are lumped (effective) parameters.

The polymeric sugars (cellulose or hemicellulose) are either divided into a fast hydrolysable fraction and a slow hydrolysable one (Nabarlatz *et al.,* 2004, Vázquez *et al.,* 2007), or considered as homogeneously reacting polymers (Aguilar *et al.*, 2002 Rodríguez-Chong *et al.*, 2004, Zhuang *et al.,* 2009, Jensen *et al.,* 2008). Solid polymers may be assumed as directly reacting to monomers (Rodríguez-Chong *et al.*, 2004, Aguilar *et al.*, 2002, Jensen *et al.,* 2008, Vázquez *et al.,* 2007) as well as indirectly through oligomers intermediates (Lee

*et al.*, 1998, Nabarlatz *et al.,* 2004, Kamio *et al.,* 2008, Zhuang *et al.,* 2009). Examples of different reaction mechanisms of this kind are schematically depicted in Figure 9.1.

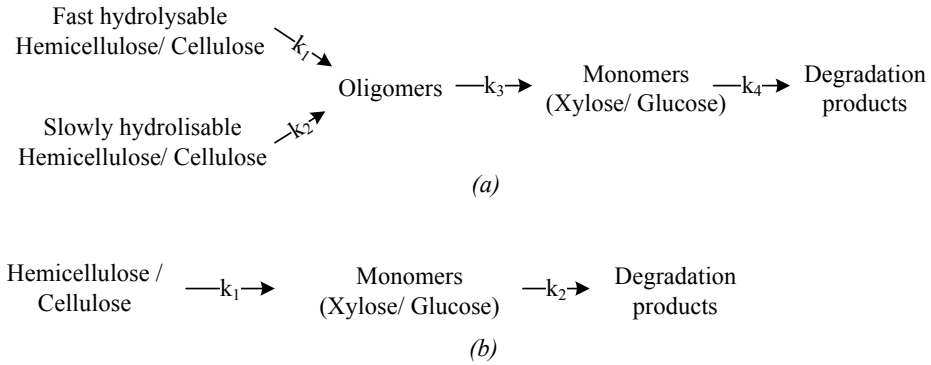


**Figure 9.1** *Different lignocellulosic materials hydrolysis reaction mechanisms: Model in which polymers are divided into a fast and a slow hydrolysable fraction and oligomers are considered (a) and model with homogeneous reacting polymers and direct formation of monomers (b).*

The existence of the two fractions defined above was first proposed for cellulose hydrolysis, based on the structural difference between amorphous and crystalline cellulose.

The same difference does not apply to hemicellulose hydrolysis, for which the two-fractions hypothesis has to be justified on the basis of other factors, such as: the influence of transport limitations (more important for bigger particle size), differences in physicochemical nature of the polymer and/or dependence of the available reaction surface on the reaction time, presence of uronic acid with reactivity lower than xylose that reduces the hemicellulose solubilization, different reaction rate of the fraction linked with lignin, variation in the surface of the interphase water-hemicellulose along with the reaction (Rodríguez-Chong *et al.,* 2004).

The prediction of the monomeric sugars concentration is the most important information concerning the acid hydrolysis of lignocellulosic biomass, because the aim of this treatment is to maximize the hydrolysis of polymeric sugars. For this reasons a kinetic like the one of Figure 9.1b is more interesting for acid hydrolysis models than for pretreatment models. If a batch reactor is used, an analytical solution can be obtained in this case:

$$C_{i,M} = C_{i,M0}\, e^{-k_2 t} + C_{i,P0}\frac{k_1}{k_2 - k_1}\left(e^{-k_1 t} - e^{k_2 t}\right) \tag{9.1}$$

where $C_{i,,M}$ and $C_{i,P}$ are the monomeric and polymeric sugars concentrations [kg/m$^3$], $t$ is the time and subscript 0 indicates initial conditions. In this case $C_{i,p}$ has to denote the total polymeric sugars (dimers included), so those only monomeric sugars are excluded.

If the LHW pretreatment is investigated these models do not give substantial information. This partial hydrolysis is only a pretreatment, whose aim is not to obtain monomeric sugars, so their concentrations are usually really small. In addition even though the solid material is solubilized, undergoes hydrolysis, and generates oligomers, these phenomena are hidden by the reaction mechanism itself. Differently, models like the one of Figure 9.1a involve also oligomers and keep track of the solubilization of the solids as well.

Once the monomeric sugars are obtained the models consider that a part of these sugars undergo degradation. Main degradation products are furfural and hydroxymethyl furfural (HMF). Actually, furfural and HMF account for only a portion of the monosaccharides loss observed during the degradation reaction. For the degradation of xylose at 19°C, at least 10 different products from the degradation besides furfural were identified, including formaldehyde, formic acid, crotonaldehyde, lactic acid, acetaldehyde, dihydroxyacetone etc (Wei *et al.,* 2008).

The real reaction mechanism would include equilibrium reactions and production of different compounds. In Figure 9.2 the glucose reaction pathways proposed by Xiang *et al*., (2004) and Conner and Lorenz (1986) are shown.

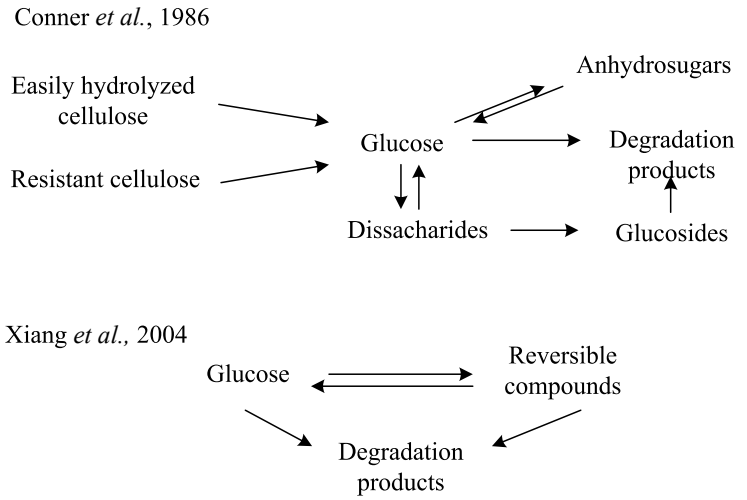


**Figure 9.2** *Glucose decomposition reactions.*

These mechanisms are usually applied to monomeric sugars degradation studies. When the pretreatment of raw materials has to be simulated, the problem is simplified so that the degraded products are considered as a unique lumped one. Again for a first order kinetic is considered the reaction (Wei *et al.,* 2008).

## 9.2 Proposed models

The two theoretical models, proposed in this Chapter, represent the pathways shown in Figure 9.3. In both the cases the solid biomass is divided in two different fractions: one that

can be dissolved and another that cannot be dissolved. This approach was applied also by: Vázquez *et al.,* (2007), to model the conversion of xylose to furfural, Aguilar *et al.,* (2002) and Kim and Lee (1987), to model the hydrolysis of hemicellulose and cellulose and by Ingram *et al.,* (2009) to simulate the dissolution of rye straw (assumed as single composite material.

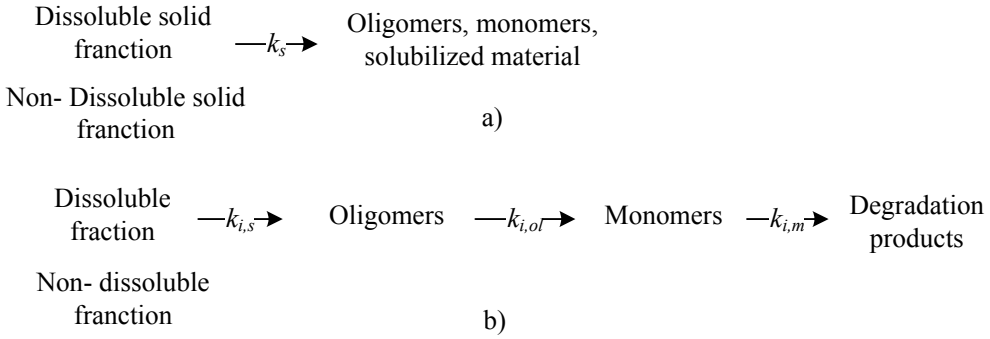


**Figure 9.3** *Model pathway for the dissolution of the biomass considered like a unique composite material (a) and divided in its constituent polymers (b).*

While our first model considers the biomass as a single (homogeneous) material, the second one distinguishes a numbers of constituent: cellulose (c), hemicellulose (h), lignin (l) and other components (o). Each of them is partially hydrolyzed and solubilized by reaction with water. Moreover cellulose and hemicellulose pathways include oligomers transformation to monomeric sugars and monomeric sugar decomposition.

## *9.2.1 Monocomponent model*

Complex approaches suffer from unknown composition of the dissolved biomass, complicated or even unknown degradation pathways, difficulties in determining the oligomeric sugars as well as the negligence of the interactions between the different compounds. The first model we have developed considers the solid material as a homogeneous material. Accordingly, the amount of experimental data needed is low, so that the model is widely applicable. However it does not give any information about the composition of the two phases but only about the macroscopic changes in the solid material amount. For these reasons the model is only useful to have an idea about the time dependence of the pretreatment and the extent of the solubilization of the solid material.
We now summarize the model hypotheses:

1. The mass balance of the solid material is written with reference to the reactor volume. This assumption is based on the experimental evidence (Lee *et al.*, 1998) that cellulose and hemicellulose solubilization kinetics can be modelled with irreversible pseudohomogeneous first-order kinetics if this basis is chosen. This behaviour valid under the assumption of monocomponent material (Ingram *et al.,* 2009);

2. The mass balance of the biomass dissolved in the liquid is referred to the liquid phase volume;
3. During the reaction the solid does not move from its initial position (see Figure 9.5) i.e. it is neither compressed at the reactor outlet section nor collapses at the reaction inlet. The cogency of this assumption depends on the type of biomass considered. For rye straw not previously chopped it can be considered as reasonable;
4. The steam present in the upper part of the reactor during the filling time has no reactivity, so only the solid wetted by water reacts;
5. There is no backmixing in the liquid phase i.e. a plug flow behaviour is assumed without changes along the radial coordinate;
6. The temperature is considered uniform throughout the reactor;
7. The solid density is constant;
8. The liquid flow rate is constant along the reactor and during the reaction time.

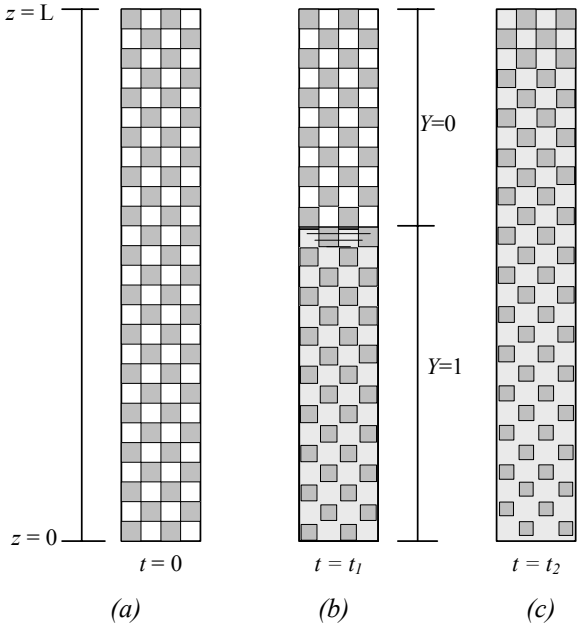


**Figure 9.4** *The reactor model. Initial condition (a), in the filling time (b) and once the reactor is completely filled (c).*

Under the hypotheses above, the equation that represents the solid solubilization is:

$$\frac{\partial C_{ss,s}(z,t)}{\partial t} = -k_s C_{ss,s}(z,t) Y(z,t) \tag{9.2}$$

with initial condition

$$C_{ss,s}(\forall z,0) = C_{s,0} \lambda_{\max}(T) \tag{9.3}$$

where $C_{ss,s}$ is the soluble solid concentration [kg/m$^3$ of reactor], $C_{s,0}$ is the total solid concentration at time zero, $\lambda_{max}$ is the maximum soluble fraction at temperature $T$ [K] and $k_s$ (T) [1/s] is the rate constant. The temperature dependence according to the Arrhenius law is:

$$k_s = A_s \cdot \exp\left(\frac{-E_{a,s}}{RT}\right) \tag{9.4}$$

where $A_s$ [1/s] is the pre-exponential factor while $E_{a,s}$ [J/mol] the activation energy, and $R$ [J/(mol K)]) the universal gas constant.

In Equation (9.2) the concentrations depend on the time and on the axial coordinate, according to the filling procedure (the filling time is around 9 min). For this reason different axial coordinates have different reaction times.

In order to simulate the filling of the reactor in Eq. (9.2), a fictitious variable $Y$ was introduced. This variable is initially set to 0 and becomes 1 when the water reaches the specific axial coordinate (Figure 9.5). Clearly, $Y$ "moves" with the same velocity of the liquid phase.

$$\frac{\partial(Y \cdot \varepsilon)}{\partial t} = v_a \frac{\partial Y(z,t)}{\partial z} \tag{9.5}$$

with initial and boundary conditions:

$$Y(\forall z,0) = 0 \; ; \; Y(0,\forall t) = 1; \tag{9.6}$$

The mass balance in the liquid is:

$$\frac{\partial(C_{ss,l} \cdot \varepsilon)}{\partial t} = v_a \frac{\partial C_{ss,l}}{\partial z} + k_s C_{ss,s} \tag{9.7}$$

where $v_a$ [m/s] is the apparent velocity calculated as the ratio between the volumetric flow rate and the reactor cross section area, $C_{ss,l}$ [kg/m$^3$ liquid] is the concentration of the solubilized solid and ε is the void volume, expressed by:

$$\varepsilon = 1 - \frac{C_s}{\rho_s} \tag{9.8}$$

whit $\rho_s$ the solid density [kg/m$^3$ solid] and $Cs$ [kg/m$^3$ reactor] total solid concentration.

The initial and boundary conditions are:

$$C_{ss,l}(\forall z,0)=0\ ;\ C_{ss,l}(0,\forall t)=0; \tag{9.9}$$

### 9.2.2 Multicomponent model

In this model the biomass is considered as made of 4 components: cellulose, hemicellulose, lignin and "others". Each of them is partially hydrolysed and solubilized by water. Cellulose and hemicellulose follow the pathway of Figure 9.4b, while it is assumed that lignin and "other" are only solubilized but not hydrolysed to monomeric units and to degradation products.

The model hypotheses are:

1 The solid polymers balance is based on the whole reactor volume, while the mass balance for the oligomers and monomers are referred to the liquid phase volume as in Lee *et al.*, 1998 (see § 9.2.1);
2 During the reaction the solid does not move from the initial position (see Figure 9.4) i.e. it is neither compressed at the reactor outlet nor collapsed at the reaction inlet;
3 The steam present in the upper part of the reactor during the filling time has no reactivity;
4 There is no backmixing in the liquid phase (plug flow behaviour is assumed);
5 No direct formation of monomers from hemicellulose or cellulose directly from the solids is considered (Nabarlatz *et al.,* 2004);
6 During the hydrolysis of the polymeric sugars a molecule of water reacts for each monomeric unit (Jensen *et al.,* 2008);
7 The solid density is constant and does not depend on the composition of the solid;
8 The liquid flow rate is constant along the reactor;
9 Hemicellulose is assumed to be made of xylose only.

For the solid material:

$$\frac{\partial C_{i,s}(z,t)}{\partial t}=-k_{i,s}C_{i,s}(z,t)Y \tag{9.10}$$

where $k_{i,s}$ (T) [1/s] is the reaction constant (see the Arrhenius law, Eq. 9.4) and $C_{i,s}$ is the concentration [kg/m$^3$ of reactor] of dissoluble component *i.*
The initial condition is:

$$C_{i,s}(\forall z,0) = C_{s,0} \cdot x_{i,s} \cdot \lambda_{i,\max} \tag{9.11}$$

where $C_{s,0}$ is the concentration [g/m$^3$ of reactor] of the raw material, $x_{i,s}$ is the mass fraction of component $i$ in the raw material and $\lambda_{\iota,\max}$ is the mass fraction of the total initial component $i$ that can be dissolved by means of LHW pretreatment. Eqs. (9.10) and (9.11) are valid for all the four components of the biomass.
The liquid phase mass balances for hemicellulose and cellulose are equivalent and modelled with the following Equations (9.12, 9.13 and 9.14), where subscript *ol* is related to the hemicellulose or cellulose oligomers while *m* to the monomeric xylose or glucose and *d* to the degradation product.

$$\frac{\partial(C_{i,ol} \cdot \varepsilon)}{\partial t} = v_a \frac{\partial C_{i,ol}}{\partial z} + k_{i,s} C_{i,s} - k_{i,ol} C_{i,ol} \varepsilon \tag{9.12}$$

,

$$\frac{\partial(C_{i,m} \cdot \varepsilon)}{\partial t} = v_a \frac{\partial C_{i,m}}{\partial z} + k_{i,ol} C_{x,ol} \varepsilon \frac{MW_{i,m}}{MW_{i,ol}} - k_{i,m} C_{x,m} \varepsilon \tag{9.13}$$

And

$$\frac{\partial(C_{i,d} \cdot \varepsilon)}{\partial t} = v_a \frac{\partial C_{i,d}}{\partial z} + \sum k_{i,m} C_{i,m} \varepsilon \frac{MW_{i,d}}{MW_{i,m}} \tag{9.14}$$

in the above equations $v_a$ [m/s] is the apparent velocity calculated as the ratio between the volumetric flow rate and the reactor cross section, $MW_{i,m}$, $MW_{i,ol}$ and $MW_{i,ol}$ are the molar weights of the monomers (Glucose = 180.16 [g/mol], Xylose= 150.13 [g/mol]) of the monomeric units present in the oligomers (Cellulose = 162.14, Hemicellulose = 132.12) and of the degradation products (HMF = 126.11, Furfural = 96.08). Concentrations $C_{i,j}$ [g/m$^3$] are referred to the liquid volume except for $C_{i,s}$ that is referred to the reactor volume. Finally, $\varepsilon$ is the void volume fraction calculated with Eq. (9.8).

In order to solve the differential equations the follows initial conditions and boundary conditions were set:
(Initial conditions):

$$C_{i,ol}(\forall z,0) = 0 \tag{9.15}$$

$$C_{i,m}(\forall z,0) = 0 \tag{9.16}$$

$$C_{i,d}(\forall z,0) = 0 \tag{9.17}$$

(boundary conditions):

$$C_{i,ol}(0,\forall t) = 0 \tag{9.18}$$

$$C_{i,m}(0,\forall t) = 0 \tag{9.19}$$

$$C_{i,d}(0,\forall t) = 0 \tag{9.20}$$

In this model lignin and "other" do not undergo hydrolysis to either monomeric units or degradation product, so the liquid mass balance is similar as for cellulose and hemicellulose, with the difference that Eqs. (9.13) and (9.14) and the last term of Eq. (9.12) are missing.

## 9.3 Results

The two models were implemented on gPROMS$^{TM}$ and tested on the data of Ingram *et al.,* (2009) about the LHW pretreatment of rye straw in a semibatch reactor.

### *9.3.1 Monocomponent model*

The experimental data about the total solid dissolution of rye straw were used in order to fit the parameters for the Arrhenius law. Table 9.1 shows the model input information.

**Table 9.1** *Simulation input data.*

| | |
|---|---|
| **Reactor diameter [m]** | 0.015 |
| **Reactor length [m]** | 0.3 |
| **Solid treated [kg]** | $1.7\ 10^{-4}$ |
| **Solid density [kg/m$^3$]** | 700 |
| **Water flow rate [m$^3$/s]** | $6.66\ 10^{-8}$ |

Additionally to Table 9.1 the maximum solid solubilization $\lambda_{max}$ at each temperature has to be supplied. The parameter was retrieved from experimental data (Figure 9.5).

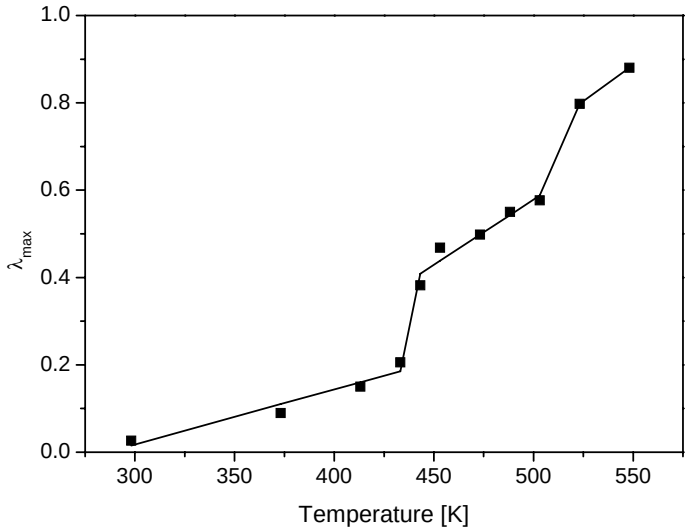


**Figure 9.5** *Fitting of the maximum solubilization parameter $\lambda_{max}$ as function of the temperature. Points are experimental data (Ingram et al., 2009) while curves were used in simulations.*

First of all the experimental data shown in Figure 9.6a were fitted and individual $k_s$ for Equation (9.2) were found. The Arrhenius plot (Figure 9.6b) allowed to calculate the parameters $A_s$ and $E_{a,s}$ that were then used as starting guess values for the simultaneous fitting of all the solubilization curves. Results are shown in Table 9.2.

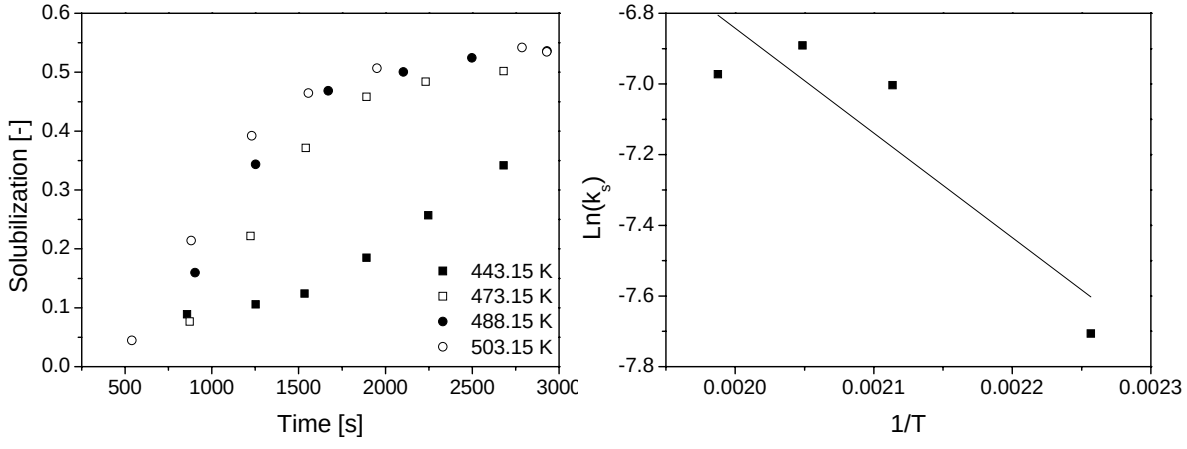


*(a)* *(b)*

**Figure 9.6** *Experimental data of solid solubilization as function of the reaction time (a) and Arrhenius plot of the individual rate constant.*

The software attempts to determine values for the unknown parameters, Φ, in order to maximise the probability that the mathematical model will predict the values obtained from the experiments. The objective function is:

$$\phi = \frac{N}{2}\ln(2\pi) + \frac{1}{2}\min_{\Theta}\left\{\sum_{i=1}^{NE}\sum_{j=1}^{NV_i}\sum_{k=1}^{NM_{ij}}\left[\ln\left(\sigma_{ijk}^2\right) + \frac{\left(\bar{z}_{ijk} - z_{ijk}\right)^2}{\sigma_{ijk}^2}\right]\right\} \tag{9.21}$$

where $N$ is the total number of measurement taken during all the experiments, $\Theta$ is the set of model parameters to be estimated, $NE$ is the number of experiments performed, $NV$ is the number of variable measured in the $i^{th}$ experiment, $NM$ the number of measurements of the $j^{th}$ variable in the $i^{th}$ experiment, $\sigma_{ij}$ the variance of the $k^{th}$ measurement of variable $j$ in experiment $i$. $\bar{z}_{ijk}$ the $k^{th}$ measured value of variable $j$ in experiment $i$ and finally $z_{ijk}$ the $k^{th}$ (model-) predicted value of variable $j$ in experiment $i$.

**Table 9.2** *Fitting results. Guess values obtained from the interpolation of the individual rate constants, and optimized values obtained from the contemporaneous fitting of all the curves.*

| | **Guess values** | **Optimized values** |
|---|---|---|
| $A_s$ **[1/s]** | 0.3995 | 0.4035 |
| $E_{a,s}$ **[J/mol]** | 24629 | 24630 |

In Figure 9.7a the comparison between experimental data (points) and curves obtained with the model proposed by Ingram *et al.,* (2009) are shown, while in Figure 9.7b the simulation of the same data is performed with the monocomponent model previously developed.

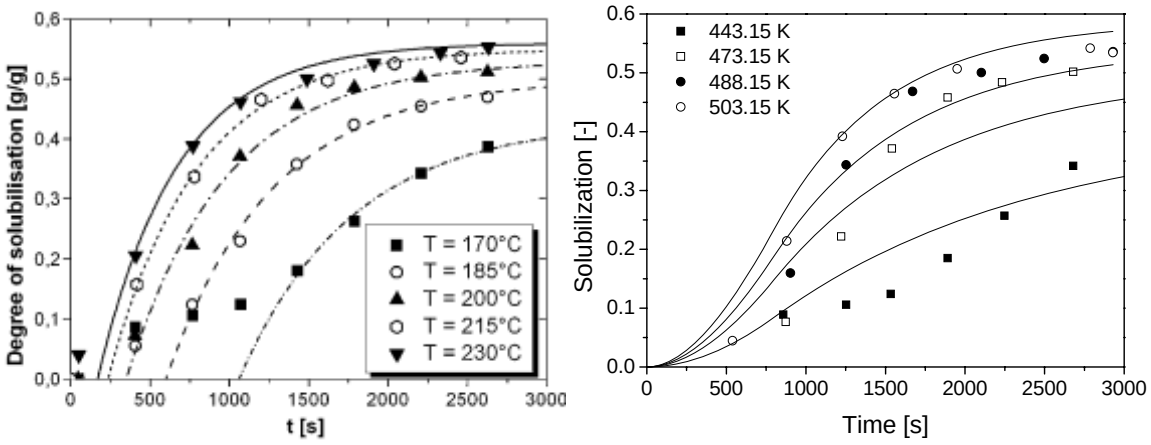


*(a)* *(b)*

**Figure 9.7** *Comparison between the performances of the model proposed by Ingram et al., (2009) (a) and the ones of the model proposed in this thesis (b).*

The model proposed by Ingram *et al.,* (2009) is derived simply from integration of a first order kinetic (Eq. 9.22) with the introduction of the maximum solubilization parameter ($\lambda_{max}$).

$$\frac{dC_s}{dt} = -k_s C_{i,s} \tag{9.22}$$

$$\Phi = \lambda_{\max}\left[1 - \exp(k_s t)\right] \tag{9.23}$$

where $\Phi$ is the solid solubilization, $C_s$ the solid concentration, and $k_s$ the rate constant. This model does not consider that the biomass at the bottom of the reactor reacts for longer time than the one on the top, so that the sigmoid behaviour cannot be reproduced. Moreover, since at time zero the value of $\Phi$ is 0, the curves were arbitrarily shifted in time due to a hypothetical reaction induction time (used as third parameter).
In conclusion the model proposed in this thesis reproduces the experimental results satisfactory by two fitting parameters only (the Arrhenius ones), thus demonstrating that the influence of the filling time cannot be neglected.

### *9.3.2 Multicomponent model*

In addition to the input information of Table 9.1, in order to use the multicomponent model the composition of the solid biomass is needed (Table 9.3).

**Table 9.3** *Rye straw composition.*

| | **Mass fraction [w/w]** |
|---|---|
| **Cellulose** | 0.436 |
| **Hemicellulose** | 0.235 |
| **Lignin** | 0.186 |
| **Others** | 0.143 |

The maximum solubilization of each component ($\lambda_{i,max}$) as a function of temperature has also to be supplied (Figure 9.8b). Compositions of the solid residue from the LHW pretreatment were available only for the treatment of 42.5 min (Figure 9.8a). As can be seen from Figure 9.7a, after this reaction time the total solubilisation of the biomass is near to the maximum value, expecially at high temperatures. For this reason those data were used to calculate the $\lambda_{i,max}$ values (Figure 9.8b).
At the temperatures investigated hemicellulose is almost totally solubilized while cellulose reacts only partially (the cellulose hydrolysis occurs at higher temperatures).

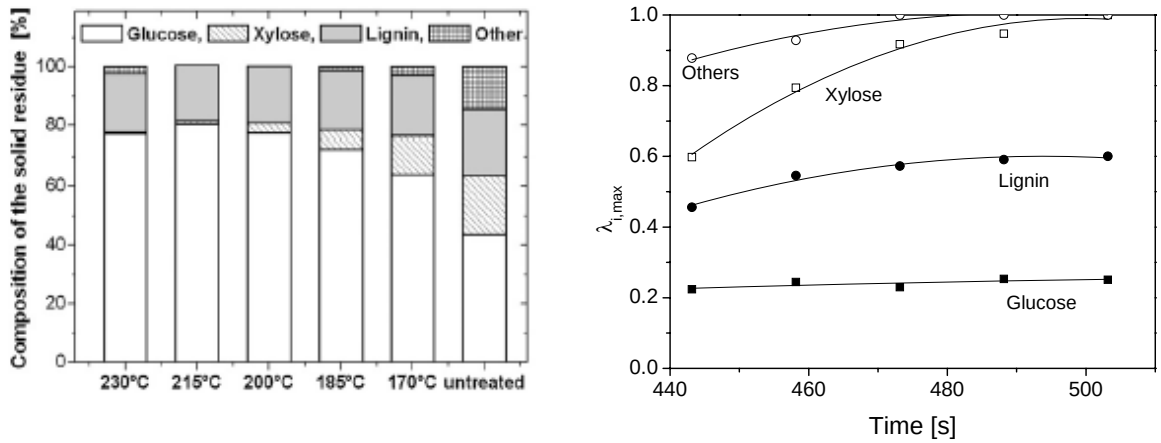


*(a)* *(b)*

**Figure 9.8** *Solid residue composition (a). Fitting of the $\lambda_{i,max}$ for each component from experimental data (b).*

As for the monocomponent model first the solubilization curves were fitted individually and the resulting rate constants ($k_{i,s}$) were plotted on the Arrhenius diagram. Then the pre-exponential factor as well as the activation energy were calculated from the graphical fitting (Figure 9.9) and used as guess value for the contemporaneous fitting of all the curves.

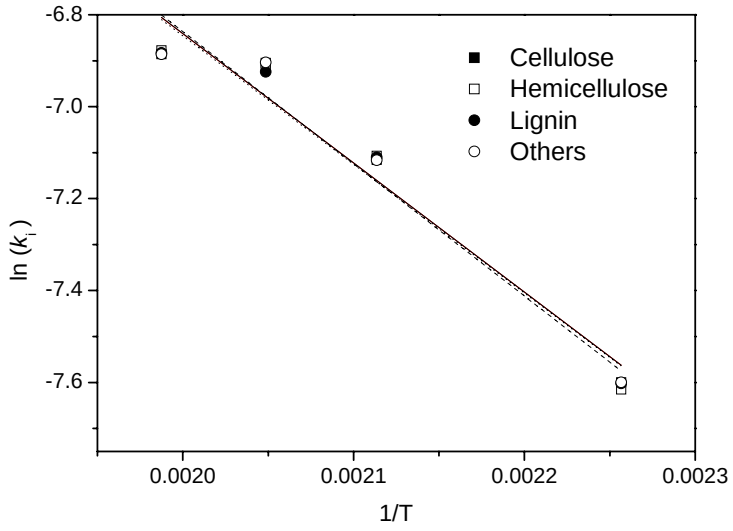


**Figure 9.9** *Linear fitting of the $k_{i,s}$ values for each component obtained by means of the individual fitting of the solubilization curves.*

The fitting results are shown in Table 9.4, while the obtained solubilization profiles in Figure 9.10.

**Table 9.4** *Fitting results. Guess values obtained from the interpolation of the individual rate constants, and optimized values obtained from the contemporaneous fitting of all the curves.*

| | Guess values | Optimized values |
|---|---|---|
| **Cellulose** | | |
| $A_{c,s}$ **[1/s]** | 0.339 | 3.821 |
| $E_{a\ s,c}$ **[J/mol]** | 23380 | 33940 |
| **Hemicellulose** | | |
| $A_{h,s}$ **[1/s]** | 0.288 | 3.087 |
| $E_{a\ h,s}$ **[J/mol]** | 23923 | 33440 |
| **Lignin** | | |
| $A_{l,s}$ **[1/s]** | 0.296 | 3.406 |
| $E_{a\ l,s}$ **[J/mol]** | 23275 | 33550 |
| **Others** | | |
| $A_{o,s}$ **[1/s]** | 0.340 | 3.612 |
| $E_{a\ o,s}$ **[J/mol]** | 23379 | 33760 |

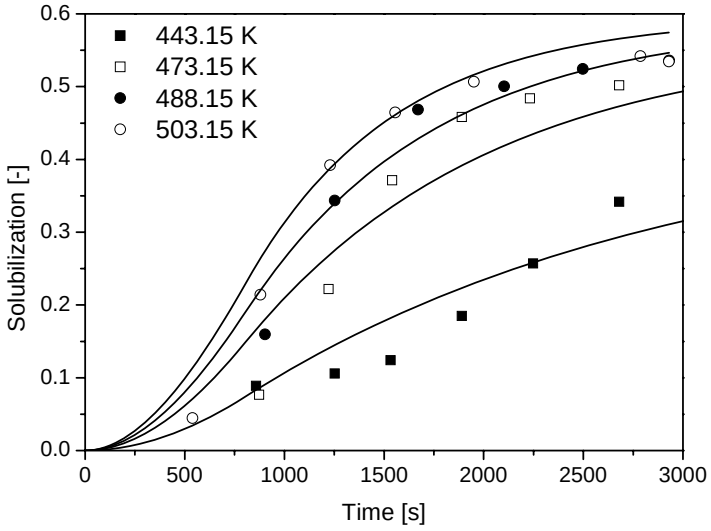


**Figure 9.10** *Solid solubilization as a function of the time if the multicomponent model is used.*

This model enables to represent very well the concentration of each species in the liquid phase. In Figure 9.11 the results for a simulation of the LHW treatment at 230°C are shown, together with the value of the filling variable. ($Y$= 1 when the water reaches the axial coordinate).

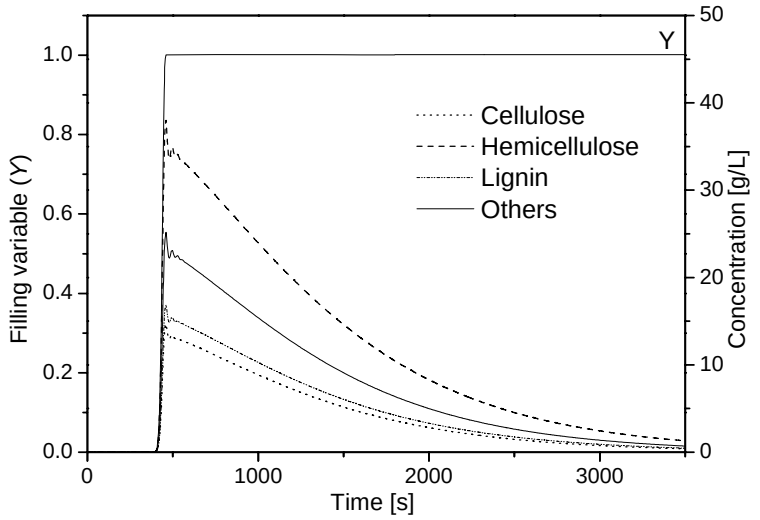


**Figure 9.11** *Hydrolysate concentrations at the reactor outlet section (z =0.3 m) for a treatment at 230 °C.*

In order to predict monomeric sugars and degradation product concentrations the constant ratio of the reaction have to be supplied to the model or retrieved from experimental data. In Table 9.5 the literature kinetic parameters for Reactions (9.24) and (9.25) are reported.

$$C_6H_{10}O_5 + H_2O \xrightarrow{k_{c,ol}} C_6H_{12}O_6 \xrightarrow{k_{c,m}} \text{Degradat.Prod} + 3H_2O \tag{9.24}$$

$$C_5H_8O_4 + H_2O \xrightarrow{k_{h,ol}} C_5H_{10}O_5 \xrightarrow{k_{h,m}} \text{Degradat.Prod} + 3H_2O \tag{9.25}$$

In Figure 9.12a the glucose concentration profiles along the reactor as function of time are presented, while in Figure 9.12b the instantaneous sugars concentration at the outlet section of the reactor are shown.

**Table 9.5** *Kinetic parameters.*

| | **Values** | **Reference** |
|---|---|---|
| **Cellulose** | | |
| $k_{c,ol}$: $E_a$ [kJ/mol]/$A$ [1/s]) | 215/ $2.33 \cdot 10^{18}$ | Mochidzuki *et al.,* 2000 |
| $k_{c,m}$: $E_a$ [kJ/mol]/$A$ [1/s]) | 118.85/$4.01 \cdot 10^{7}$ | Qi and Xiuyang, 2008 |
| **Hemicellulose** | | |
| $k_{h,ol}$: $E_a$ [kJ/mol]/$A$ [1/s]) | 65.58/ $7.33 \cdot 10^{2}$ | Zhuang *et al.,* 2009 |
| $k_{h,m}$: $E_a$ [kJ/mol]/$A$ [1/s]) | 147.21/ $3.39 \cdot 10^{132}$ | Zhuang *et al.,* 2009 |

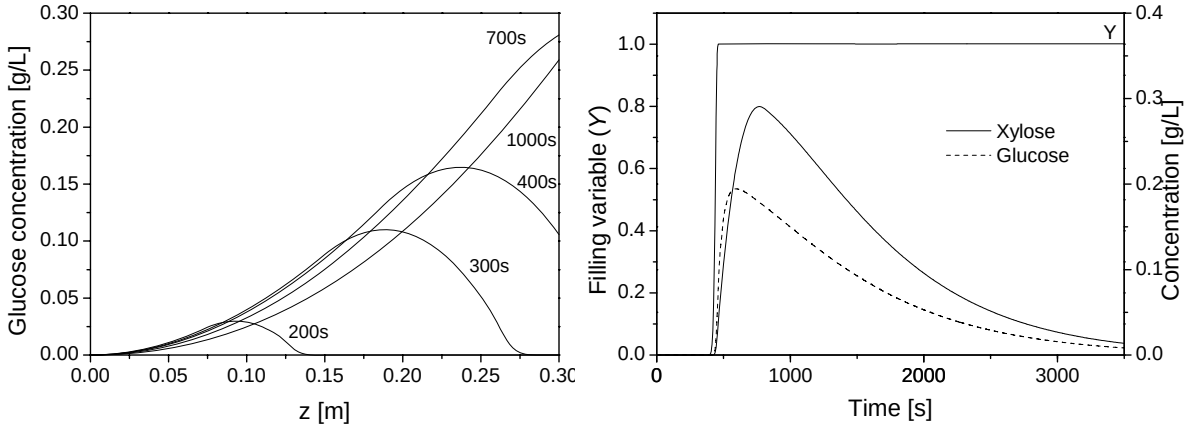


**Figure 9.12** *Glucose concentration along the reactor as function of the time (a) sugar concentrations at the reactor outlet section (b). (Treatment at 230 °C)*

The sugars concentration presents a maximum accordingly to the experimental result (Ingram *et al.,* 2009 and by Ji *et al.,* 2009).

## 9.4 Conclusions and future works

Two models for the semi-continuous LHW treatment of the biomass were developed and tested on experimental data about the treatment of rye straw. These models, even though very simple, perform better than those presently available in literature. They permit to simulate the solid solubilization and allow having an idea about the concentration of monomeric sugars and degradation products obtained from the pretreatment. The fitting of the experimental points is quite good. Better performance could probably be obtained by introducing a delay time in the reaction of the solid.

## 9.5 Nomenclature

$A_s$ = Arrhenius law pre exponential factor (1/s)
$C_{i,,M}$ = monomeric sugar concentration (g/m$^3$)
$C_{i,P}$ = polymeric sugar concentration (g/m$^3$)
$C_s$ = total solid concentration (g/m$^3$ of reactor)
$C_{ss,s}$ = soluble solid concentration in the solid phase (g/m$^3$ of reactor)
$C_{ss,l}$ = solubilized solid concentration in the liquid phase (g/m$^3$ liquid)
$C_{i,s}$ = concentration of dissoluble component *i* in the solid (g/m$^3$ of reactor)
$C_{i,m}$ = monomer concentration of component *i* (g/m$^3$ liquid)
$C_{i,ol}$ = oligomer concentration of component *i* (g/m$^3$ liquid)
$C_{i,d}$ = degradation product concentration of component *i* (g/m$^3$ liquid)

| | | |
|---|---|---|
| $E_{a,s}$ | = | activation energy (J/mol) |
| $k_s$ | = | rate constant (1/s) |
| $k_{i,s}$ | = | rate constant of component *i* in the solid (1/s) |
| $k_{i,m}$ | = | monomer rate constant (1/s) |
| $k_{i,ol}$ | = | oligomer rate constant (1/s) |
| $MW_{i,j}$ | = | molar weight (g/mol) |
| $R$ | = | universal gas constant (J/(mol K)) |
| $T$ | = | temperature (K) |
| $v_a$ | = | apparent velocity (m/s) |
| $x_{i,s}$ | = | mass fraction of component *i* in the raw material (-) |
| $t$ | = | time (s) |
| $Y$ | = | filling variable |
| $z$ | = | axial coordinate (m) |

Greek letters:

| | | |
|---|---|---|
| $\lambda_{max}$ | = | maximum soluble fraction of the solid (-) |
| $\lambda_{i,max}$ | = | mass fraction of the total initial component *i* that can be dissolved (-) |
| $\varepsilon$ | = | void volume (-) |
| $\rho_s$ | = | solid density (g/m$^3$ solid) |

Subscript:

| | | |
|---|---|---|
| s | = | solid phase |
| ss | = | soluble solid |
| l | = | liquid hydrolysate phase |
| *ol* | = | oligomers |
| *m* | = | monomeric xylose or glucose. |
| h | = | hemicellulose |
| c | = | cellulose |
| l | = | lignin |
| o | = | others |

## 9.6 References

Aguilar, R., J.A. Ramírez, G. Garrote, and M. Vázquez (2002). Kinetic Study of the Acid Hydrolysis of Sugar Cane Bagasse. *J. Food Eng.,* **55**, 309–318.

Carrasco, F. and C. Roy (1992). Kinetic Study of Dilute-acid Prehydrolysis of Xylan-Containing Biomass. *Wood Sci. Technol.,* **26**, 189-208.

Conner, A.H. and L.F. Lorenz (1986). Kinetic Modeling of Hardwood Prehydrolysis. Part III: Water and Dilute Acetic Acid Prehydrolysis of Southern Red Oak. *Wood Fiber Sci.,* **18**, 248-263.

Gámez, S., J.A. Ramírez, G. Garrote, and M. Vázquez (2006). Hydrolysis of Sugar Cane Bagasse Using Phosphoric Acid at Autoclave Pressure. *J. Food Eng.*, **74**, 78–88.

Garrote, G., H. Domínguez, and J.C. Parajó (1999). Hydrothermal Processing of Lignocellulosic Materials. *Holz Roh Werkst*., **57**, 191-202.

Ingram, T. (2008). Thermal and Thermal-Enzymatic Hydrolysis of Ligno- cellulosic Biomass for the Production of Bioethanol. *Master thesis*, TU Hamburg-Harburg.

Ingram, T., T. Rogalinski, V. Bockemühl, G. Antranikian, G. Brunner (2009). Semi-Continuous Liquid Hot Water Pre-treatment of Rye Straw for Bioethanol Production. *J. Supercrit. Fluids,* **48,** 238-246.

Jensen, J., J. Morinelly, A. Aglan, A. Mix, and D.R. Shonnard (2008). Kinetic Characterization of Biomass Dilute Sulfuric Acid Hydrolysis: Mixtures of Hardwoods, Softwood, and Switchgrass. *AIChE J.,* **54**, 1637-1645.

Ji, Y., S. Viamajala, M.H. Selig, T. Vinzant, and M.P. Tucker (2009). Comparison of Kinetics of Xylose and Lignin Removal During Hot Water and Dilute-Acid Pretreatment of Corn Stover using a Continuous Flow-Through Reactor. Poster presented at: *31st Symposium on Biotechnology for Fuels and Chemicals*, San Francisco (U.S.A.), May 3-6.

Kamio, E., H. Sato, S. Takahashi, H. Noda, C. Fukuhara, and T. Okamura (2008). Liquefaction Kinetics of Cellulose Treated by Hot Compressed Water Under Variable Temperature Conditions. *J Mater. Sci.*, **7**, 2179-2188.

Kim, S.B. and Y.Y. Lee (1987). Kinetics in Acid-catalyzed Hydrolysis of Hardwood Hemicellulose. Biotechnology Bioengineering Symposium, 17, 71–84.

Lee, Y.Y., P. Iyer, Q. Xiang, and J. Hayes (1998). *Kinetic and Modeling Investigation to Provide Design Guidelines for the NREL Dilute- Acid Process Aimed at Total Hydrolysis/Fractionation of Lignocellulosic Biomass*. NERL report SR-510-36392.

Liu, C. and C.E. Wyman (2004). Impact of Fluid Velocity on Hot Water Only Pretreatment of Corn Stover in a Flowthrough Reactor. *Appl. Biochem. Biotech*., **113–116**, 977-987.

Mochidzuki, K., A. Sakoda, M. Suzuki (2000). Measurement of the Hydrothermal Reaction Rate of Cellulose Using Novel Liquid-Phase Thermogravimetry. *Thermochimica Acta*, **348**, 69-76.

Nabarlatz, D., X. Farriol, and D. Montané (2004). Kinetic Modeling of the Autohydrolysis of Lignocellulosic Biomass for the Production of Hemicellulose-Derived Oligosaccharides. *Ind. Eng. Chem. Res*., **43**, 4124-4131.

Qi, J. and L. Xiuyang (2008). Kinetics of Non-catalyzed Decomposition of Glucose in High-temperature Liquid Water. *Chin. J. Chem. Eng*., **16**, 890-894.

Rodríguez-Chong, A., J.A. Ramírez, G. Garrote, and M. Vázquez (2004). Hydrolysis of Sugar Cane Bagasse Using Nitric Acid: a Kinetic Assessment. *J. Food Eng.,* **61**, 143–152.

Saeman, J.F. (1945). Kinetics of Wood Saccharification. Hydrolysis of Cellulose and Decomposition of Sugars in Dilute Acid at High Temperature. *Ind. Eng. Chem*., **37**, 43-52.

Vázquez, M., M. Oliva, S.J. Téllez-Luis, and J.A. Ramírez (2007). Hydrolysis of Sorghum Straw Using Phosphoric Acid: Evaluation of Furfural Production. *Bioresour. Technol.,* **98**, 3053–3060.

Wei, Q., Z. Su-ping, X. Qing-li, R. Zheng-wei, and Y. Yong-jie (2008). Degradation Kinetics of Xylose and Glucose in Hydrolysate Containing Dilute Sulfuric Acid. *Chin. J. Proc. Eng*., **8**, 1132-1137.

Xiang, Q., Y.Y. Lee, and R.W. Torget (2004). Kinetics of Glucose Decomposition During Dilute-Acid Hydrolysis of Lignocellulosic Biomass. *Appl. Biochem. Biotechnol.,* **113-116**, 1127-1138.

Zhuang, X., Z. Yuan, L. Ma, C. Wu, M. Xu, J. Xu, S. Zhu, and W. Qi (2009). Kinetic Study of Hydrolysis of Xylan and Agricultural Wastes with Hot Liquid Water. *Biotechnol. Adv.,* **27**, 578–582.

# Conclusions

The problem of the extensive production of bioethanol as an alternative fuel for transportation has been addressed in this PhD thesis, with specific reference to a number of issues under current scientific investigation. Namely, the aim of the thesis was to analyse the main obstacles to the widespread diffusion of bioethanol and to give contributions, for both "first generation" and "second generation" processes, in order to find technical and economical alternatives, that could improve the plant performance and profitability.

The literature work reported in the *Introduction* and in *Chapter 1* permitted to identify bioethanol as the front runner among the different possibilities to replace fossil fuels in the short period. According to the fact that ethanol from sugar cane is definitely economic and the production process is already optimized, the hot research topics were identified in developing the processes to produce ethanol from corn and from lignocellulosic materials. In the first case industrial plants are already in operation, but the production is not economic yet in comparison to gasoline, whereas no industrial applications of lignocellulosic ethanol are reported yet, as in this case problems still arise from both the economical and technical points of view. Anyway, lignocellulosic bioethanol is the true alternative to gasoline because it is more environmentally friendly and does not require raw materials in competition with food.

In *Chapter 2* a detailed simulation of the ethanol from corn process allowed developing a tool for quantitative sensitivity analyses. For instance, calculations showed that if the corn starch content were increased by 16.8%, corn consumption and DDGS amount would be reduced as well (respectively, 14.3% and 35.6% less). As DDGS is presently sold at 300 €/t, higher revenue from higher alcohol production could almost be reset by the drop in the revenue from DDGS. Differently, if an increased tolerance of yeasts to ethanol were obtained (i.e. from 0.109% w/w to 0.210% w/w into the fermenter) this would lead to 20% less steam consumption thanks to the easier separation downstream.

Finally, it was shown that the production cost is primarily due to the corn itself (68.8%), and secondly (16.2%) to the energetic needs of the processes. Due to the impossibility to act on the corn cost, which depends on the market, the further step was to find an alternative to decrease the energy consumption of the process. It was underlined that thermal integration is a must when promoting this process for large scale applications, so that all technical alternatives proposed should be aimed to maximize the possible energy recoveries.

In *Chapter 3* and *Chapter 4* the possibility to use supercritical $CO_2$ extraction instead of distillation to recover ethanol from the mixture exiting the fermenter, was investigated from a technical and economical standpoint. The results presented in *Chapter 4* show that for

both the process options considered the supercritical extraction is not economic because of the high capital investment required and the high operating costs, which shift the payback period to completely unrealistic values.

It the following *Chapters* the "second generation" ethanol process was examined. In particular focus was given to the pretreatment step. The liquid hot water (LHW) treatment was identified as one of the most promising, and for this reason it was investigated deeply both by means of simulation and from the experimental point of view.

In *Chapter 5* a production process from rye straw to ethanol was modelled and simulated. For both the distillation configurations considered it was demonstrated that all the energy needs of the process can be covered by burning the solid residue in a combined heat and power (CHP) plant. An excess of 82.6 (1$^{st}$ conf.) and 65.8 MW (2$^{nd}$ conf.) of electricity could also be sold to the grid.

*Chapter 6* addresses some economic issues concerning "second generation" ethanol plants. The hemicellulose fraction of the biomass was identified as a possible source of an additional valuable product that could increase the profitability of the plant. The economical analysis of a plant producing ethanol from the hexoses part of the biomass and xylitol from the xylose one permitted to demonstrate that such option could effectively help to increase the overall process profitability.

In *Chapter 7* and *Chapter 8* the LHW pretreatment was experimentally studied. As only a few works on semibatch pretreatment are available in literature, and due to the advantages of such a technical solution, the attention was focused on this type of reactor.

The solubilization of the wheat bran was extensively studied as a function of temperature and for different water/solid ratios in *Chapter 7*. Only small differences in the solubilization of the biomass and its components were found when shifting from water/solid ratio of 6.4 to 12.8. Longer experiments did not lead to better performances. It was moreover discovered that temperatures above 200 °C lead to the formation of degradation products, which negatively influence the final fermentation step. At 200 °C almost 80% of the biomass was solubilized and the enzymatic treatment of the two fractions obtained allowed a total recovery of 80% of glucose, 85% of xylose, and 40% of the arabinose. According to the experimental tests on wheat bran, it was concluded that lignocellulosic biomass can be converted in valuable monomeric sugars, and LHW provides an excellent reaction medium for the pretreatment of biomass.

In *Chapter 8* an experimental apparatus that permits to perform LHW pretreatment in semibatch reactor with and without the addition of $CO_2$ as a catalyst was designed, built, and tested. Preliminary results on the treatment of white office paper showed that it could be hydrolysed by water at high temperature, achieving almost the 100% of solubilization. After an enzymatic treatment it was possible to obtain monomeric sugars suitable for fermentation

(with large amount of enzymes about 0.55 g glucose and 0.15 g of xylose for grams of paper treated with LHW where obtained).
Two simple models to describe the LHW treatment in semibatch reactor were proposed in *Chapter 9*. They permitted to simulate the solid solubilization and to have an idea about the concentration of monomeric sugars and degradation products obtained in the pretreatment. The fitting of the experimental points was quite satisfactory. It was concluded that the filling time is crucial in order to simulate the sigmoid behaviour of the solubilization of the biomass.

In summary, lignocellulosic bioethanol is the best way forward to follow in order to replace gasoline, but big breakthroughs are still needed. As the economical aspect is the limiting factor to industrial scale diffusion, the first step has to be done in this direction. Industrial-scale biorefineries have been identified as the most promising route to the creation of a sustainable bio-based economy. A biorefinery would integrate a variety of conversion processes to produce multiple product streams such as motor fuels, heat, electricity, and chemicals from biomass. As demonstrated also in this thesis, the need to obtain fuel can be economically supported by the simultaneous productions of other high value products.

# Acknowledgments

This work could not been completed without the collaboration of many people and without the financial support of some institutions.
I should therefore thank, first of all, Prof. Alberto Bertucco, that gave me the opportunity to work on this PhD project. I'm really grateful to my supervisor for his continuous help and in particular for believing in me.
I would like to thank also Prof. Gerd Brunner and Prof. Irina Smirnova of the TUHH University of Hamburg (Germany), that gave me the possibility to spend nine very constructive and positive months studying the LHW pretreatment.
I am also grateful to my colleagues: the PhD students of the Department DIPIC of the University of Padua for the friendly atmosphere that went along during this year. And finally, I want to thank the colleagues of the TUHH University that made me spend really nice moments.
I am grateful to Ministero Italiano dell'Università e della Ricerca and Fondazione Aldo Gini, for the financial support to the research activities.

# Appendix A

In this appendix the Fortran subroutines used to simulate the equilibrium in the simulations of Chapter 4 are shown.

Equilibrium at 100 bar and 333.15 K:

```
        SUBROUTINE USRKLL (T,     P,       X1,     X2,     NCP,
     2                     IDX,   NBOPST,  KDIAG,  KBASE,  RK,
     3                     RDUM,  KER,     NINT,  INT,    NREAL,
     4                     REAL,  ISTAGE,  IBASIS)

        IMPLICIT NONE

C       DECLARE VARIABLES USED IN DIMENSIONING

        INTEGER NCP,NINT

       #include "ppexec_user.cmn"
        EQUIVALENCE (RMISS, USER_RUMISS)
        EQUIVALENCE (IMISS, USER_IUMISS)

C       DECLARE ARGUMENTS

        INTEGER IDX(NCP),NBOPST(6),    KDIAG, KBASE, KER,
     +        INT(NINT),   NREAL, ISTAGE,IBASIS,I,IPCO2,IPETOH,IPW
        REAL*8 X1(NCP), X2(NCP), RK(NCP), T,     P,
     +       RDUM

C       DECLARE LOCAL VARIABLES

        INTEGER IMISS, NCOMP,ICO2,IETOH,IW,DMS_KFORMC
        REAL*8 REAL(NREAL), RMISS,yW,xW,yCO2,xCO2, yET, xET,ketoh, XETOH,
     +                      YETOH

C       BEGIN EXECUTABLE CODE

        DO I=1,NCP
          RK(I)=1
        ENDDO

        IETOH=DMS_KFORMC('C2H6O-2')
        ICO2=DMS_KFORMC('CO2')
        IW=DMS_KFORMC('H2O')

        DO I=1,NCP
          IF (IDX(I).EQ.IETOH)THEN
            IPETOH=I
          ELSE IF (IDX(I).EQ.ICO2)THEN
            IPCO2=I
          ELSE IF (IDX(I).EQ.IW) THEN
            IPW=I
         ENDIF
        ENDDO

        XETOH=X1(IPETOH)/(X1(IPETOH)+X1(IPW))

        IF (X1(IPETOH).LE.(0.23634429))THEN
```

```
          xET=-0.681184*XETOH**3-0.030098*XETOH**2+0.983785*XETOH
        ELSEIF(X1(IPETOH).GT.(0.23634429)) THEN
          xET=-0.972615*XETOH**2 + 1.39964*XETOH-0.05463
        ENDIF

        xW=(1-XETOH)*xET/XETOH
        xCO2=1-xW-xET
        ketoh=-1.38288*XETOH**6+4.5638*XETOH**5-5.37123*XETOH**4 +
       + 2.54282*XETOH**3 + 0.06039*XETOH**2 - 0.45096*XETOH + 0.15623
        yET=ketoh*xET

        IF (X1(IPETOH).LE.(0.030260296))THEN
          YETOH=3333218.407163*X1(IPETOH)**5-404801.9525*X1(IPETOH)**4+
       +   24977.392587*X1(IPETOH)**3-921.904202*X1(IPETOH)**2+
       +   26.81259*X1(IPETOH)
        ELSEIF(X1(IPETOH).GT.(0.030260296)
       +.AND.X1(IPETOH).LE.(0.122375059)) THEN
          YETOH=42.126283*XETOH**5-97.313955*XETOH**4+85.081528*XETOH**3-
       +   34.604258*XETOH**2+6.650468*XETOH+0.232598
        ELSEIF(X1(IPETOH).GT.(0.122375059)
       +.AND.X1(IPETOH).LE.(0.99391438)) THEN
          YETOH=2.87345*XETOH**5-10.2011*XETOH**4+13.5792*XETOH**3-
       +   7.95137*XETOH**2+2.20857*XETOH+0.48961
        ELSEIF(X1(IPETOH).GT.(0.99391438)) THEN
          YETOH=0.87391*XETOH+0.12609
        ENDIF

        yW=(1-YETOH)*yET/YETOH
        yCO2=1-yW-yET

        RK(IPETOH)=yET/xET
        RK(IPCO2)=yCO2/xCO2
        RK(IPW)=yW/xW

        RETURN
        END
```

Equilibrium at 140 bar and 333.15 K:

```
        SUBROUTINE KLLDEC (T,     P,       X1,     X2,     NCP,
      2                   IDX,   NBOPST,  KDIAG,  KBASE,  RK,
      3                   RDUM,  KER,     NINT,   INT,    NREAL,
      4                   REAL,  ISTAGE,  IBASIS)

        IMPLICIT NONE

C     DECLARE VARIABLES USED IN DIMENSIONING

        INTEGER NCP,NINT
      #include "ppexec_user.cmn"

        EQUIVALENCE (RMISS, USER_RUMISS)
        EQUIVALENCE (IMISS, USER_IUMISS)

C     DECLARE ARGUMENTS

        INTEGER IDX(NCP),NBOPST(6),    KDIAG, KBASE, KER,
      +        INT(NINT),NREAL,ISTAGE,IBASIS,I,IPCO2,IPETOH,IPW
```

```
        REAL*8 X1(NCP),X2(NCP),RK(NCP),T,P,
     +       RDUM

C     DECLARE LOCAL VARIABLES

        INTEGER IMISS, NCOMP,ICO2,IETOH,IW,DMS_KFORMC
        REAL*8 REAL(NREAL), RMISS, Zy, Zx

C     BEGIN EXECUTABLE CODE

        DO I=1,NCP
          RK(I)=1
        ENDDO

        IETOH=DMS_KFORMC('C2H6O-2')
        ICO2=DMS_KFORMC('CO2')
        IW=DMS_KFORMC('H2O')

        DO I=1,NCP
        IF (IDX(I).EQ.IETOH)THEN
          IPETOH=I
        ELSE IF (IDX(I).EQ.ICO2)THEN
          IPCO2=I
        ELSE IF (IDX(I).EQ.IW) THEN
          IPW=I
        ENDIF
        ENDDO

        IF(X1(IW).LE.(0.5610)) THEN
          RK(IPW)=0.0125*(X1(IW))**(-1.9669)
          RK(IPETOH)=-36.66*X1(IW)**5+106.9*X1(IW)**4-122.5*X1(IW)**3+
     +   +69.92*X1(IW)**2-20.15*X1(IW)+2.62
          Zy=(-53.653*(X2(IETOH)/(X2(IETOH)+X2(IW)))**2 +
     +   -119.92*(X2(IETOH)/(X2(IETOH)+X2(IW)))+127.1)*(X2(IETOH)+X2(IW))
          Zx=0.0196*EXP(6.2753*(X1(IETOH)/(X1(IETOH)+X1(IW))))
     +   *(X1(IETOH)+X1(IW))
          RK(IPCO2)=Zy/Zx
        ELSE IF(X1(IW).GT.(0.5610)) THEN
          RK(IPW)=-0.07*log(X1(IW))+0.007
          RK(IPETOH)=-0.003*X1(IW)**2+0.249*X1(IW)+0.106
          Zy=(-53.563*(X2(IETOH)/(X2(IETOH)+X2(IW)))**2 +
     +   -119.92*(X2(IETOH)/(X2(IETOH)+X2(IW)))+127.1)*(X2(IETOH)+X2(IW))
          Zx=0.0196*EXP(6.2753*(X1(IETOH)/(X1(IETOH)+X1(IW))))
     +   *(X1(IETOH)+X1(IW))
          RK(IPCO2)=Zy/Zx
        END IF

            RETURN
            END
```